U.S. Department of Transportation

Federal Railroad Administration

SAFETY OF PASSENGER VEHICLE DYNAMICS

Simulation and Test Correlations for a Passenger Car with Non-Equalized Trucks

Office of Research and Development
Washington, DC 20590

G. Samavedam
J. Gomes
D. Wormley

Foster-Miller, Inc.
350 Second Avenue
Waltham, MA 02451-1196

DOT/FRA/ORD-

Draft Final Report
January 1999

SAFETY OF PASSENGER VEHICLE DYNAMICS
Simulation and Test Correlations for a Passenger Car with Non-Equalized Trucks

G. Samavedam
J. Gomes
D. Wormley

Foster-Miller, Inc.
350 Second Avenue
Waltham, MA 02451-1196
(781) 684-4000

Draft Final Report

January 1999

REPORT DOCUMENTATION PAGE

Form Approved
OMB No. 0704-0188

1. AGENCY USE ONLY *(Leave blank)*	2. REPORT DATE January 1999	3. REPORT TYPE AND DATES COVERED January 1997 - January 1999

4. TITLE AND SUBTITLE
Safety of Passenger Vehicle Dynamics: Simulation and Test Correlations for a Passenger Car with Non-Equalized Trucks

5. FUNDING NUMBERS
DTFR53-95-C-00049

6. AUTHOR(S)
G. Samavedam, J. Gomes, D. Wormley**

7. PERFORMING ORGANIZATION NAME(S) AND ADDRESS(ES)
Foster-Miller, Inc.
350 Second Avenue
Waltham, MA 02451-1196

8. PERFORMING ORGANIZATION REPORT NUMBER

9. SPONSORING/MONITORING AGENCY NAME(S) AND ADDRESS(ES)
U.S. Department of Transportation*
Federal Railroad Administration
Office of Research and Development
Washington, D.C. 20593

10. SPONSORING/MONITORING AGENCY REPORT NUMBER
DOT/FRA/ORD-

11. SUPPLEMENTARY NOTES
*COTR: Dr. Thomas N. Tsai
**Consultant

12a. DISTRIBUTION/AVAILABILITY STATEMENT
This document is available to the public throuh the National Technical Information Service, Springfield, VA 22161

12b. DISTRIBUTION CODE
N/A

13. ABSTRACT *(Maximum 200 words)*

This report presents a summary of the field test results and correlations with computer simulation for a rail passenger car which has non-equalized trucks. The tests and OMNISIM simulation correlations included vehicle response to variations in vertical alignment, steady curving with spirals, dynamic curving, yaw and sway, twist and roll, pitch and bounce, and hunting with initial alignment defects. For each dynamic test, a description, correlation and conclusions are provided.

The purpose of the work is to validate the methodology previously developed for vehicle dynamic safety evaluations, which requires the application of simulation tools as well as testing of vehicles under different track scenarios. This report specifically addresses the evaluation of the tasks in the methodology related to measurement of vehicle and track parameters, test conduct, and correlation of the test results with computer simulation results.

14. SUBJECT TERMS
Passenger rail vehicles, non-equalized trucks, OMNISIM

15. NUMBER OF PAGES
152

16. PRICE CODE
N/A

17. SECURITY CLASSIFICATION OF REPORT	18. SECURITY CLASSIFICATION OF THIS PAGE	19. SECURITY CLASSIFICATION OF ABSTRACT	20. LIMITATION OF ABSTRACT
Unclassified	Unclassified	Unclassified	Unlimited

NSN 7540-01-280-5500

Standard Form 298 (Rev. 2-89)
Prescribed by ANSI Std. 239-18

PREFACE

This report presents a summary of the testing and correlation with computer simulation results for a rail passenger car which has non-equalized trucks. The testing was performed at the Transportation Technology Center (TTC), Pueblo, CO. All testing was done from June to August 1997. The vehicle response to variations in vertical alignment tests and the dynamic curving tests were conducted from July 28-29 on the Wheel Rail Mechanisms (WRM) loop. The hunting test with initial alignment defects was conducted on July 24 on the Railroad Test Track (RTT). The steady curving with spirals tests were conducted in the months of June and July on the RTT. Testing on the Precision Test Track (PTT) was done on August 1. The PTT is used for the yaw and sway, twist and roll, and pitch and bounce tests.

The work reported here has been performed under the contract DTFR53-95-C-00049 from the Federal Railroad Administration (FRA). Dr. Thomas Tsai of the FRA is the Technical Monitor. The authors wish to thank Dr. Fred Blader and Mr. John Elkins for their valuable technical inputs throughout the program. The technical input from Dr. Herbert Weinstock of the Volpe Center is gratefully acknowledged. The support of Dr. Andrew Kish of the Volpe Center in the development of the OMNISIM code is also acknowledged.

The authors wish to thank Mr. Steve Belport of TTC for the conduct of the tests. Thanks are also due to Messrs. Ken Laine and David Cackovic of TTC for their test support.

METRIC/ENGLISH CONVERSION FACTORS

ENGLISH TO METRIC		METRIC TO ENGLISH	
LENGTH (APPROXIMATE)		**LENGTH (APPROXIMATE)**	
1 inch (in)	= 2.5 centimeters (cm)	1 millimeter (mm)	0.04 inch (in)
1 foot (ft)	= 30 centimeters (cm)	1 centimeter (cm)	0.4 inch (in)
1 yard (yd)	= 0.9 meter (m)	1 meter (m)	3.3 feet (ft)
1 mile (mi)	= 1.6 kilometers (km)	1 meter (m)	1.1 yards (yd)
		1 kilometer (k)	0.6 mile (mi)
AREA (APPROXIMATE)		**AREA (APPROXIMATE)**	
1 square inch (sq in, in^2)	= 6.5 square centimeters (cm^2)	1 square centimeter (cm^2)	0.16 square inch (sq in, in^2)
1 square foot (sq ft, ft^2)	= 0.09 square meter (m^2)	1 square meter (m^2)	1.2 square yards (sq yd, yd^2)
1 square yard (sq yd, yd^2)	= 0.8 square meter (m^2)	1 square kilometer (km^2)	0.4 square mile (sq mi, mi^2)
1 square mile (sq mi, mi^2)	= 2.6 square kilometers (km^2)	10,000 square meters (m^2)	1 hectare (he) = 2.5 acres
1 acre = 0.4 hectare (he)	= 4,000 square meters (m^2)		
MASS - WEIGHT (APPROXIMATE)		**MASS - WEIGHT (APPROXIMATE)**	
1 ounce (oz)	= 28 grams (gm)	1 gram (gm)	0.036 ounce (oz)
1 pound (lb)	= 0.45 kilogram (kg)	1 kilogram (kg)	2.2 pounds (lb)
1 short ton = 2,000 pounds (lb)	= 0.9 tonne (t)	1 tonne (t) = 1,000 kilograms (kg)	1.1 short tons
VOLUME (APPROXIMATE)		**VOLUME (APPROXIMATE)**	
1 teaspoon (tsp)	= 5 milliliters (ml)	1 milliliter (ml)	0.03 fluid ounce (fl oz)
1 tablespoon (tbsp)	= 15 milliliters (ml)	1 liter (l)	2.1 pints (pt)
1 fluid ounce (fl oz)	= 30 milliliters (ml)	1 liter (l)	1.06 quarts (qt)
1 cup (c)	= 0.24 liter (l)	1 liter (l)	0.26 gallon (gal)
1 pint (pt)	= 0.47 liter (l)		
1 quart (qt)	= 0.96 liter (l)		
1 gallon (gal)	= 3.8 liters (l)		
1 cubic foot (cu ft, ft^3)	= 0.03 cubic meter (m^3)	1 cubic meter (m^3)	36 cubic feet (cu ft, ft^3)
1 cubic yard (cu yd, yd^3)	= 0.76 cubic meter (m^3)	1 cubic meter (m^3)	1.3 cubic yards (cu yd, yd^3)
TEMPERATURE (EXACT)		**TEMPERATURE (EXACT)**	
[(x-32)(5/9)] °F	= y °C	[(9/5) y + 32] °C	x °F

QUICK INCH - CENTIMETER LENGTH CONVERSION

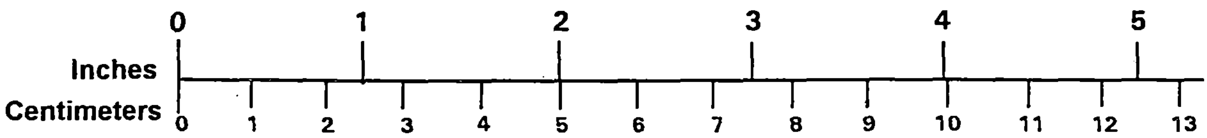

QUICK FAHRENHEIT - CELSIUS TEMPERATURE CONVERSION

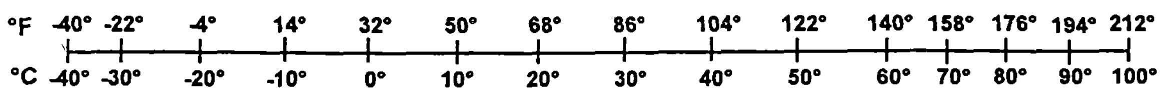

For more exact and or other conversion factors, see NBS Miscellaneous Publication 286, Units of Weights and Measures. Price $2.50 SD Catalog No. C13 10286

Updated 1/23/95

CONTENTS

ILLUSTRATIONS

Figure **Page**

Figure		Page

Figure **Page**

Figure **Page**

1. INTRODUCTION

The 1994 amendment of the Federal Railroad Safety Act requires that the FRA establish regulations for minimum safety standards of conventional railroad passenger vehicles. Passenger rail vehicles have to operate on a variety of track geometries: tangent, curved and spirals connecting tangents to constant radius curves. The maximum levels of vertical and lateral misalignment and the maximum amount of crosslevel variation that can be safely negotiated are important in safety evaluations. Derailments occur for a variety of reasons, including track failures, equipment failures, and improper train operation. A number of scenarios need to be identified for investigation including vehicle transient response to vertical and lateral perturbations in the track alignment, steady-state curving, dynamic curving, and truck hunting. As a part of this mission, FRA initiated the development of a methodology for vehicle dynamic safety evaluations. The methodology is described in Refs. (1,2), and requires the application of simulation tools as well as testing of vehicles under different track scenarios.

Figure 1-1 indicates the overall methodology being pursued for vehicle safety evaluation. Tasks 1 to 4 in this figure represent determination of car and track parameters, which are inputs, to the analysis. Task 5 focuses on wheel climb/wheel lift failure modes for application in the methodology. In Task 6, OMNISIM has been chosen as a candidate tool for safety evaluations. Using this tool, vehicle dynamic response and safety have been studied for several scenarios such as:

- Hunting.
- Steady curving.
- Dynamic curving.
- Gage narrowing.
- Response to individual and combined lateral and vertical track perturbations.

This report specifically addresses the evaluation of the tasks in the methodology related to measurement of vehicle and track parameters, test conduct, and correlation of the test results with computer simulation results. These are critical tasks in the overall safety methodology and require direct evaluation. In this evaluation a car with non-equalized trucks is considered while in a subsequent evaluation a car with equalized trucks will be considered.

The report is organized as follows. Section 2 presents a brief description of the simulation program, OMNISIM. Section 3 gives a description of the car used in all the tests. Section 4 presents the stationary testing which includes track stiffness, static suspension system characterization, rigid body modal characterization, and track and wheel profile measurements.

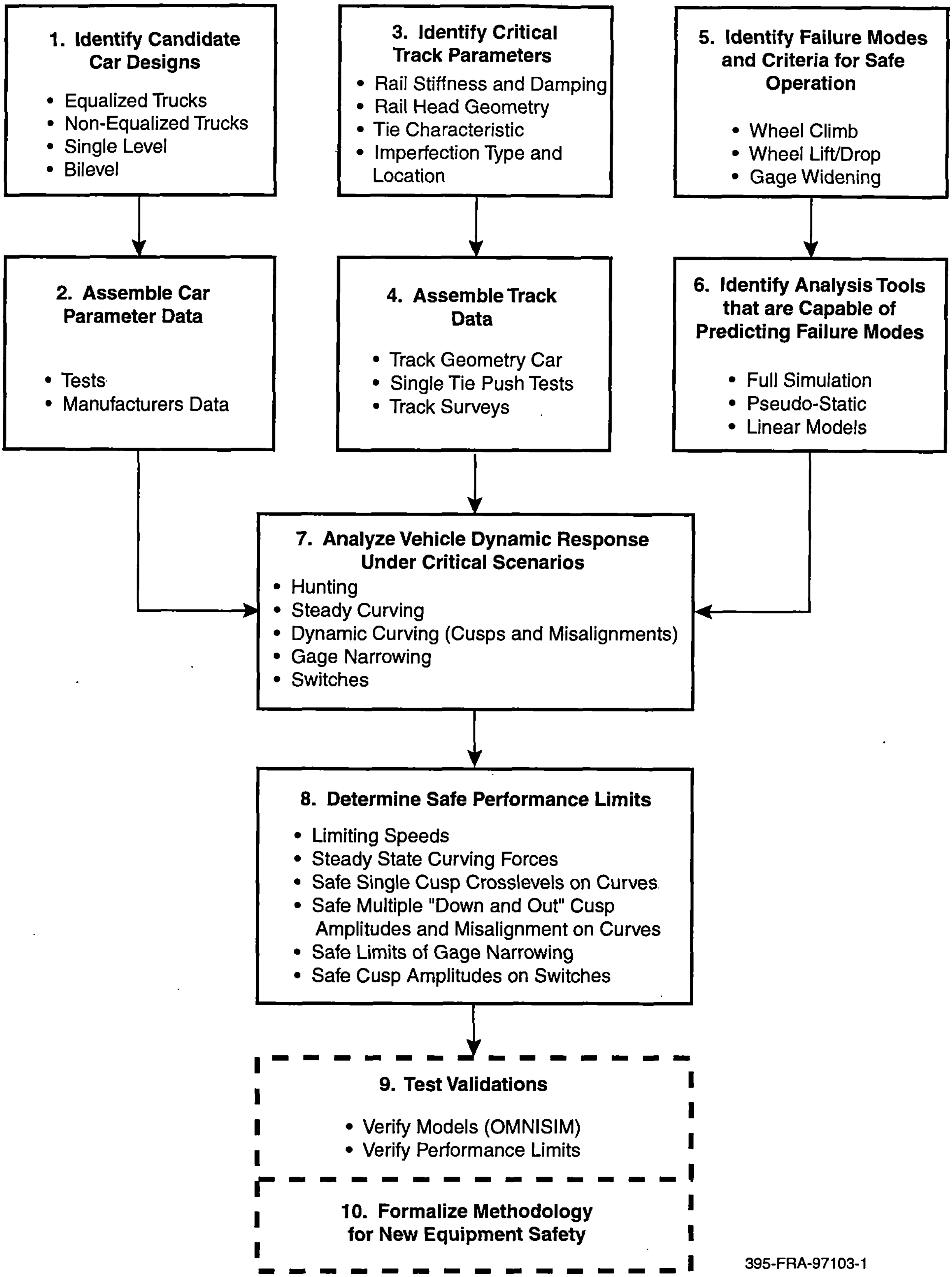

Figure 1-1. Overall methodology

Section 5 presents the dynamic testing and includes correlations with simulation results. For each dynamic test, description, correlation and conclusions are provided. The simulation results are compared with the test data, and overall conclusions of practical interest derived from the study are presented in Section 6.

1.1 Objectives

The overall objective of the testing is to validate the proposed rail vehicle safety evaluation methodology through testing two different types of vehicles and trucks under several track scenarios. The specific objectives followed in this work are:

1. Evaluate by full-scale tests the dynamic performance of a bi-level vehicle with non-equalized trucks for track scenarios including vertical track perturbations, steady curving, dynamic curving, and perturbations generating: yaw and sway, twist and roll, pitch and bounce, and hunting. Identify unsafe behavior of the car, such as wheel climb and wheel lift.

2. Characterize the parameters of vehicles and the track segments required for the OMNISIM simulation code to predict the observed response.

3. Compare the OMNISIM simulation results with the test data on lateral and vertical loads and on lateral and vertical accelerations. Evaluate the OMNISIM code capability to predict the unsafe vehicle behavior observed in the test.

4. Identify the inadequacies, if any, in the overall safety methodology and the limitations of the code and test techniques.

2. SIMULATION TOOL - OMNISIM

OMNISIM (3) has been used for the evaluation of the dynamic performance of commuter passenger vehicles. OMNISIM is a multi-body system simulation program, modeling both vehicle and supporting structures in a generalized manner. Each system modeled is represented as a group of bodies, each having its own inertial properties and position in space. These bodies are connected by appropriate interconnections, which may be defined as having special properties, such as suspensions or the rolling connection between the wheel and rail, or being very stiff such as metal-to-metal contact. The program can predict the behavior of the bodies in transient and steady-state response in the time domain. OMNISIM also permits the bodies to be represented as having simple flexible properties. This is useful, for example, to simplify the representation of the torsional rigidity of a vehicle body when negotiating track crosslevel gradients.

OMNISIM can work with English or metric units and with measured or analytically constructed inputs or a combination of both. It presents a unified approach to predicting rail vehicle response to a variety of inputs, such as those from the track, actuator or wind forces. Vehicle ride quality may also be assessed. The flexible structure of the input allows the user to model any new or existing vehicle design. In addition to the main run processor, pre- and post-processing programs have also been created. Each system is defined in a text file called the definition file, using an appropriate word processor. This file is then preprocessed to the required format and units by the preprocessing program DEFINE. This program rearranges the data and the system units and permits the user to see the system in diagrammatic form, displaying its geometry and characteristics. DEFINE will also display previously pre-processed files.

Means are provided in the definition file to identify the degrees of freedom for each body required in the model. The potential choices include all translational and rotational rigid body motions and the first beamlike free-free flexible modes in twist and in vertical and lateral bending. The interaction of rigid or flexible bodies is defined through hard or soft connections (e.g., metal to metal or suspension elements). The program requires the user to define a vehicle and track system model with inertial and geometric properties, connection characteristics, wheel/rail geometry data, and displacement or force inputs.

There are a number of different types of track and vehicle interbody connections available. Their characteristics range from simple spring and damper pairs in parallel or in series to more complex friction elements. The characteristic of each spring and damper is defined using piecewise linear functions of displacement and velocity, respectively. Hysteresis requires two piecewise linear functions that represent the asymptotic loading and unloading curves. Additional information, such as that which controls the speed of closure to the asymptote in hysteresis, may also be specified.

The present wheel/rail connection assumes no roll rotation of the rail, with the vehicle and track system in the same moving coordinates. This is equivalent to a track model that generates the same behavior at the wheel as the vehicle moves down the track. Although useful in identifying rail motions, further improvements are contemplated. These will allow the rails to be modeled as a stationary continuum with a potential reduction in the number of degrees of freedom, and will release the rail support model from moving with the vehicle.

Each individual wheel/rail connection uses a look-up table representing the required variables at the point of contact between the wheel and rail so that the rolling contact forces may be calculated for the steel wheels on steel rails. The profile data tables are precomputed using a more flexible version of Law and Cooperrider's program WHRAILA (4), named PROFIT, for PROfile FIT. A four-dimensional look-up table of creep force coefficients, according to Kalker (5) and as adapted by British Rail, is used in determining the forces and moments on each wheel. The rotational speed of the wheel or axle, which may be a solid or have independently rotating wheels, is regarded as a special variable and is required to obtain the wheel/rail forces. The method assumes that the dominant changes in the wheel/rail contact geometry are those due to local relative displacement between each wheel and the rail to which it is connected.

The inputs to the system under study may be measured or analytically constructed in segments using several optional functions. Those representative of laboratory simulation, generally as a function of time, can be formed in the input text file that is read directly by the stepping processor at commencement. A swept frequency sine wave allows vibration testing of a stationary vehicle. However, at the option of the user, the input file may request some or all of the data from a file of either measured or analytically defined histories, formed using the preprocessor called INFORM. This may be filtered and is formatted as digital information in steps along a chosen path or track. If measured data is to be used, it is called into INFORM, from a measured track geometry file. INFORM uses a text setup file to identify the source and preprocess the path and input data that may be of mixed measured and analytic origins.

The short wavelength inputs are regarded as local perturbations, and are introduced as variations in lateral or vertical position of the rails or guideway. For the analytically defined inputs, a repeated shape and amplitude for a segment of the rail may be chosen from a combination of cusps, bends, or sine waves. The long wavelength variations define the overall path and are linearly interpolated from positions along the track at which curvature and superelevation are either chosen analytically or taken from the measured data set. These are transformed into components of the connection strokes, so that the degrees of freedom for each body remain those relative to its local inertial coordinate system. Provision is made to allow both external displacement and forcing inputs to the model. Rail perturbations are an example of displacement inputs; whereas coupler loads due to train action is an example of a forcing input.

For post-processing, PLOTS produces graphs of the output for monitor display or for hardcopy output. TEXTS produces numerical information for viewing or passing to other post-processors, such as a spreadsheet, for further manipulation. Much of the work in this report was postprocessed using a spreadsheet program.

3. VEHICLE AND MODEL DESCRIPTION

3.1 The Test Vehicle

The vehicle used for testing is a modern bi-level passenger car with non-equalized trucks. It has an axle load of 34 kips. It uses an H truck frame and bolster with outside journal bearings. A schematic of a generic non-equalized truck is shown in Figure 3-1. The frame is welded steel and consists of two box sections for the side beams and two circular sections for the lateral beams. The truck bolster is a welded box structure that is also used as an auxiliary air supply for the air springs. A center pivot provides the interface between the frame and truck bolster with a nylon bushing.

A radius arm between the truck frame and the journal bearing provides wheelset guidance. The primary suspension is a set of steel coil springs supported on the journal bearing through a rubber pad.

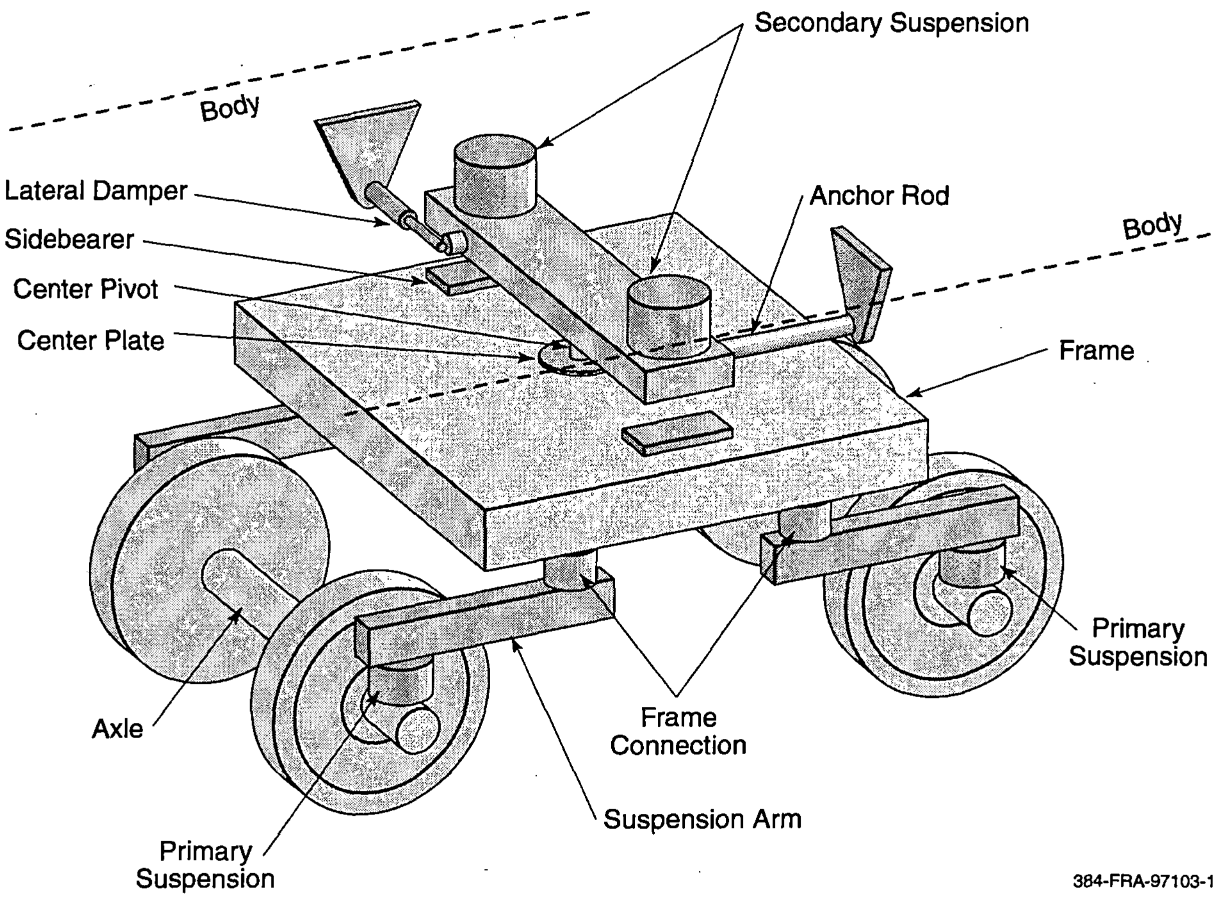

Figure 3-1. Schematic of non-equalized truck

The vehicle uses an air bag secondary suspension. An air spring with a back-up rubber spring is used as an emergency if air is lost. There are stops to limit both vertical and lateral movement. The lateral stops are on the truck bolster and the vertical stops are between the carbody and truck bolsters. Rotary dampers provide damping in the lateral and vertical directions and are connected between the truck bolster and carbody.

3.2 The Vehicle Model

The vehicle is represented by a multi-body model consisting of springs, dampers and masses that represent the carbody, primary and secondary suspensions, trucks, axles, and wheels. The track structure is also represented with springs, dampers and masses. These parameters are identified on the basis of manufacturer's data or measured by testing as explained in Section 4. A list of input parameters required for the computer simulation program is shown in Table 3-1.

The carbody is represented with lateral, vertical, pitch, yaw, roll, torsional and bending degrees of freedom (DOF). The suspension between the carbody is represented with longitudinal, lateral, and vertical DOF's. The truck is represented with longitudinal, lateral, vertical, pitch, yaw and roll DOF's. The primary suspension between the truck and axle is represented with longitudinal, lateral, and vertical DOF's. Each wheelset has longitudinal, vertical, lateral, pitch and roll DOF's. The wheel-rail contact model uses the Kalker formulation as described in Ref. (5). The model parameters are summarized in Table 3-2.

Table 3-1. ***Required parameters***

I. Vehicle Parameters -			
Body	**Weight**		
Car Body			
Bogie Frame			
Axle			
Suspension/Connection Parameters -			
Suspension	**Degree of Freedom**	**Stiffness**	**Damping**
Primary Suspension	Lateral		
(Axle to Bogie)	Vertical		
	Yaw		
Secondary Suspension	Lateral		
(Bogie to Car)	Vertical		
	Yaw		
Wheel Profile/Type of Wheel			
II. Track Parameters -			
Parameter	**Required Value**		
Rail Size	AREA Designation		
Tie Mass	Mass		
Tie Spacing (Δ)			
Tie Peak Resistance (F_P)			
Tie Deflection at Peak Resistance (w_P)			
Tie to Ballast Friction Coefficient (μ_f)			
Track Foundation Modulus (k_v)			
Track Curvature			
Spiral Length			
Track Superelevation			
II. Track Connections -			
Connection	**Degree of Freedom**	**Stiffness**	**Damping**
Rail to Tie	Lateral		
	Vertical		
Tie to Ballast	Lateral		
	Vertical		
Rail Module to Module	Lateral Shear		N/A
	Lateral Bending		N/A
	Vertical Shear		N/A
	Vertical Bending		N/A

Table 3-2. Car physical characteristics

Unit	Parameter Description	Value
lb-s^2/in.	Carbody mass	257.91
lb-s^2/in.	Truck bolster mass	5.24
lb-s^2/in.	Truck frame mass	15.86
lb-s^2/in.	Wheelset mass	11.33
in.	Truck wheelbase	102
in.	Truck center spacing	714
in.	Wheel radius	18
in.	Carbody center of gravity from top of rail	99.00
in.	Bolster center of gravity from top of rail	30.21
in.	Truck frame center of gravity from top of rail	23.40
in.	Wheelset center of gravity from top of rail	18.00
in.	Transverse secondary spring spacing	79.02
in.	Transverse secondary damper spacing	107.01
in.	Transverse bolster anchor rod spacing	107.01
in.	Transverse wear plate spacing	45.67
in.	Transverse primary spring spacing	79.02
in.	Center of air spring height from top of rail	40.04
in.	Center of lateral damper height from top of rail	33.10
in.	Center of bolster anchor rod height from top of rail	20.95
lb-s^2-in.	Carbody roll moment of inertia	9.89E+05
lb-s^2-in.	Carbody pitch moment of inertia	2.70E+07
lb-s^2-in.	Carbody yaw moment of inertia	2.70E+07
lb-s^2-in.	Truck bolster roll moment of inertia	5.98E+03
lb-s^2-in.	Truck bolster pitch moment of inertia	2.21E+02
lb-s^2-in.	Truck bolster yaw moment of inertia	5.78E+03
lb-s^2-in.	Truck frame roll moment of inertia	1.31E+04
lb-s^2-in.	Truck frame pitch moment of inertia	1.56E+04
lb-s^2-in.	Truck frame yaw moment of inertia	2.83E+04
lb-s^2-in.	Wheelset roll moment of inertia	8.03E+03
lb-s^2-in.	Wheelset pitch moment of inertia	1.49E+03
lb-s^2-in.	Wheelset yaw moment of inertia	8.03E+03
lb/in.	Primary longitudinal stiffness (per wheel)	4.27E+04
lb/in.	Primary lateral stiffness (per wheel)	4.20E+04
lb/in.	Primary vertical stiffness (per wheel)	2.00E+05
lb/in.	Secondary suspension lateral stiffness (per spingset)	3.00E+03
lb/in.	Secondary suspension vertical stiffness (per spingset)	1.88E+04
lb-s/in.	Secondary lateral damping (per truck)	5.60E+02

4. PARAMETER CHARACTERIZATION

To validate the software, input data describing the car and track characteristics are required in the simulation runs. The data collected included:

- Track lateral and vertical stiffness.
- Vehicle static suspension characterization.
- Vehicle rigid body modal characterization.
- Track and wheel profile measurements.

4.1 Track Lateral and Vertical Stiffness

The lateral resistance of the track was measured using the Single Tie Push Test (STPT) fixture. This device can be used to measure the lateral resistance of both wood and concrete tie track. The measurements were made on the test tracks in various locations. The vertical track stiffness was also measured at various locations along the test track. The lateral and vertical stiffnesses are used in the OMNISIM vehicle/track model.

4.2 Static Suspension System Characterization

The purpose of the static characterization is to measure the load-displacement characteristics for the primary and secondary suspensions. Load measuring instrumented rails combined with displacement transducers were used to obtain stiffness data (force-vs.-displacement) for each suspension element. The method typically used to measure the vertical suspension characteristics is shown in Figure 4-1, where the carbody is unloaded and deflections are measured on the primary and secondary suspension elements. Unloading of the wheels was achieved using pneumatic floor jacks and overhead cranes. The physical characteristics are as shown in Table 3-2.

4.3 Rigid Body Modal Characteristics

The modal characterization tests were conducted to obtain rigid body modal frequencies and damping for each dynamic vehicle mode. These values are used in the OMNISIM vehicle model. The primary dynamic modes of vibration tested are shown in Figure 4-2. By exciting the carbody at selected locations, these vibration modes were generated and the frequency response was measured. The result is the frequency of the acceleration response. The damping coefficients are evaluated by measuring the hysteresis of force-vs.-displacement plots for each suspension element. The measured values of frequency for the rigid body modes are summarized in Table 4-1.

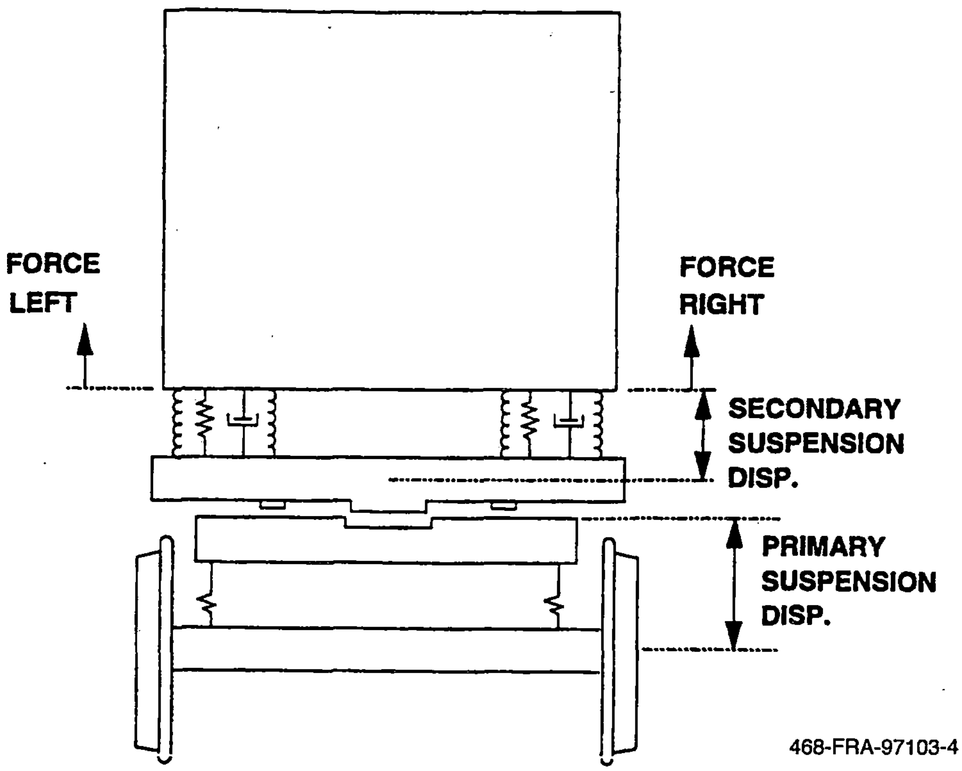

Figure 4-1. Vertical suspension characterization test setup

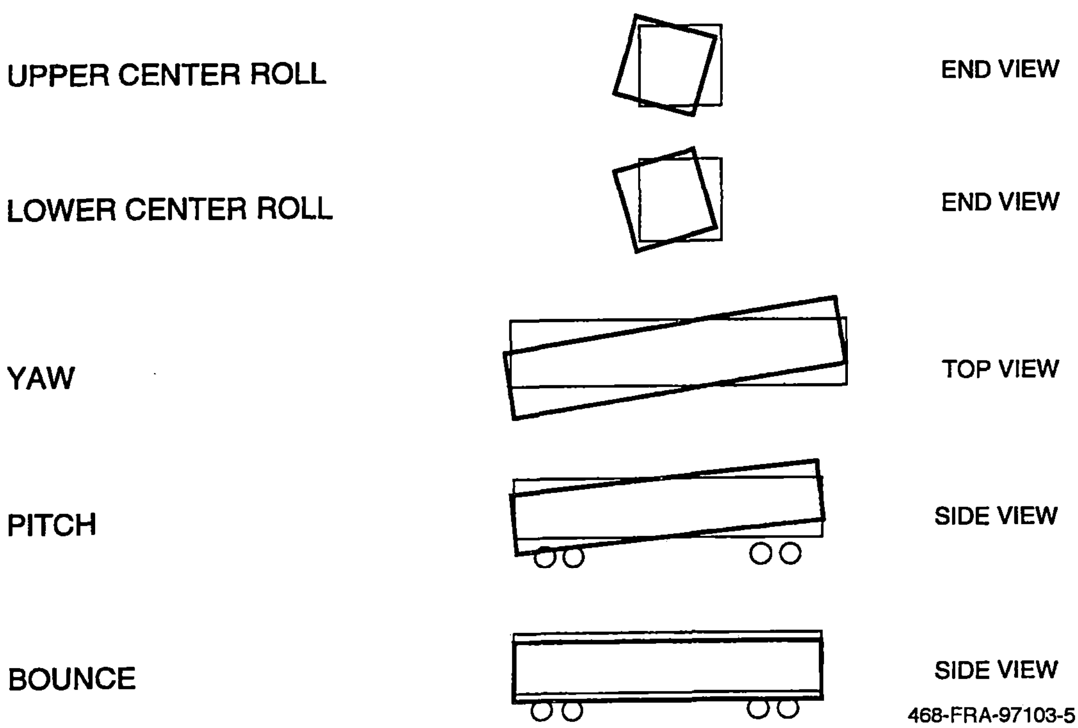

Figure 4-2. Rigid body modes

Table 4-1. Rigid body modal characterization

Mode	Frequency (Hz)
Bounce	1.17
Lower Center Roll	0.40
Upper Center Roll	1.25
Pitch	1.17
Yaw	1.08

4.4 Track and Wheel Profile Measurements

To accurately predict dynamic vehicle behavior, representative wheel and rail profile shapes were recorded using a portable profilometer.

The wheel profilometer magnetically attaches to the wheel while a digitization probe rolls over the wheel surface. Data was obtained using a notebook PC for graphical display and data processing for modeling requirements. Wheel profile processing also included measurements of wheel diameter. Rail profile measurements were obtained using similar instrumentation. Each rail was measured with reference to the opposite rail for measurements of relative cant and gage. The wheel/rail profile (rolling radius difference vs. wheelset lateral) is shown in Figure 4-3. A rail tribometer was also used to measure the rail coefficient of friction.

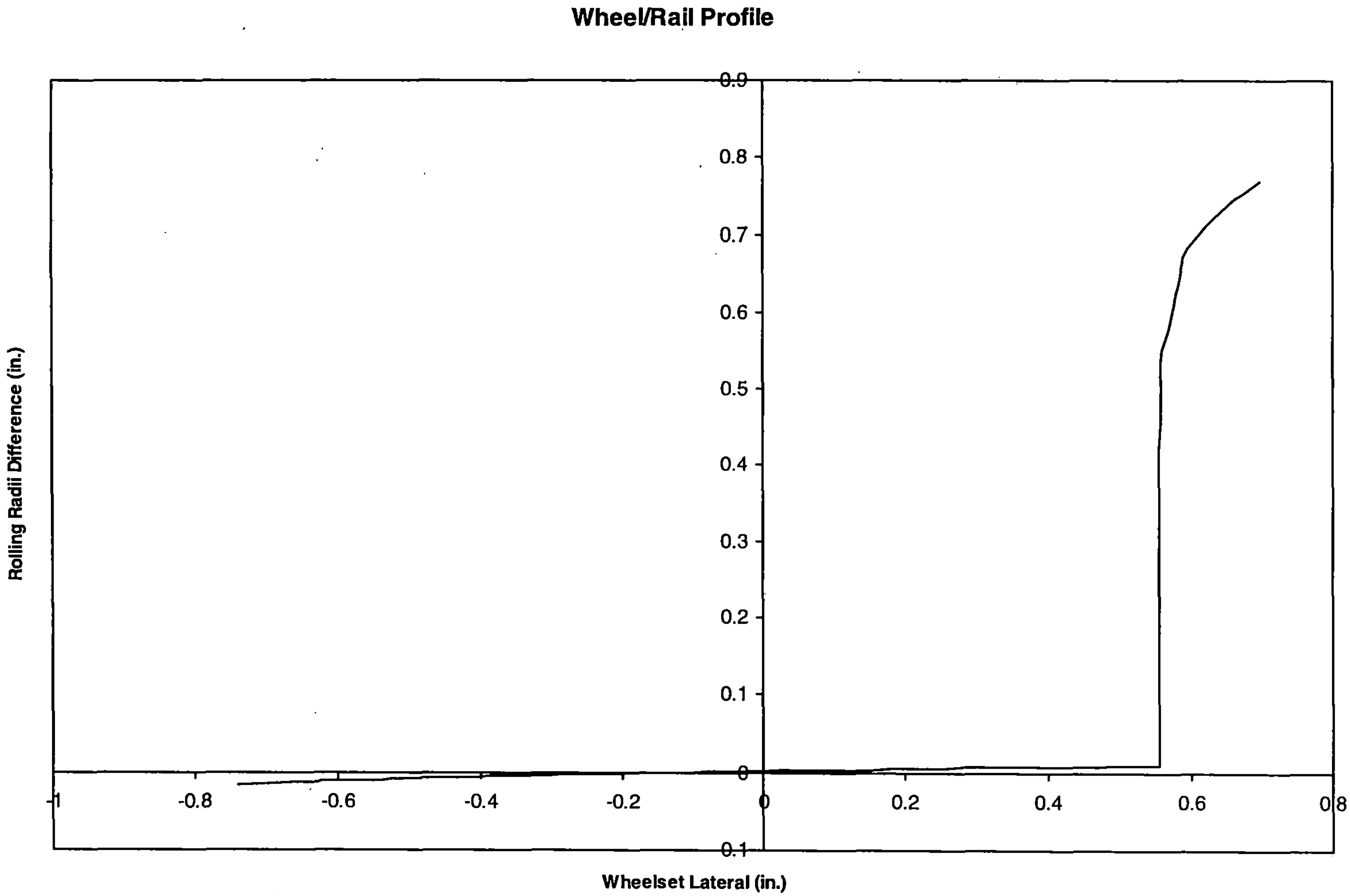

Figure 4-3. Wheel/rail profile

5. DYNAMIC TESTING – COMPARISON OF TESTS TO SIMULATIONS

The dynamic tests discussed in the following sections were performed on various test tracks located at TTC. The track configurations are shown in Figure 5-1.

The car tested was the cab car in a three car consist. The car was tested in both pull and push modes. When the car was pulled the instrumented wheelset was trailing and conversely when the test car was pushed the instrumented wheelset was leading. Data including wheel vertical and lateral forces were measured on each of the two AAR instrumented wheelsets.

Simulations were run using the computer program OMNISIM on a Pentium PC. The track scenarios were modeled and the program was exercised to produce lateral and vertical forces. Time history plots were developed for the simulation and compared to time histories of the test

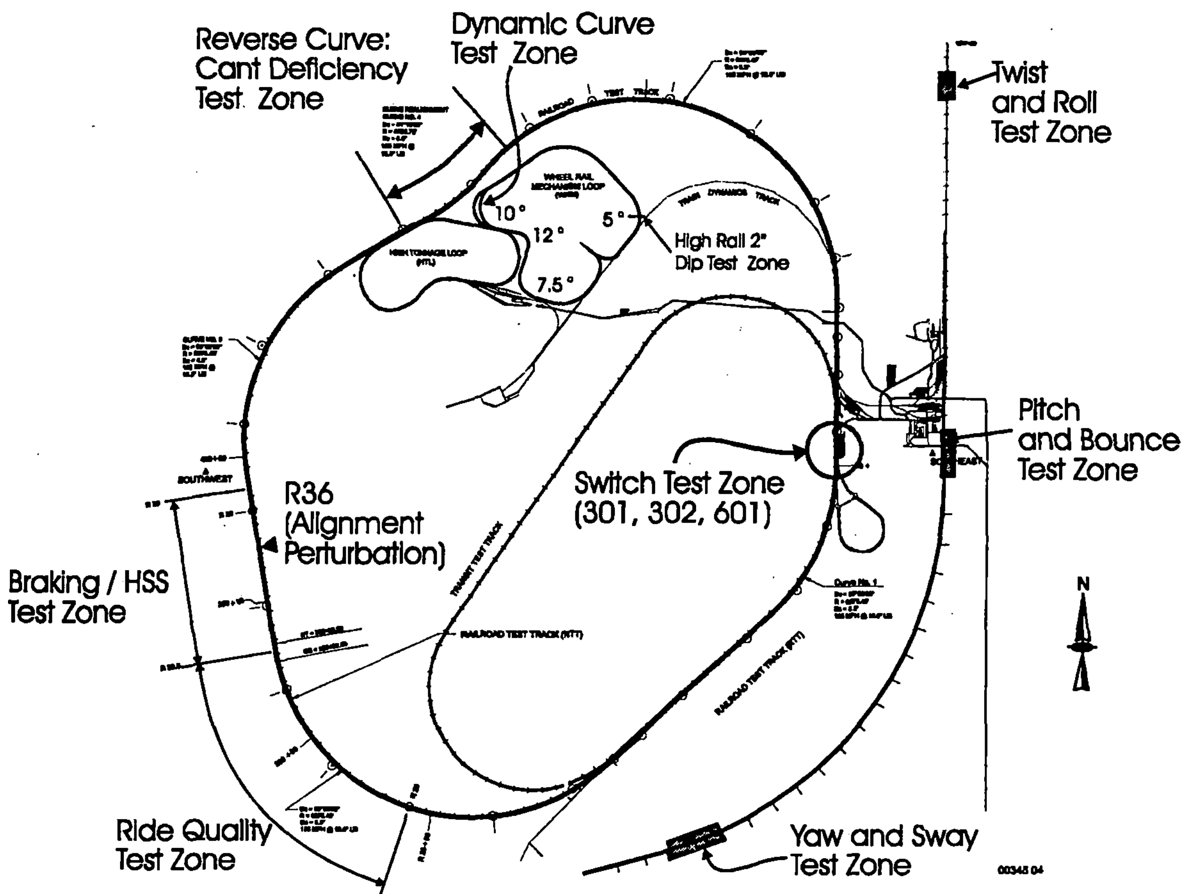

Figure 5-1. TTC test tracks

data. Comparisons were made for the maximum lateral force and the minimum vertical force. These were chosen because the maximum lateral force coupled with the minimum vertical force produce the largest L/V ratio. Also maximum carbody lateral acceleration is presented for the range of test speeds. The following sections give a description of each test, a comparison of the test data to the simulation results, and conclusions.

5.1 Vehicle Response to Variations in Vertical Alignment

Test Description

Test with variations in curved track vertical alignment were conducted to measure the test car's ability to operate in low speed curves at permissible speeds and to predict the potential of wheel lift. This test is also referred to as the vertical dip test. Test runs were performed on the 5 deg portion of the Wheel Rail Mechanisms (WRM) loop. The 5 deg curve has a 20 mph balance speed and has concrete ties on granite ballast. A vertical perturbation of 2 in. on the outer rail was installed on the track. Figure 5-2 shows the vertical dip that was installed in the 5 deg curve. The test was run for a range of speeds (5 to 22 mph) in forward and reverse directions. A video camera was also deployed on the carbody focussing on the primary suspension to capture its movement under potential wheel lift situations.

Correlation

Test data and simulation results for the wheel vertical and lateral forces resulting from the traverse of the vertical dip are displayed in Figures 5-3 and 5-4 for 20 mph operation and in Figures 5-5 and 5-6 for 15 mph. The simulation and the test data indicate a wheel lift condition occurring at 20 mph. At the point where wheel lift occurs, the simulation is discontinued. For both 15 and 20 mph cases, good agreement is found between the predicted and measured vertical forces at all four wheels of the instrumented truck.

At 20 mph, the outer wheel of the lead axle vertical force increases to a value of approximately 17 to 18 kips just prior to reducing to zero (wheel lift condition). At 15 mph, the outer wheel of the lead axle vertical force similarly increases to a value of approximately 17 kips, decreases to a minimum of approximately 7 kips and then increases again to approximately 24 kips with good correspondence between the test data and simulation.

The measured and predicted lateral forces have similar shapes and levels of magnitude, however, the correlations are not as good as found for the vertical force. For the 20 mph case, the lateral force on the lead axle prior to entering the dip is approximately 5.5 kips (simulation) and 7.5 kips (test) for the outer wheel and 6.75 kips (simulation) and 9 kips (test) for the inner wheel. The lateral forces for both the simulation and test data on the outer and inner wheel changes abruptly at the point of wheel lift. The trailing axle lateral forces test data are in the approximately ±2.0 kips range for the outer wheel and –0.5 to 4 kips range for the inner wheel. The simulation results have similar waveforms but at reduced levels with the outer wheel lateral forces varying from –0.75 to 0.25 kips and the inner wheel lateral force a maximum of 1.25 kips.

At 15 mph the lateral force test data have relatively good agreement with the simulation data for the initial lateral force values prior to entering the dip. The waveforms of the simulations are similar to the test data during passage through the dip, but have smaller amplitudes than the test data by 4 to 5 kips for the lead axle outer wheel, and 2 kips for the trailing axle outer wheel.

A plot of the minimum vertical force occurring during negotiation of the dip for a range of speeds is shown in Figure 5-7 for the outer wheel on the lead axle of the trailing truck. Good correlation is shown over the speed range for the vertical force and also the zero force value when wheel lift occurs.

Conclusion

The simulation shows very good correlation of the vertical force for negotiation of the vertical dip at all speeds; however, the correlation for the lateral force is not as good. The simulation tool predicts wheel lift at the correct speed and no wheel lift at the lower speeds, consistent with tests.

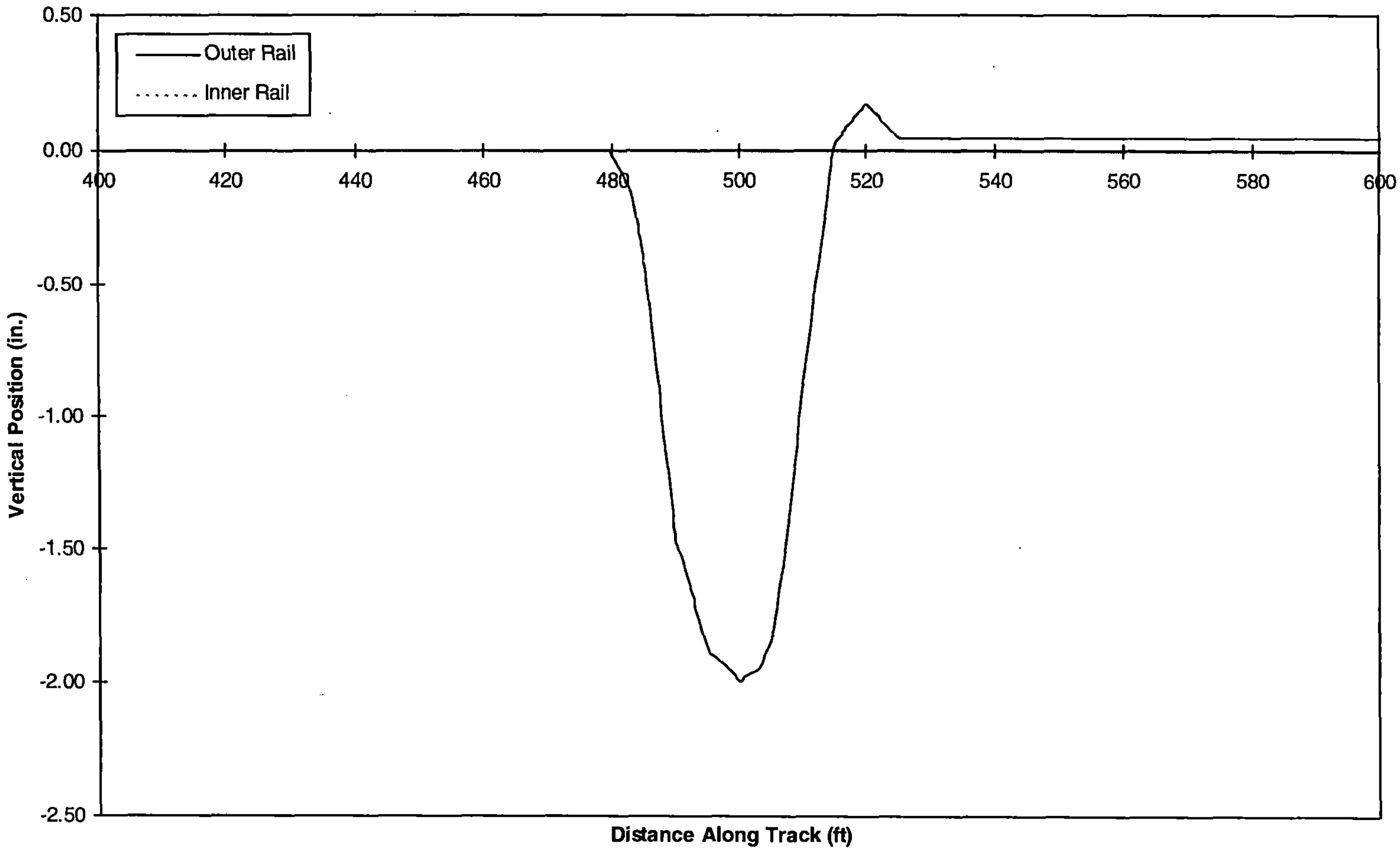

Figure 5-2. *Vertical dip in the 5 deg curve*

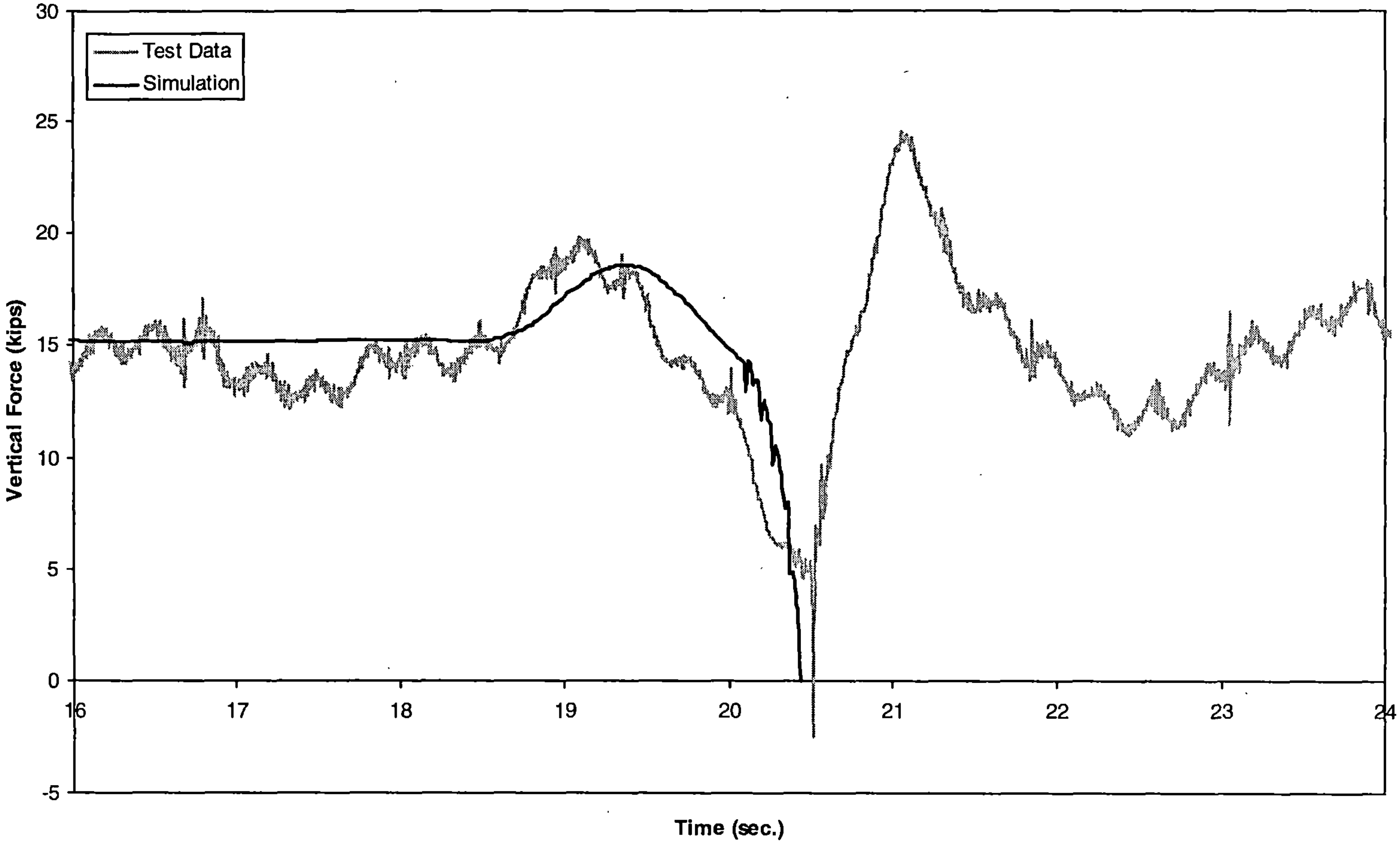

Figure 5-3(a). Vertical dip test – vertical force time history, 20 mph (lead outer wheel)

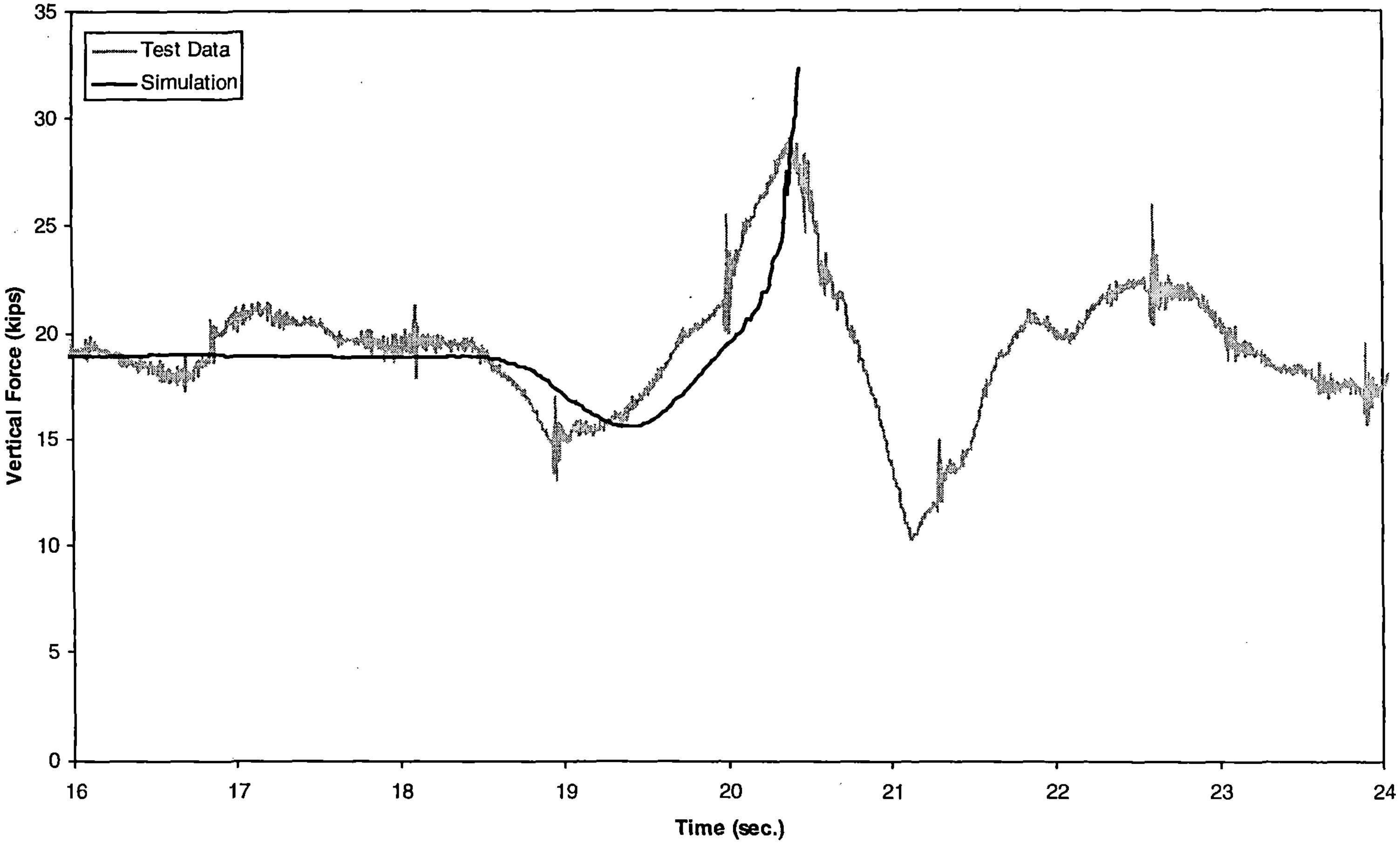

Figure 5-3(b). Vertical dip test – vertical force time history, 20 mph (lead inner wheel)

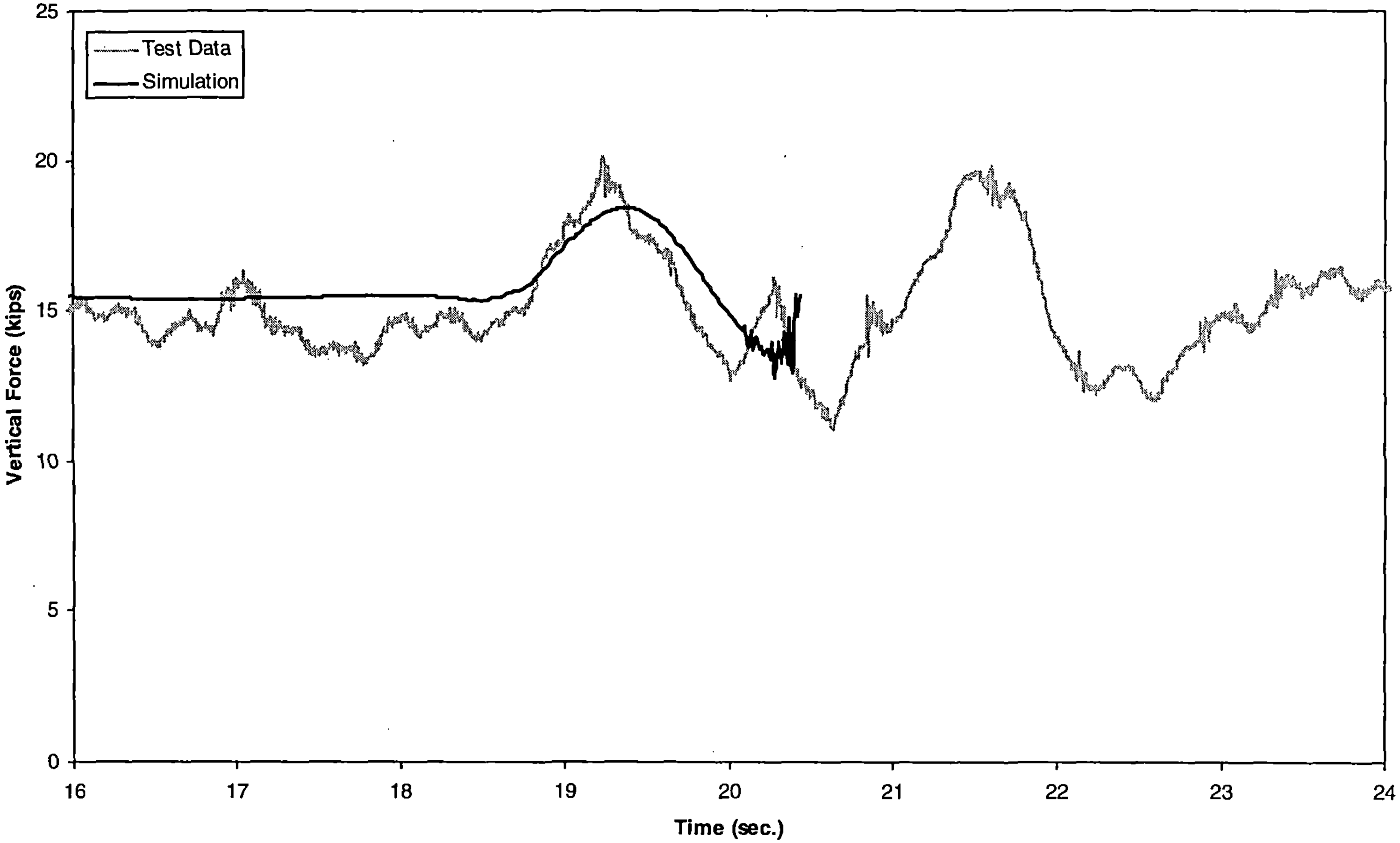

Figure 5-3(c). Vertical dip test – vertical force time history, 20 mph (trailing outer wheel)

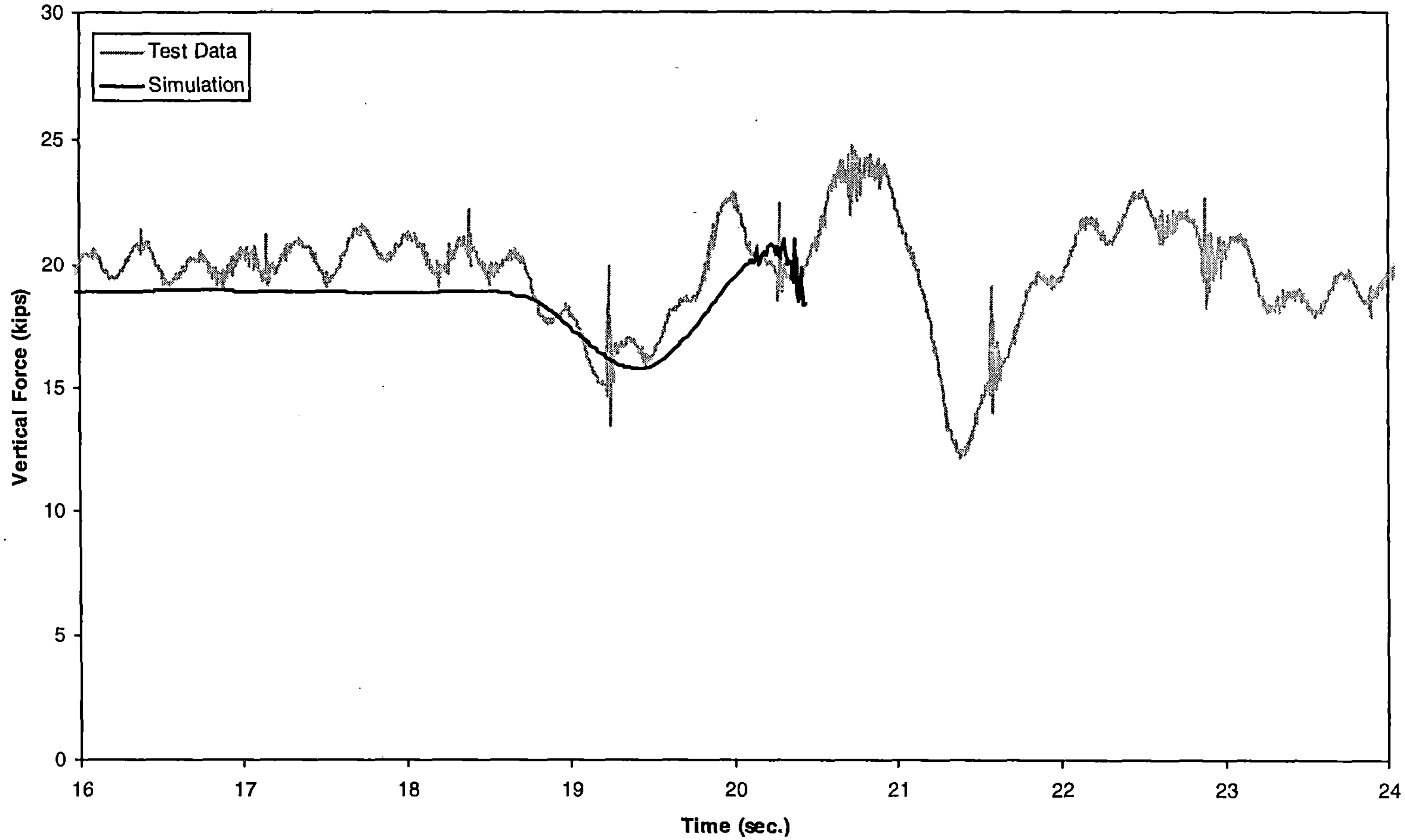

Figure 5-3(d). Vertical dip test – vertical force time history, 20 mph (trailing inner wheel)

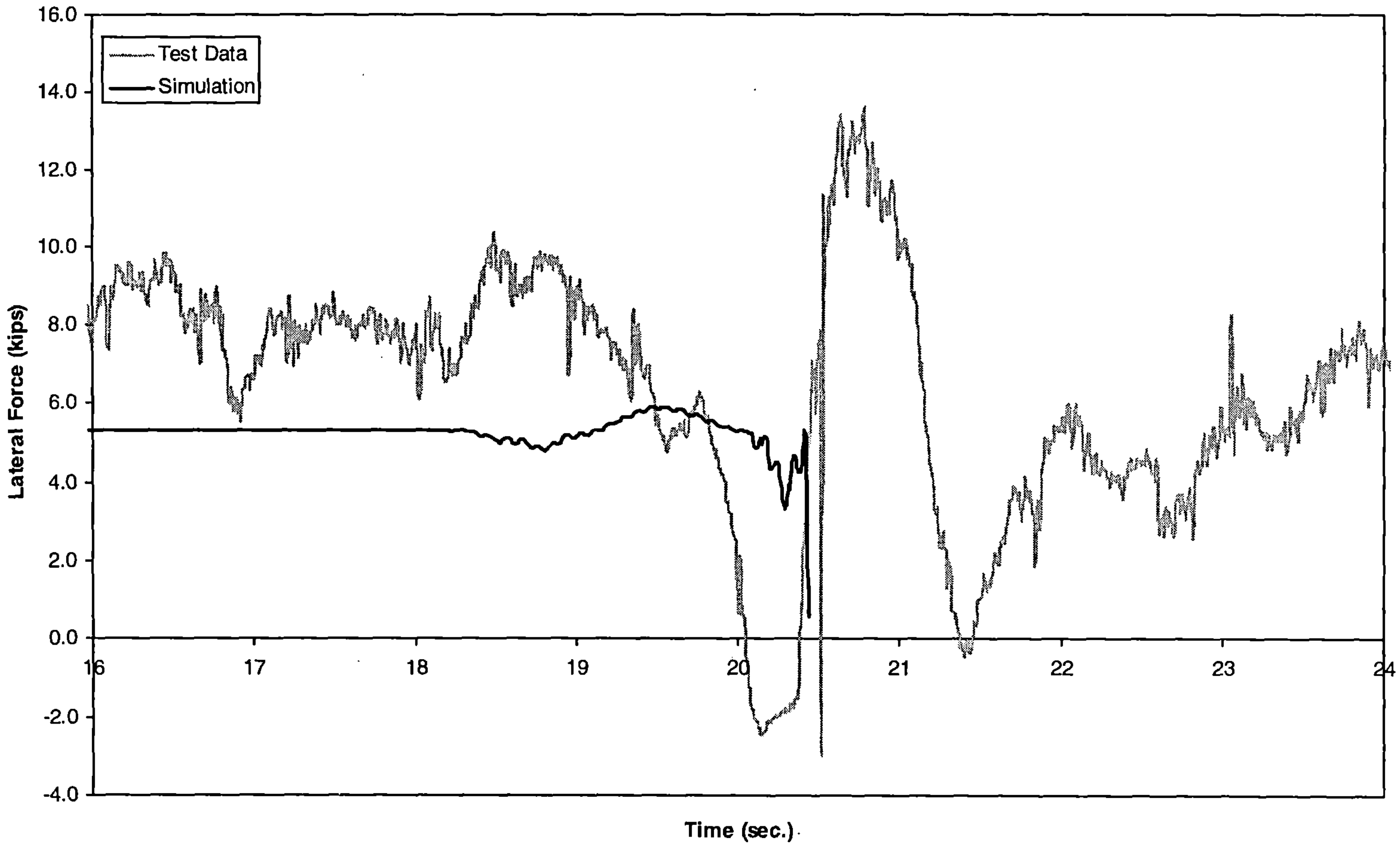

Figure 5-4(a). Vertical dip test – lateral force time history, 20 mph (lead outer wheel)

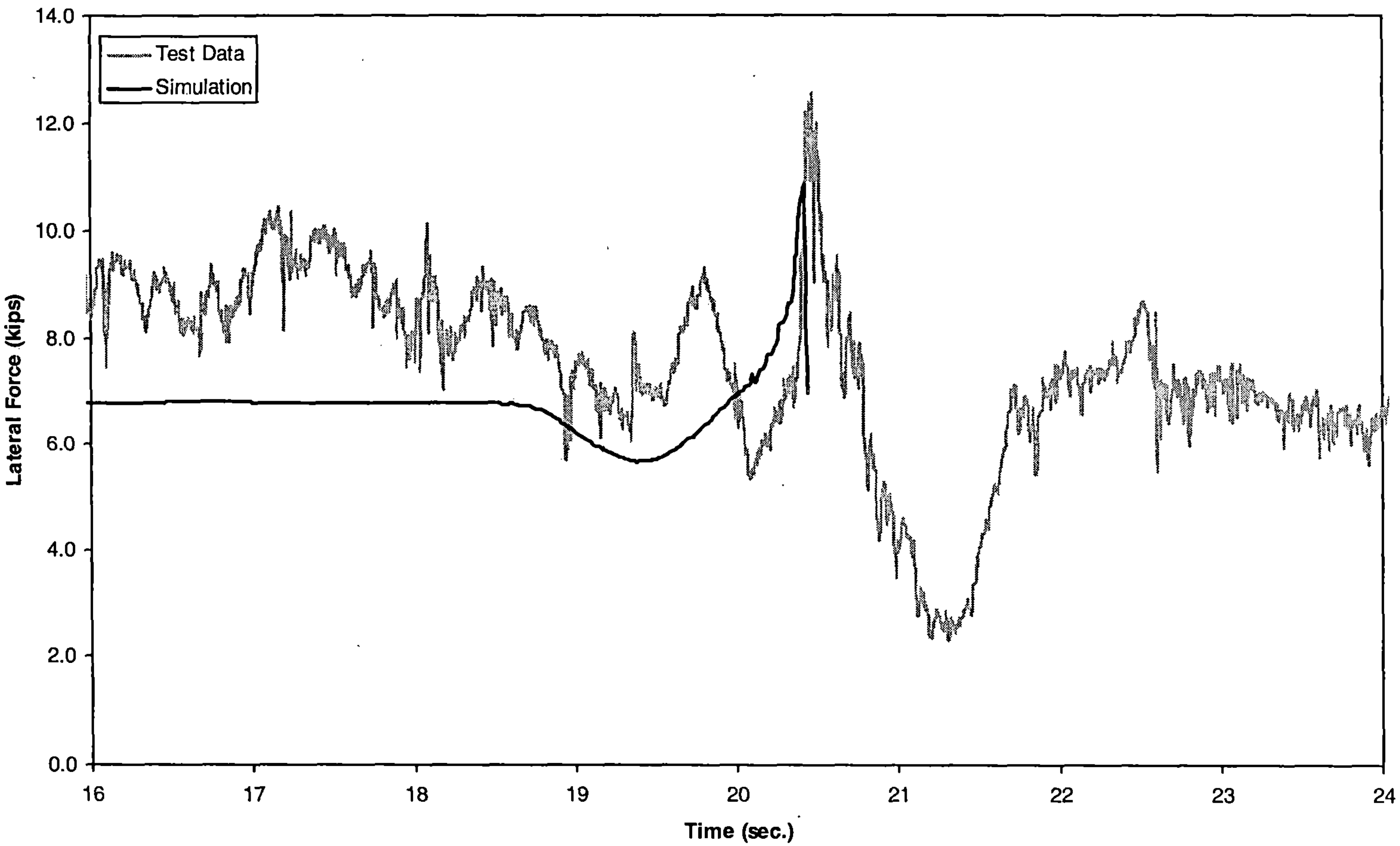

Figure 5-4(b). Vertical dip test – lateral force time history, 20 mph (lead inner wheel)

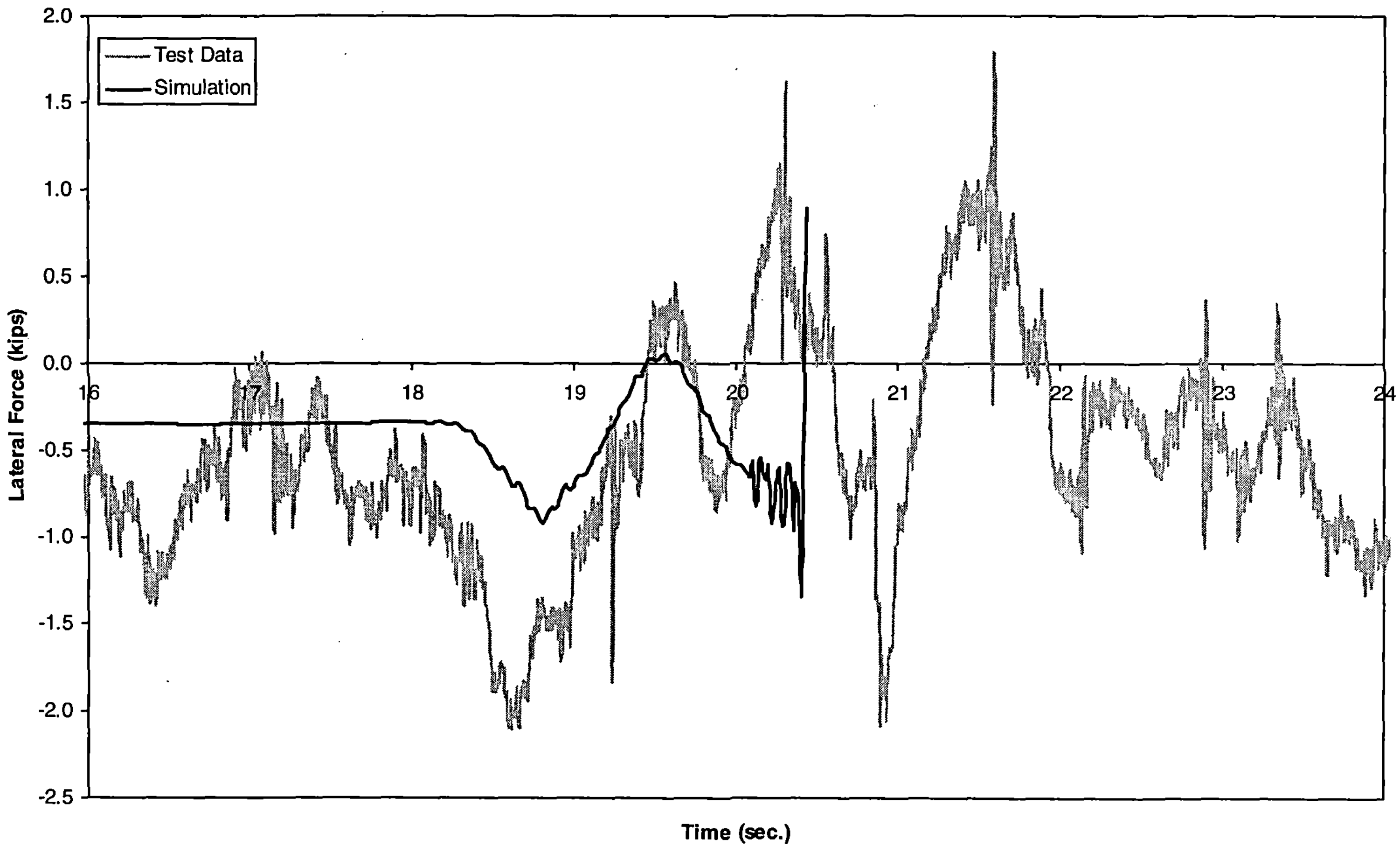

Figure 5-4(c). Vertical dip test – lateral force time history, 20 mph (trailing outer wheel)

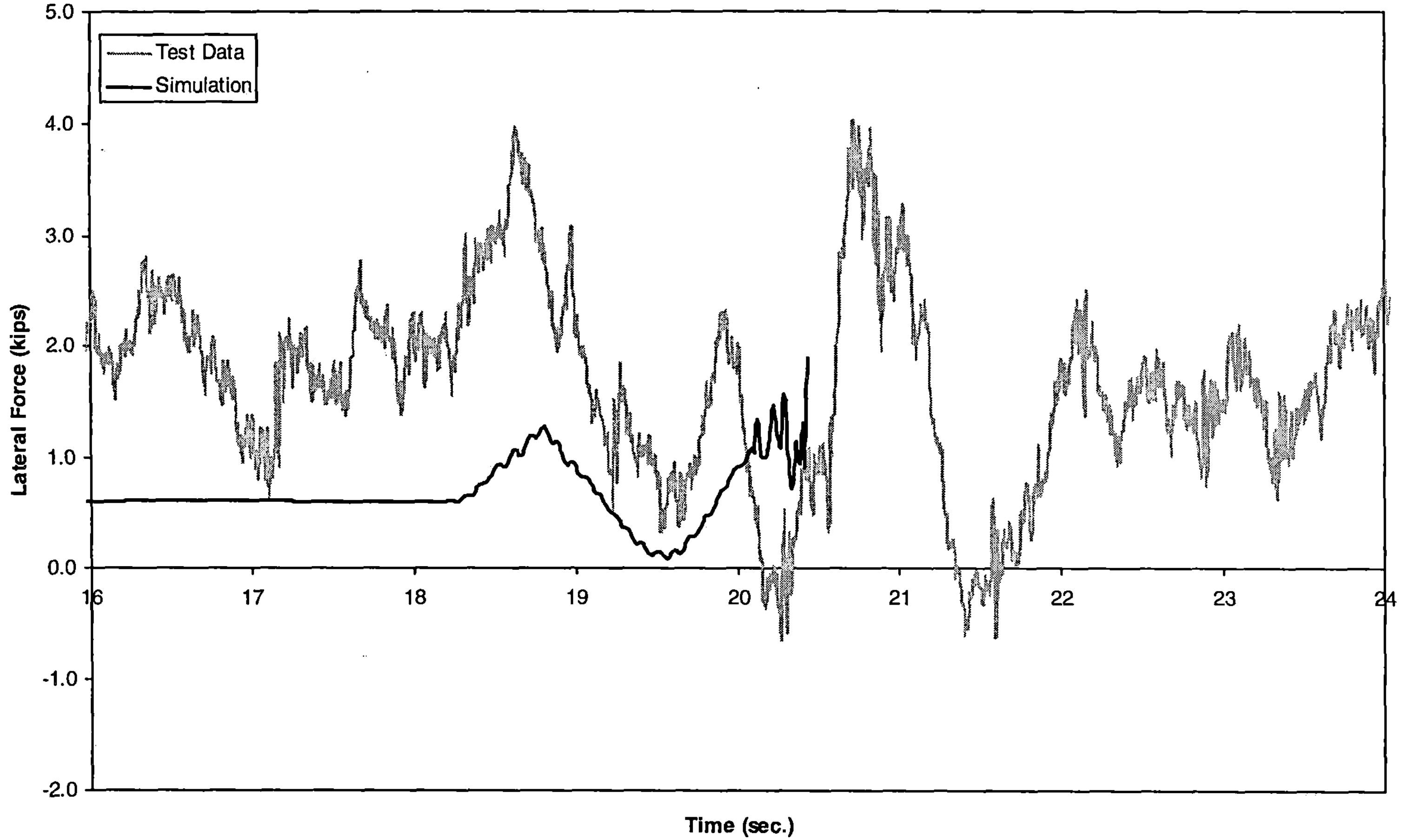

Figure 5-4(d). Vertical dip test – lateral force time history, 20 mph (trailing inner wheel)

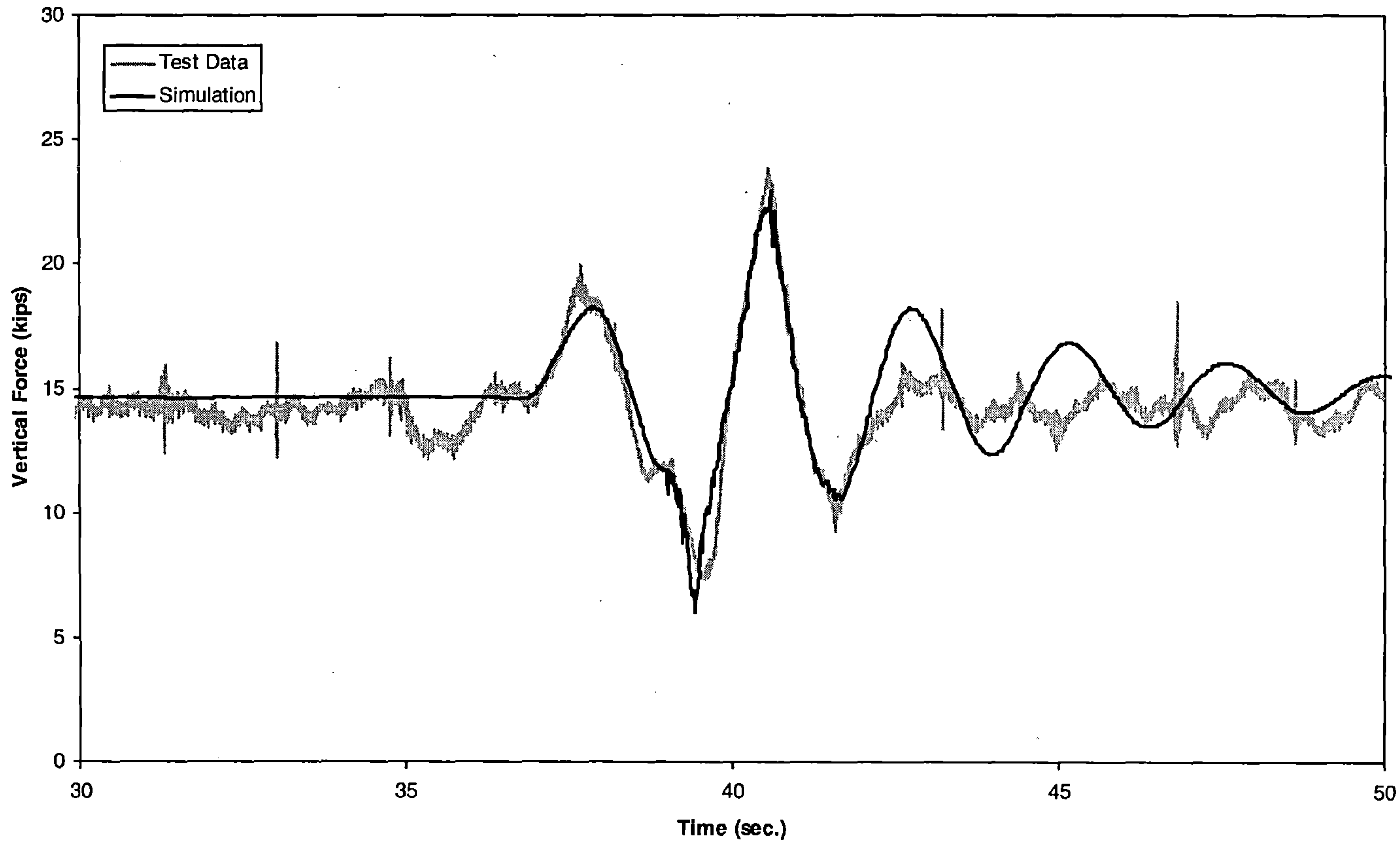

Figure 5-5(a). Vertical dip test – vertical force time history, 15 mph (lead outer wheel)

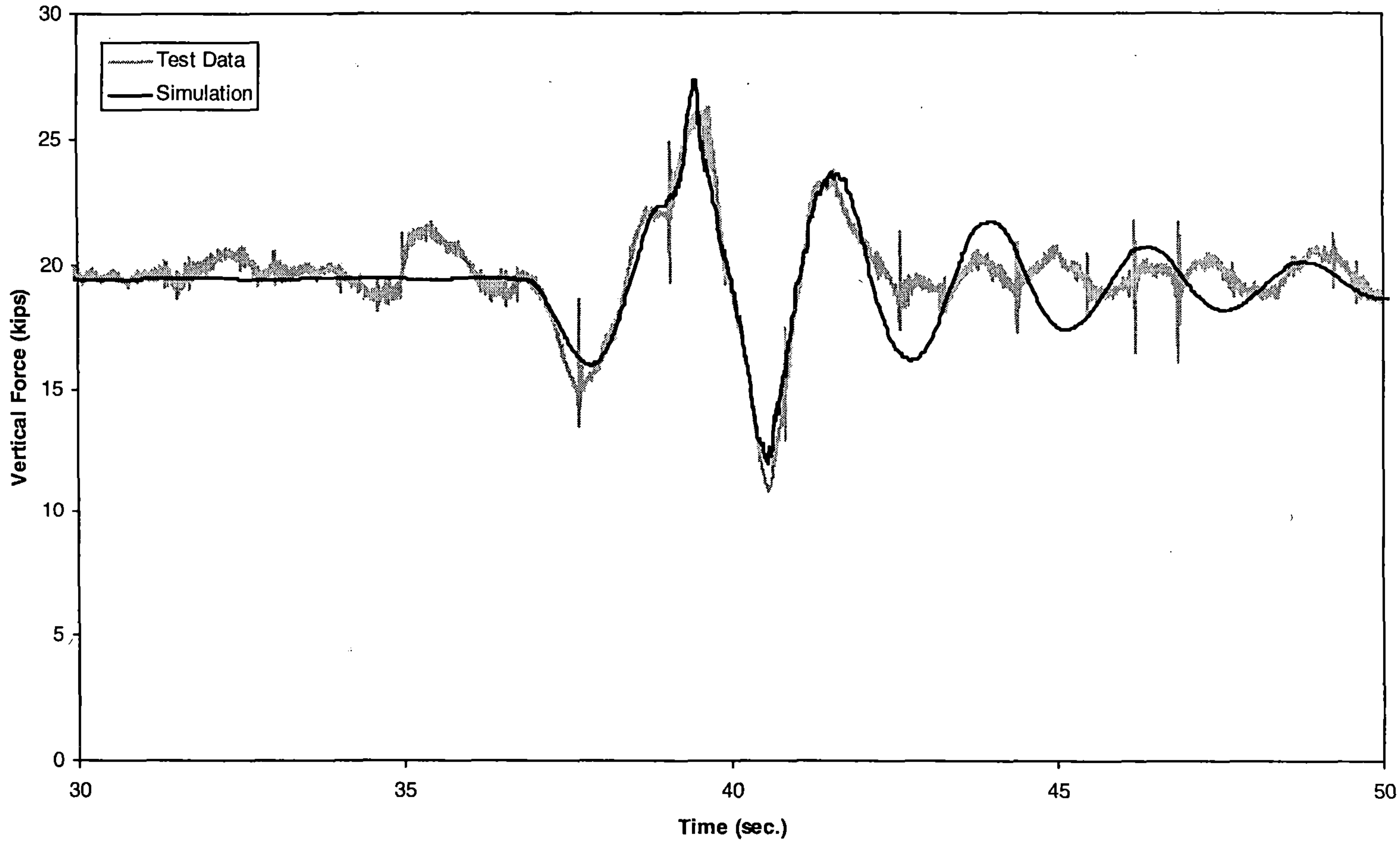

Figure 5-5(b). Vertical dip test – vertical force time history, 15 mph (lead inner wheel)

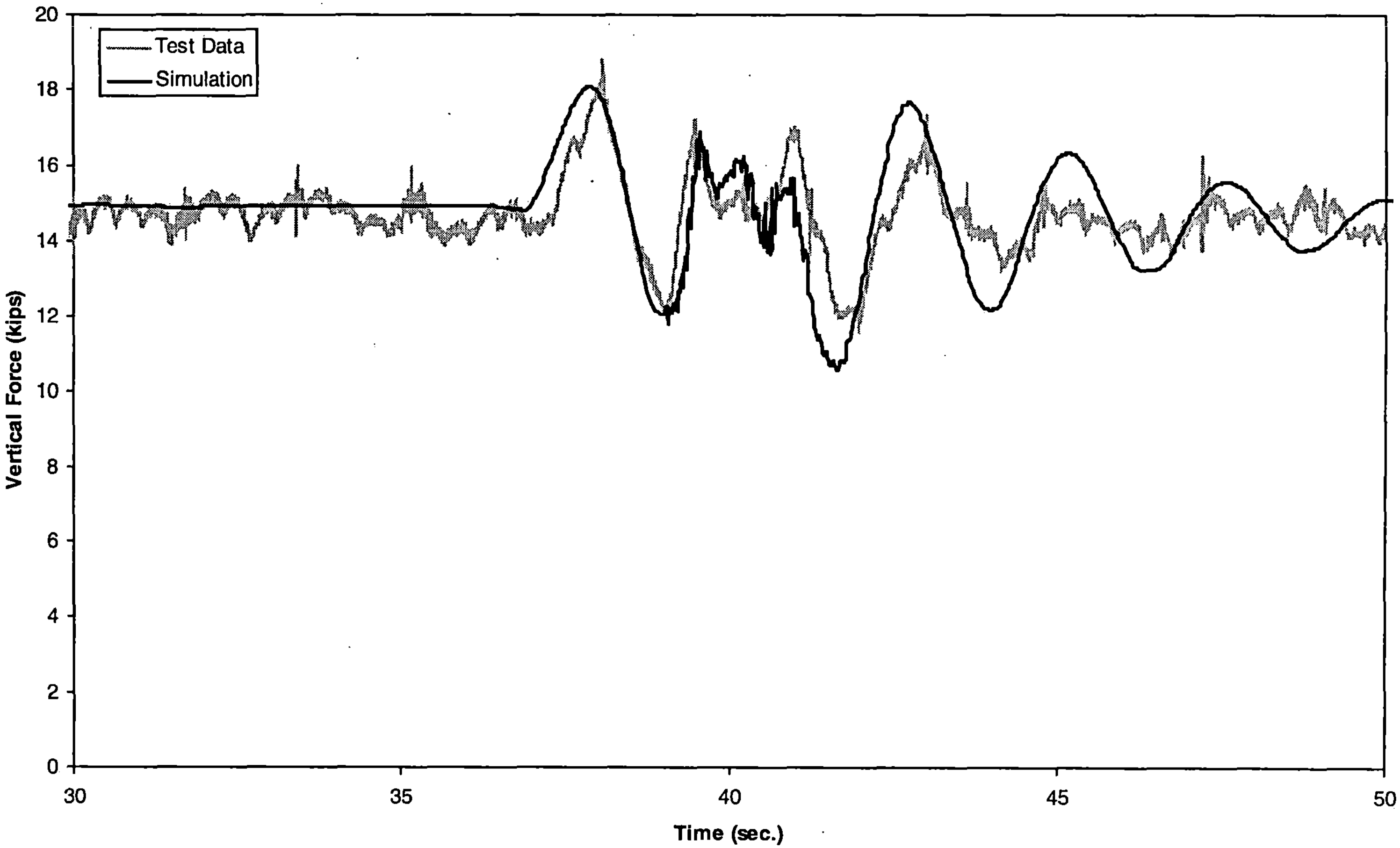

Figure 5-5(c). Vertical dip test – vertical force time history, 15 mph (trailing outer wheel)

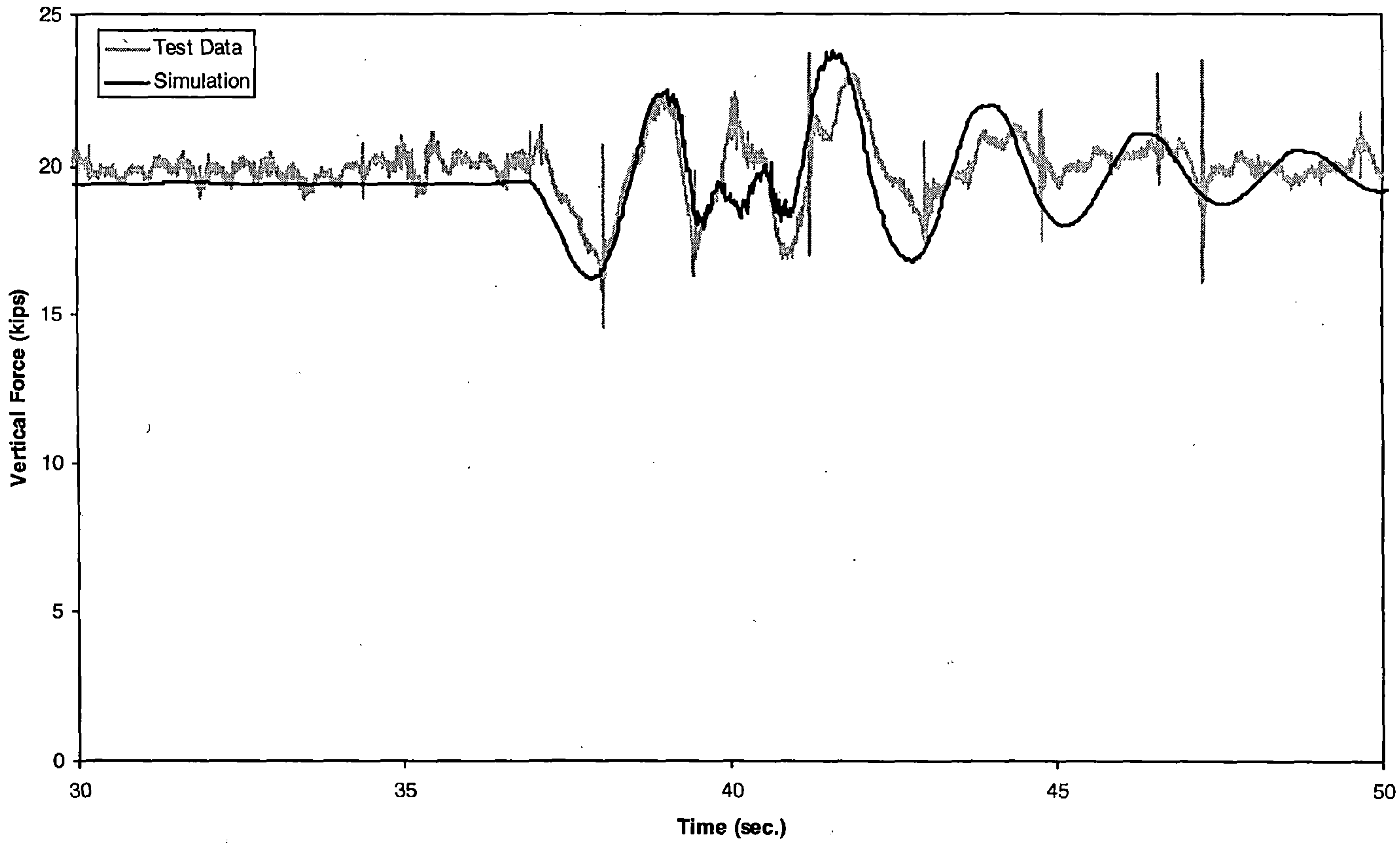

Figure 5-5(d). Vertical dip test – vertical force time history, 15 mph (trailing inner wheel)

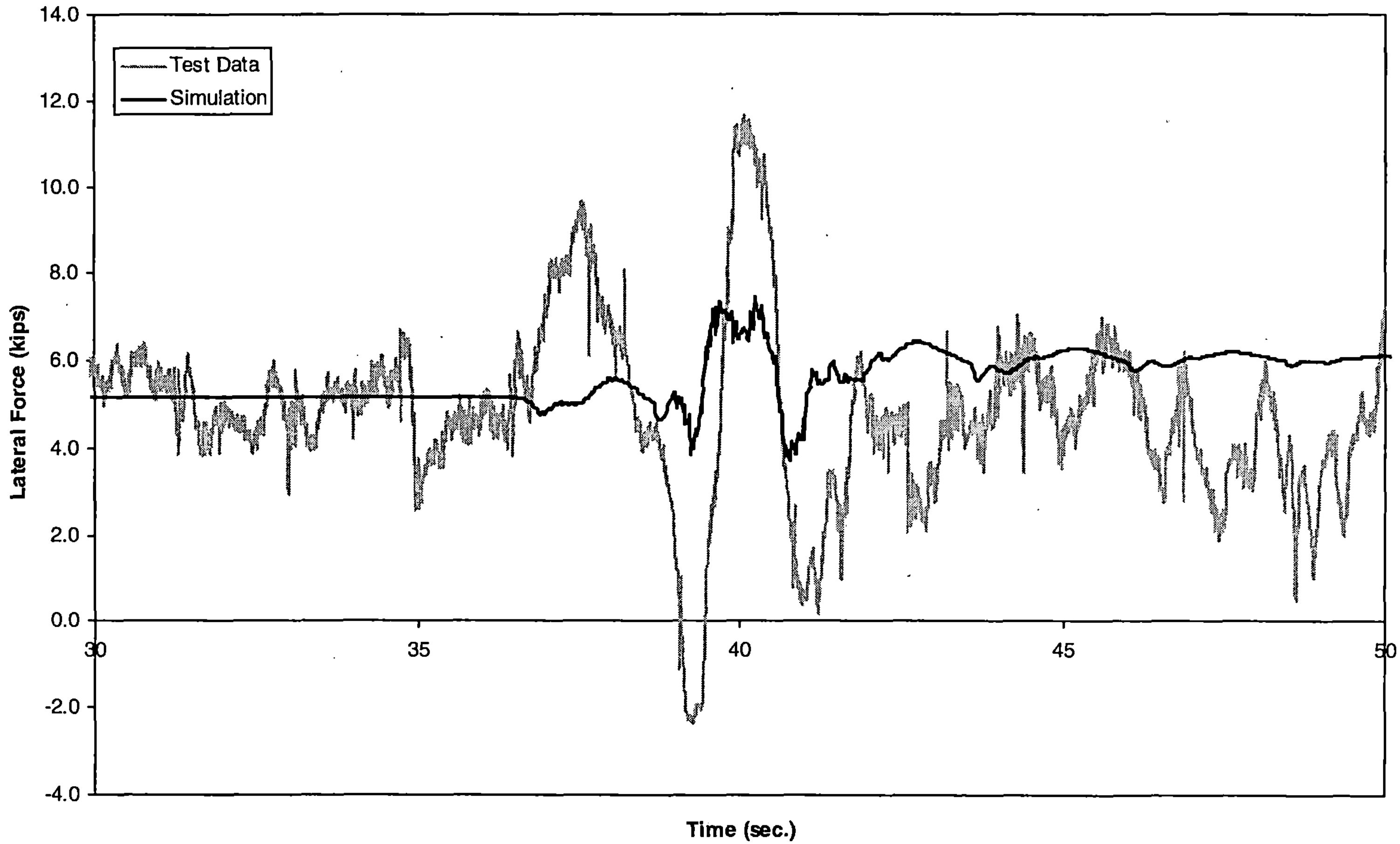

Figure 5-6(a). Vertical dip test – lateral force time history, 15 mph (lead outer wheel)

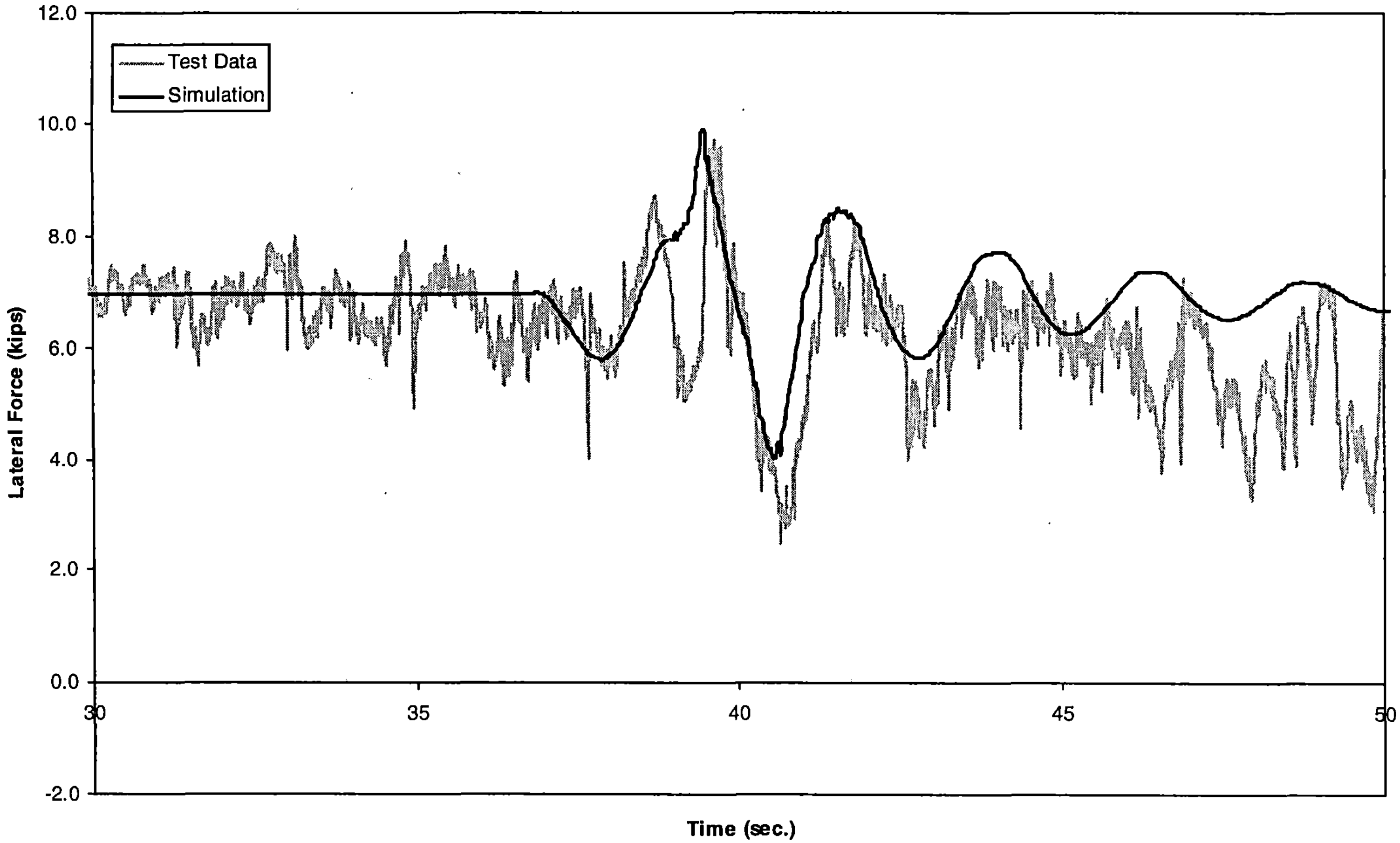

Figure 5-6(b). Vertical dip test – lateral force time history, 15 mph (lead inner wheel)

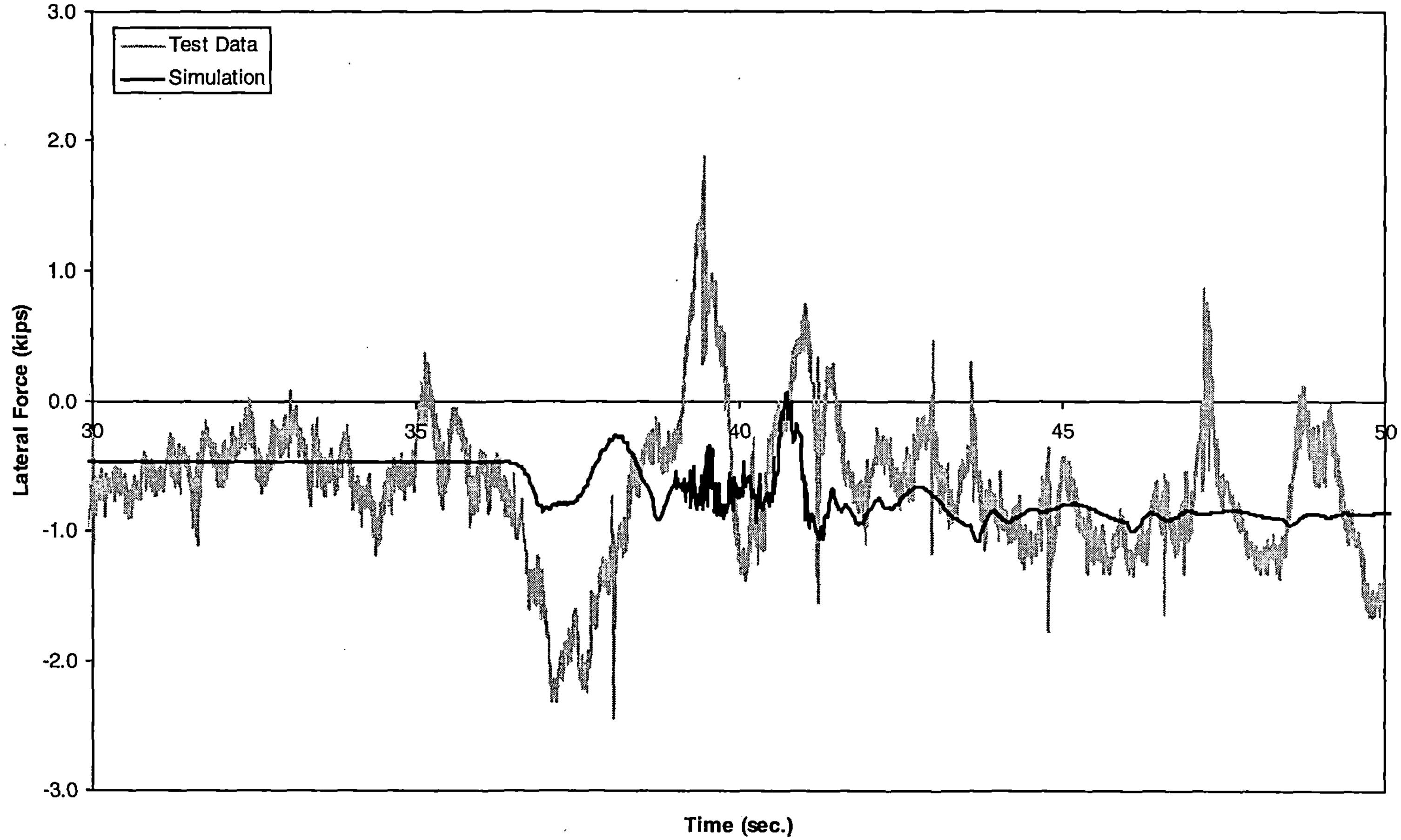

Figure 5-6(c). Vertical dip test – lateral force time history, 15 mph (trailing outer wheel)

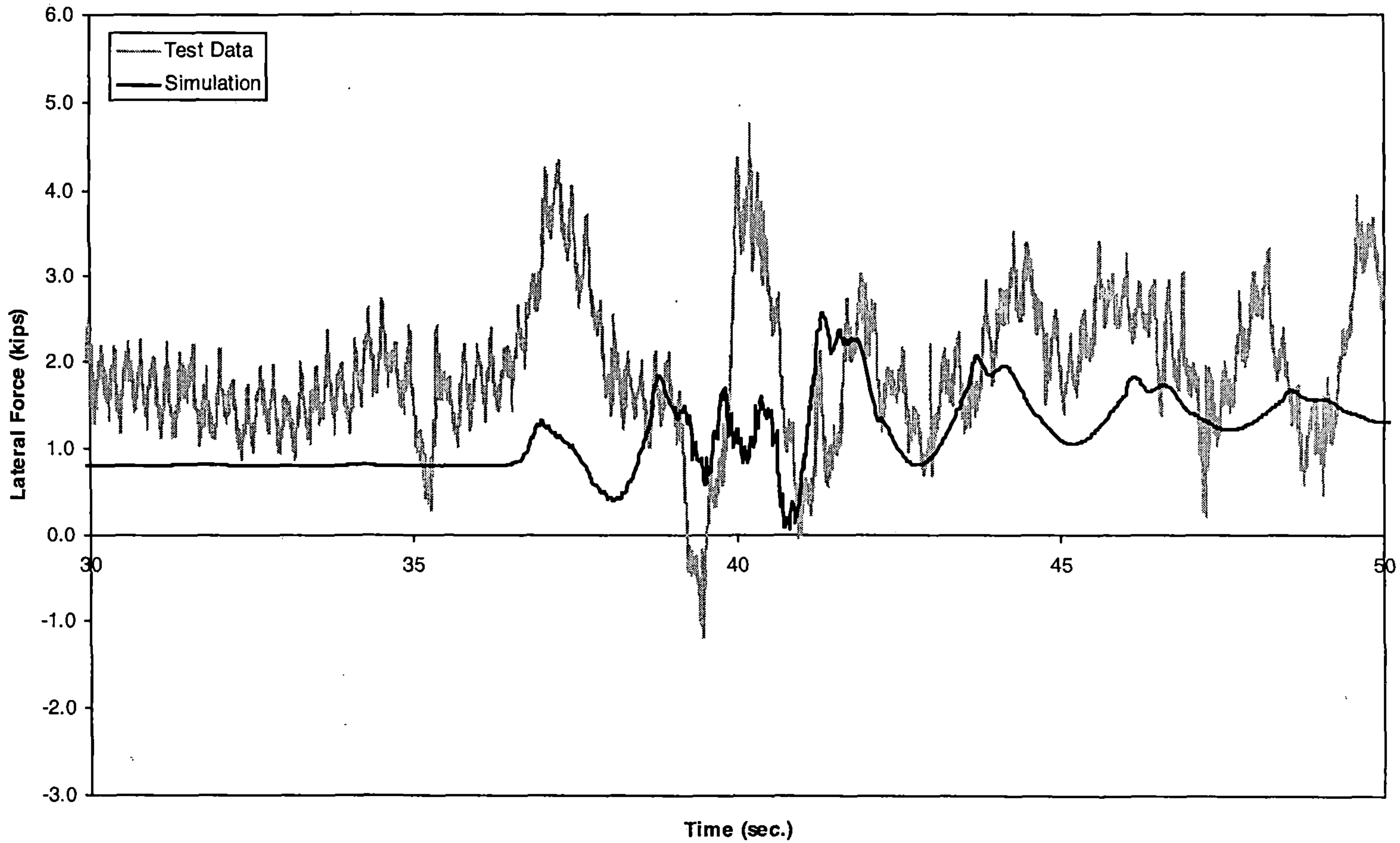

Figure 5-6(d). Vertical dip test – lateral force time history, 15 mph (trailing inner wheel)

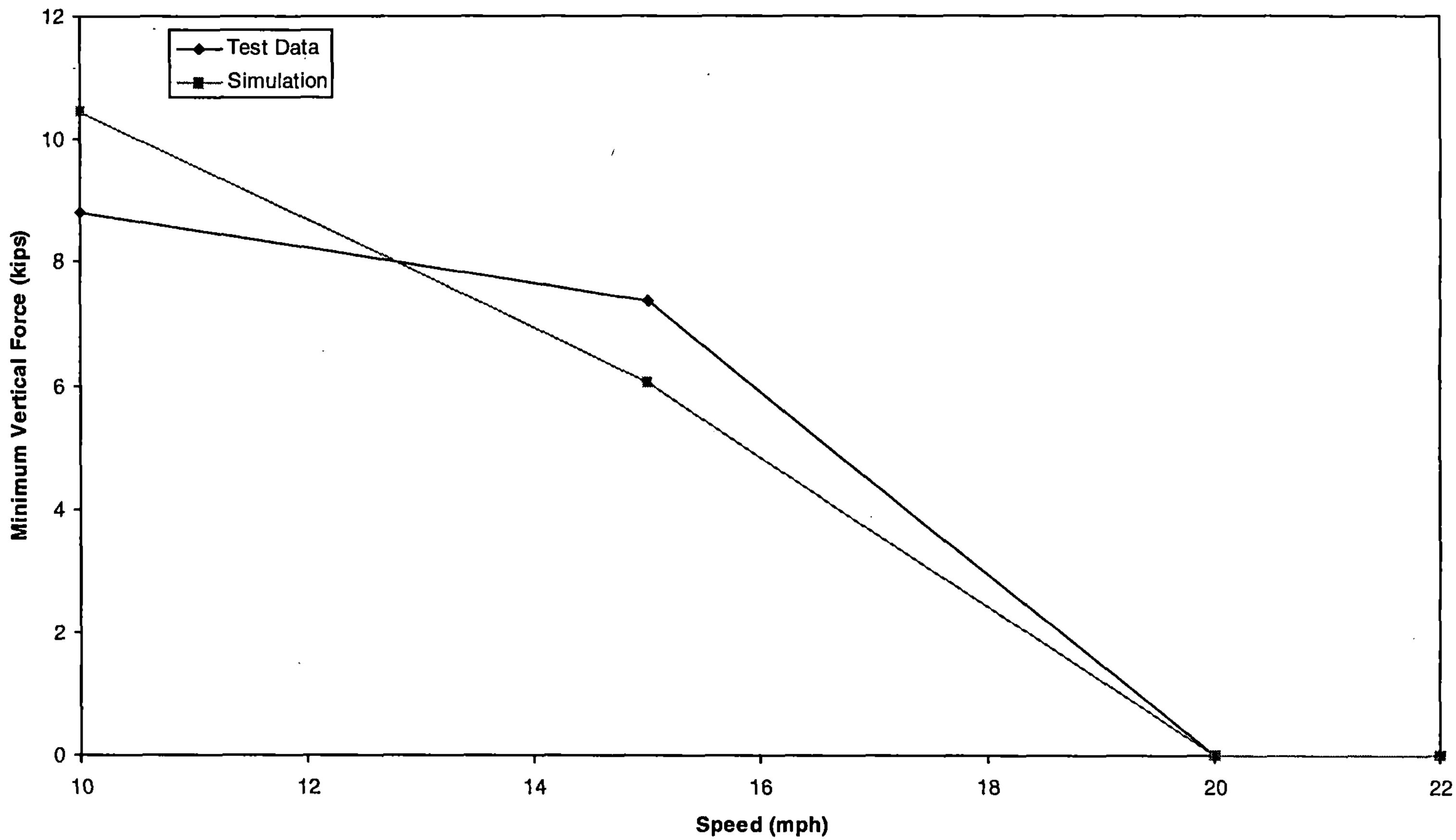

Figure 5-7. Vertical dip test – minimum vertical force

5.2 Steady Curving with Spirals

Test Description

Steady curving tests were conducted to measure the test car's ability to operate on high speed curves. The test consist was operated at speeds from the balance speed up to an unbalanced (cant deficiency) condition of ~7 in. Unbalance is defined as the additional height in inches, which if added to the rail in a curve at a certain car speed would provide a single resultant force, (combined effect of weight and centrifugal force on the car) in a direction perpendicular to the plane of the track. A constant 1-degree 15-minute reverse curve with 6 in. superelevation, on the Railroad Test Track (RTT) was used for all tests. Test runs were performed over Class 5 through 6 track, at speeds of 84 mph (balance speed) to 124 mph (~7 in. unbalance) on the RTT. The tracks have AREA 136 rail and wood ties with cut spike construction on slag ballast.

Correlation

Test data and simulation results for passage through the curve; are presented in Figures 5-8, 5-9 and 5-10 for operation at 84 mph and in Figures 5-11, 5-12 and 5-13 for operation at 124 mph. Vertical force data in Figure 5-10 for operation at balance speed show that both the test data and simulation indicate that the vertical forces remain very close to their nominal values for all four wheels during the curve negotiation. The variations in the test data (Figure 5-8) from the nominal value are believed due to local track perturbations. The lateral data (Figure 5-9) for the individual wheels do not have close agreement between the simulation and the test data. The lead axle test data is 3 to 3.5 kips less than the simulation value for the outer and inner wheels. The trailing axle test data is 2.5 to 3 kips greater than the simulation data for the outer and inner wheels. Comparison of the simulation and test data for the net lateral force on the lead and trailing axles, summarized in Figure 5-10, has closer correlations. For the lead axle, simulation gives 1.0 kip compared with test data of approximately 0.75 kip. For the trailing axle, simulation gives –1.0 kip, which is almost the same value as the test data. Thus though the individual wheel lateral loads are not in good agreement, the net axle lateral loads from the simulation and test agree. The sum of the two net axle loads is approximately zero for operation at balance speed in both the simulation and test data, as one would expect.

The vertical force data, presented in Figure 5-11, shows that at 124 mph, the outer wheel vertical force increases to approximately 22 to 23 kips and the inner wheel value decreases to approximately 10 kips for both axles. The test and simulation data are close. Lead axle lateral force data (Figure 5-12) shows that the outer wheel is approximately 6 kips for the simulation in comparison to 4 kips for the test data, whereas the inner wheel is 1.0 kip for the simulation and approximately -0.5 kip for the test data. The trailing axle lateral force for the outer wheel is 2 kips in the simulation and approximately 3.5 kips in the test data and for the inner wheel is -1.0 kip for the simulation in comparison to approximately -0.75 kips for the test data.

The net axle lateral force for both axles is presented in Figure 5-13. The lead axle net lateral force is approximately 5 kips with close agreement between the simulation and test data while the trailing axle lateral force is 3 kips for the simulation and approximately 3.5 kips for the test data. The net axle lateral forces are in relatively good agreement between the simulation and test data and reflect a net track lateral force of approximately 8 to 8.5 kips for the over balance speed of approximately 7 in.

Conclusion

The test and simulation data for the vertical forces on each wheel of the track are in close agreement for operation at all speeds on the curve. The lateral force data for individual wheels was not in such close agreement. Differences of up to 3.5 kips occurred at both balance and higher speeds. However, when the net axle loads on the leading and trailing axles were compared, differences between the simulation and test data were less than 0.5 kips.

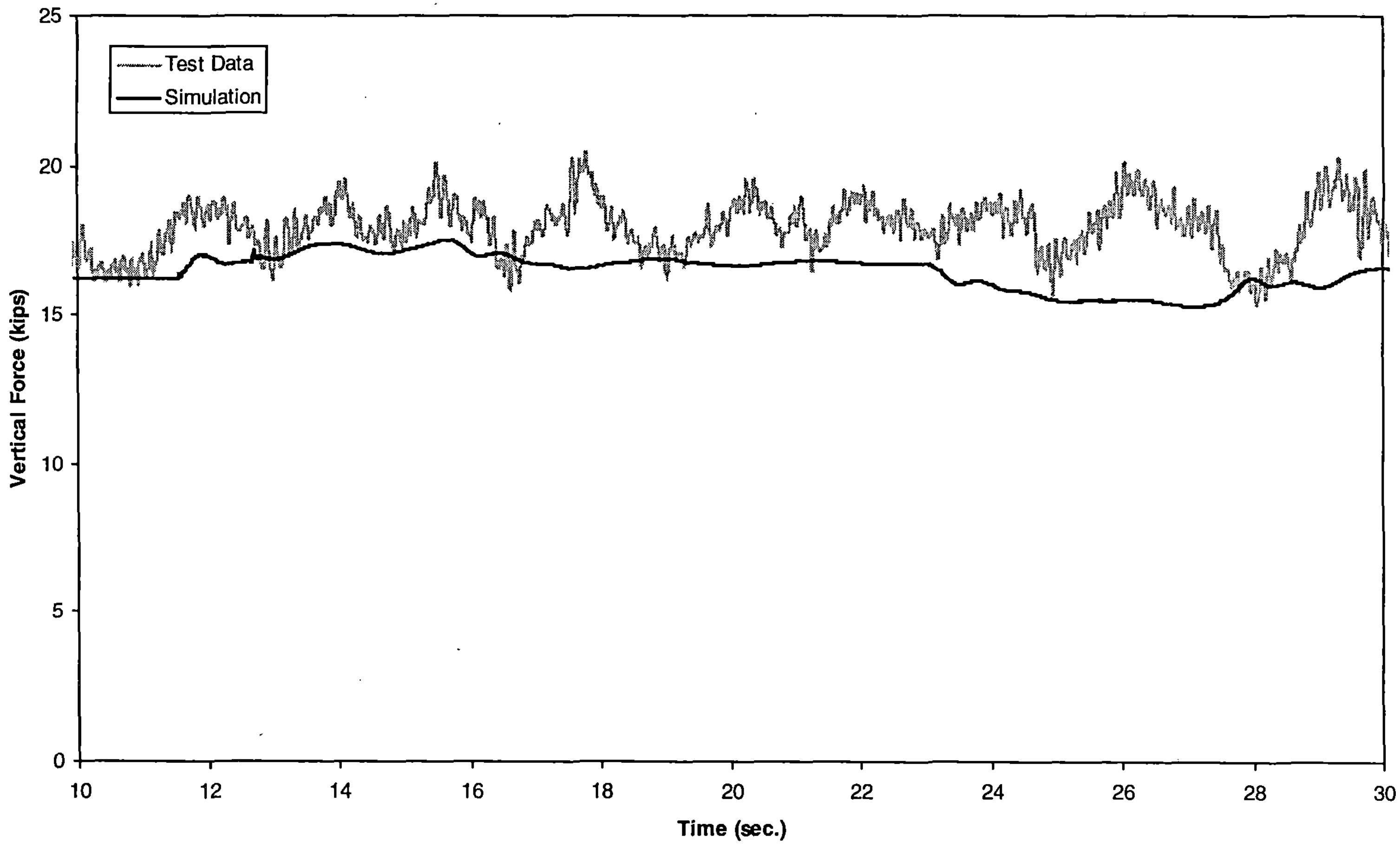

Figure 5-8(a). Steady curving – vertical force time history, 84 mph (lead outer wheel)

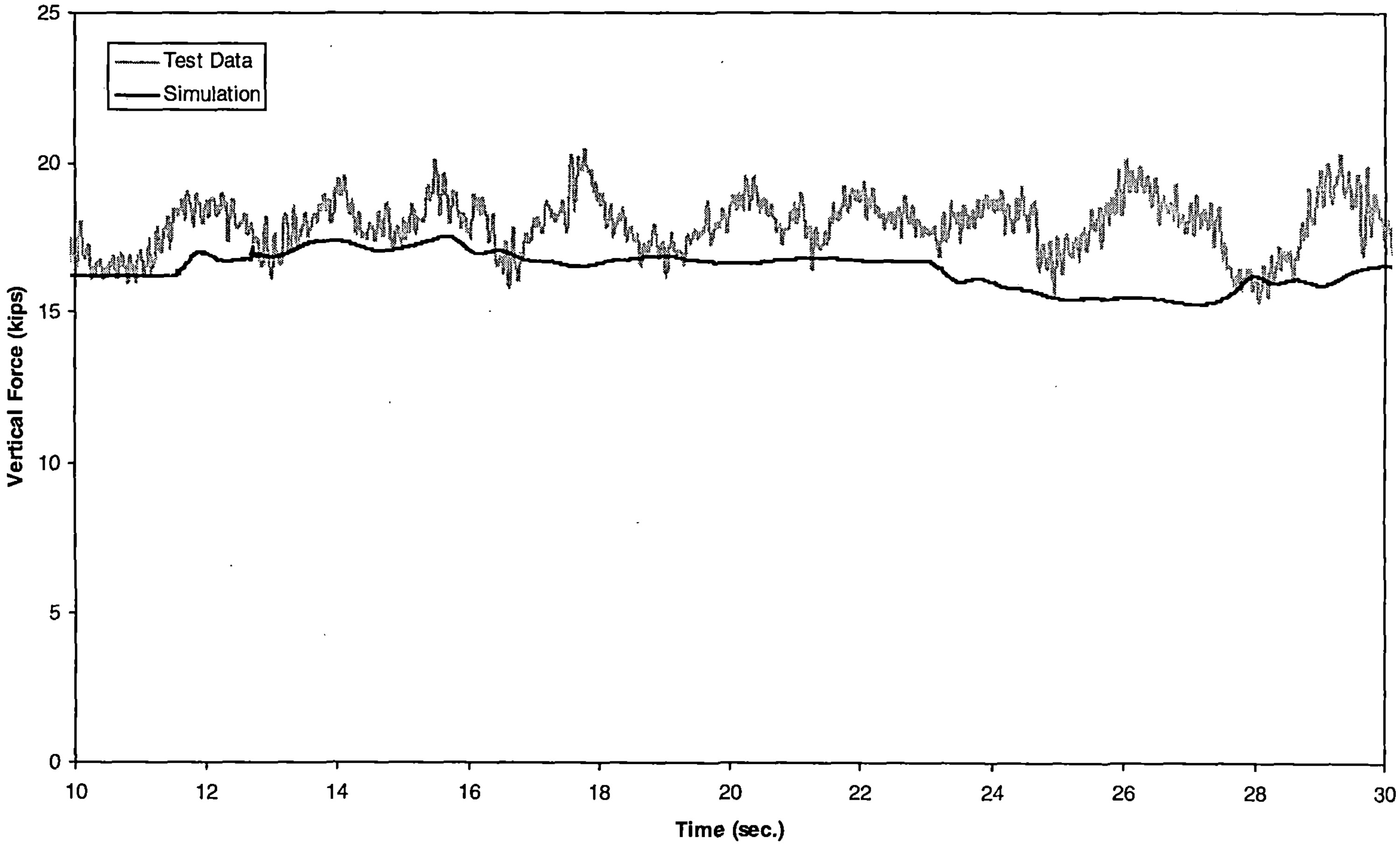

Figure 5-8(b). Steady curving – vertical force time history, 84 mph (lead inner wheel)

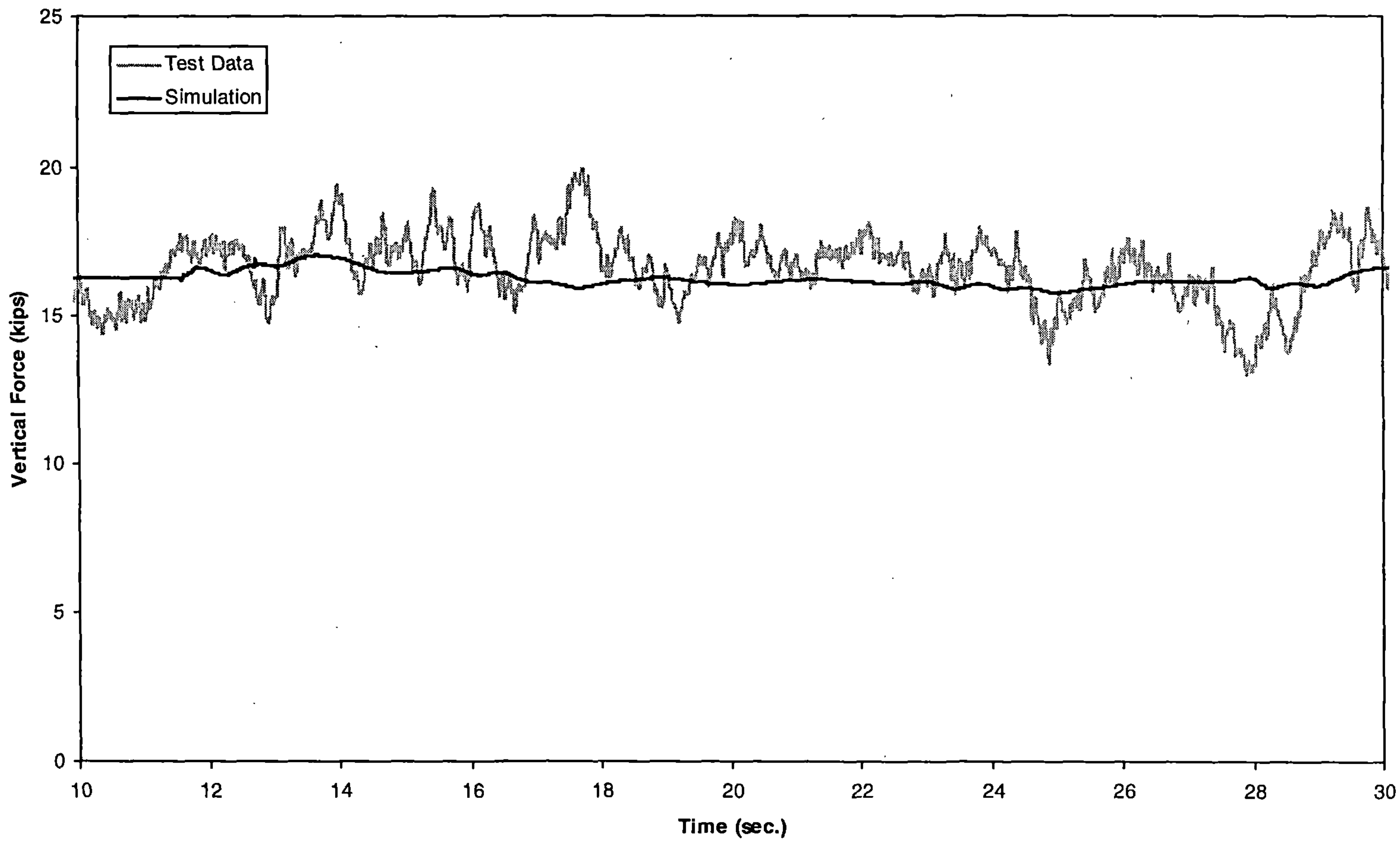

Figure 5-8(c). ***Steady curving – vertical force time history, 84 mph (trailing outer wheel)***

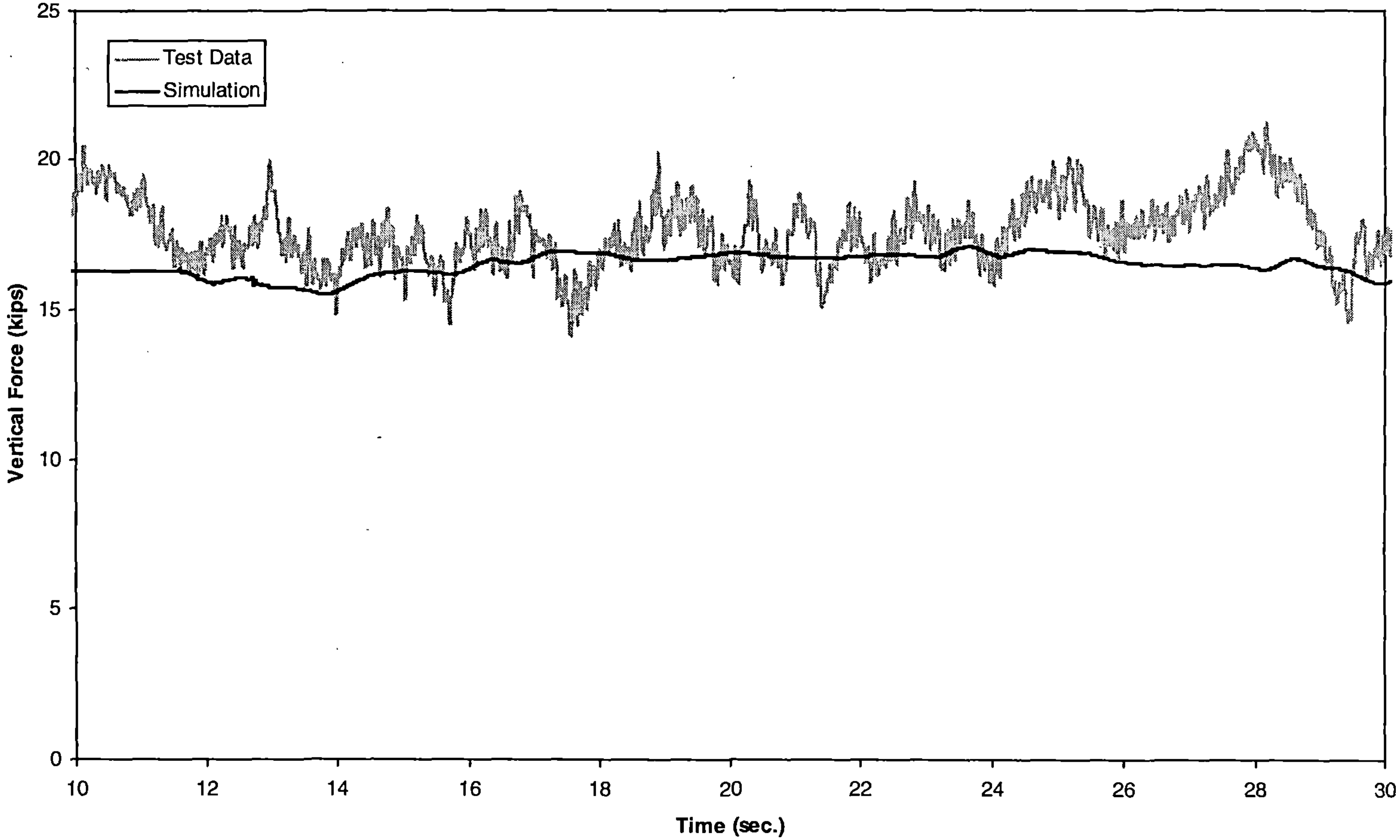

Figure 5-8(d). Steady curving – vertical force time history, 84 mph (trailing inner wheel)

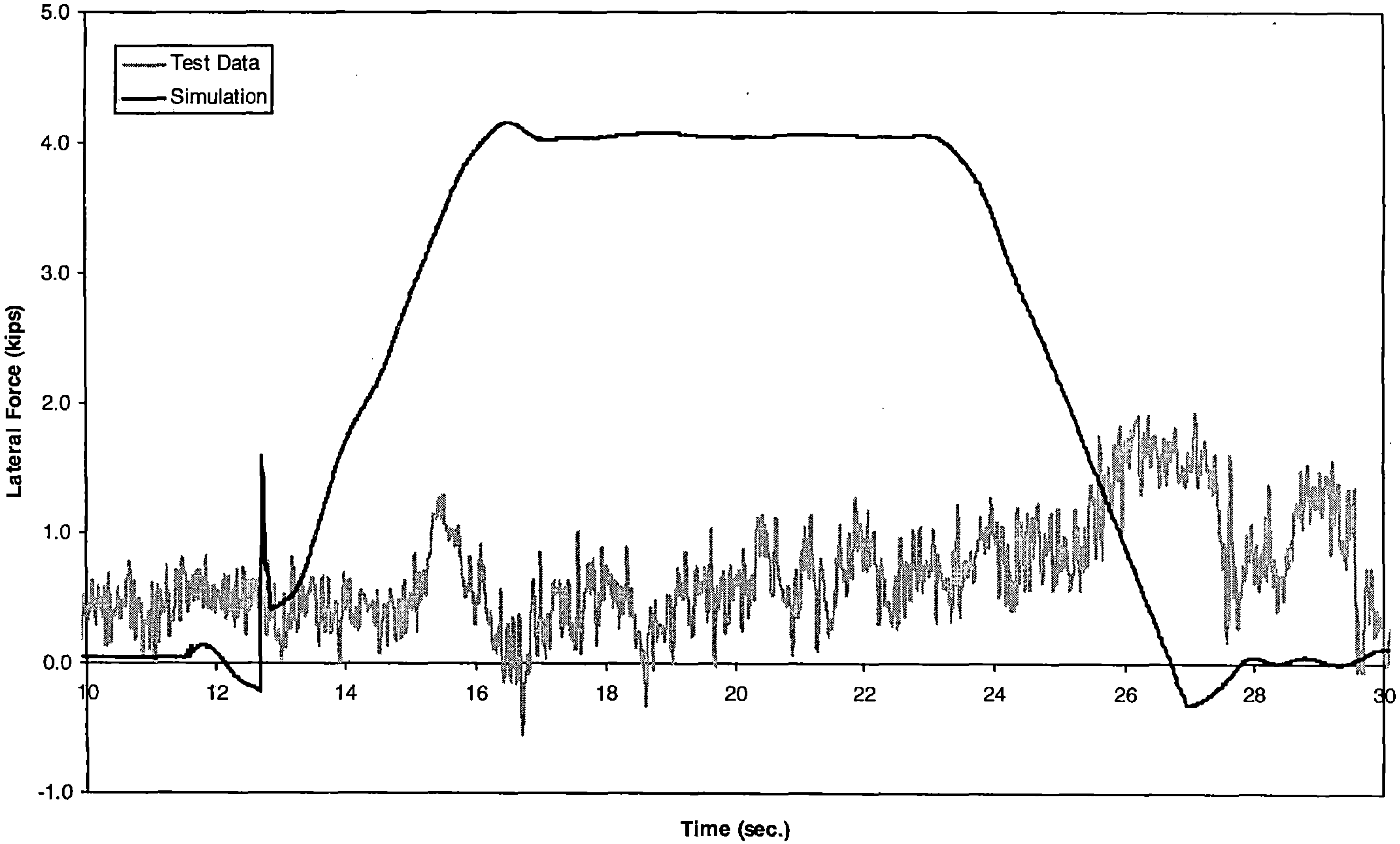

Figure 5-9(a). Steady curving – lateral force time history, 84 mph (lead outer wheel)

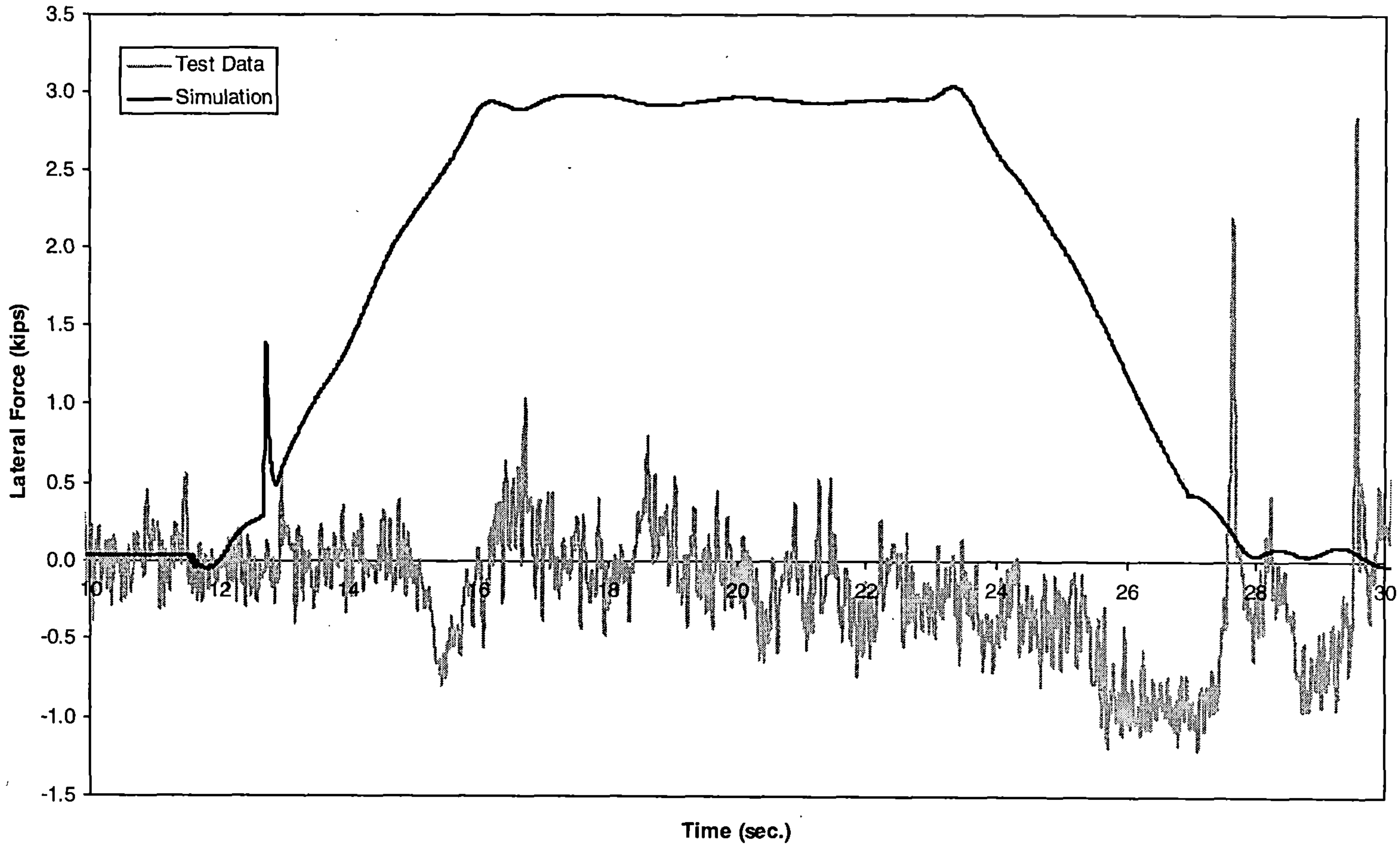

Figure 5-9(b). Steady curving – lateral force time history, 84 mph (lead inner wheel)

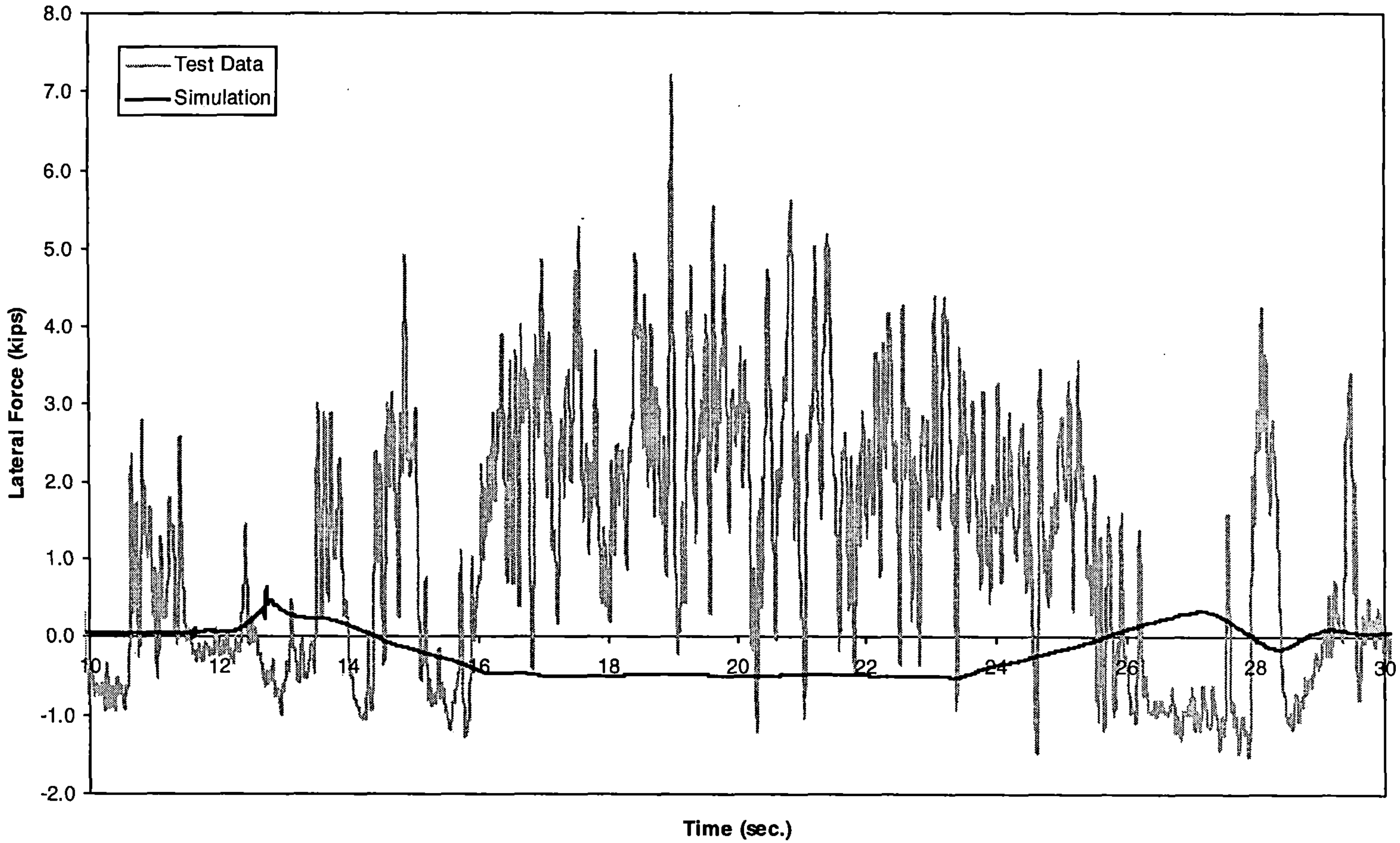

Figure 5-9(c). Steady curving – lateral force time history, 84 mph (trailing outer wheel)

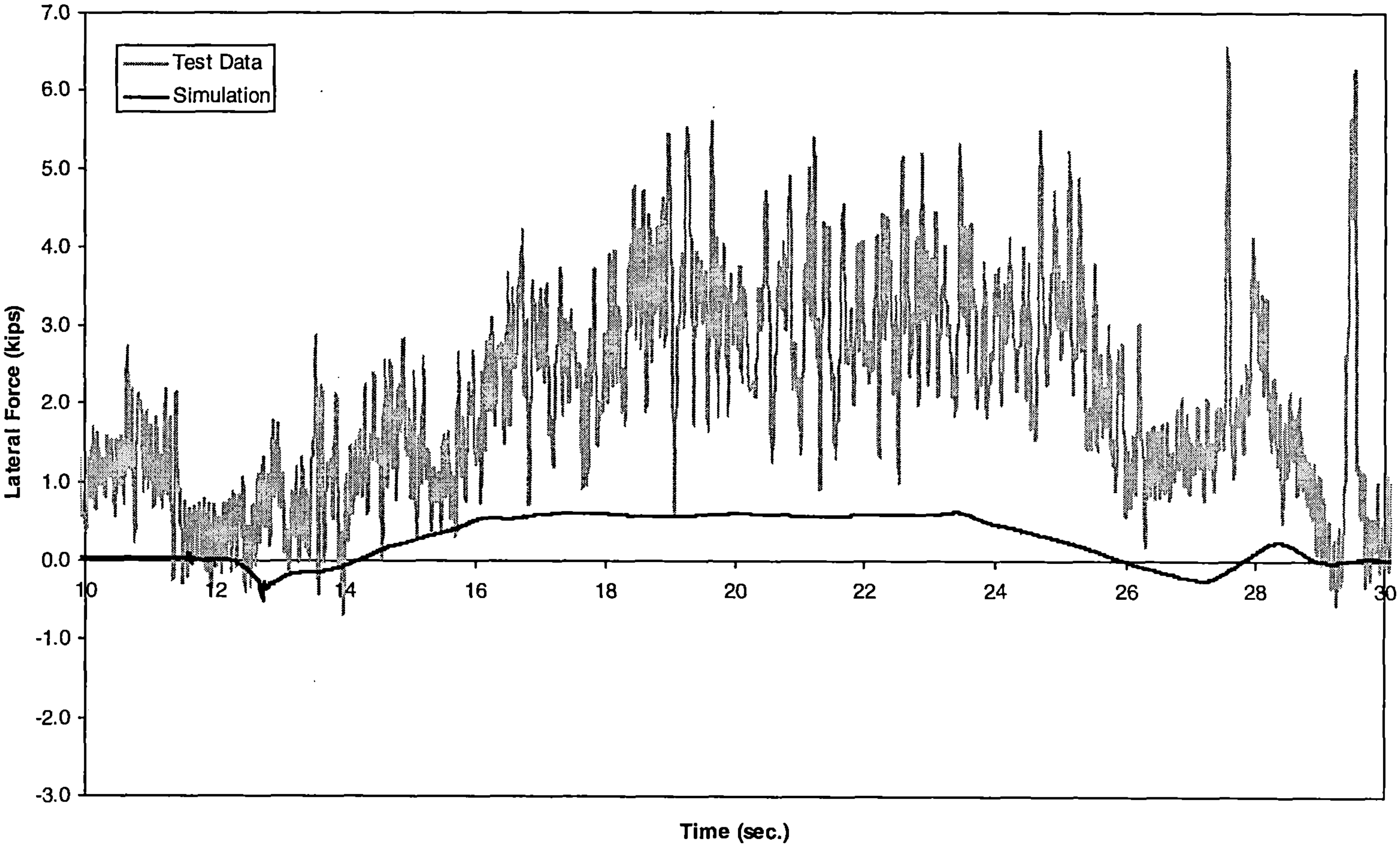

Figure 5-9(d). Steady curving – lateral force time history, 84 mph (trailing inner wheel)

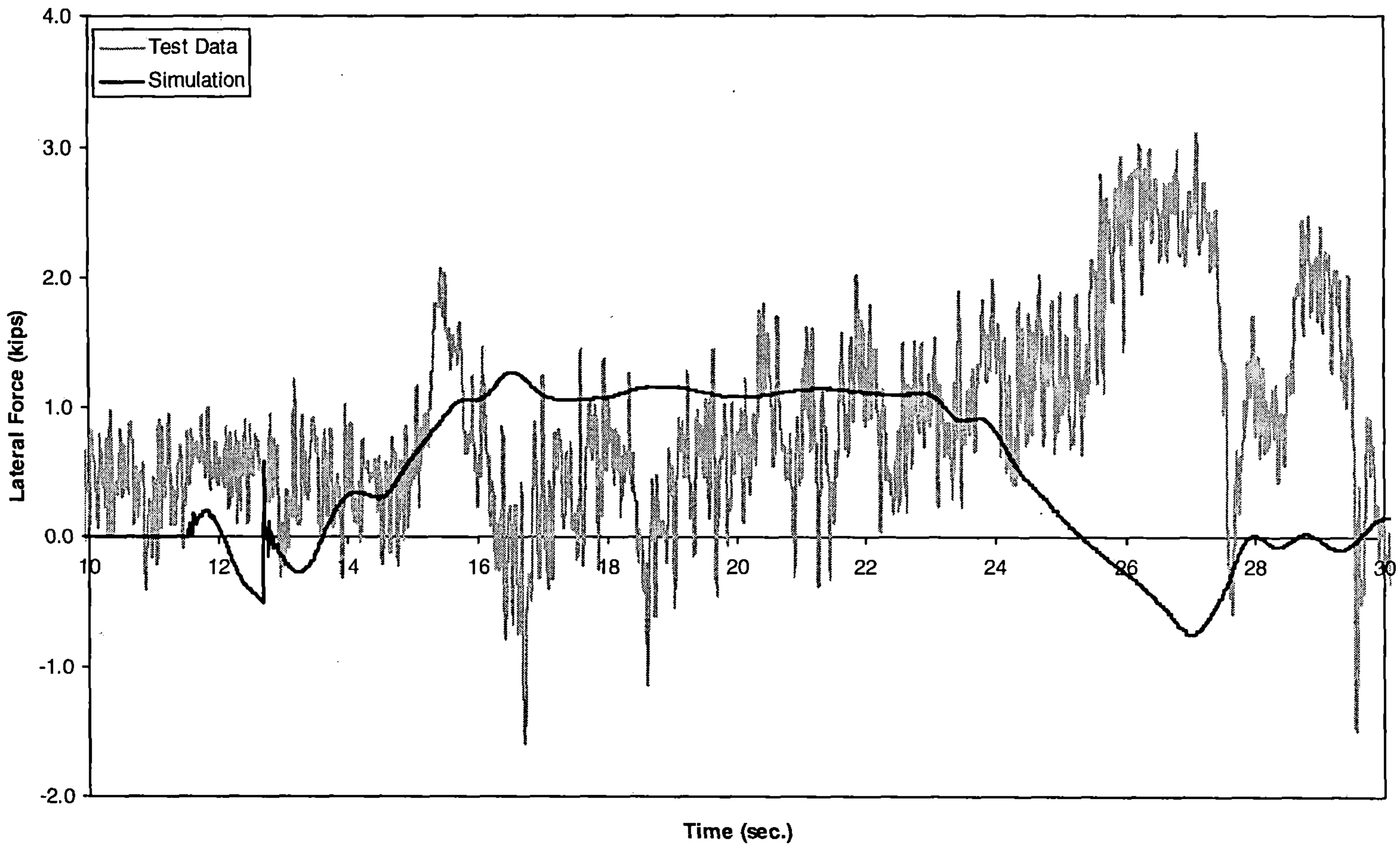

Figure 5-10(a). Steady curving – net axle lateral force time history, 84 mph (lead axle)

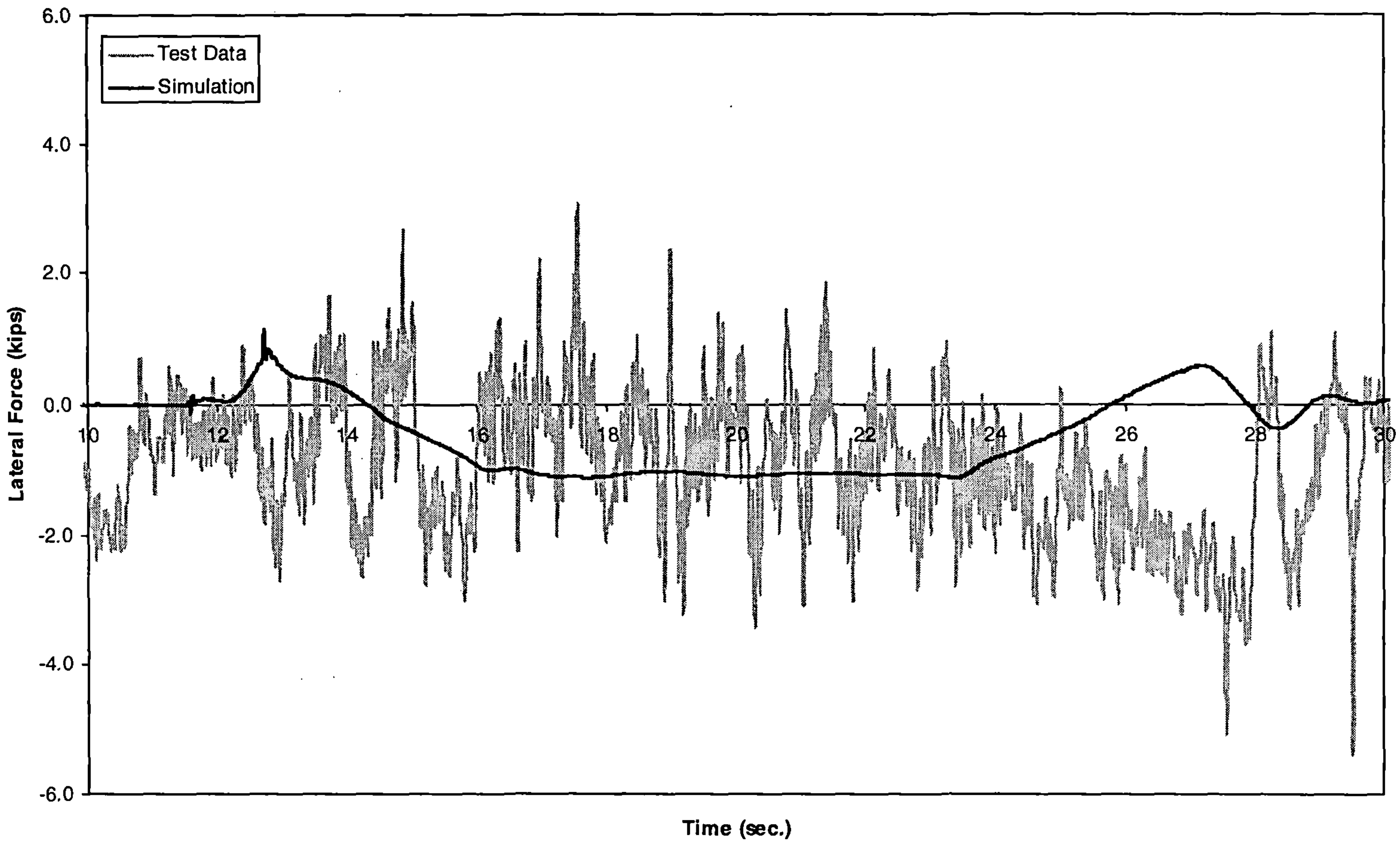

Figure 5-10(b). Steady curving – net axle lateral force time history, 84 mph (trailing axle)

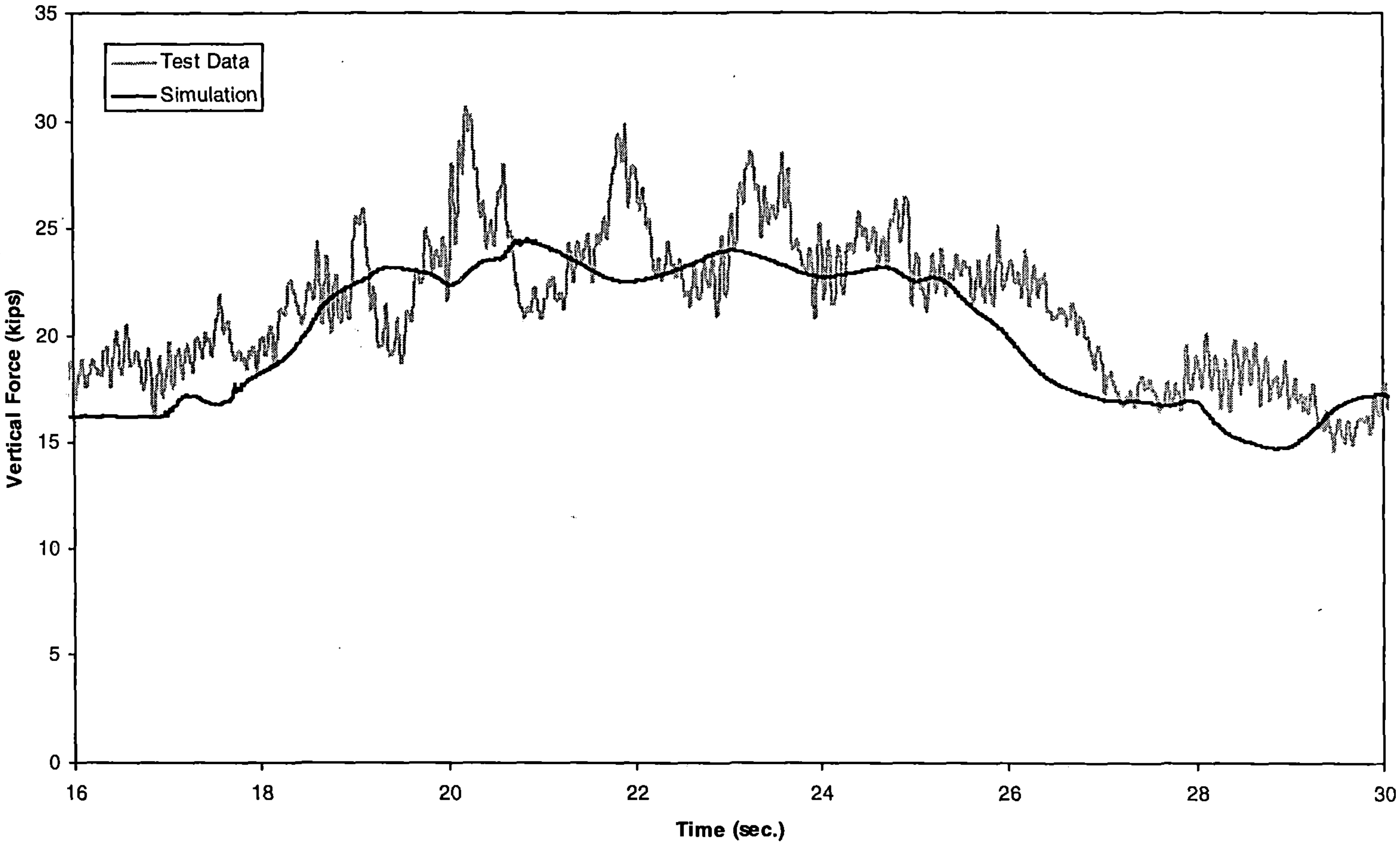

Figure 5-11(a). Steady curving – vertical force time history, 124 mph (lead outer wheel)

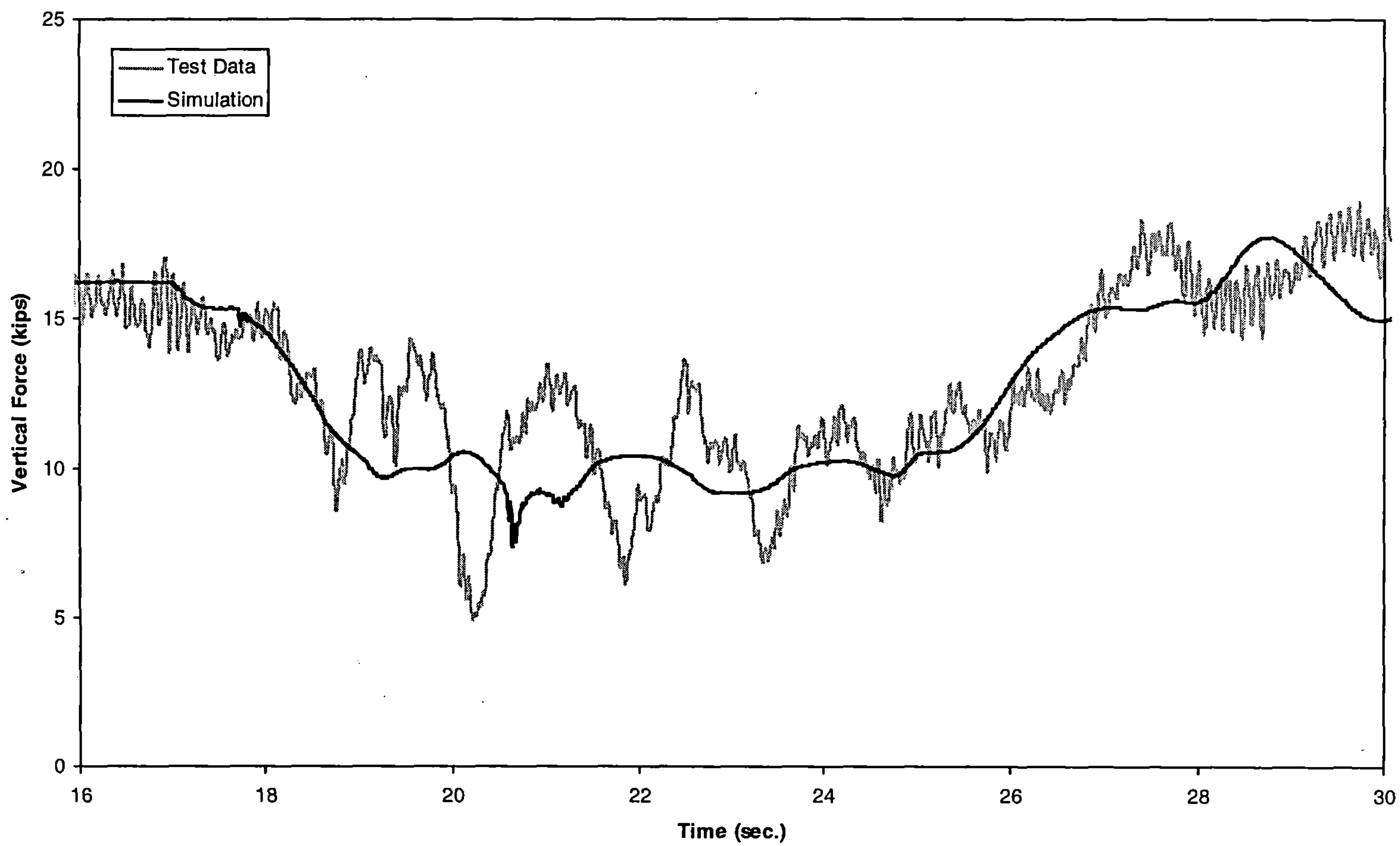

Figure 5-11(b). Steady curving – vertical force time history, 124 mph (lead inner wheel)

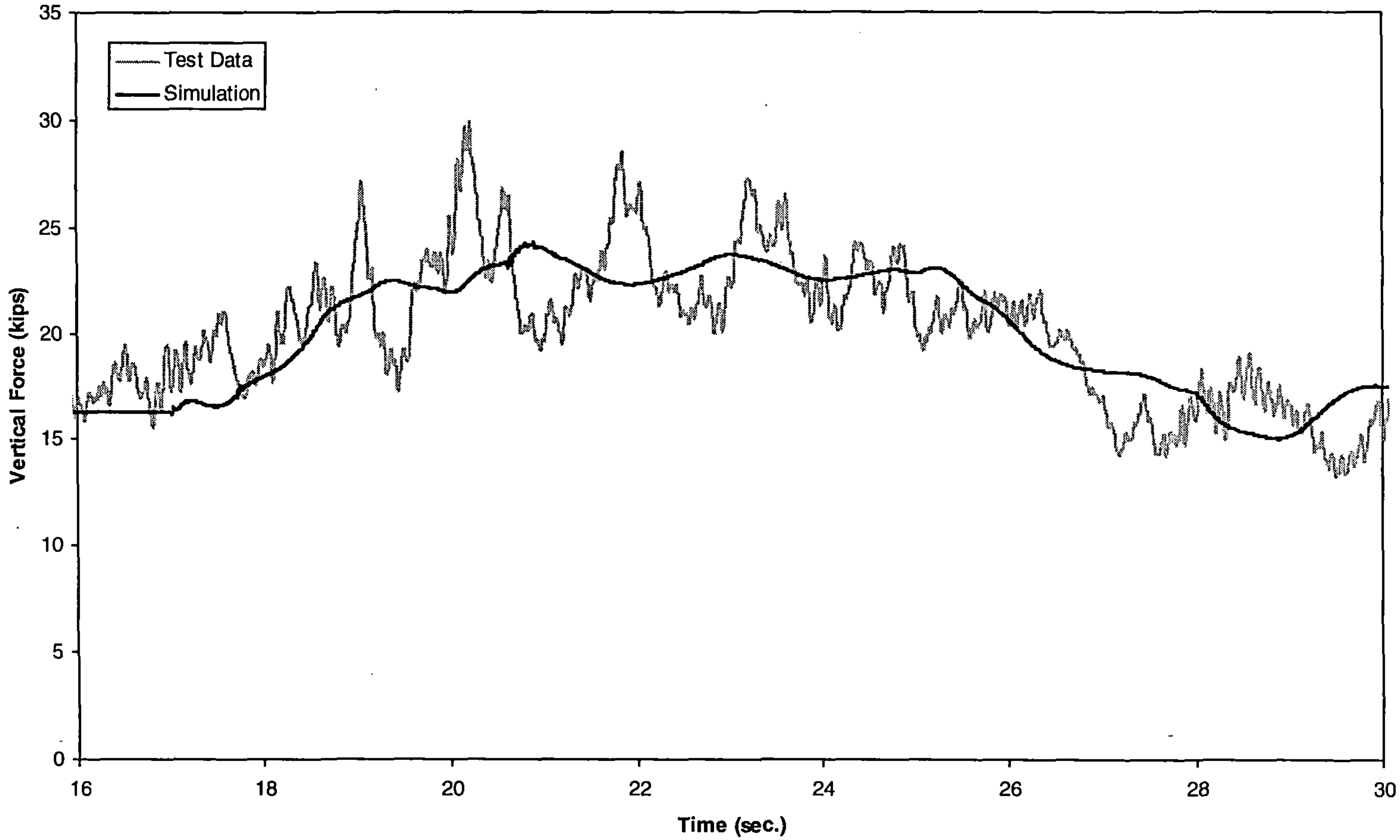

Figure 5-11(c). Steady curving – vertical force time history, 124 mph (trailing outer wheel)

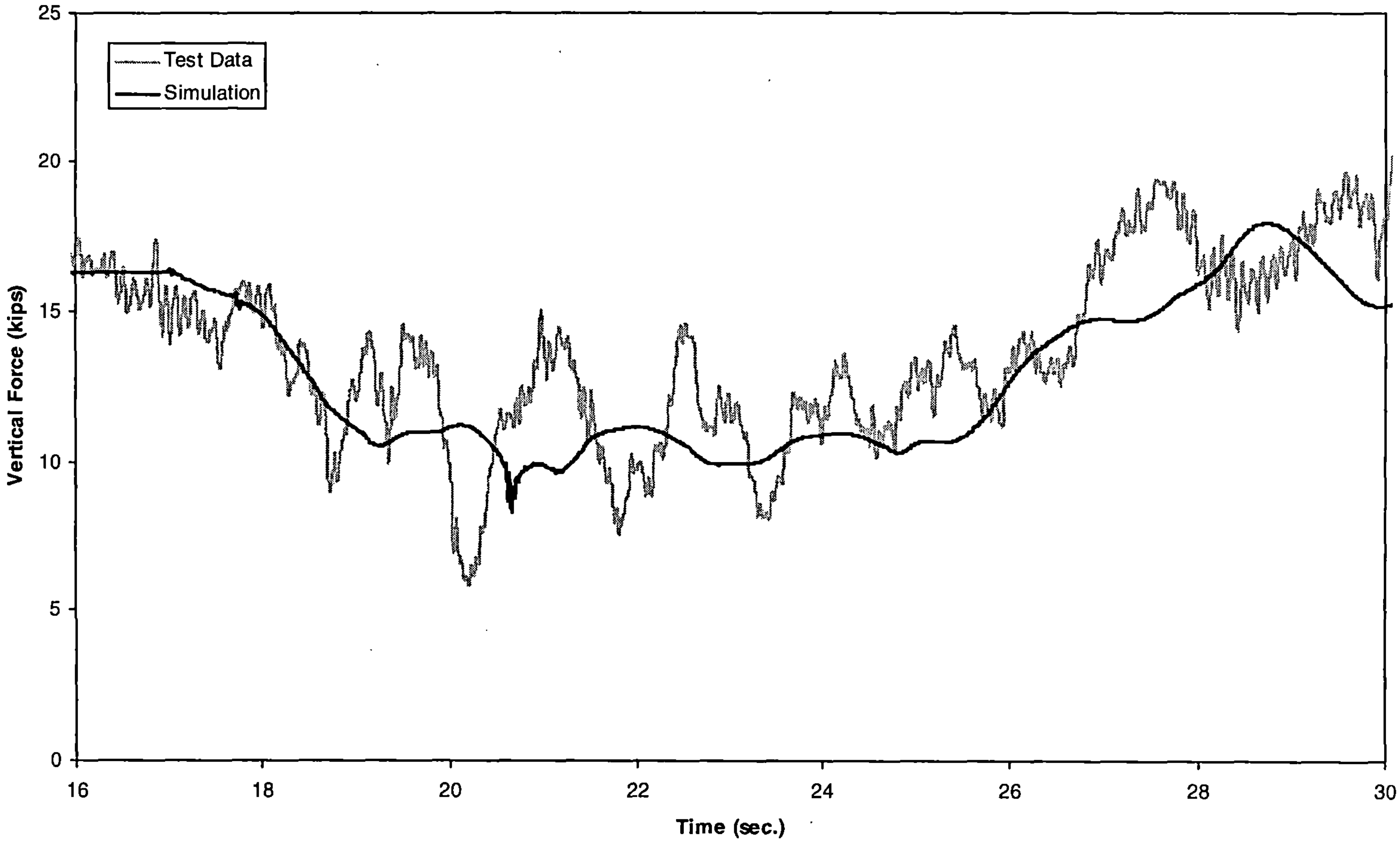

Figure 5-11(d). Steady curving – vertical force time history, 124 mph (trailing inner wheel)

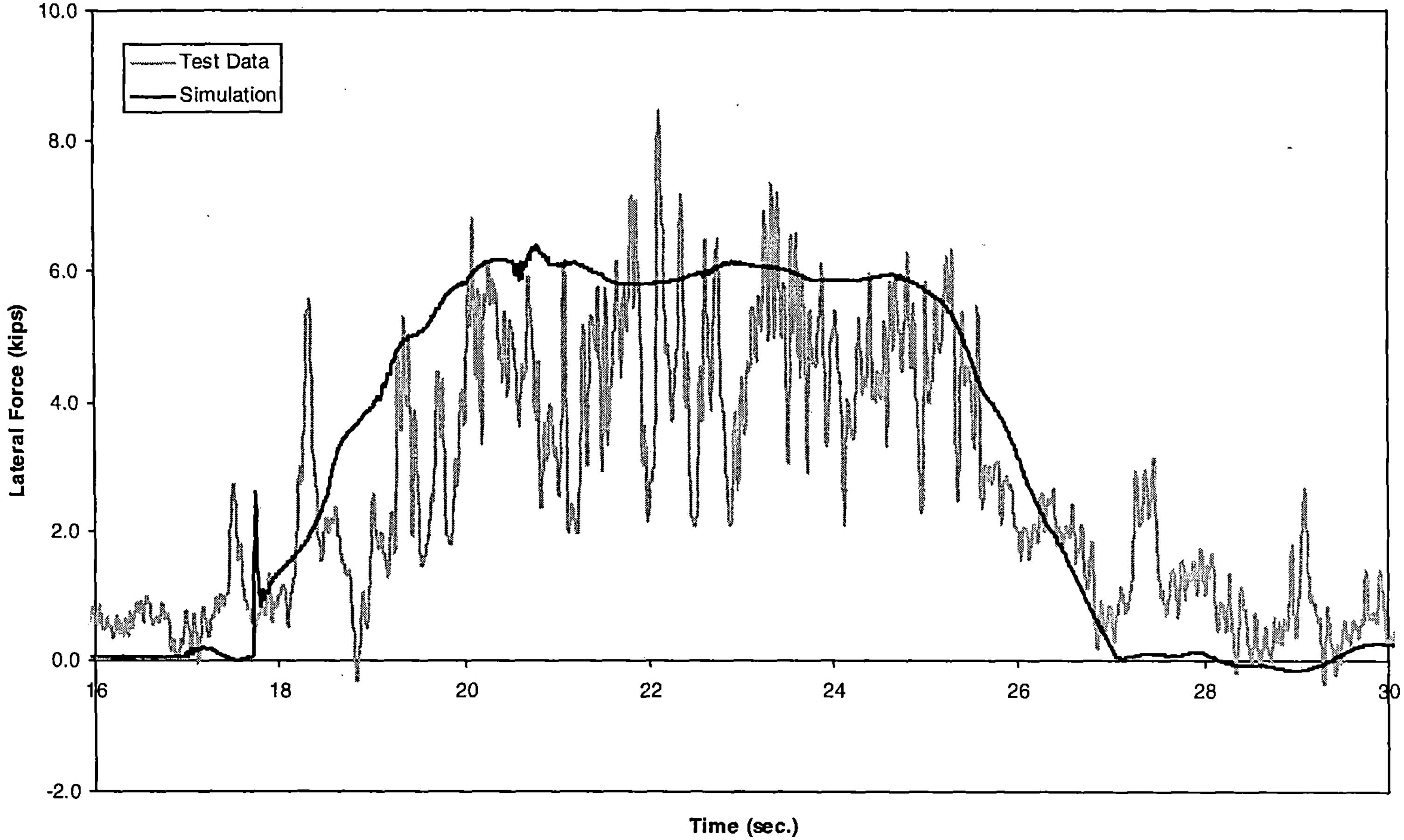

Figure 5-12(a). Steady curving – lateral force time history, 124 mph (lead outer wheel)

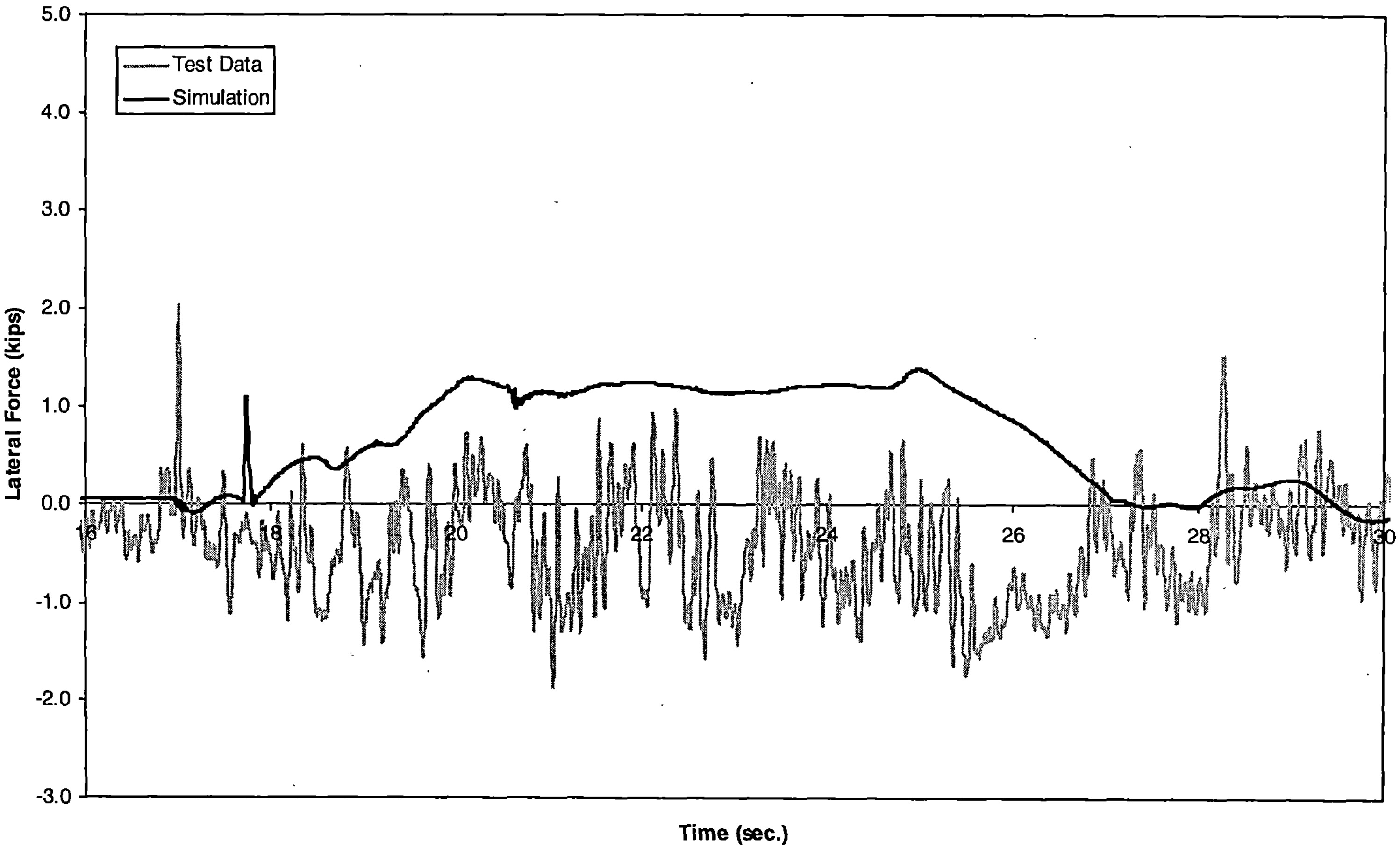

Figure 5-12(b). Steady curving – lateral force time history, 124 mph (lead inner wheel)

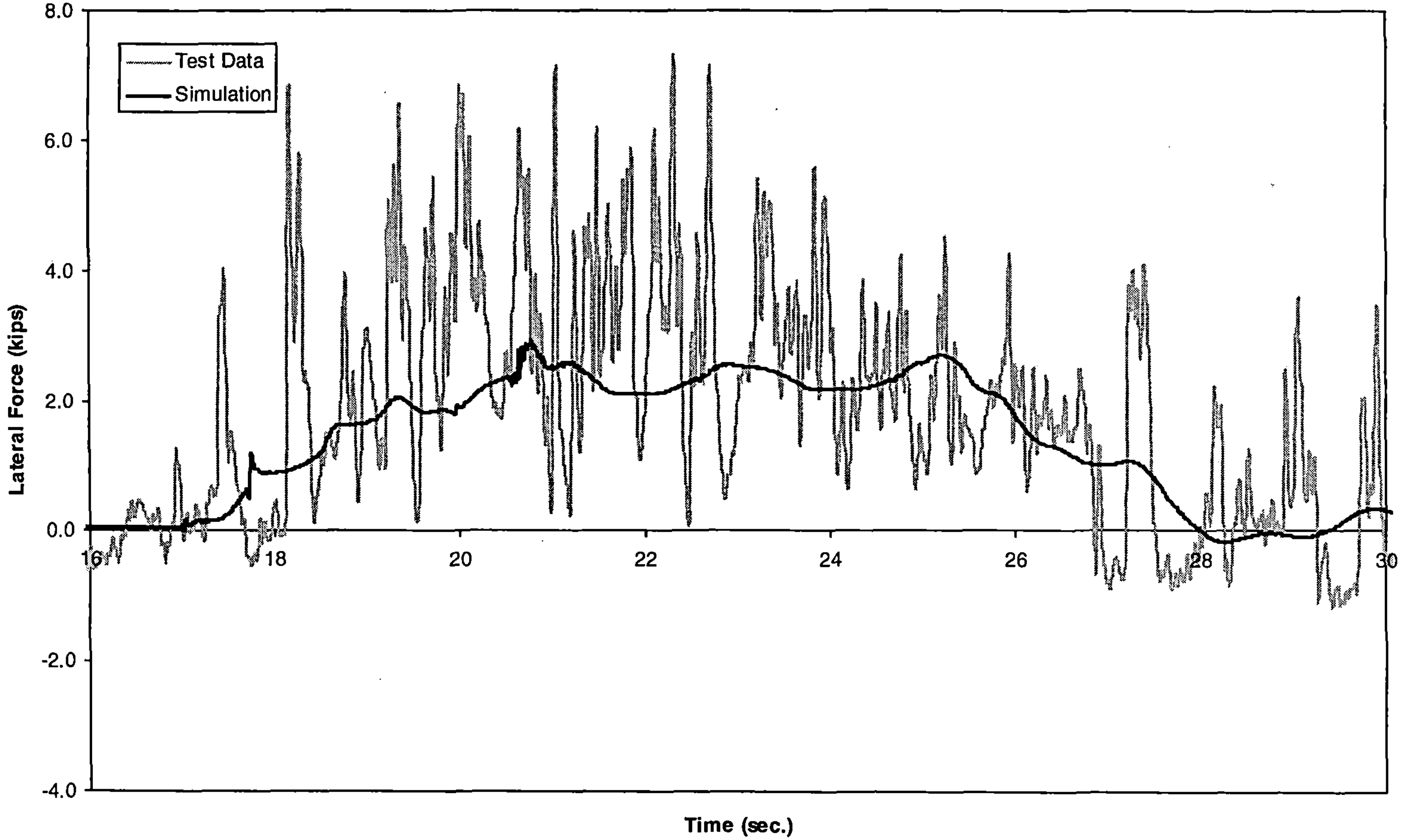

Figure 5-12(c). Steady curving – lateral force time history, 124 mph (trailing outer wheel)

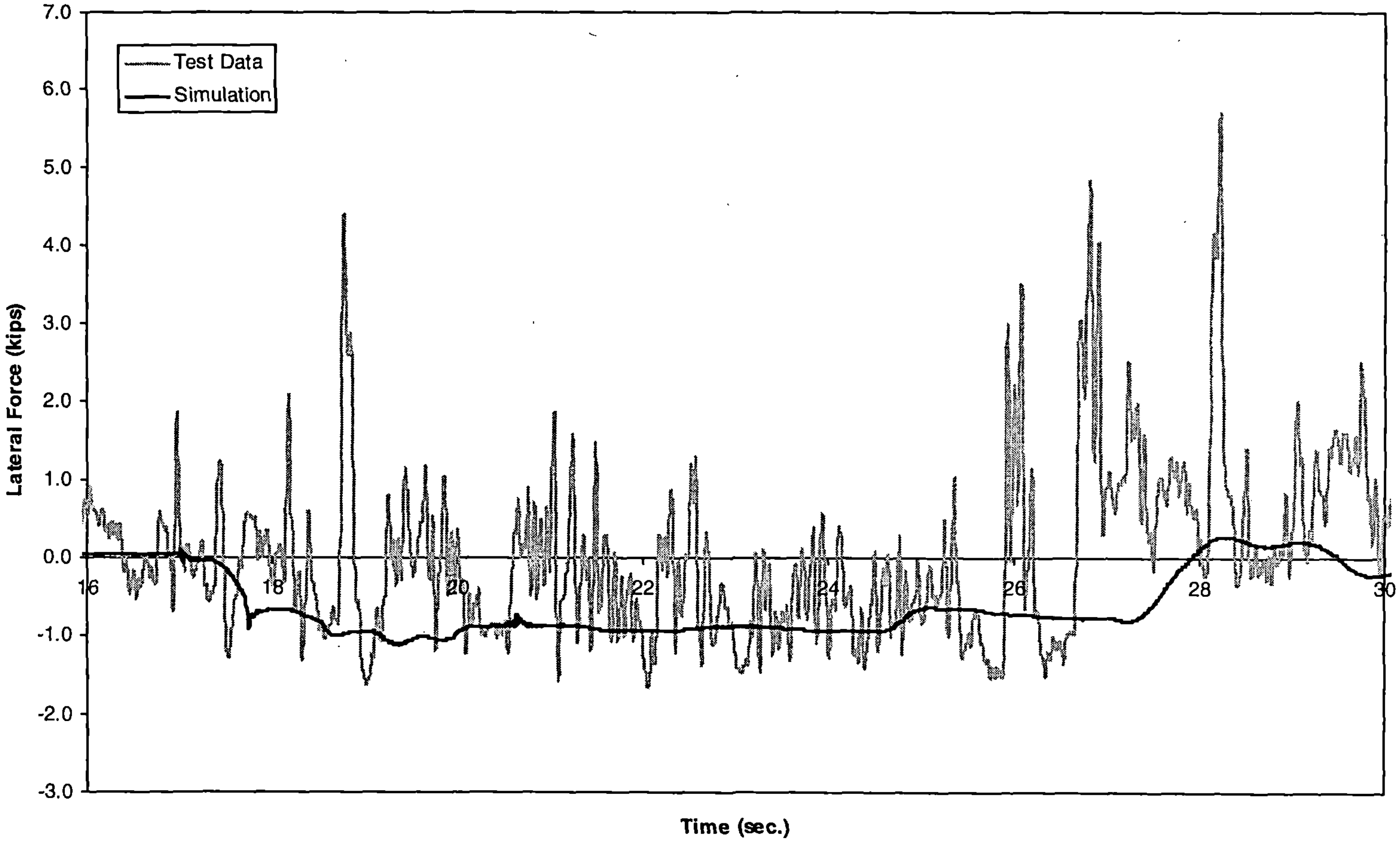

Figure 5-12(d). Steady curving – lateral force time history, 124 mph (trailing inner wheel)

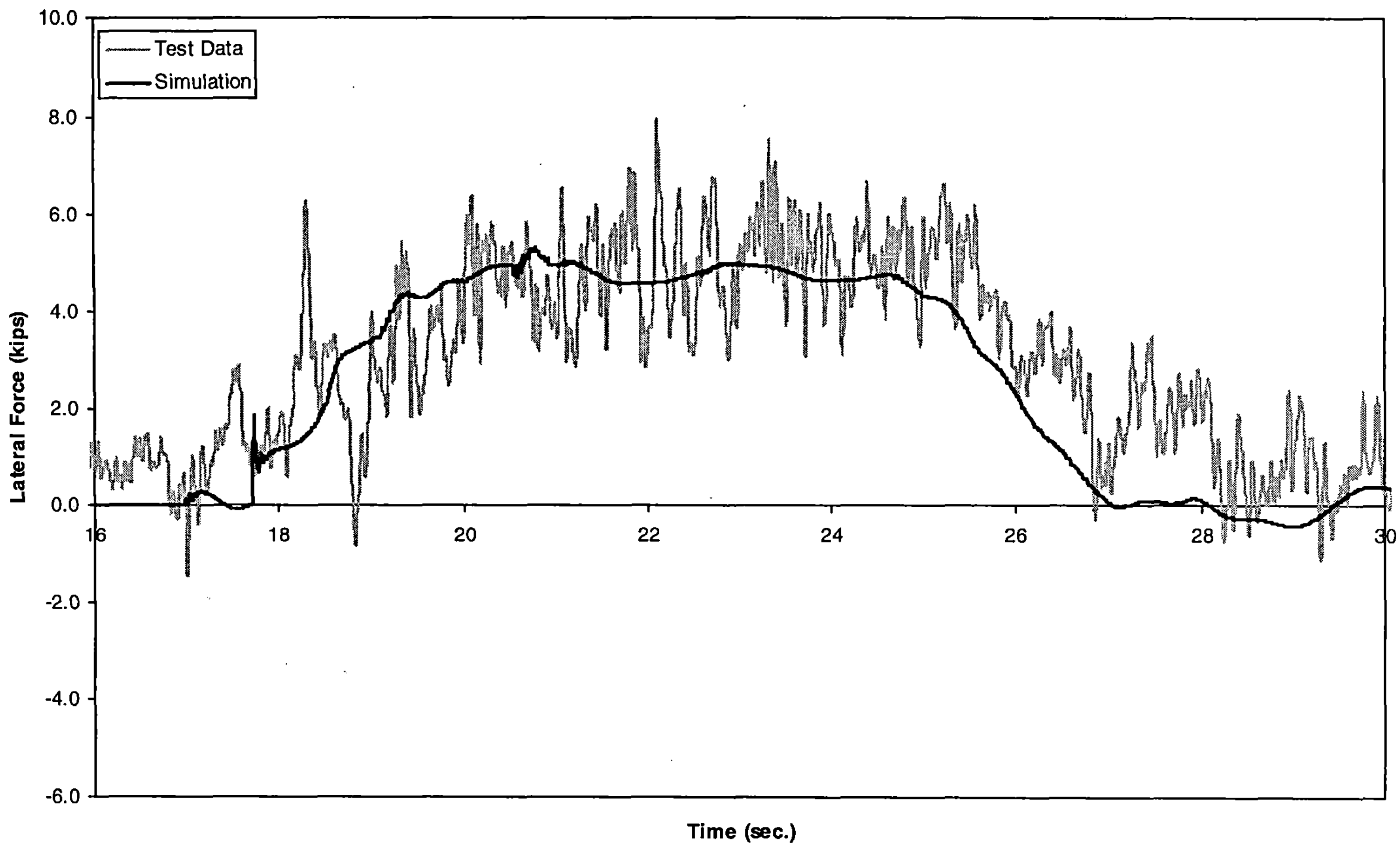

Figure 5-13(a). Steady curving – net axle lateral force time history, 124 mph (lead axle)

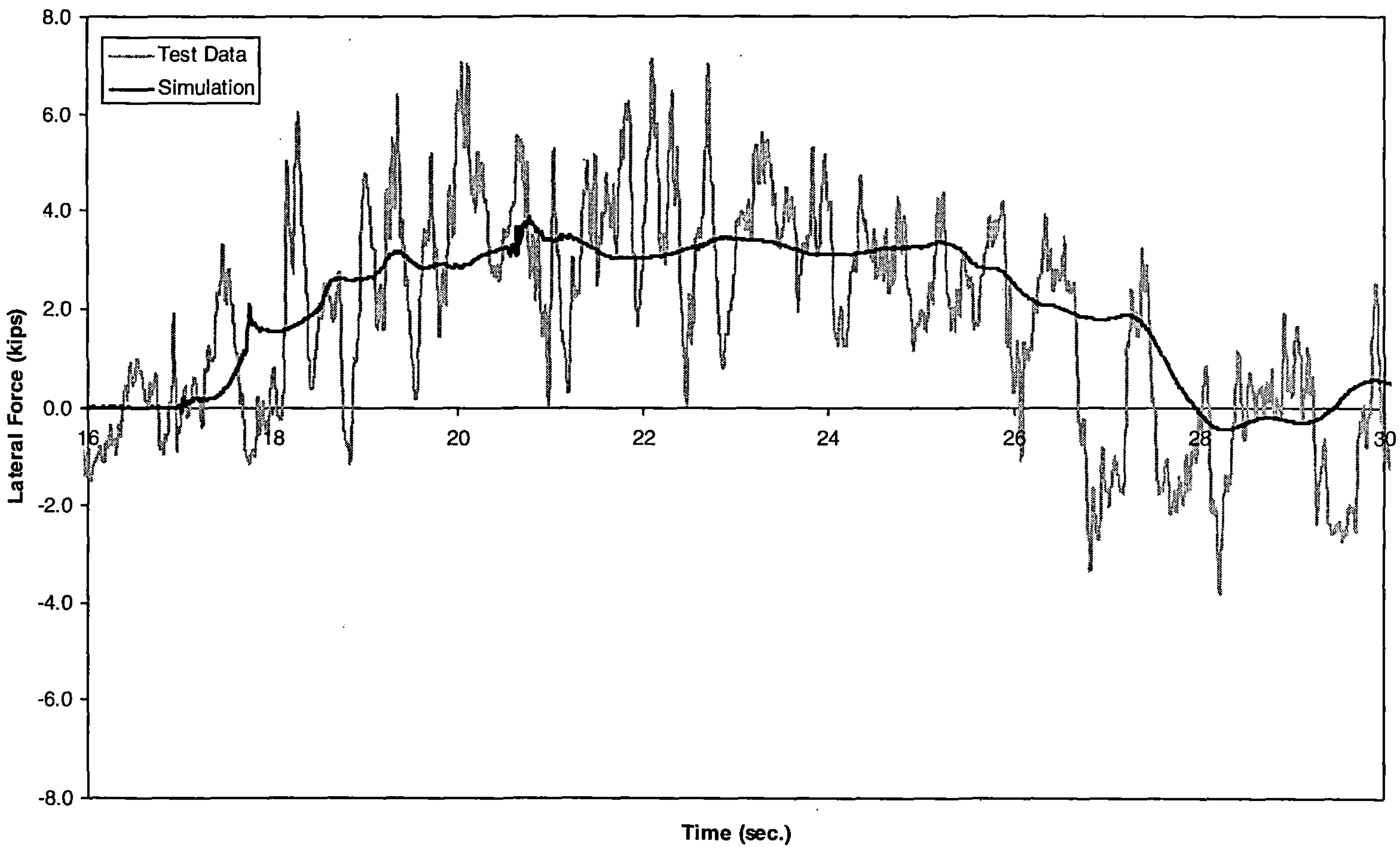

Figure 5-13(b). Steady curving – net axle lateral force time history, 124 mph (trailing axle)

5.3 Dynamic Curving

Test Description

The test for dynamic curving was designed to evaluate safety of the car as it negotiates combinations of vertical profile irregularities and crosslevel in jointed tracks. The resulting forces between the wheel and rail should have an adequate margin of safety against any tendency of the wheel to climb. The 10 deg curved track for dynamic curving consists of five staggered vertical perturbations over a wavelength of 39 ft, with a crosslevel of 0.5 in. (see Figure 5-14). The latter was achieved by appropriately shimming the rails, which also creates combined gage and alignment variations. The maximum gage of 57.5 in. corresponds to the low points of the outer rail. The minimum gage of 56.5 in. corresponds to the low points on the inner rail. This is shown in Figure 5-15. The tests were performed at speeds in the range of 10 to 32 mph.

Correlation

The vertical and lateral forces for the trailing truck wheels are shown in Figures 5-16 and 5-17, respectively for operation at 20 mph. The vertical force simulation and test data are in good agreement. The vertical forces vary from 14 to 20 kips as the perturbations are negotiated. The lateral force waveforms for the simulation and test data are similar for the trailing axle wheels, and the amplitudes are in good agreement. For the lead axle, simulation data shows higher (by approximately 4 kips) average values of force on both the outer and inner wheels. (This difference is similar to the difference seen in the steady-state curving tests.)

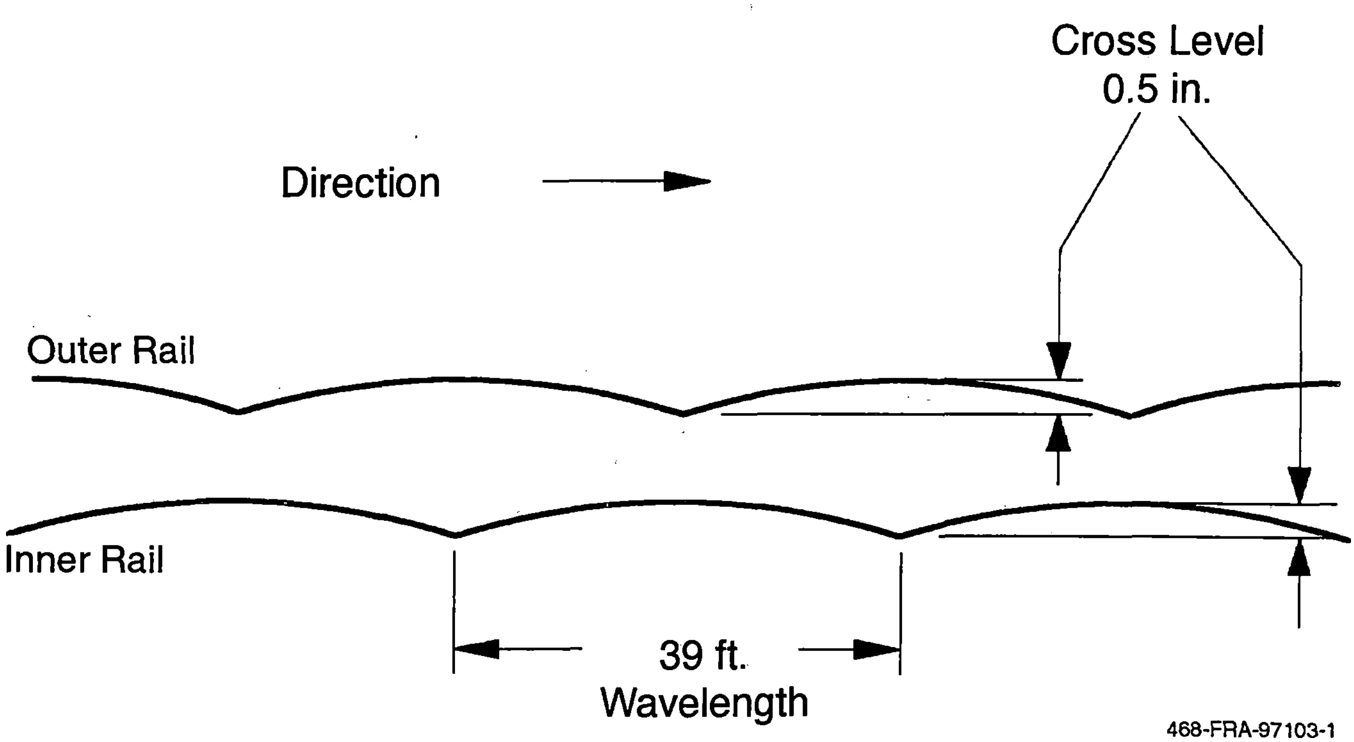

Figure 5-14. Crosslevel variation for dynamic curving

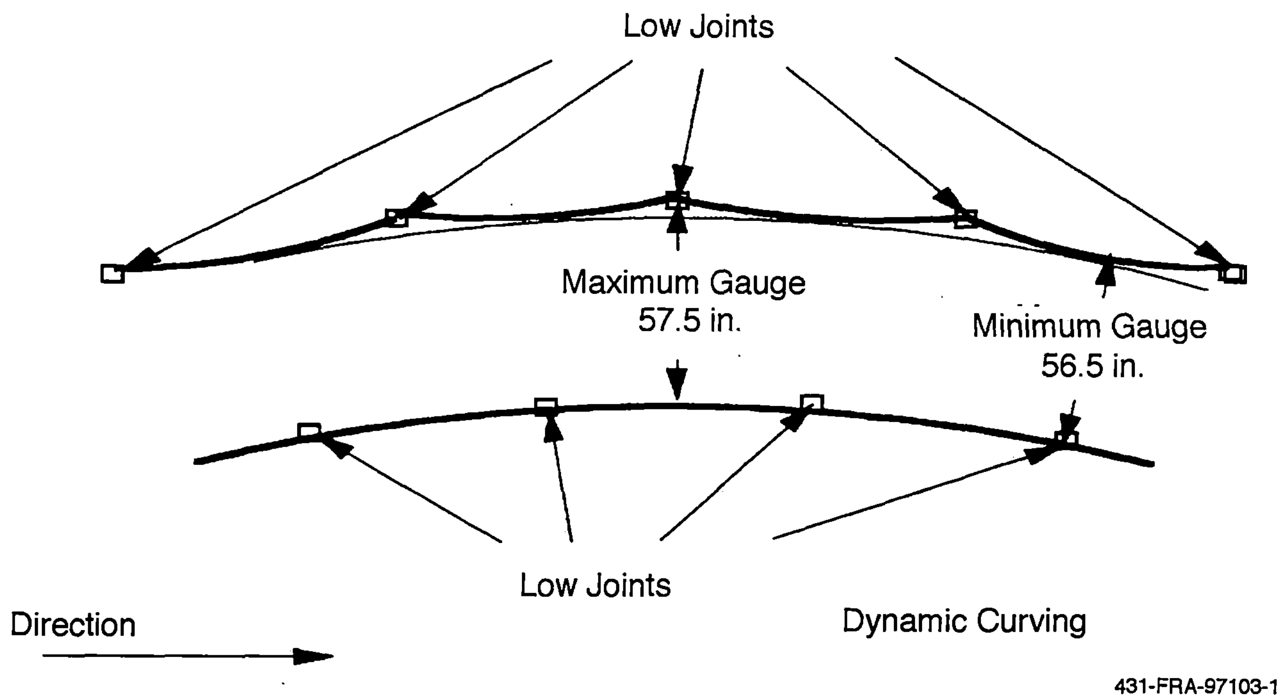

Figure 5-15. Gage and alignment variation for dynamic curving

Data for operation at 28 mph, illustrated in Figure 5-18, also indicate good correspondence between the vertical forces predicted and measured for all four wheels. The lateral force data of Figure 5-19 for the trailing axle are also in reasonable agreement. The lead axle simulation has an average value of approximately 3 to 4 kips greater than the test data for the inner and outer wheels.

A plot of the minimum vertical force and maximum lateral force occurring during the tests is shown in Figures 5-20 and 5-21. Good correlation is shown through the speed range for the vertical force. The lateral force correlation is not as good. The maximum absolute lateral carbody acceleration at the "B" end is shown in Figure 5-22. The test data have lower values of acceleration than the simulation over the speed range.

Conclusion

The simulation has good correlation for the vertical force at all speeds, however, the correlation for the lateral force is not as good. The simulation predicts well the shape and amplitude of the vertical forces. The predicted lateral forces have the same shape as test lateral forces but their amplitudes are larger. The overall safe behavior of the vehicle observed in the test is consistent with the simulation predictions.

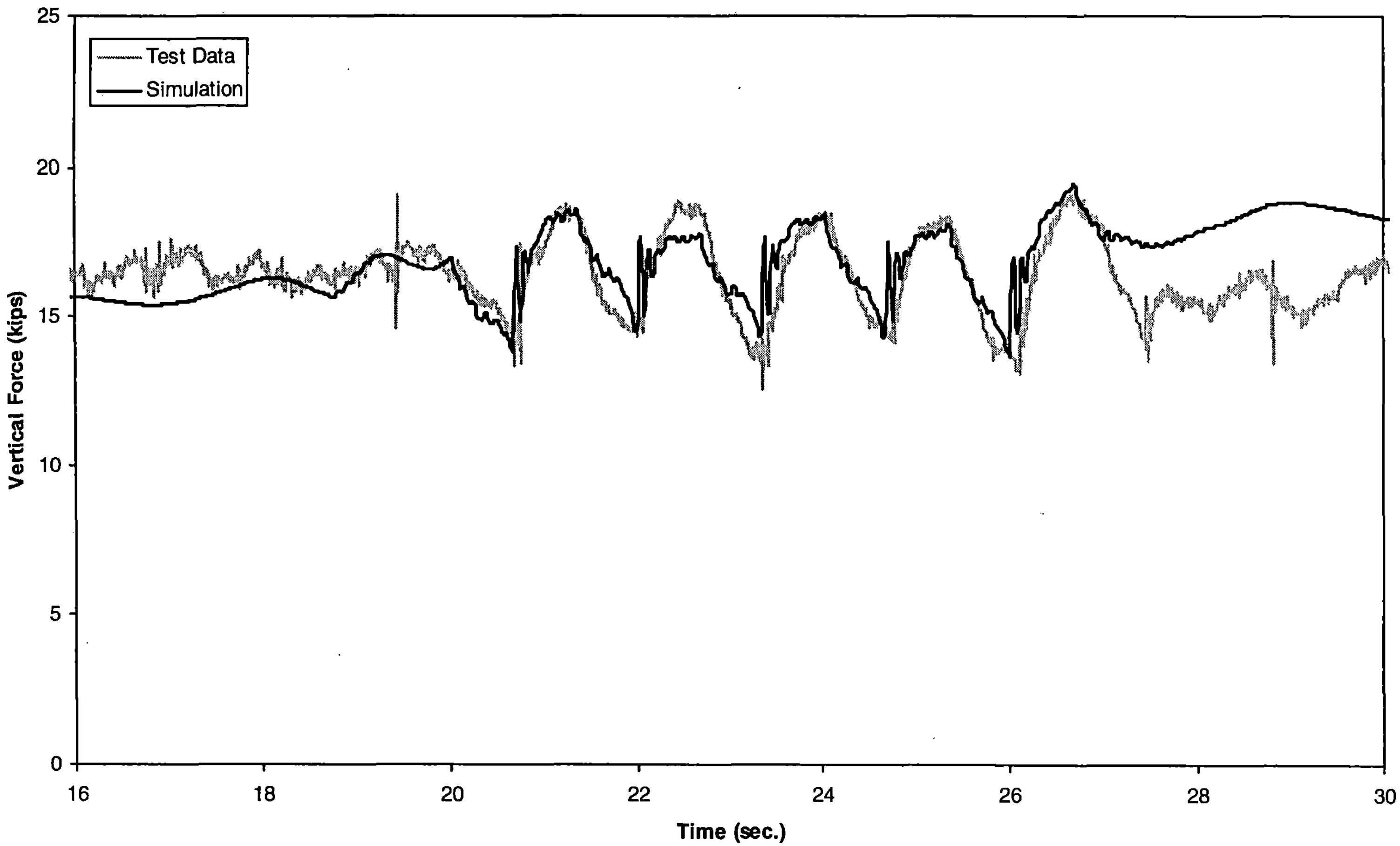

Figure 5-16(a). Dynamic curving – vertical force time history, 20 mph (lead outer wheel)

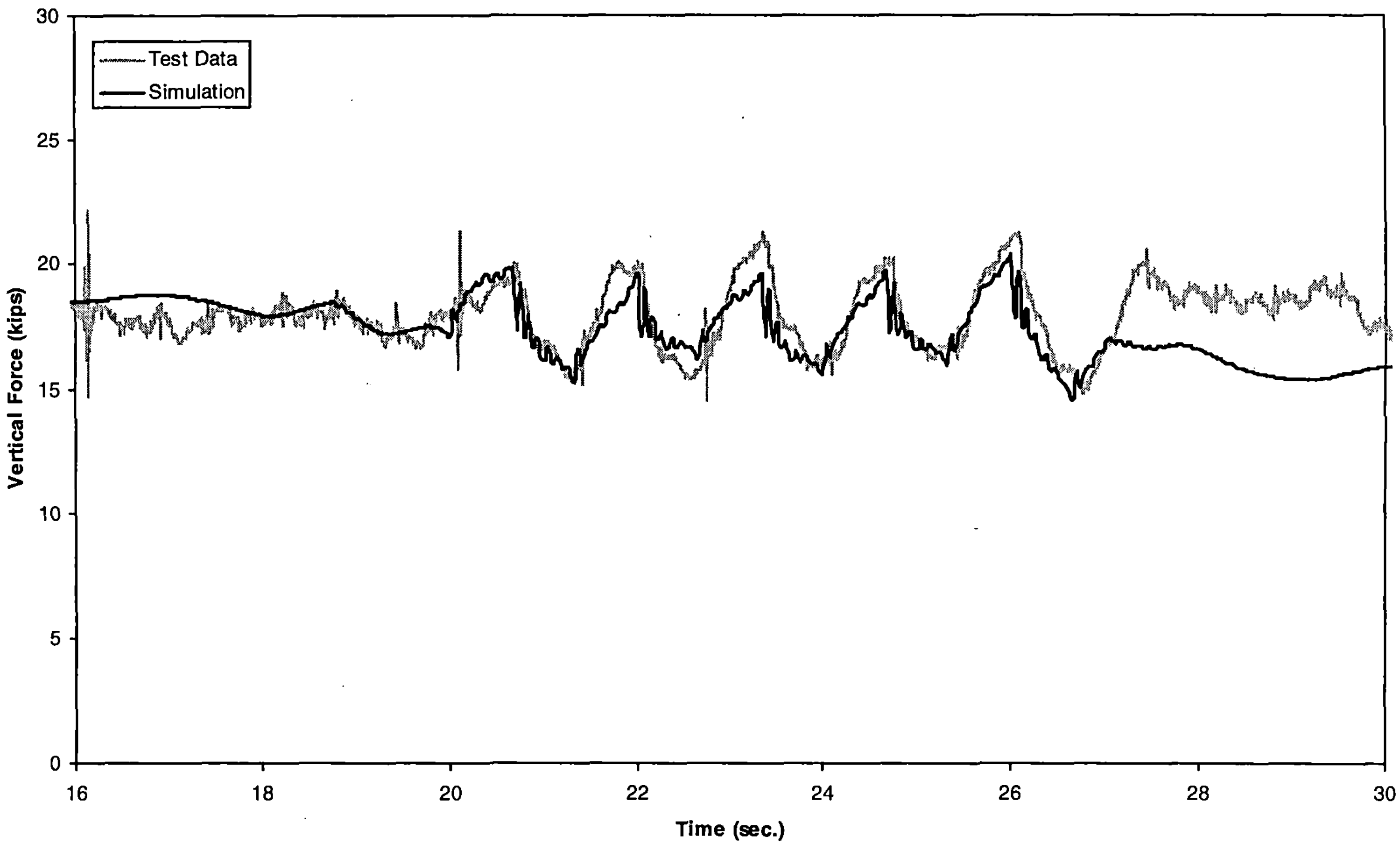

Figure 5-16(b). Dynamic curving – vertical force time history, 20 mph (lead inner wheel)

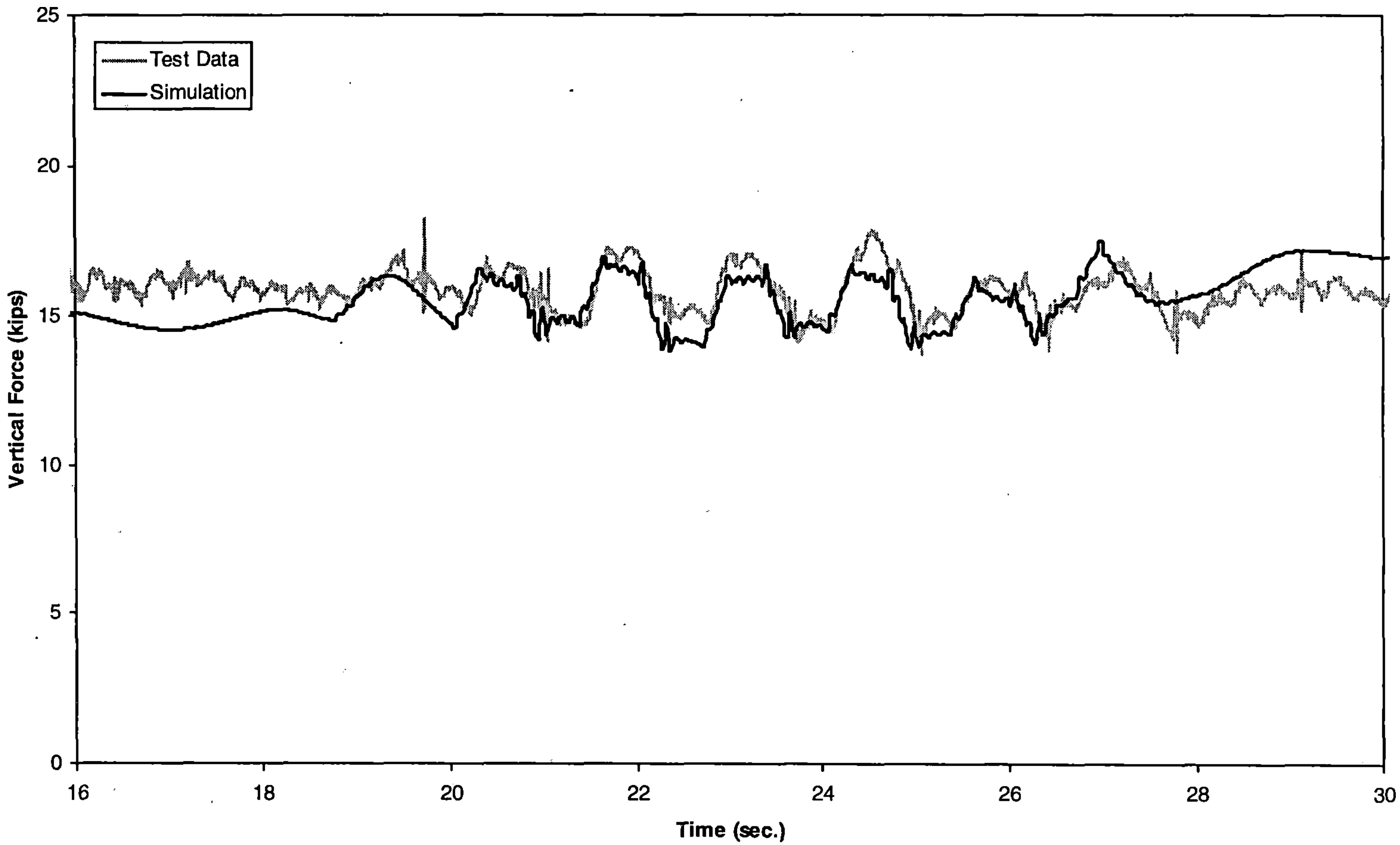

Figure 5-16(c). Dynamic curving – vertical force time history, 20 mph (trailing outer wheel)

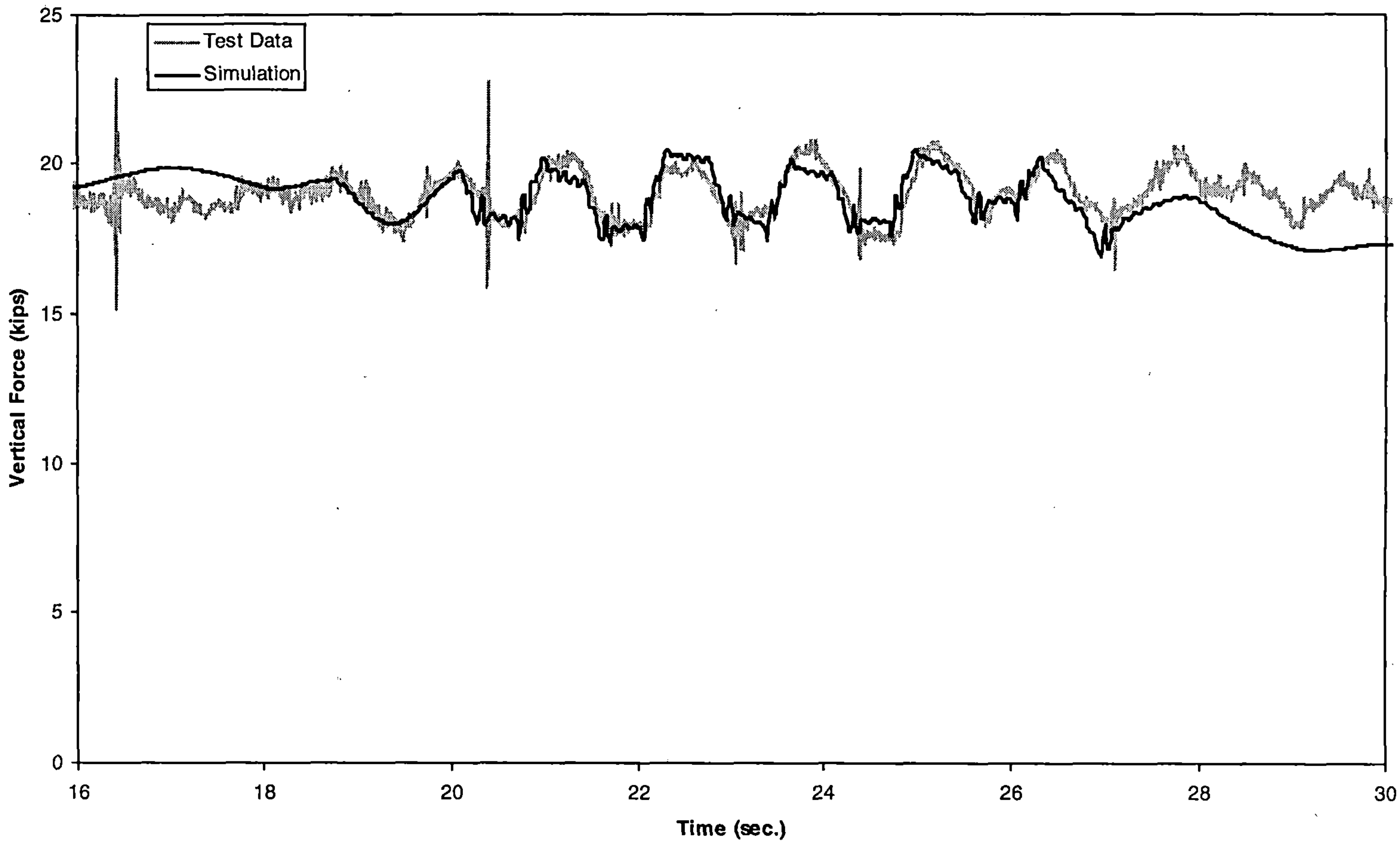

Figure 5-16(d). Dynamic curving – vertical force time history, 20 mph (trailing inner wheel)

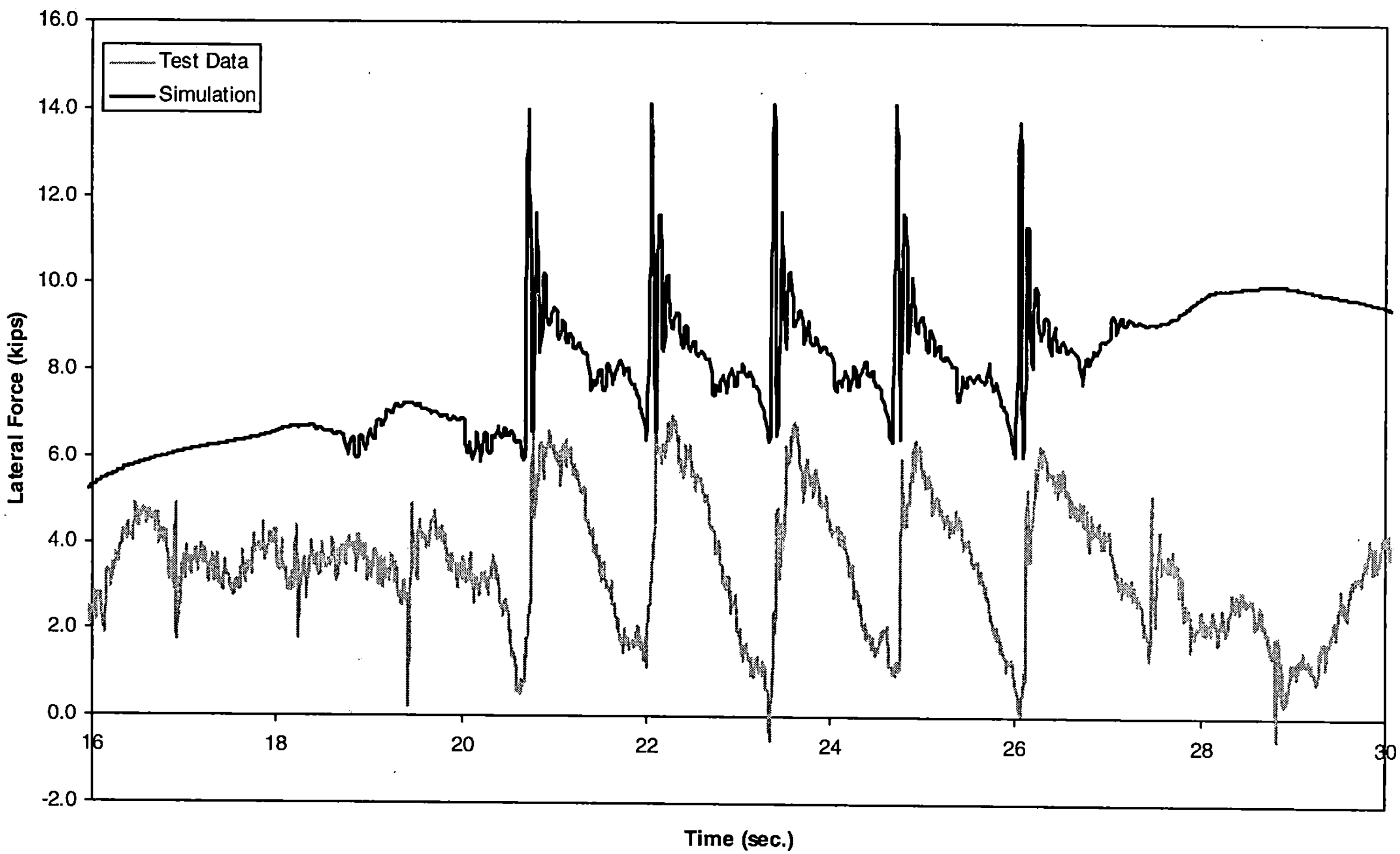

Figure 5-17(a). Dynamic curving – lateral force time history, 20 mph (lead outer wheel)

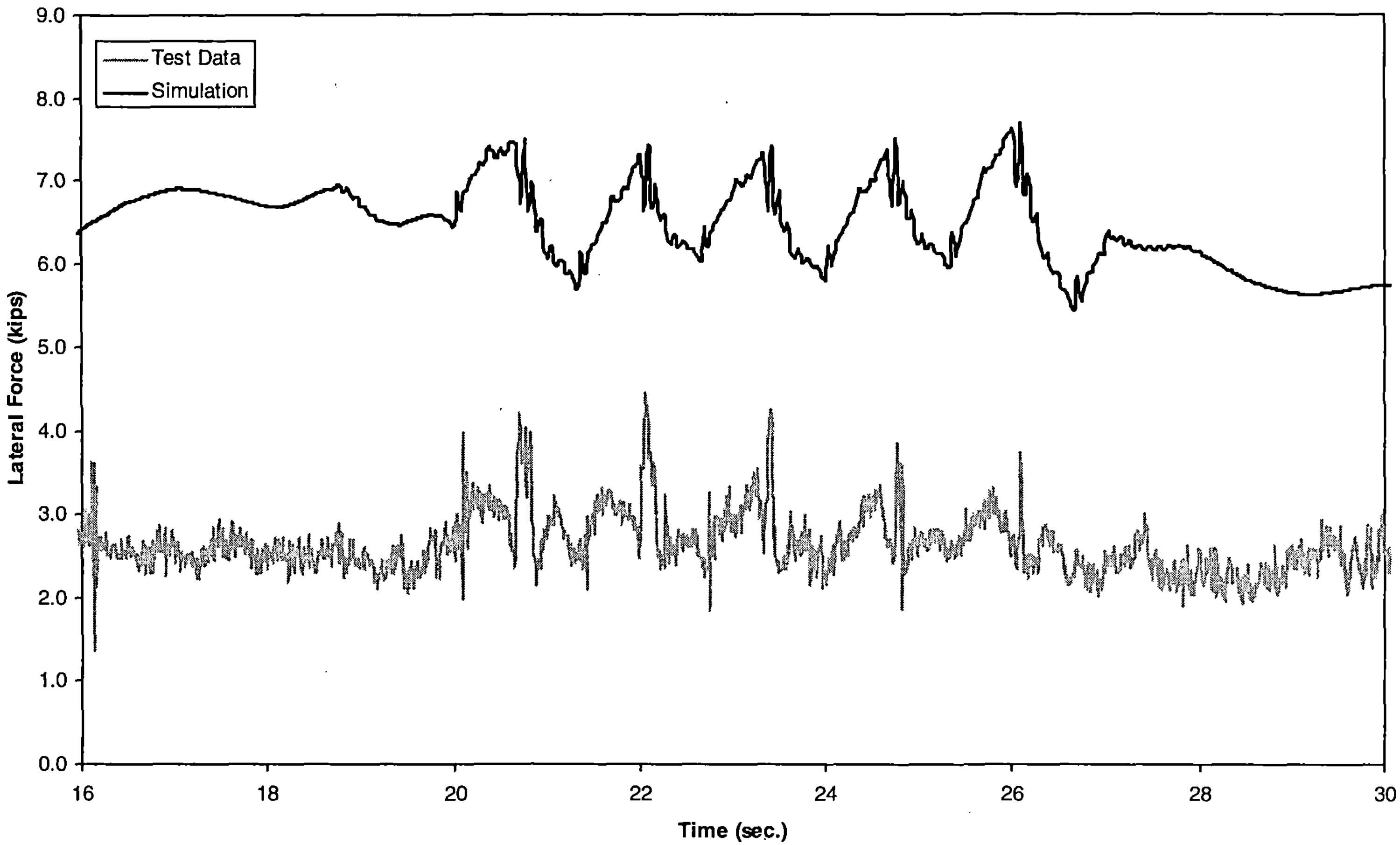

Figure 5-17(b). Dynamic curving – lateral force time history, 20 mph (lead inner wheel)

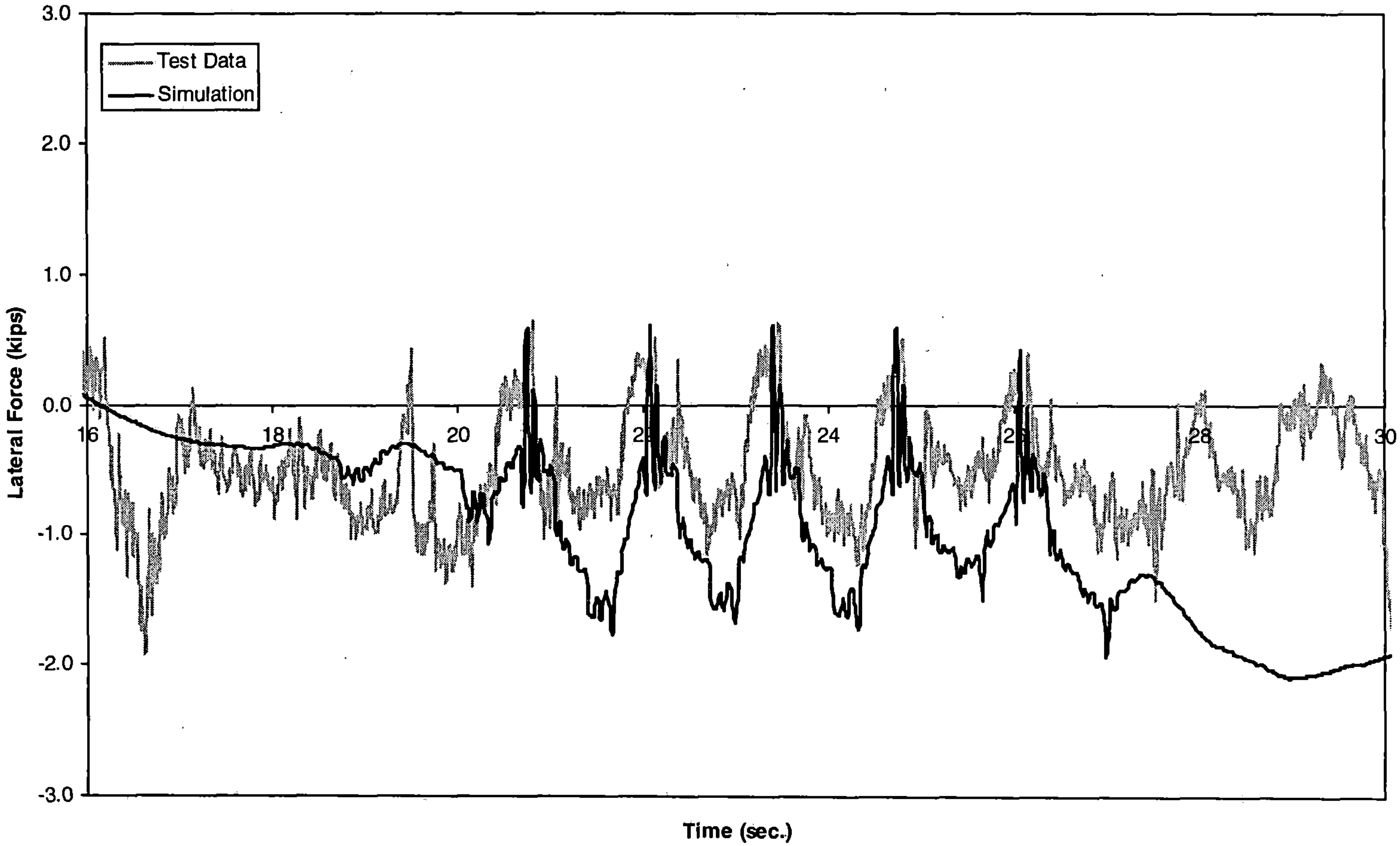

Figure 5-17(c). Dynamic curving – lateral force time history, 20 mph (trailing outer wheel)

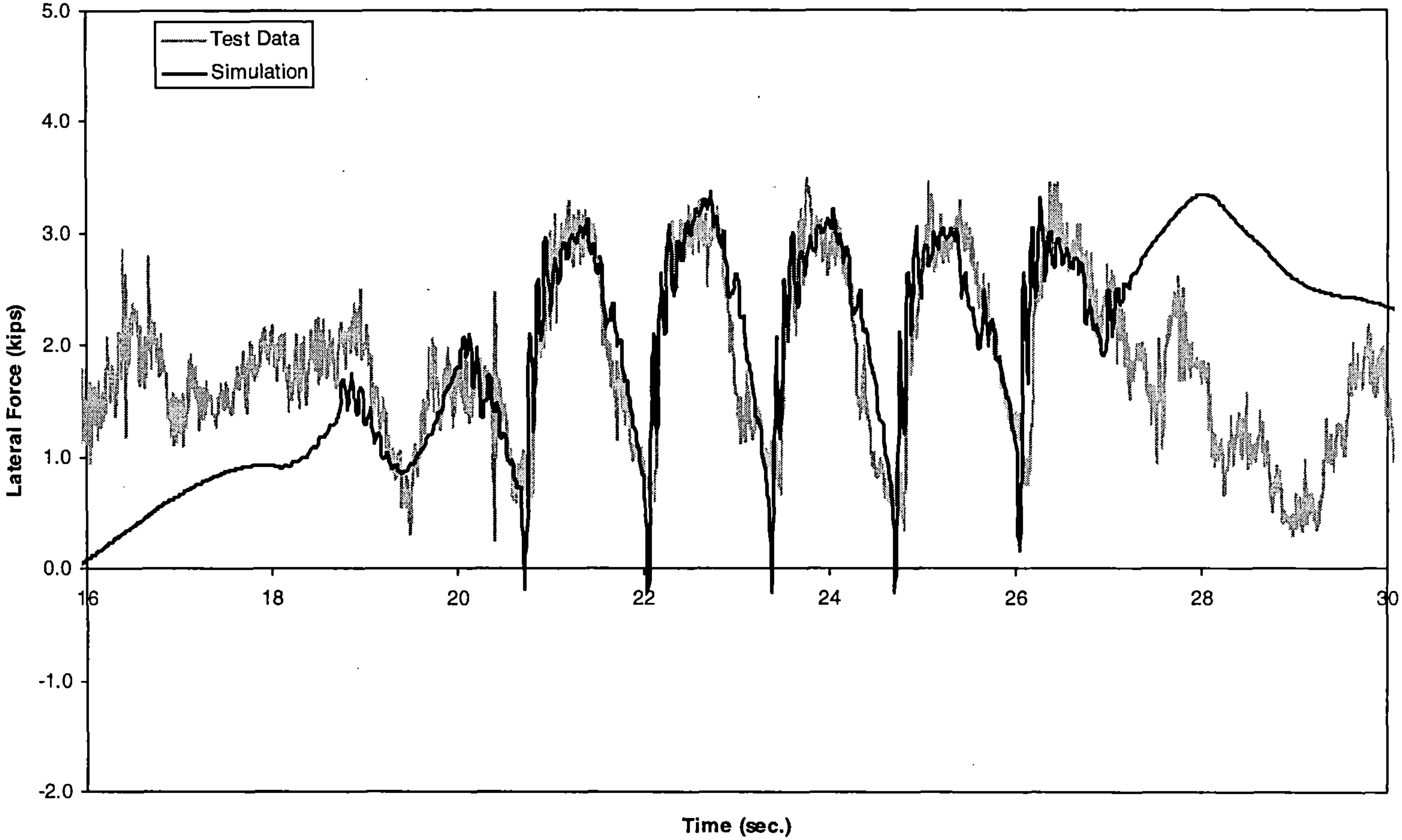

Figure 5-17(d). Dynamic curving – lateral force time history, 20 mph (trailing inner wheel)

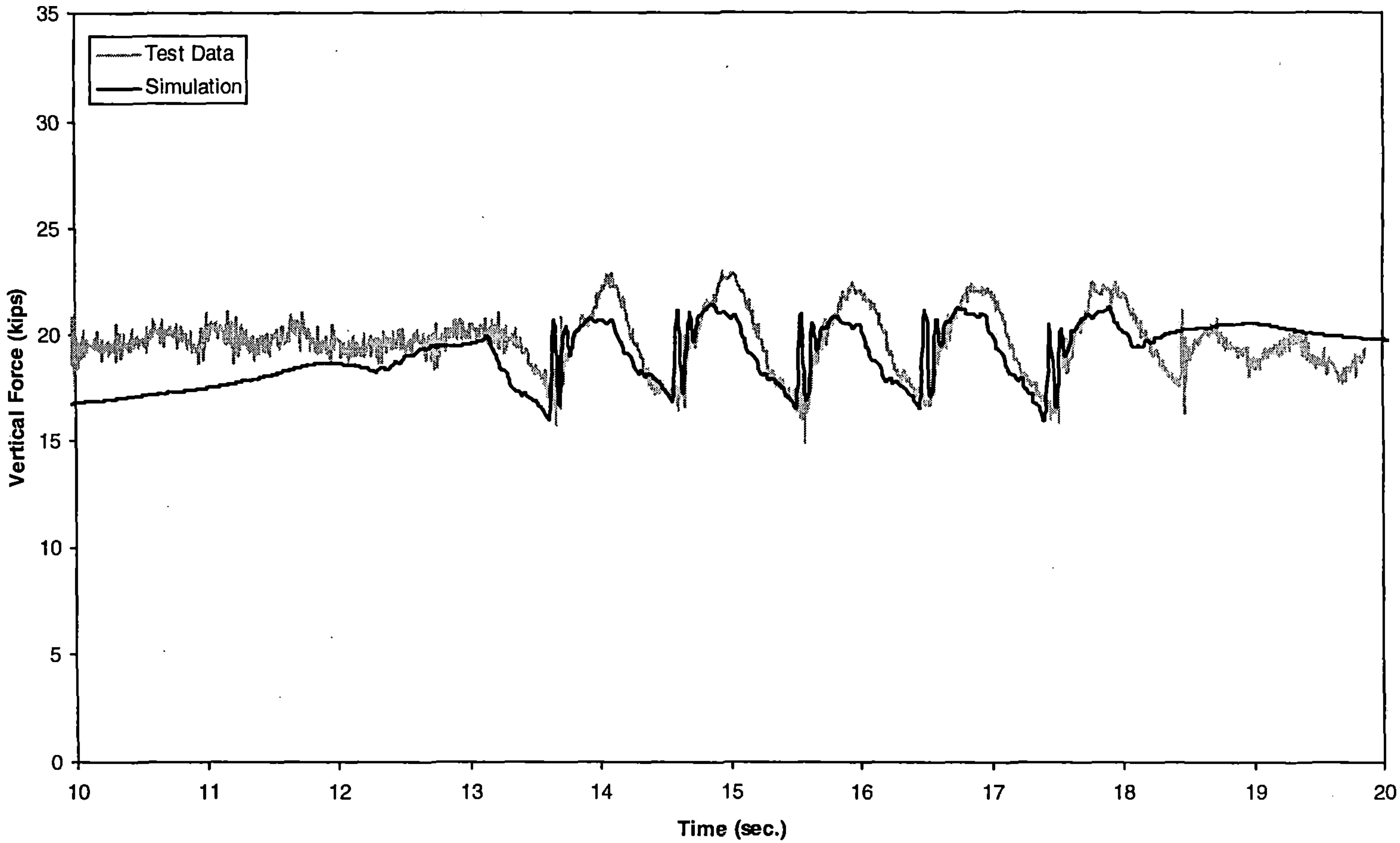

Figure 5-18(a). Dynamic curving – vertical force time history, 28 mph (lead outer wheel)

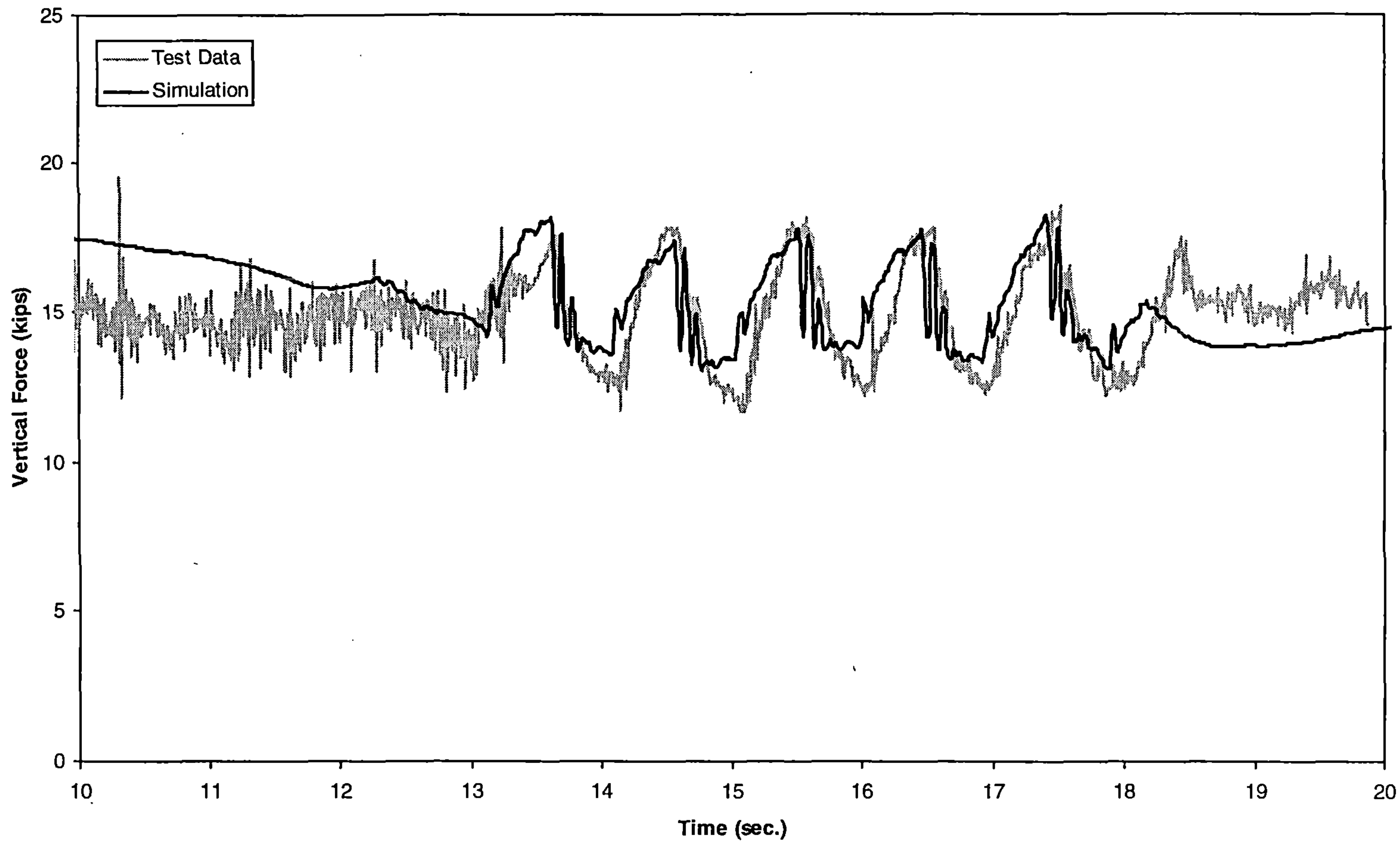

Figure 5-18(b). Dynamic curving – vertical force time history, 28 mph (lead inner wheel)

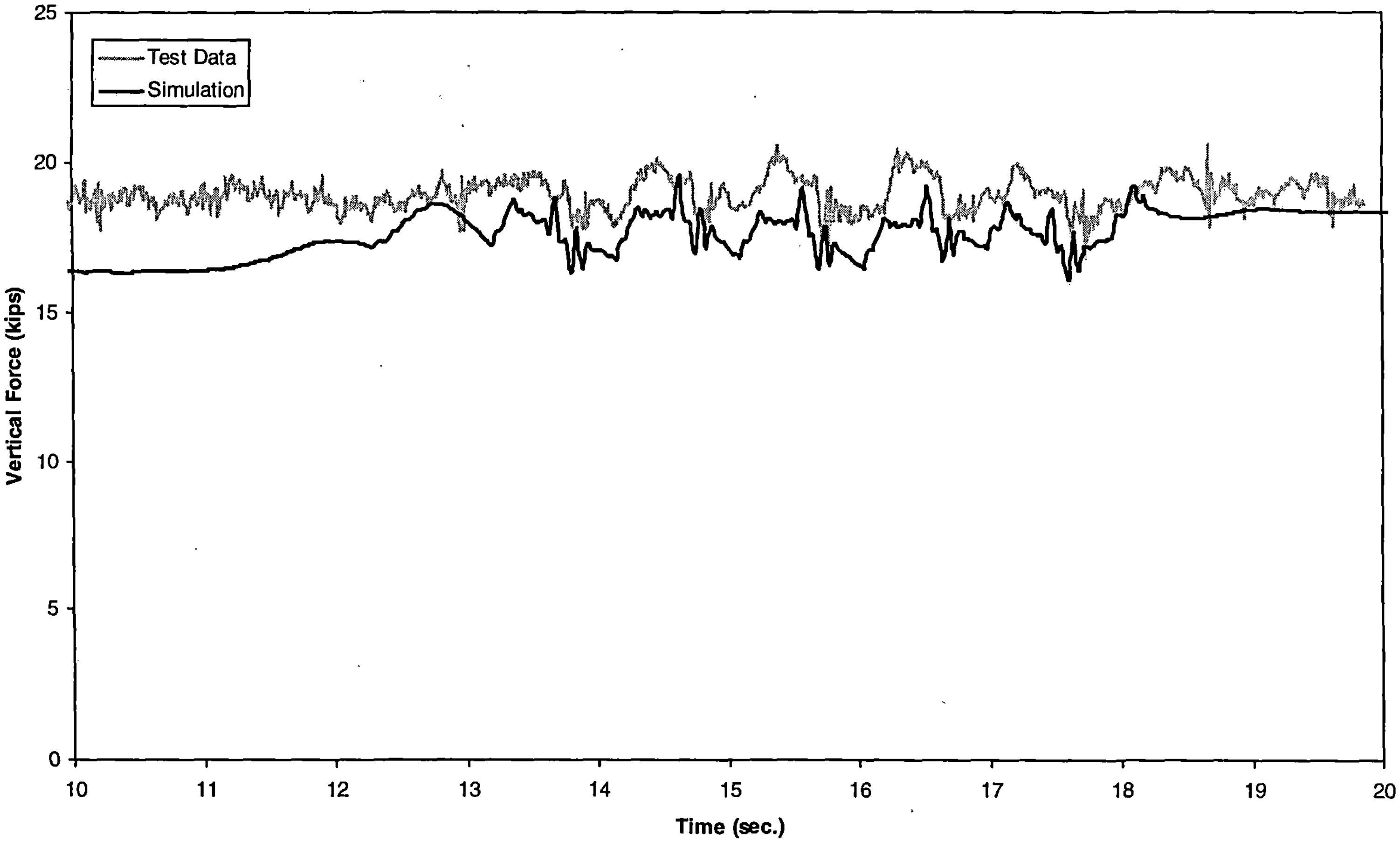

Figure 5-18(c). Dynamic curving – vertical force time history, 28 mph (trailing outer wheel)

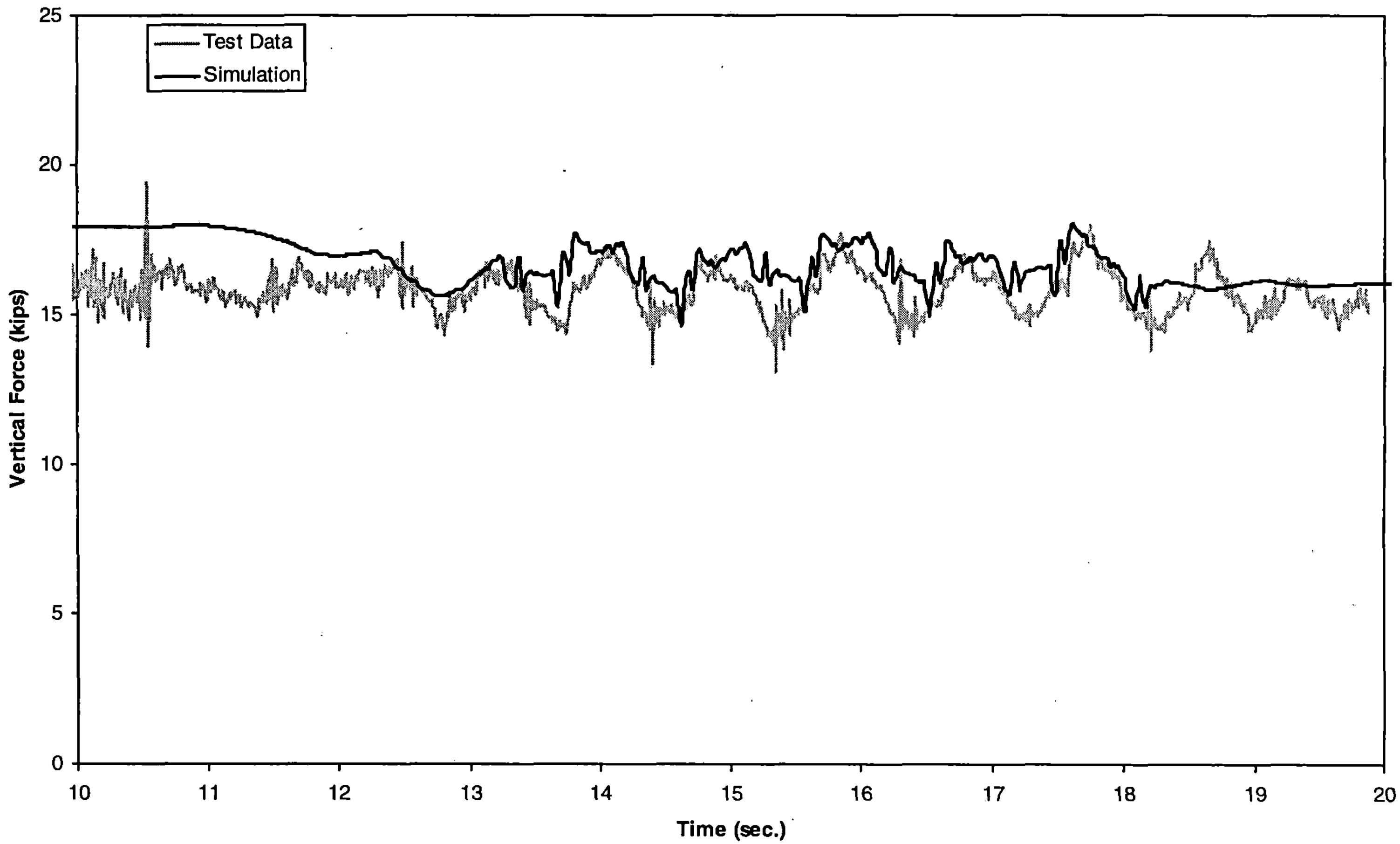

Figure 5-18(d). Dynamic curving – vertical force time history, 28 mph (trailing inner wheel)

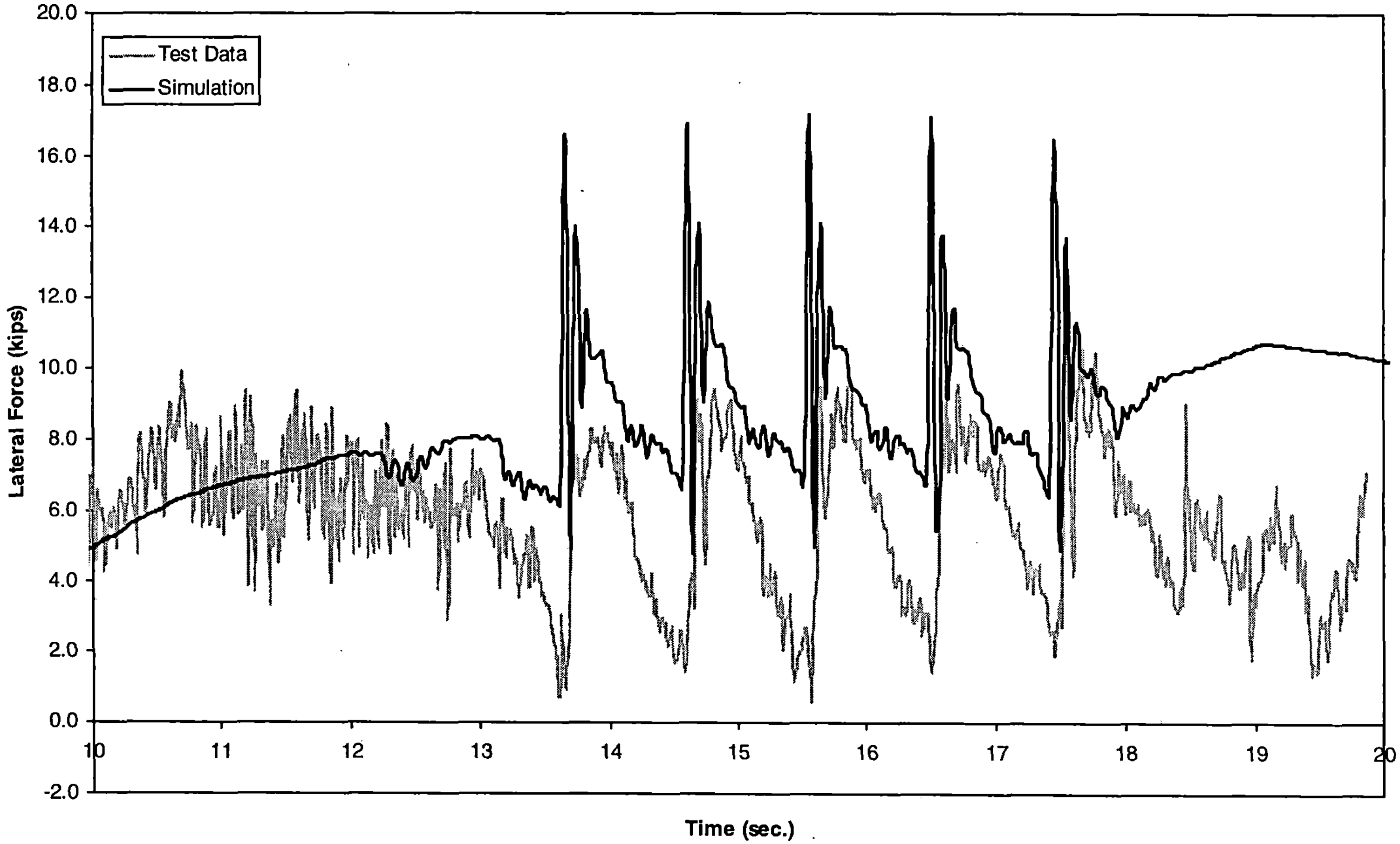

Figure 5-19(a). Dynamic curving – lateral force time history, 28 mph (lead outer wheel)

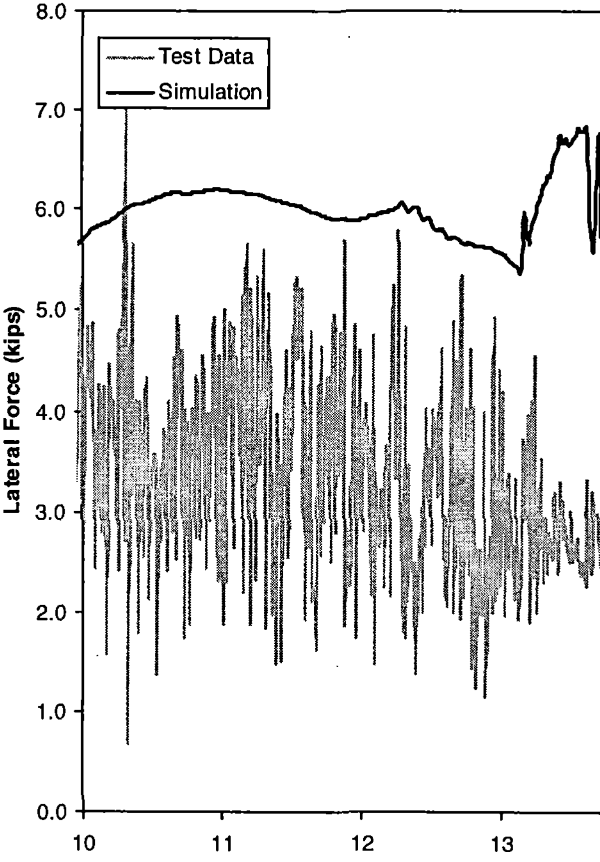

Figure 5-19(b). Dynamic curving –

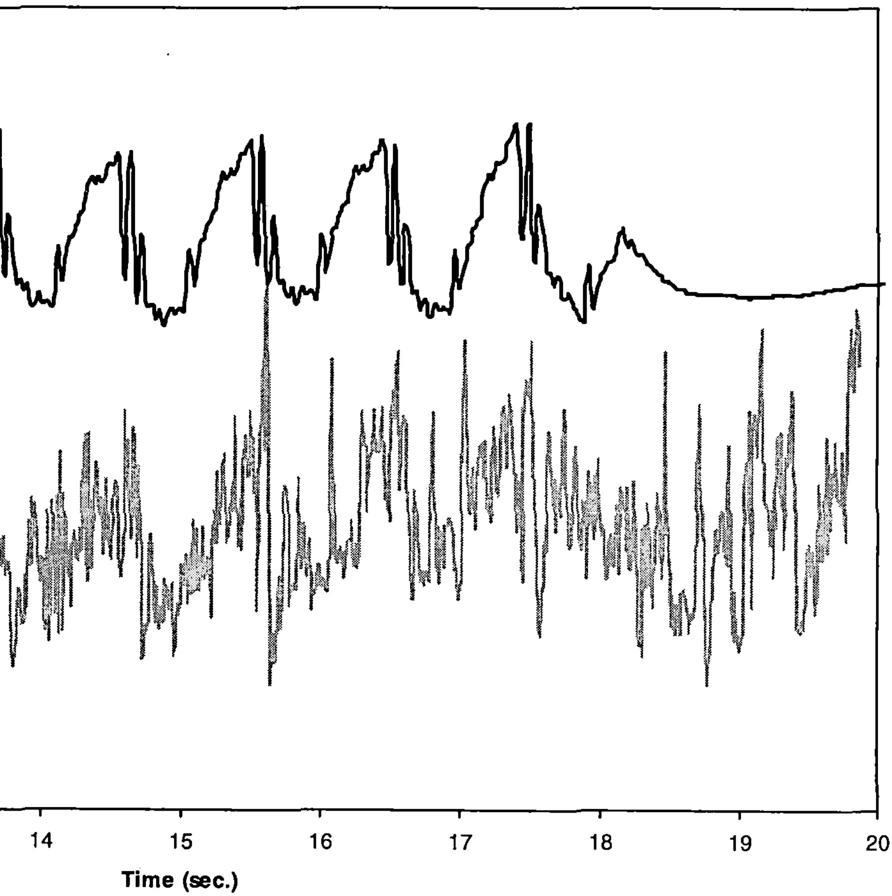

- lateral force time history, 28 mph (lead inner wheel)

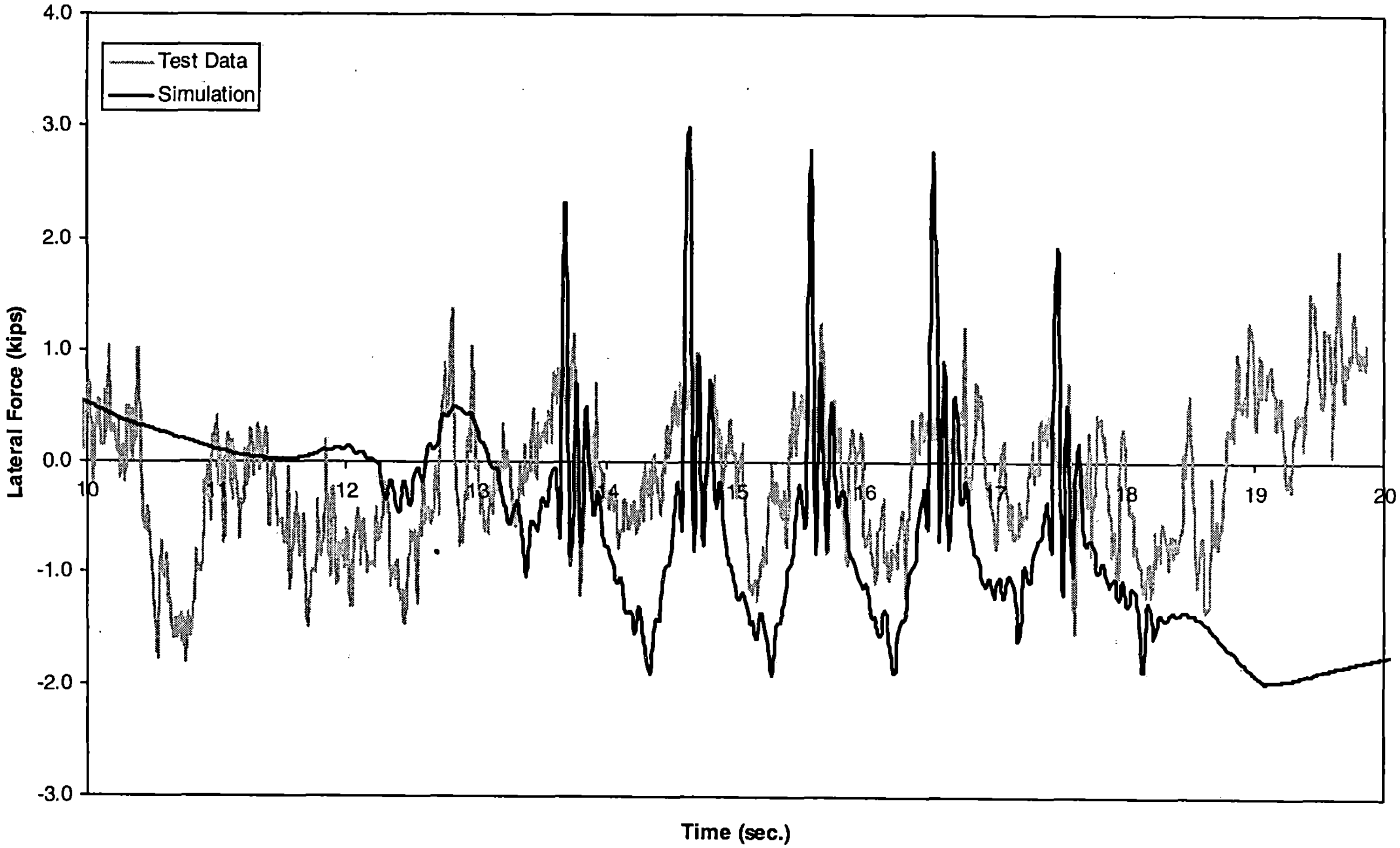

Figure 5-19(c). Dynamic curving – lateral force time history, 28 mph (trailing outer wheel)

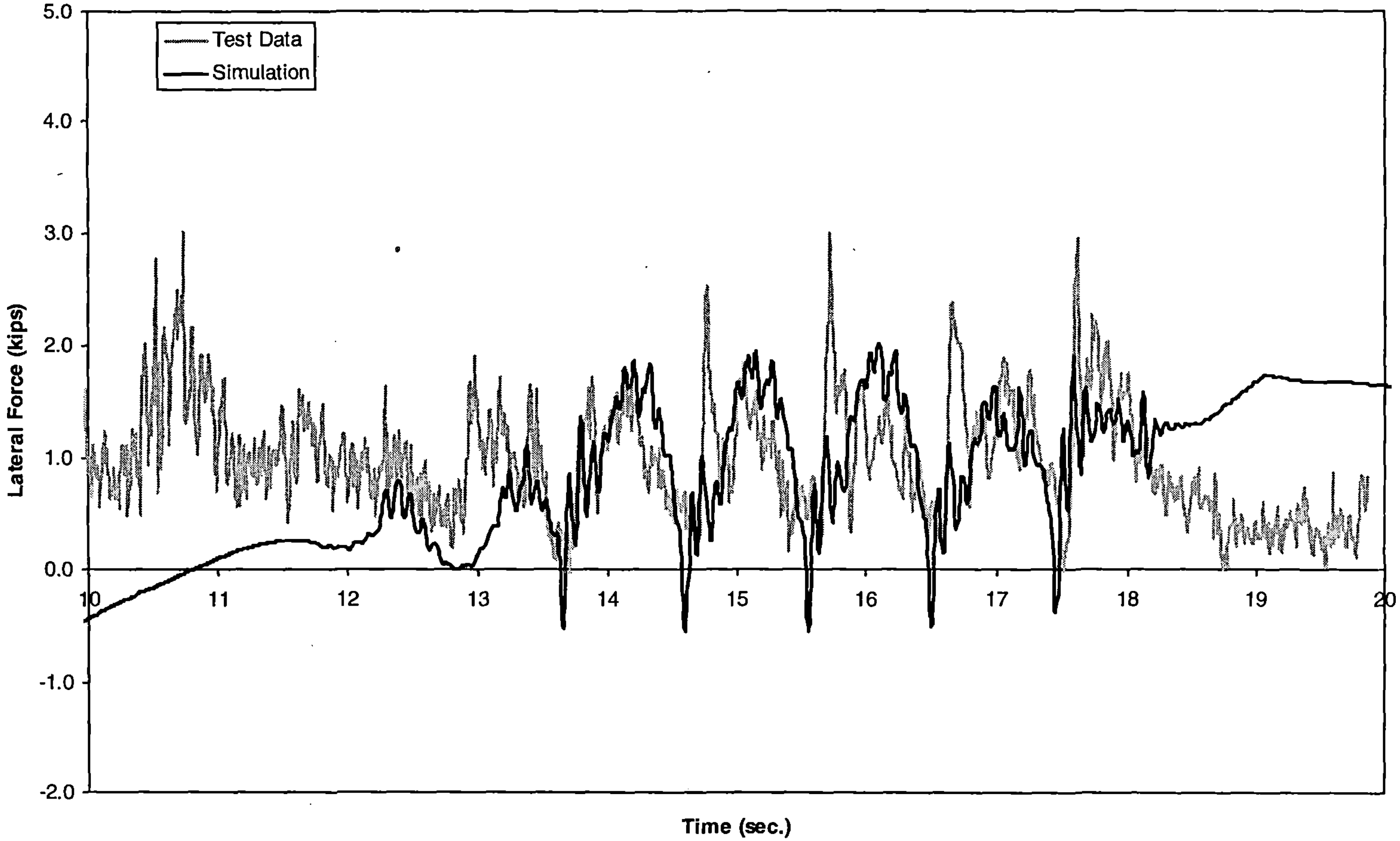

Figure 5-19(d). Dynamic curving – lateral force time history, 28 mph (trailing inner wheel)

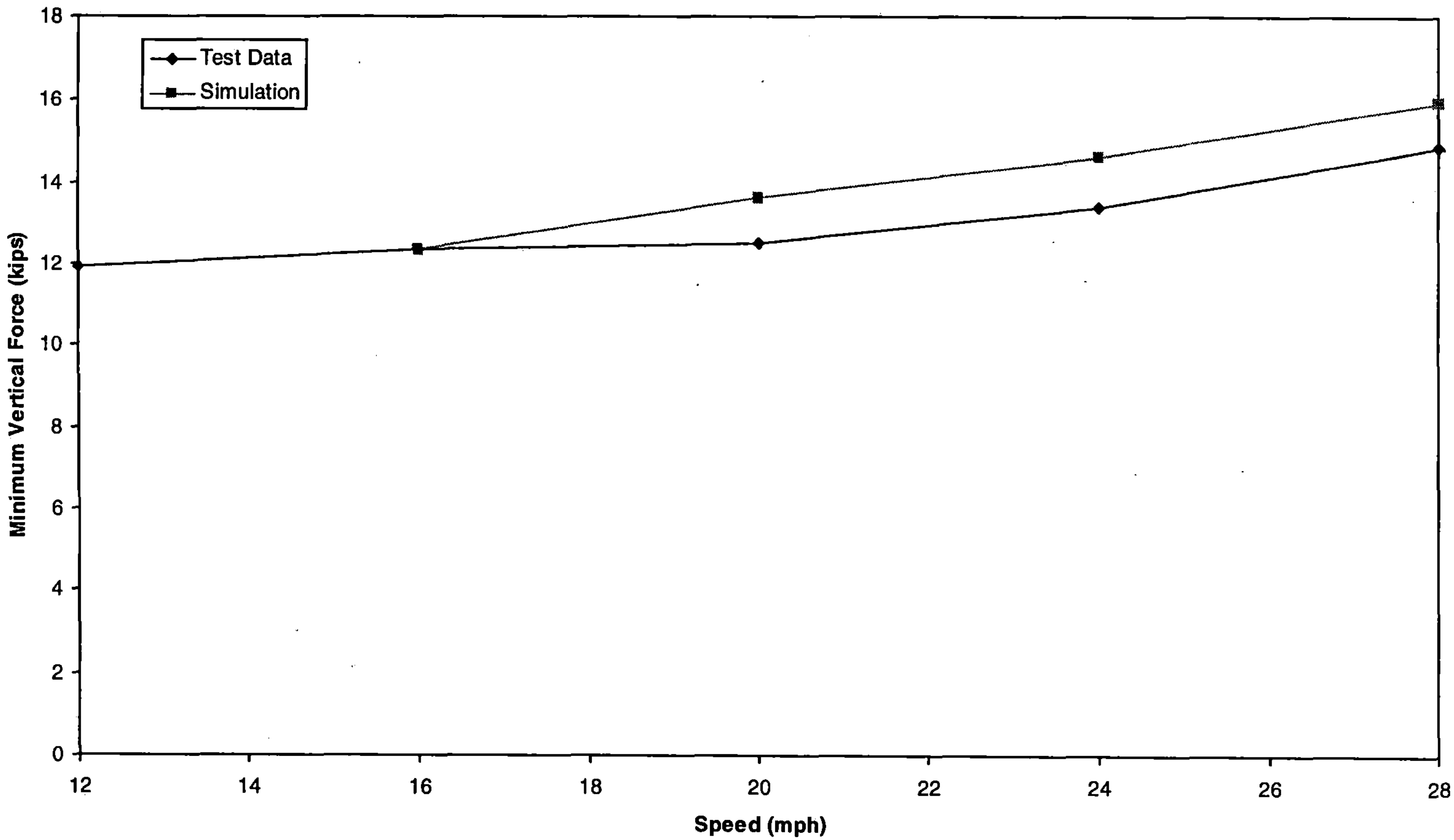

Figure 5-20. Dynamic curving – minimum vertical force

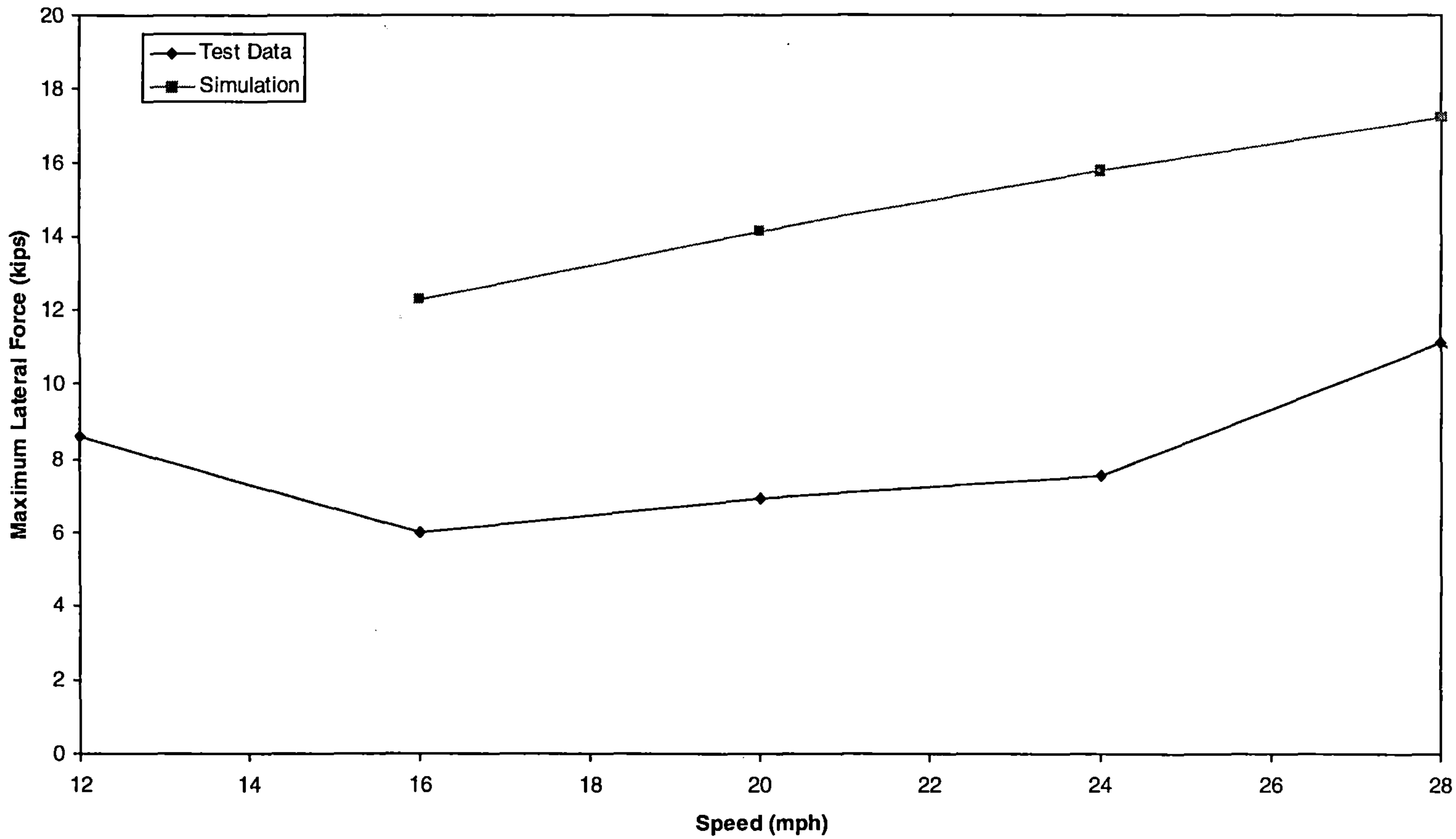

Figure 5-21. ***Dynamic curving – maximum lateral force***

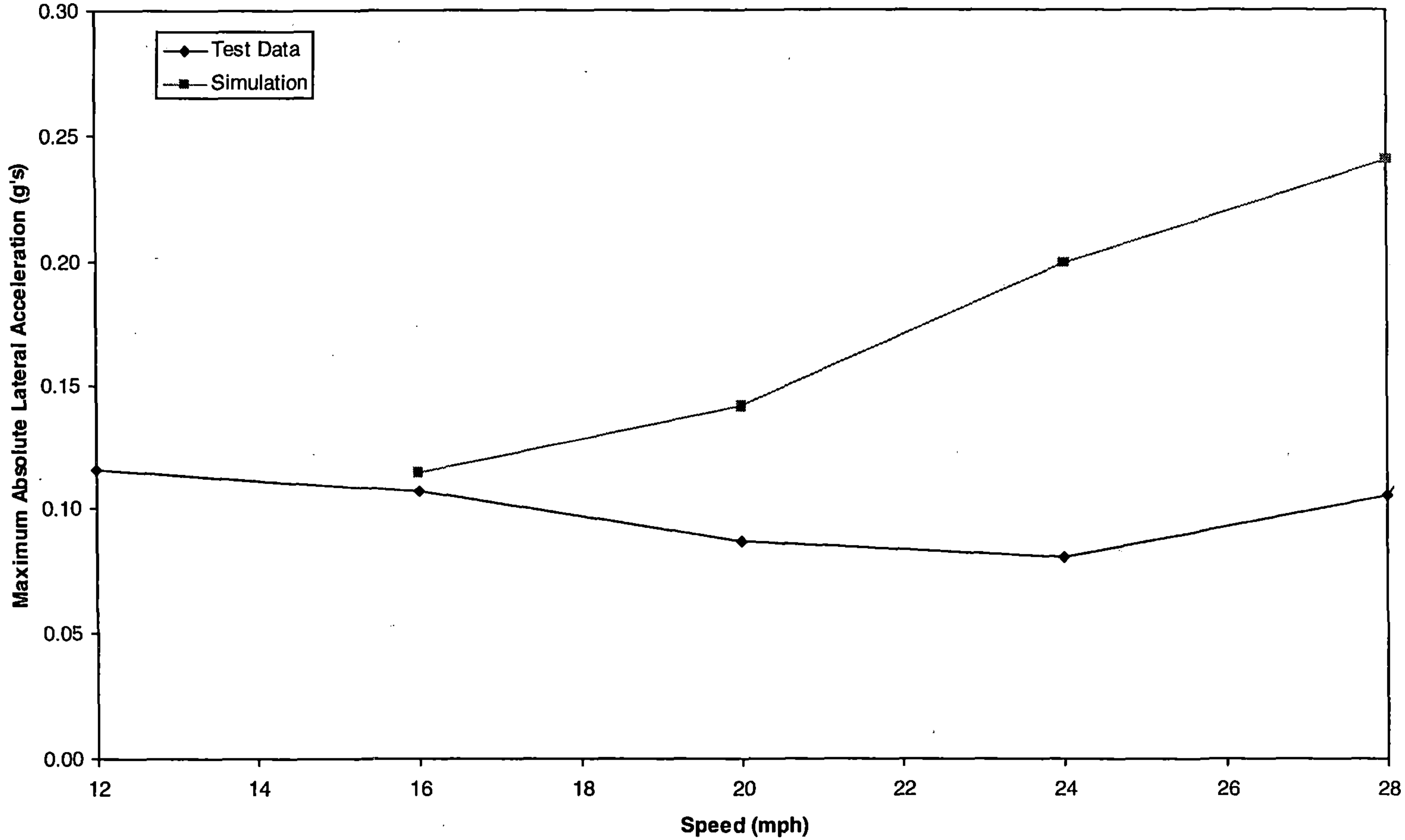

Figure 5-22. Dynamic curving – maximum absolute lateral carbody acceleration

5.4 Yaw and Sway

Test Description

This test was designed to evaluate vehicle safety in its negotiation of track perturbations that generate yaw and sway oscillations. The resulting forces between the wheel and rail should have an adequate margin of safety against any tendency for the car to derail. The car was excited by a symmetric, sinusoidal track alignment deviation with a wavelength of 39 ft on tangent track. Each simulation included five parallel, lateral perturbations with a sinusoidal double amplitude of 1.25 in. peak to peak on both rails and a constant wide gage (see Figure 5-23). The tests were performed at speeds in the range of 15 to 90 mph, ensuring the capture of the resonant speed.

Correlation

Comparisons of the test and simulation data are shown in Figures 5-24 and 5-25 for vertical and lateral forces, respectively for 20 mph and in Figures 5-26 and 5-27 for 60 mph. For the tests at both speeds, the vertical data have relative small variations on the order of ±1 kip from the nominal value of vertical load of 17 kips. While the lead axle test data indicates nominally equal loads on each wheel, the trailing axle test data shows a nominal load of 15.5 kips on the left wheel and 18.5 kips on the right wheel. The five cycle variation in vertical load illustrated in the simulation is also reflected in the test data. The lateral test data on all four wheels at both speeds have a series of sharp "spikes" of lateral force with amplitudes typically of 3 to 7 kips. These spikes occur at 39 ft intervals and are attributed to the track joints. The gaps at the joints are not modeled in the simulation which assumed a smooth sinusoidal alignment variation. Hence the simulation results do not show the "spikes" observed in the tests.

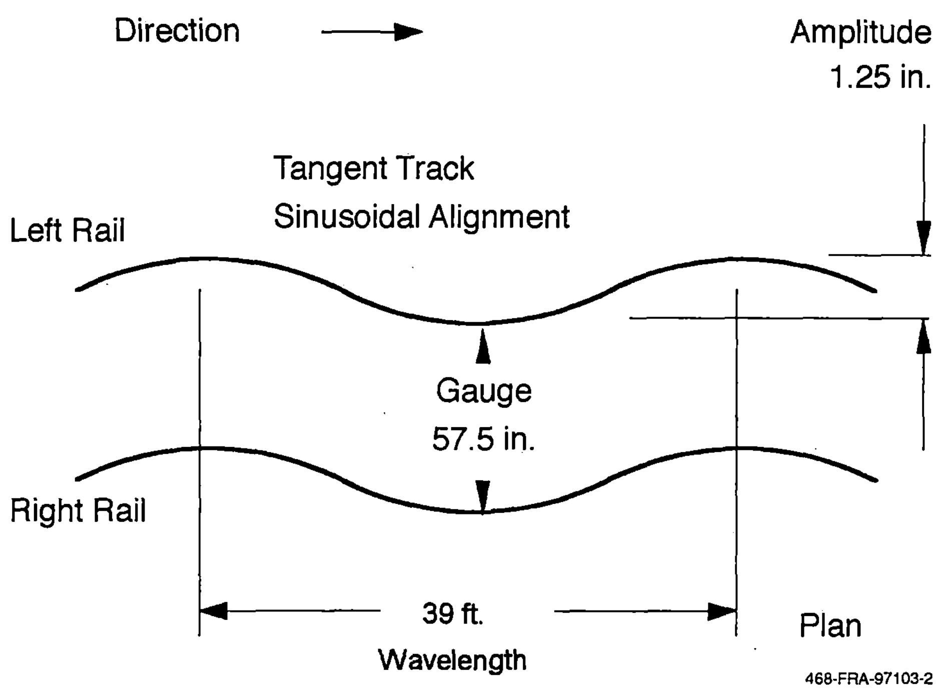

Figure 5-23. Track alignment variation for yaw and sway

The minimum vertical force over the speed range of 15 to 90 mph occurring during a test run is plotted in Figure 5-28 for the left front axle wheel. The maximum lateral force and maximum lateral carbody acceleration at the B end are plotted respectively in Figures 5-29 and 5-30. The lateral maximum wheel force and carbody acceleration data exceed the simulation data significantly if the "spikes" in the test data due to the joints are included. The resonant condition is not obvious from the test data possibly due to large damping in the system.

Conclusion

Relatively good agreement occurs between the test and simulation data for the vertical forces in the test series. The lateral forces had poor agreement believed primarily due to lateral force "spikes" generated by the rail joints. This series of tests indicates the need to improve the simulations.

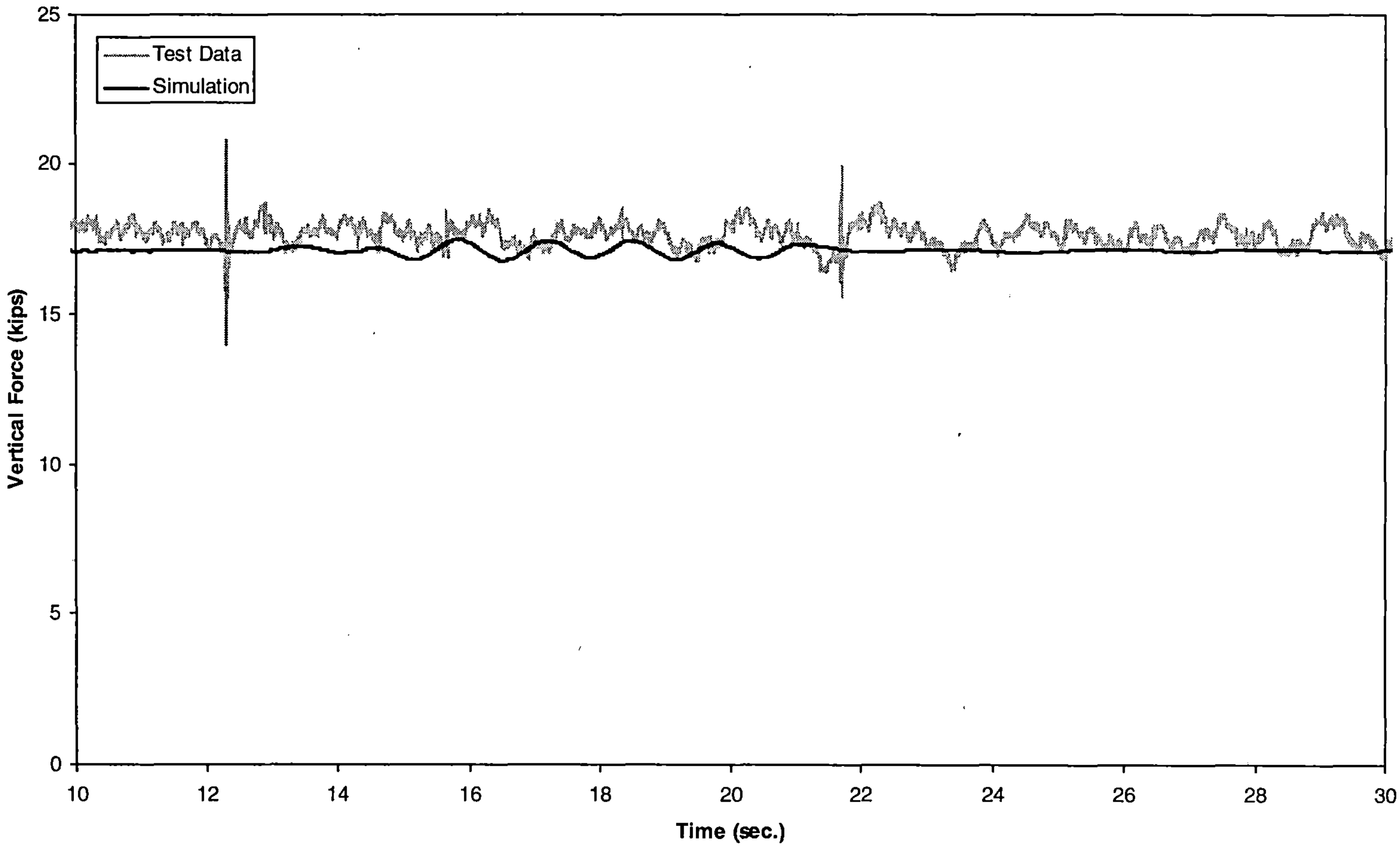

Figure 5-24(a). Yaw and sway – vertical force time history, 20 mph (lead left wheel)

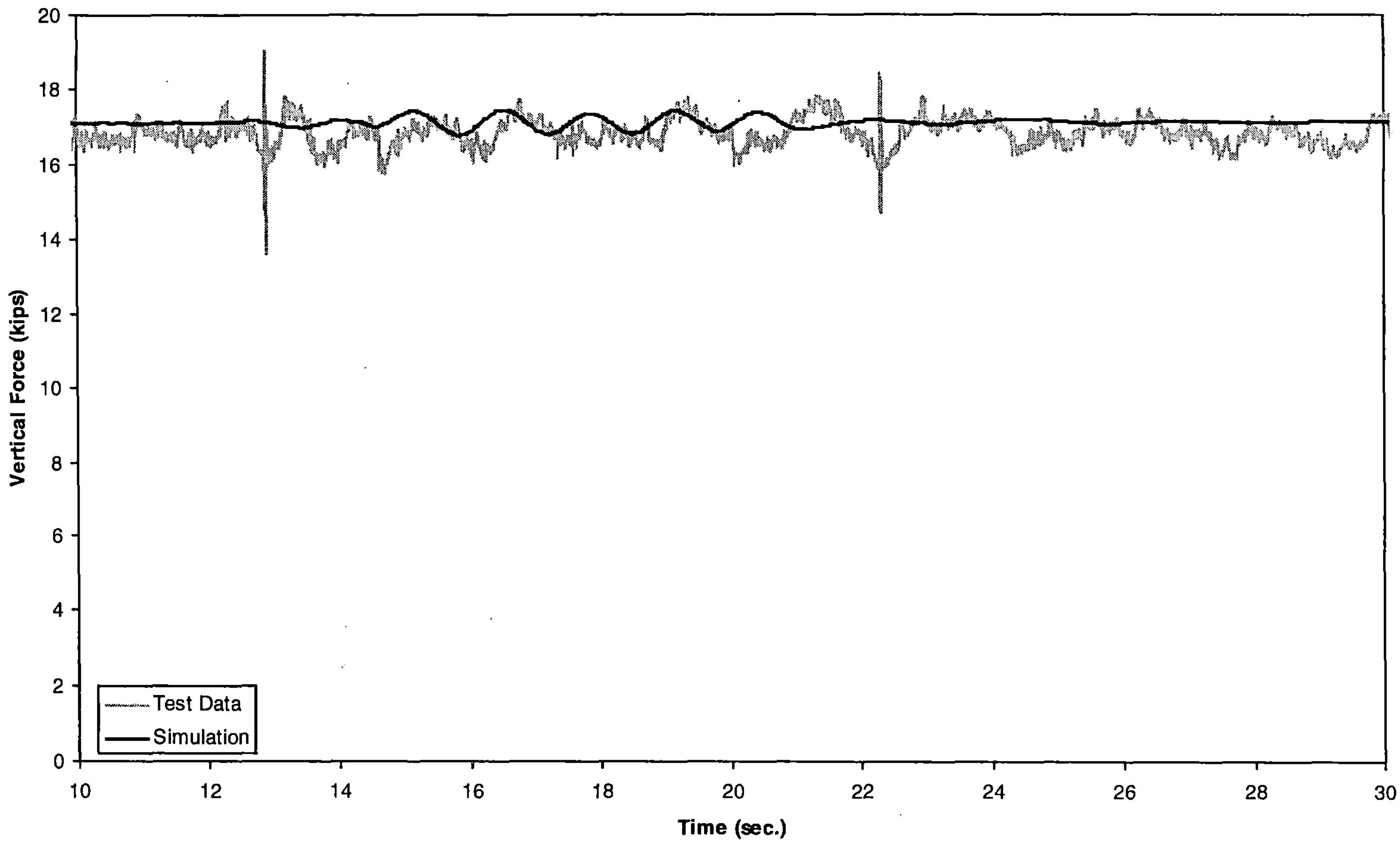

Figure 5-24(b). Yaw and sway – vertical force time history, 20 mph (lead right wheel)

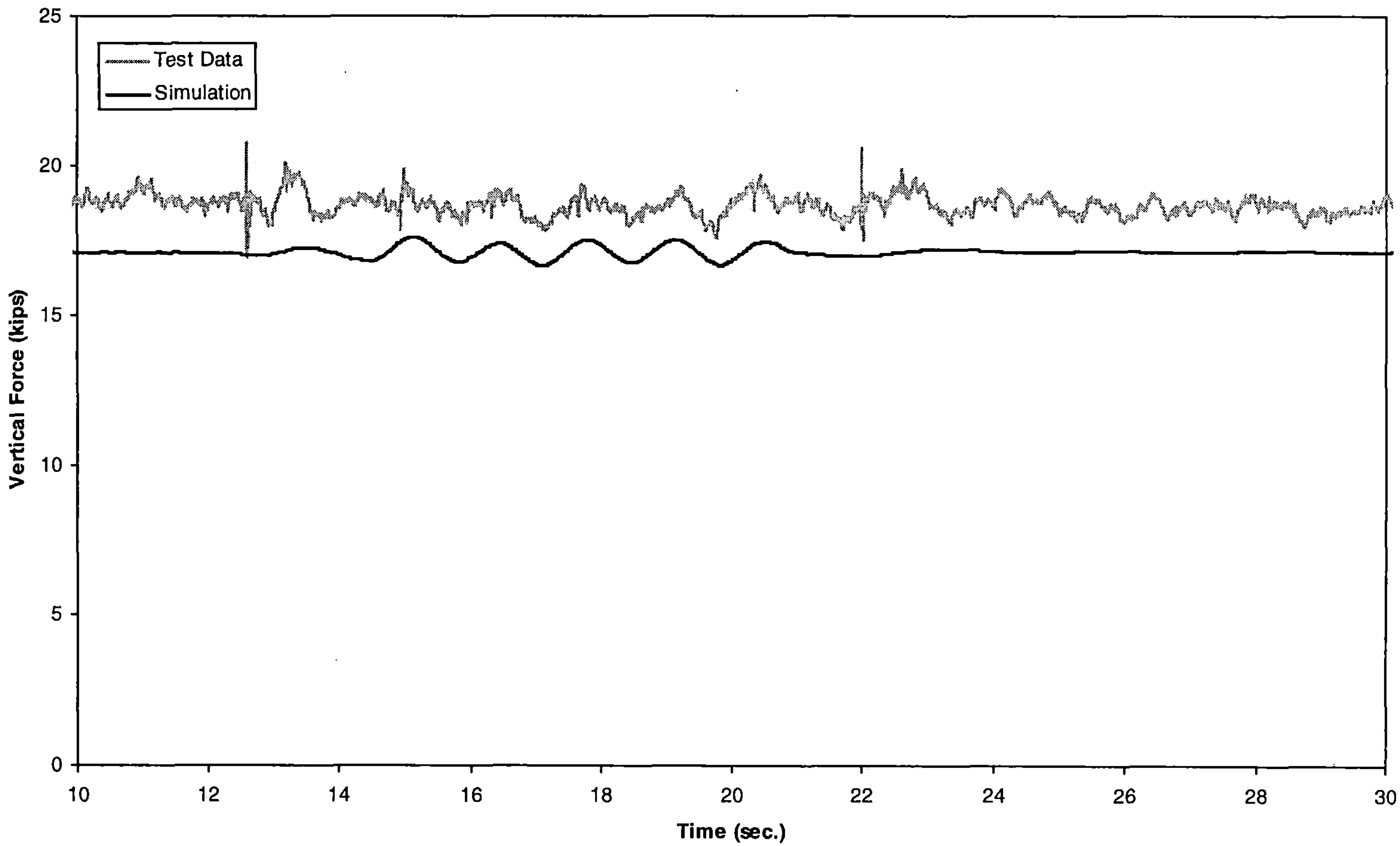

Figure 5-24(c). Yaw and sway – vertical force time history, 20 mph (trailing left wheel)

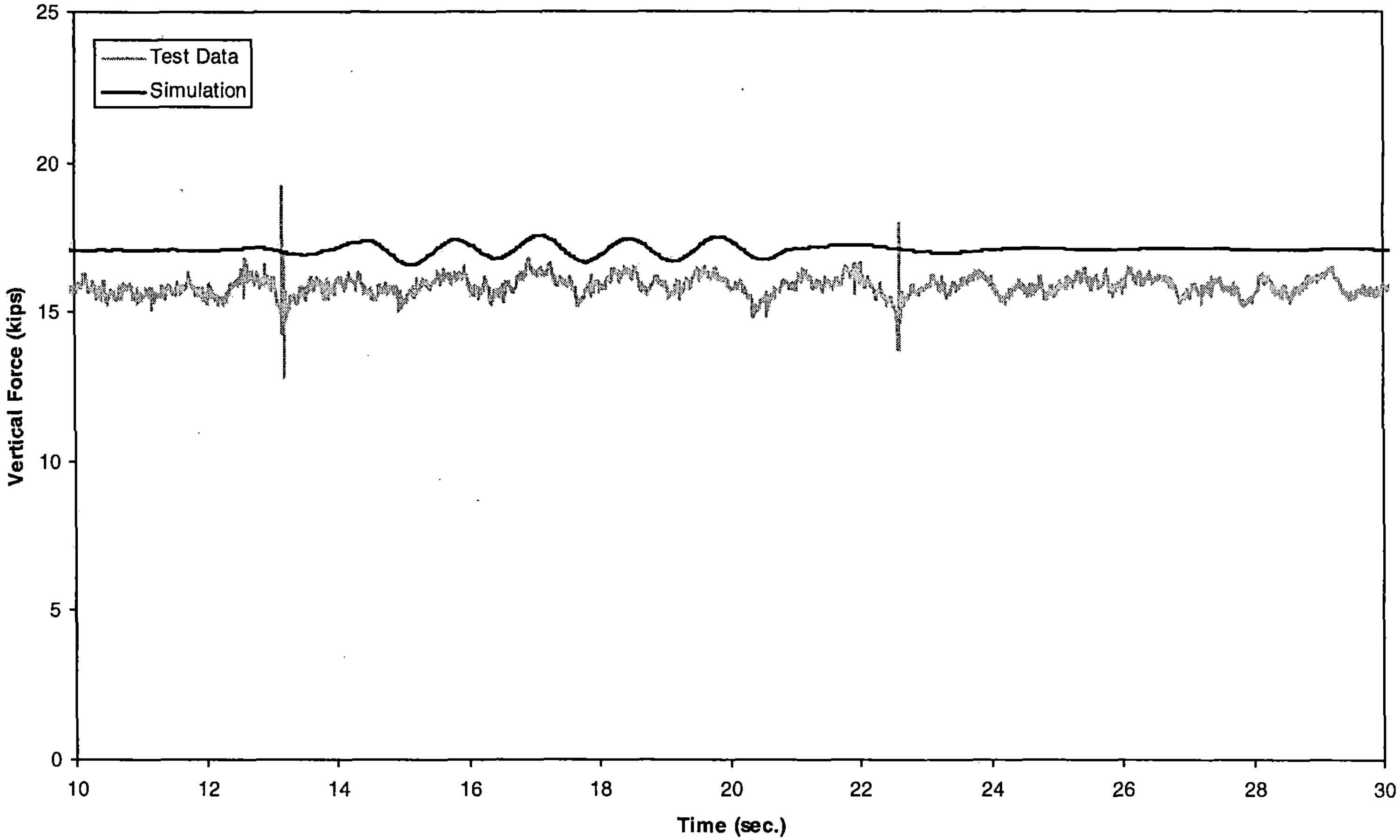

Figure 5-24(d). Yaw and sway – vertical force time history, 20 mph (trailing right wheel)

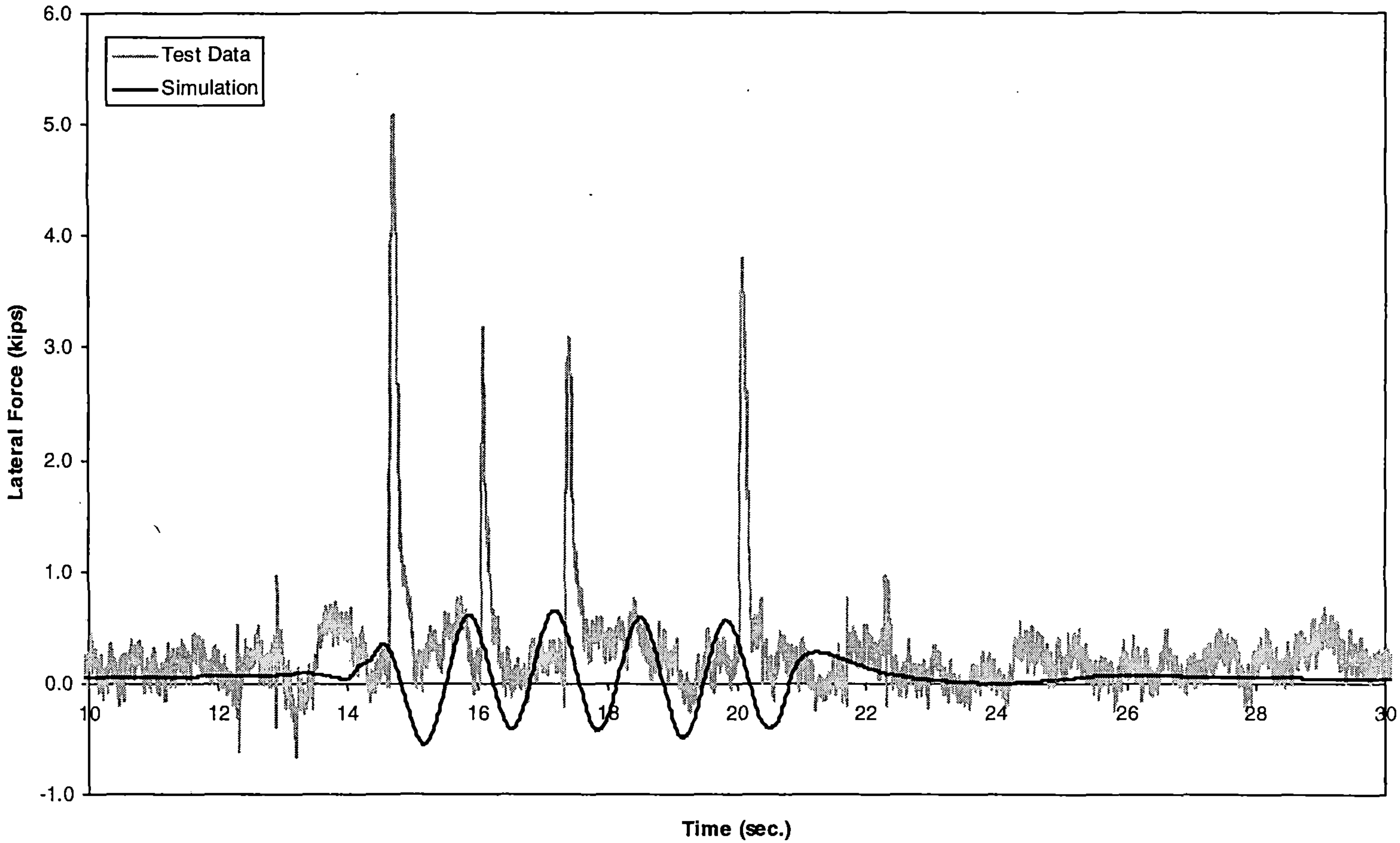

Figure 5-25(a). Yaw and sway – lateral force time history, 20 mph (lead left wheel)

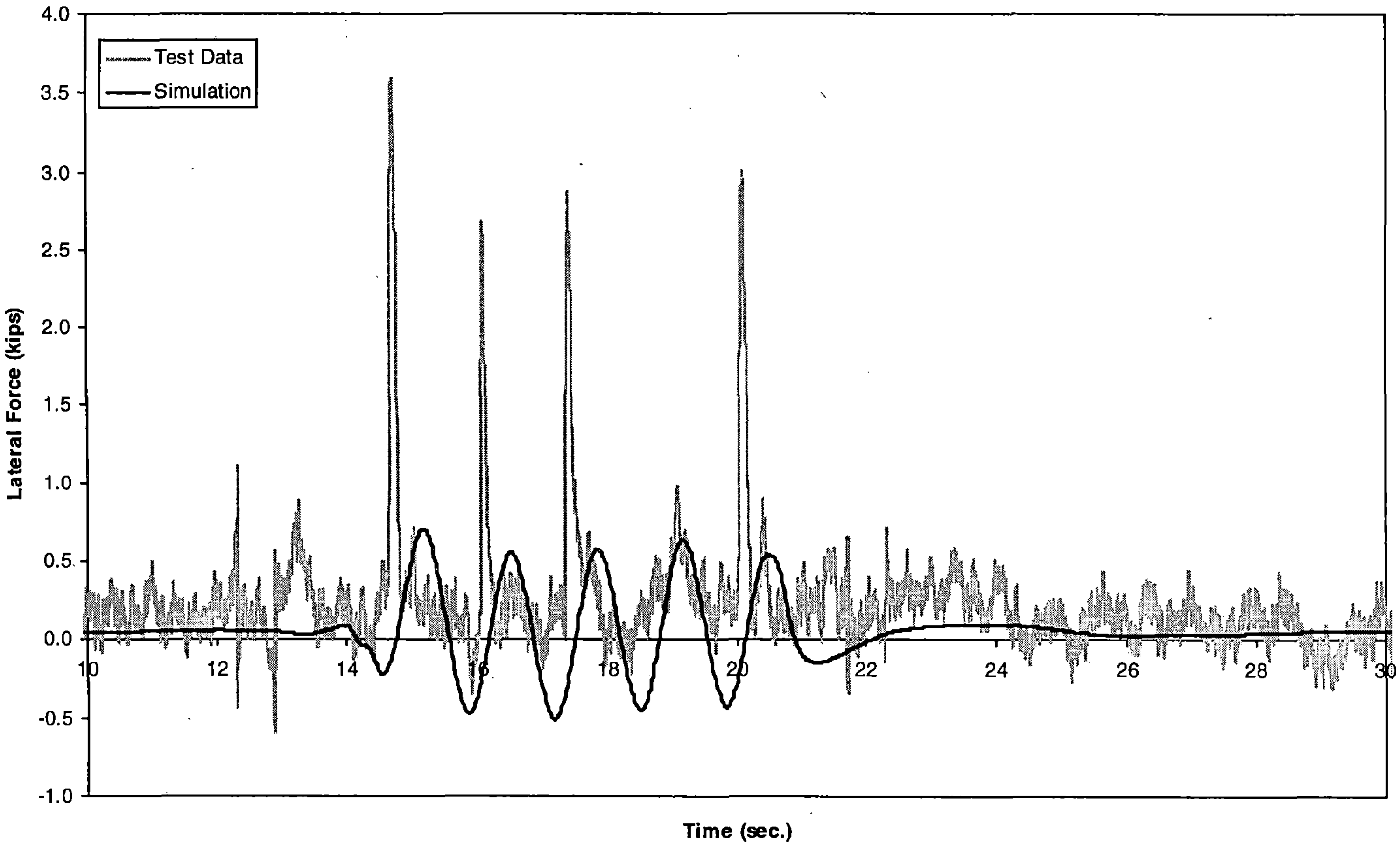

Figure 5-25(b). Yaw and sway – lateral force time history, 20 mph (lead right wheel)

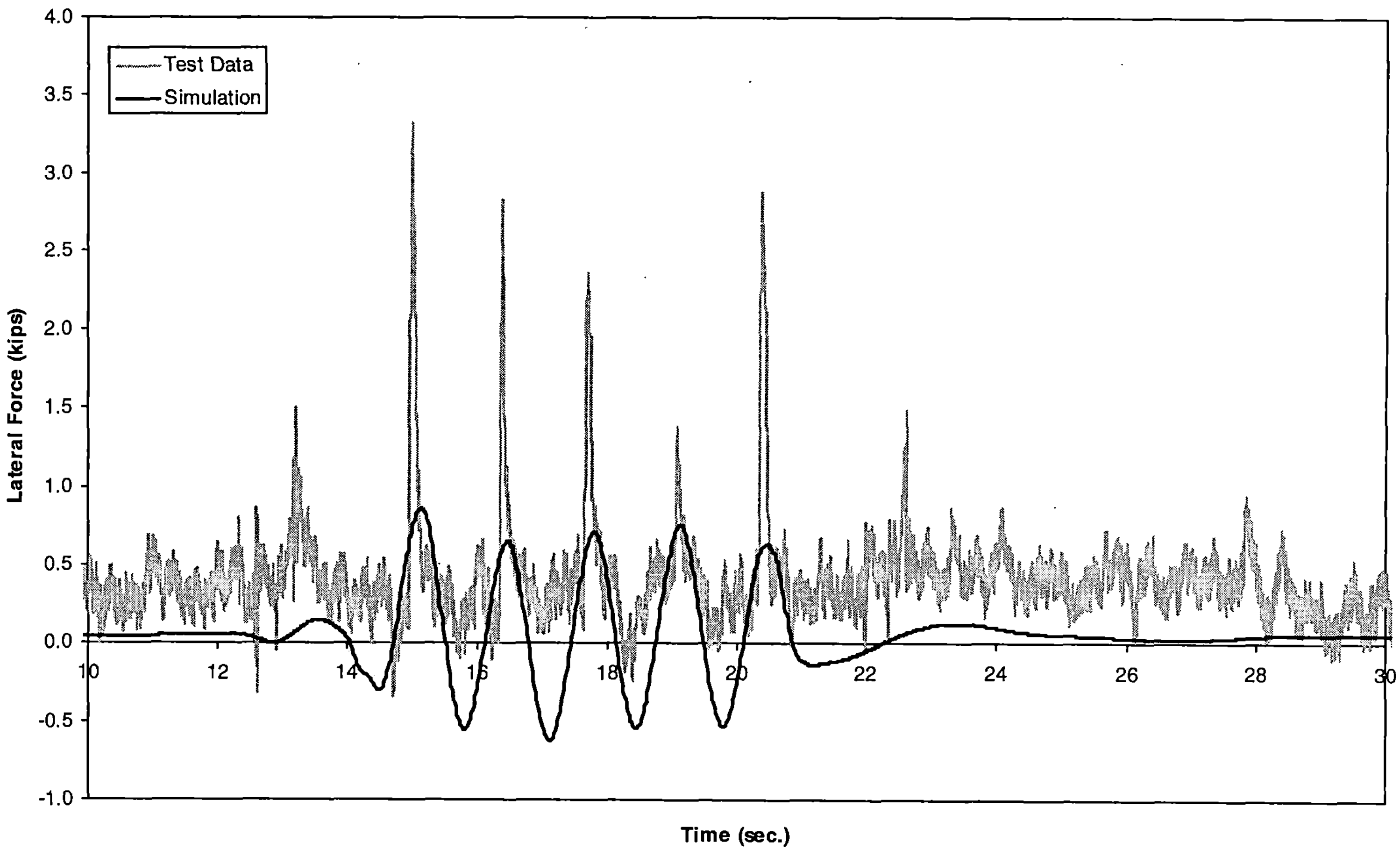

Figure 5-25(c). Yaw and sway – lateral force time history, 20 mph (trailing left wheel)

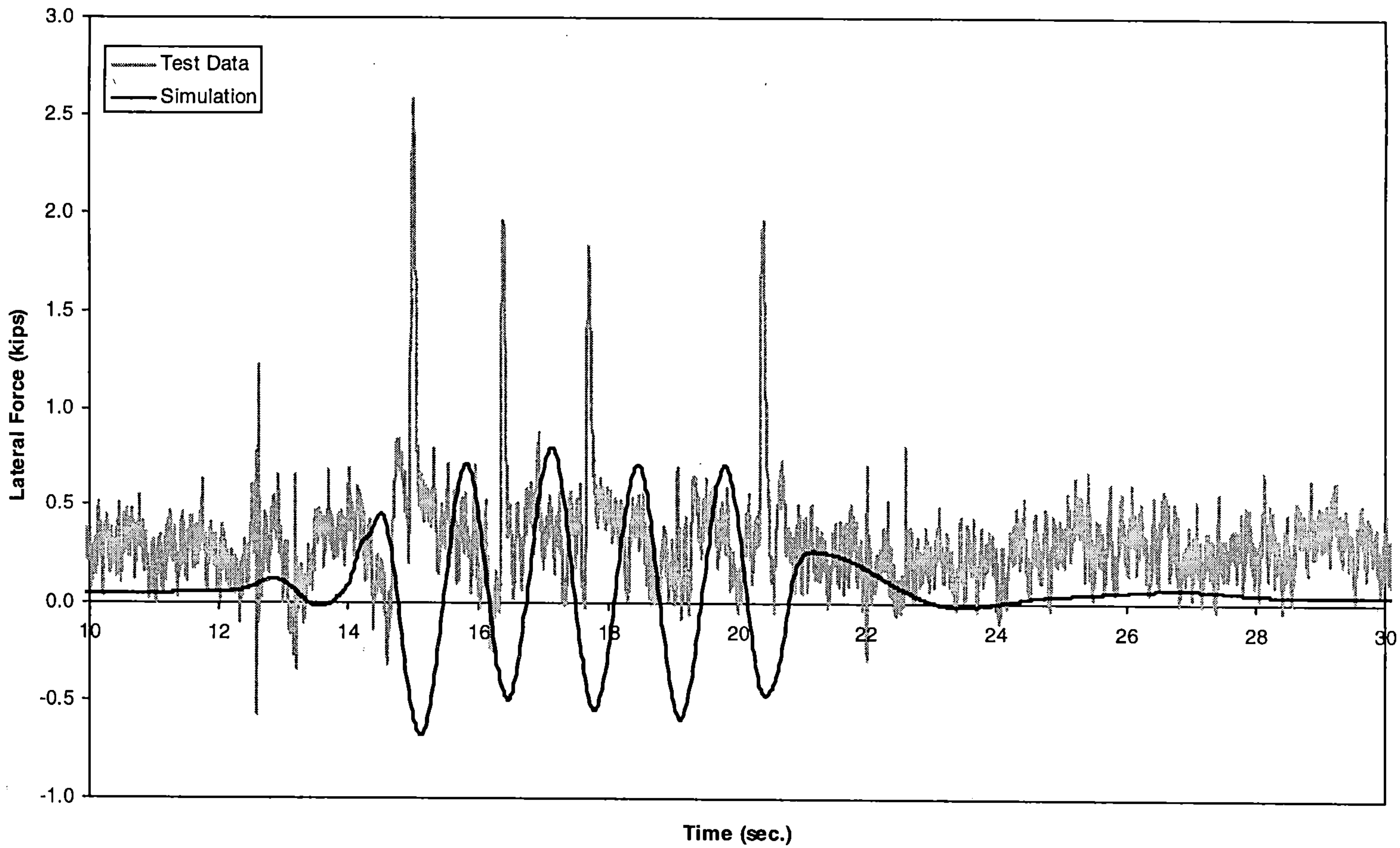

Figure 5-25(d). Yaw and sway – lateral force time history, 20 mph (trailing right wheel)

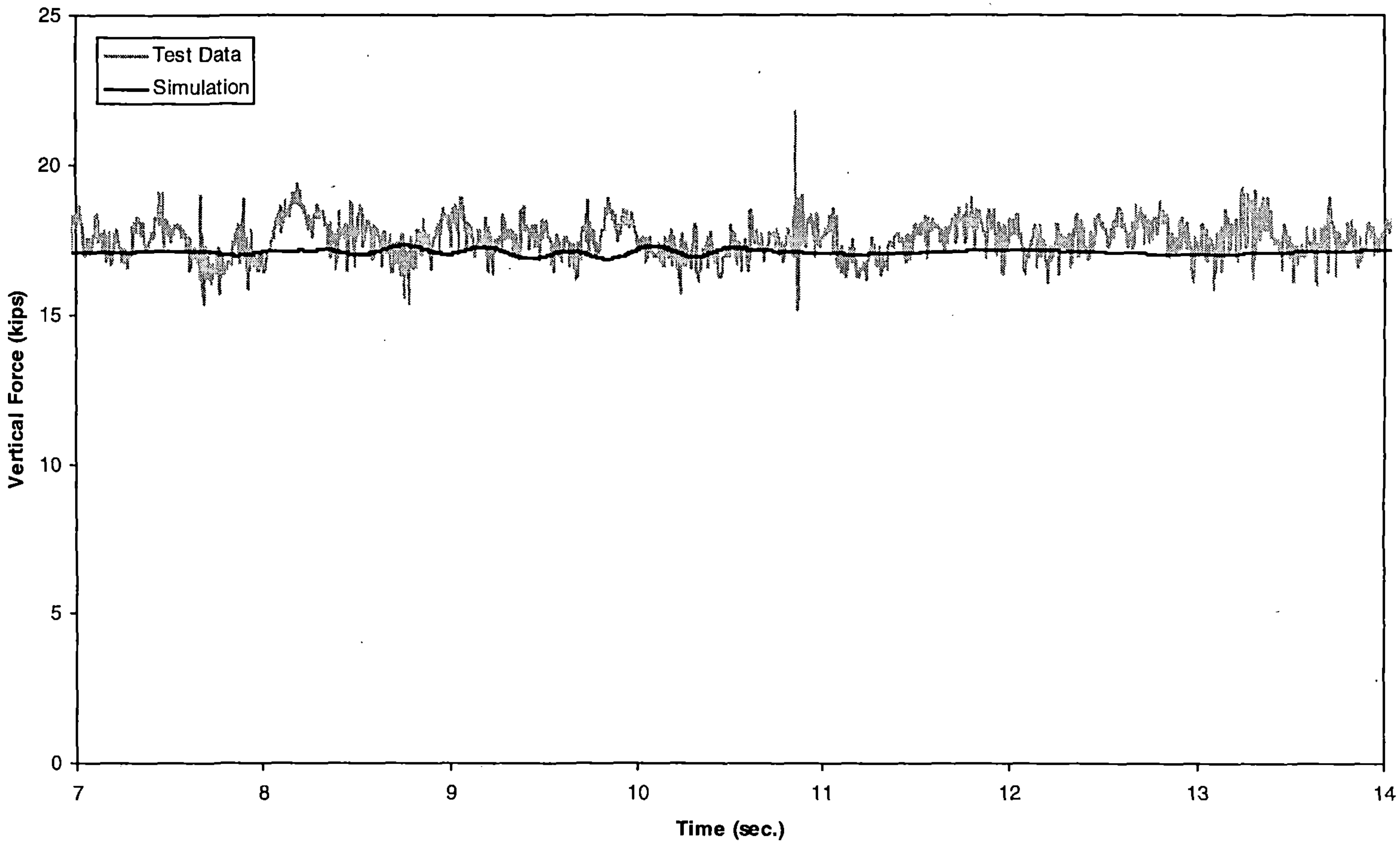

Figure 5-26(a). Yaw and sway – vertical force time history, 60 mph (lead left wheel)

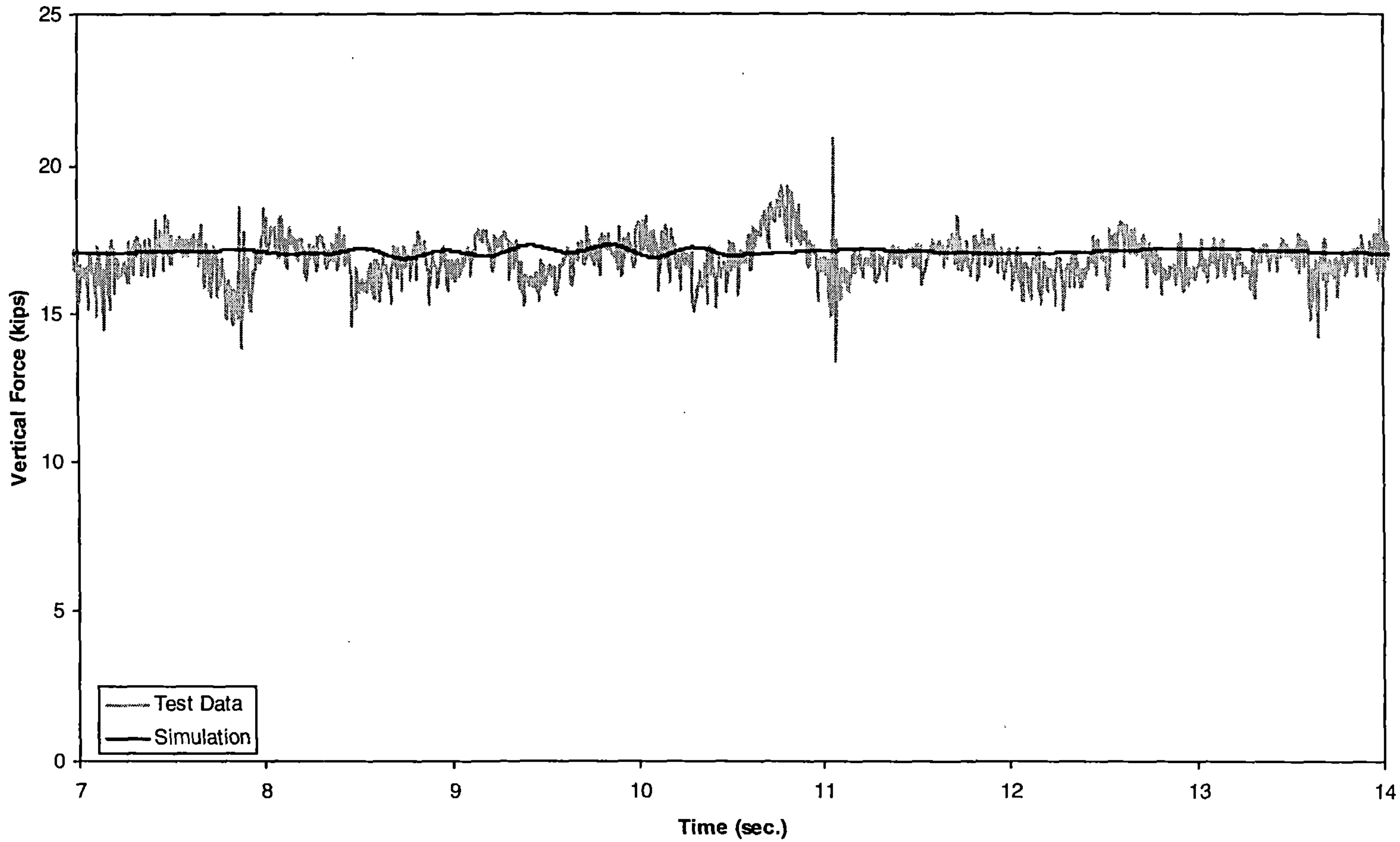

Figure 5-26(b). Yaw and sway – vertical force time history, 60 mph (lead right wheel)

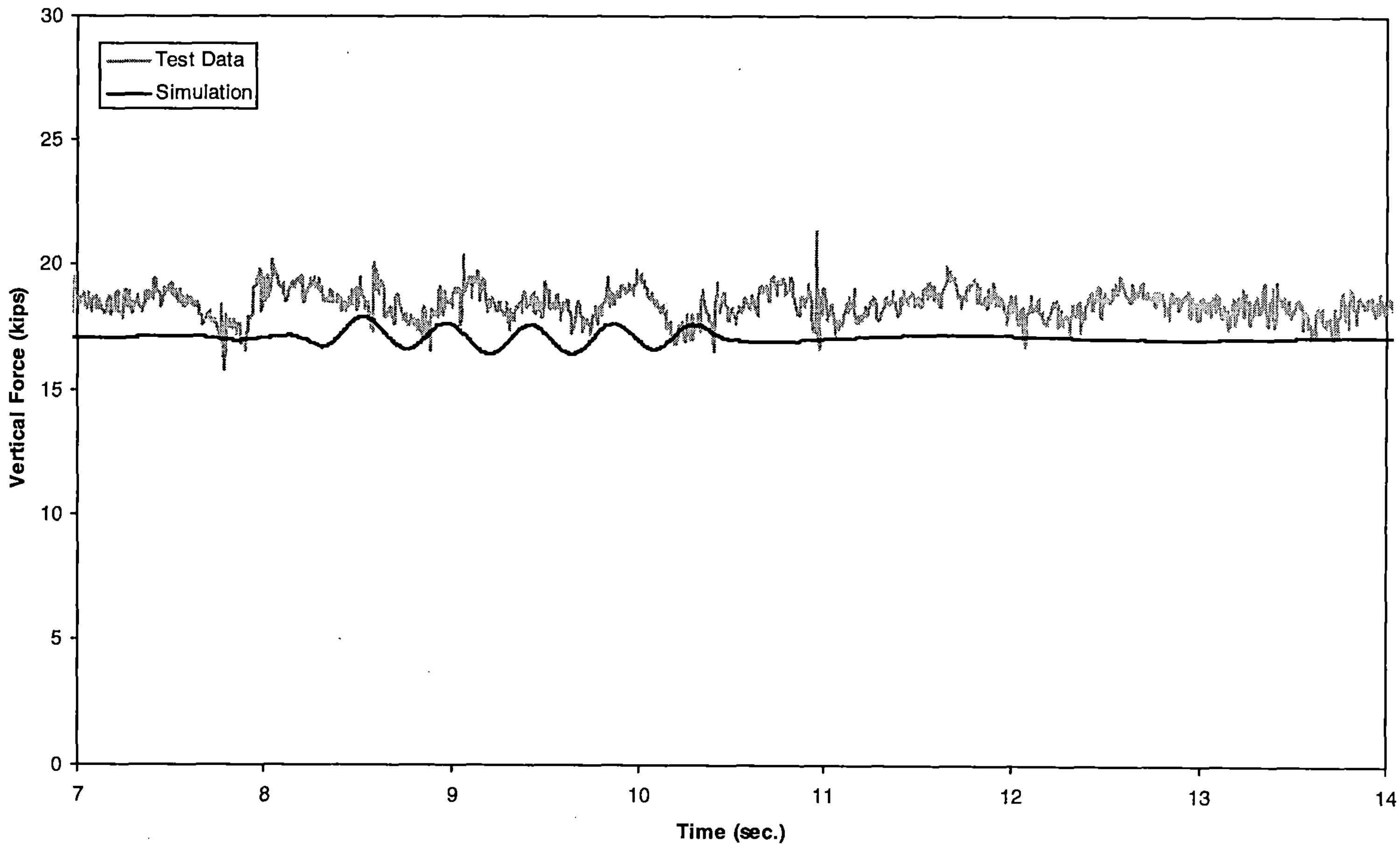

Figure 5-26(c). Yaw and sway – vertical force time history, 60 mph (trailing left wheel)

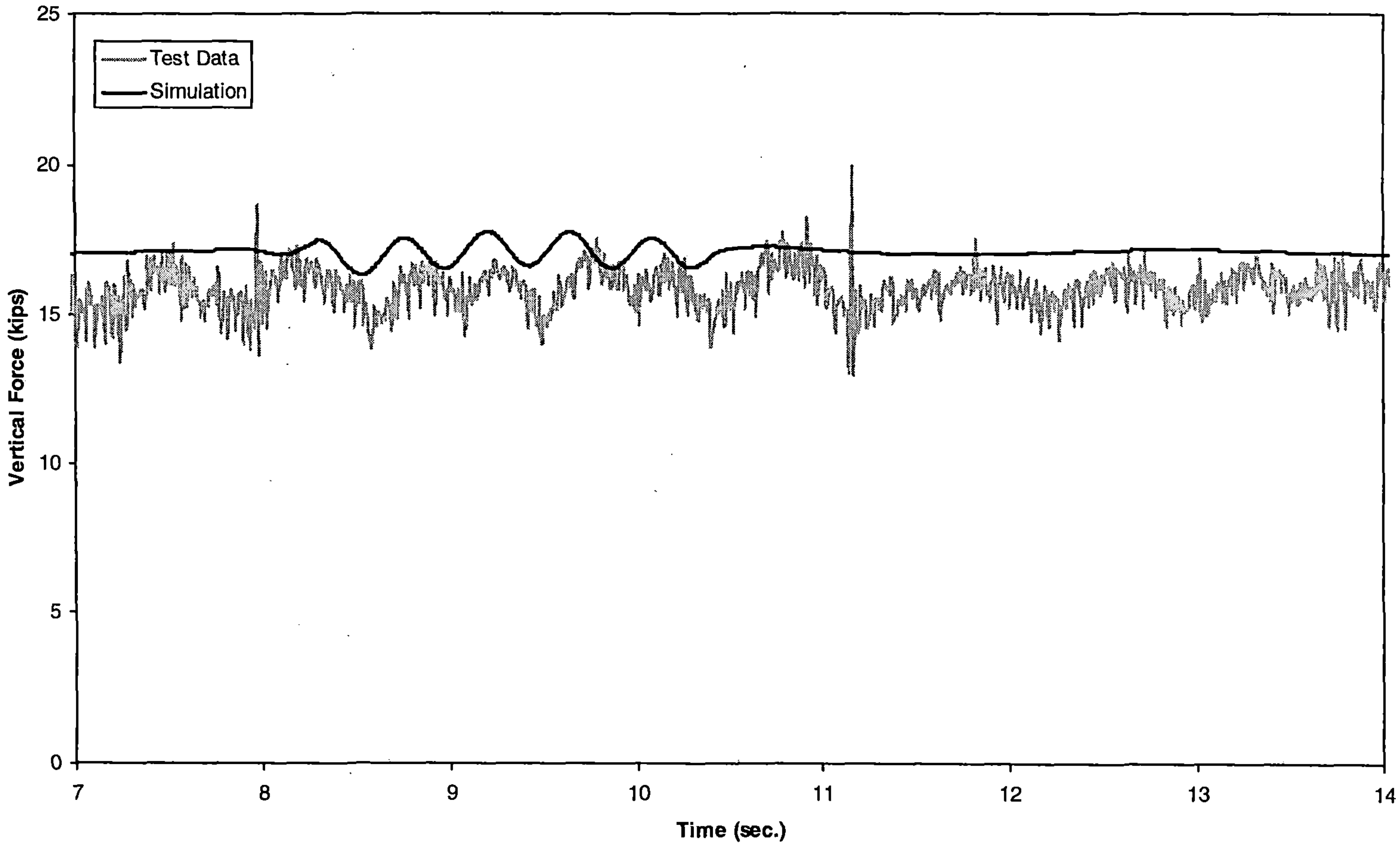

Figure 5-26(d). Yaw and sway – vertical force time history, 60 mph (trailing right wheel)

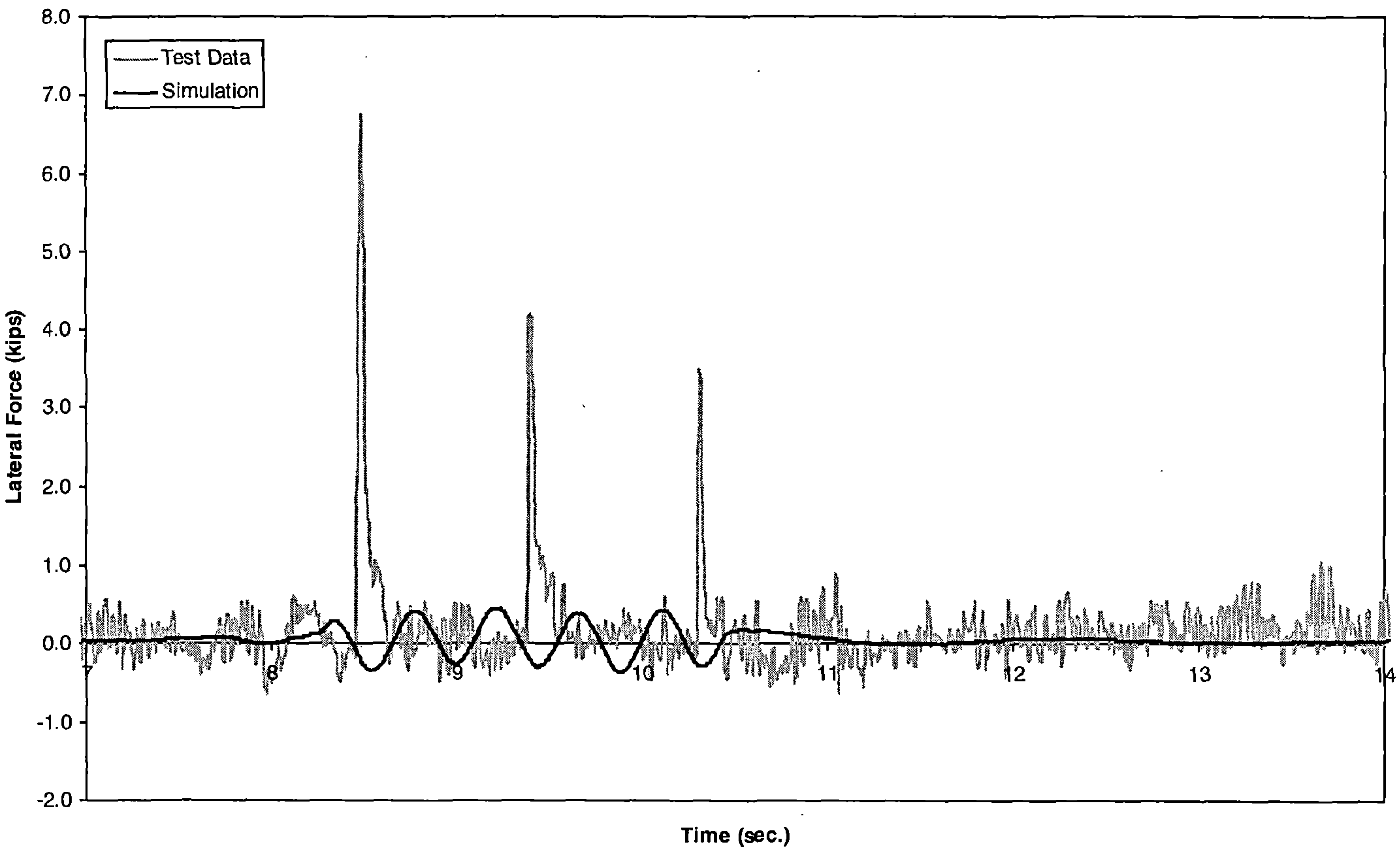

Figure 5-27(a). Yaw and sway – lateral force time history, 60 mph (lead left wheel)

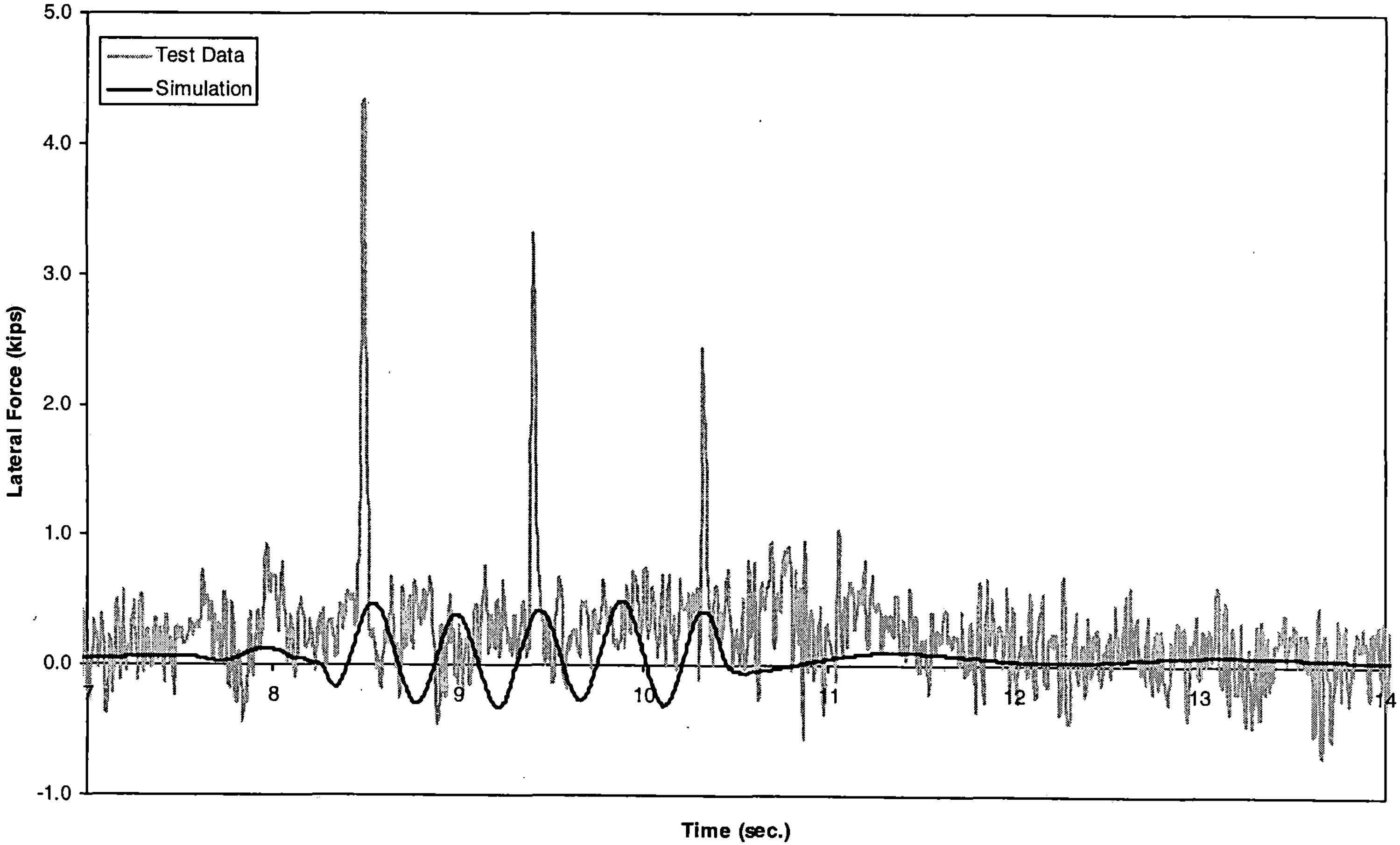

Figure 5-27(b). Yaw and sway – lateral force time history, 60 mph (lead right wheel)

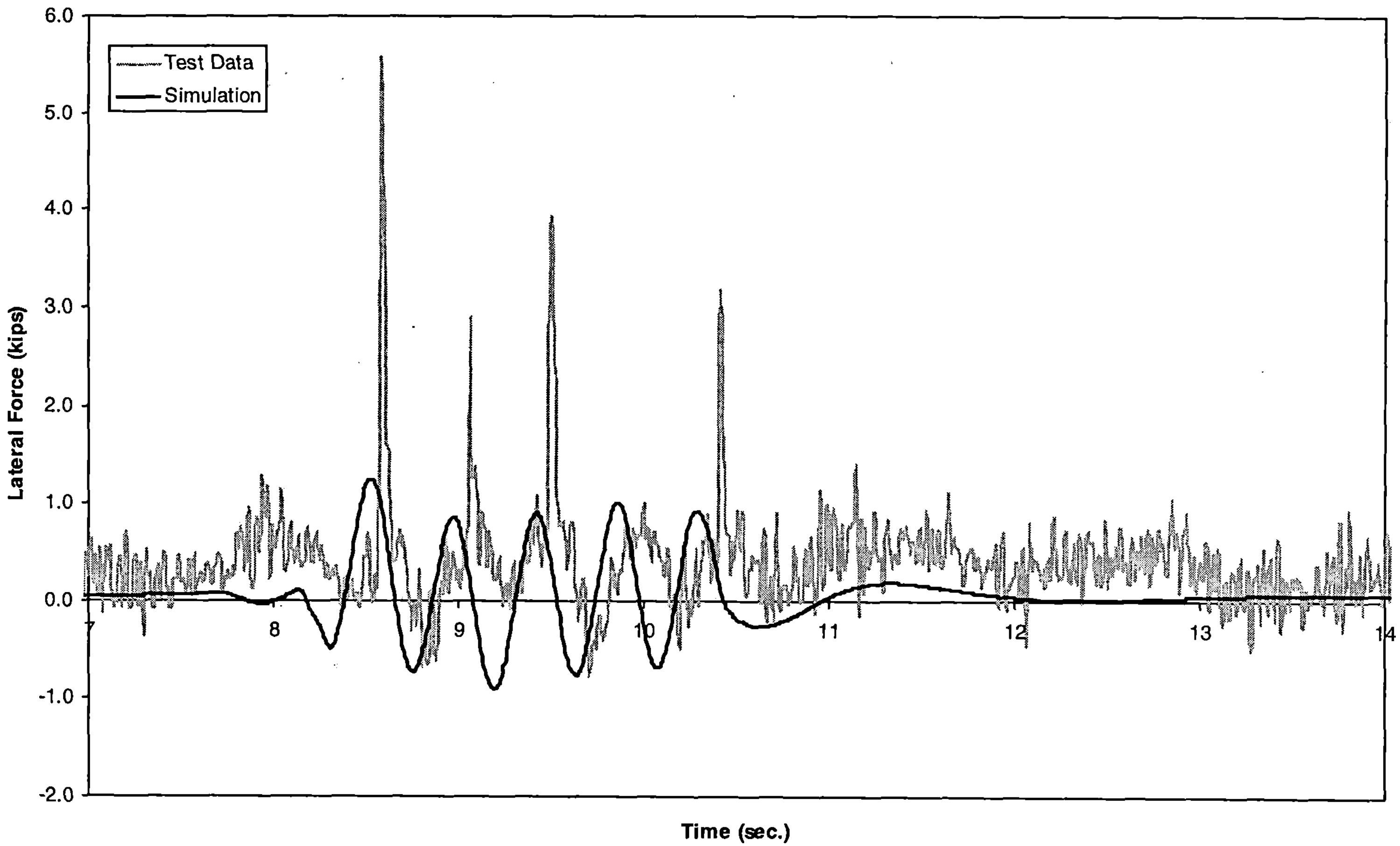

Figure 5-27(c). Yaw and sway – lateral force time history, 60 mph (trailing left wheel)

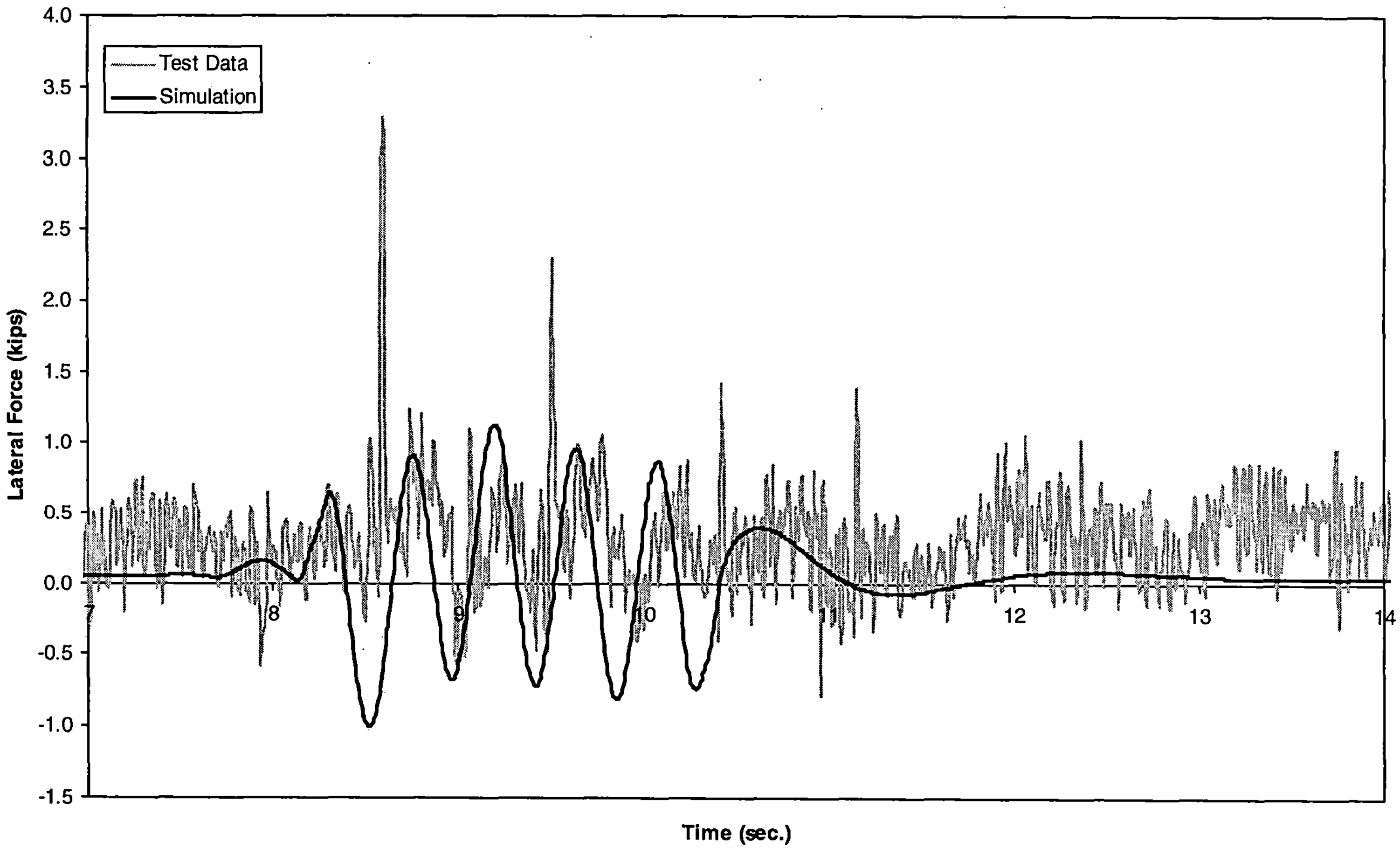

Figure 5-27(d). Yaw and sway – lateral force time history, 60 mph (trailing right wheel)

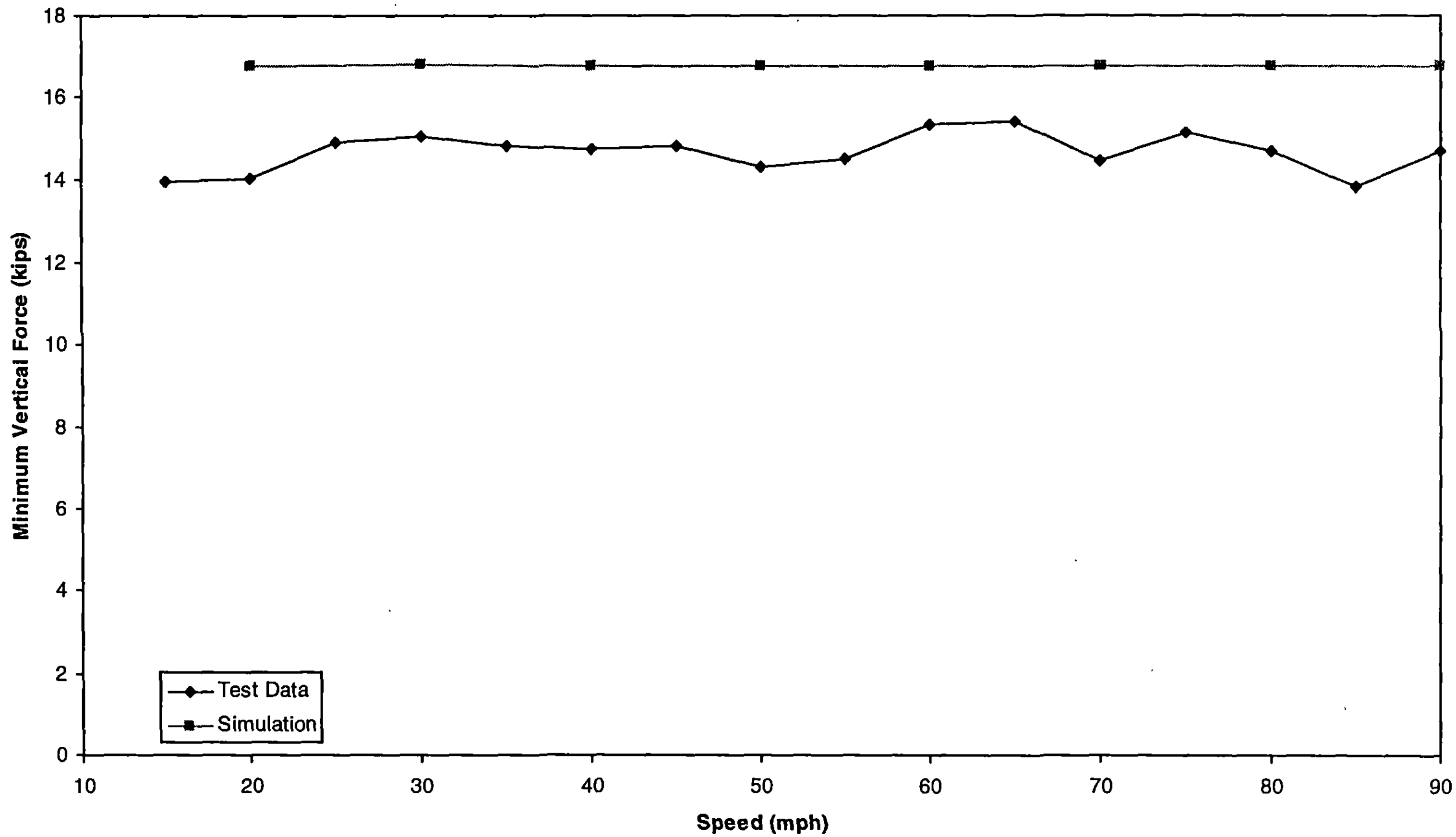

Figure 5-28. Yaw and sway – minimum vertical force

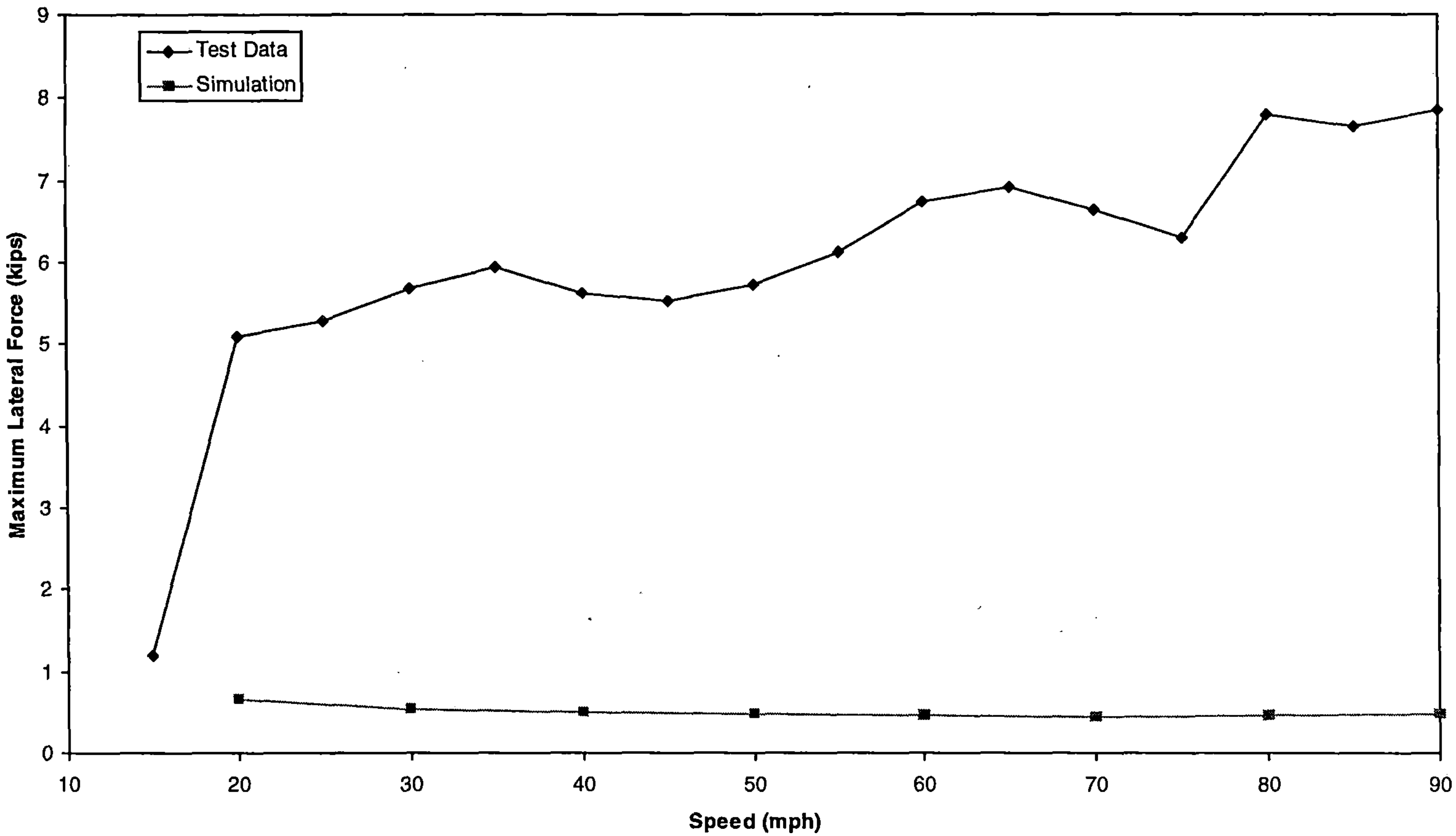

Figure 5-29. Yaw and sway – maximum lateral force

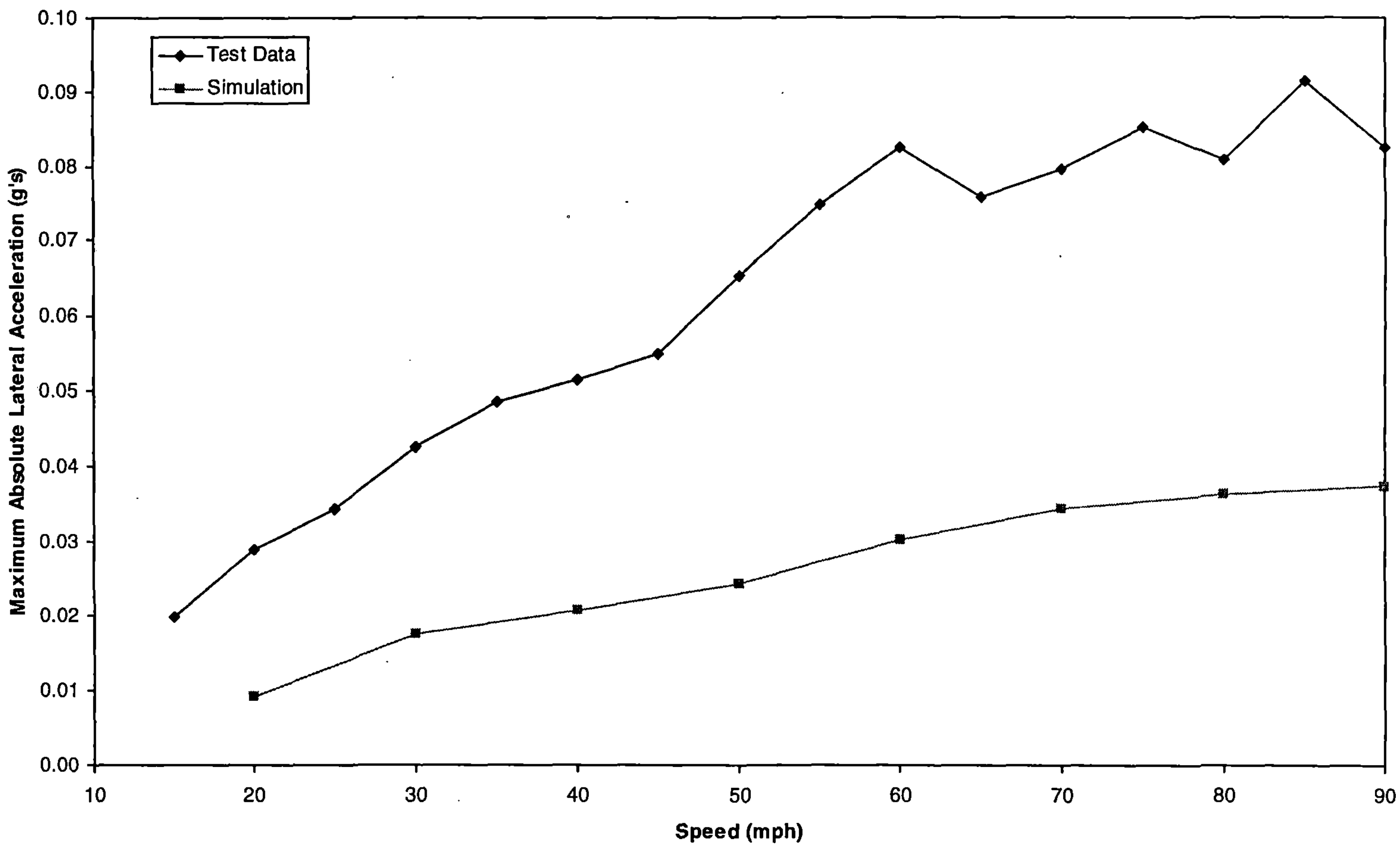

Figure 5-30. Yaw and sway – maximum absolute lateral carbody acceleration

5.5 Twist and Roll

Test Description

Successive crosslevel excitation of cars may lead to large car roll and twist amplitudes, which should be limited for car safety assurance. The analyses and tests are required to evaluate the margin of safety against derailment. The test and simulation track sections included 10 vertical perturbations 39 ft apart, staggered each with an amplitude of 0.75 in. (see Figure 5-31). The cusp shaped perturbations were located on each rail to generate the lower and upper roll and twist resonance modes. The tests were performed at speeds in the range of 10 to 70 mph.

Correlation

Comparisons of the test data for all four wheels of the trailing truck vertical and lateral forces are summarized in Figures 5-32 and 5-33 for 20 mph and Figures 5-34 and 5-35 for 60 mph tests. The comparisons illustrate good agreement in vertical force waveforms and amplitudes.

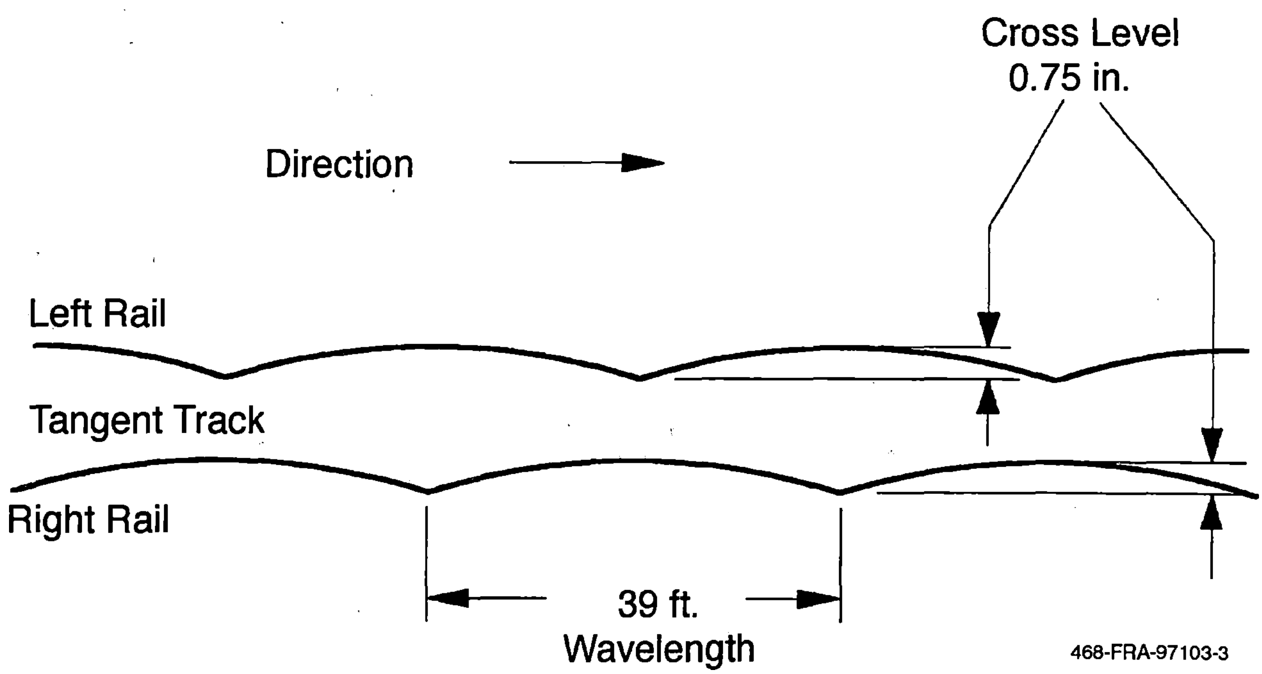

Figure 5-31. Crosslevel variation for twist and roll

The data at 20 mph indicate that in the first few cycles of the test, a "phase shift" between the test data and simulation is seen which is attributed to some uncertainty in the vehicle test speed. The vertical force amplitude of the four wheels varies between approximately 13 and 22 kips and shows good agreement between the test and simulation. The lateral force data for the lead axle vary between about –1.0 to +1.7 kips and also shows good agreement between the test and simulation. The lateral force data for the trailing axle vary from –0.5 to +1.5 kips for the tests and ±0.5 kips in the simulation and are considered to be approaching values small enough to represent the test accuracy limits. The vertical force test and simulation data at 60 mph vary from approximately 12.5 to 22 kips and are in excellent agreement. The test and lateral force simulation data for the lead axle vary from approximately –1.5 to +2.5 kips and are in relatively good agreement. The lateral test and simulation force data for the trailing axle vary from –1.0 to +1.5 kips with the general levels in agreement.

Plots of the test and simulation of minimum vertical force and maximum lateral force are shown in Figures 5-36 and 5-37 for the lead axle left wheel of the trailing truck. Good correlation is seen for the vertical force in the speed range while the lateral force test data is approximately 25 percent greater than the simulation. The maximum absolute lateral carbody acceleration at the "B" end is shown in Figure 5-38. The simulation underestimates the values by 0.04g, though the general trend of the car body acceleration with speed is well predicted by the simulation.

Conclusion

The simulation has relatively good correlation for the amplitude of the vertical and lateral force at all speeds. Simulation predictions for both vertical and lateral force in the twist and roll tests are reasonable.

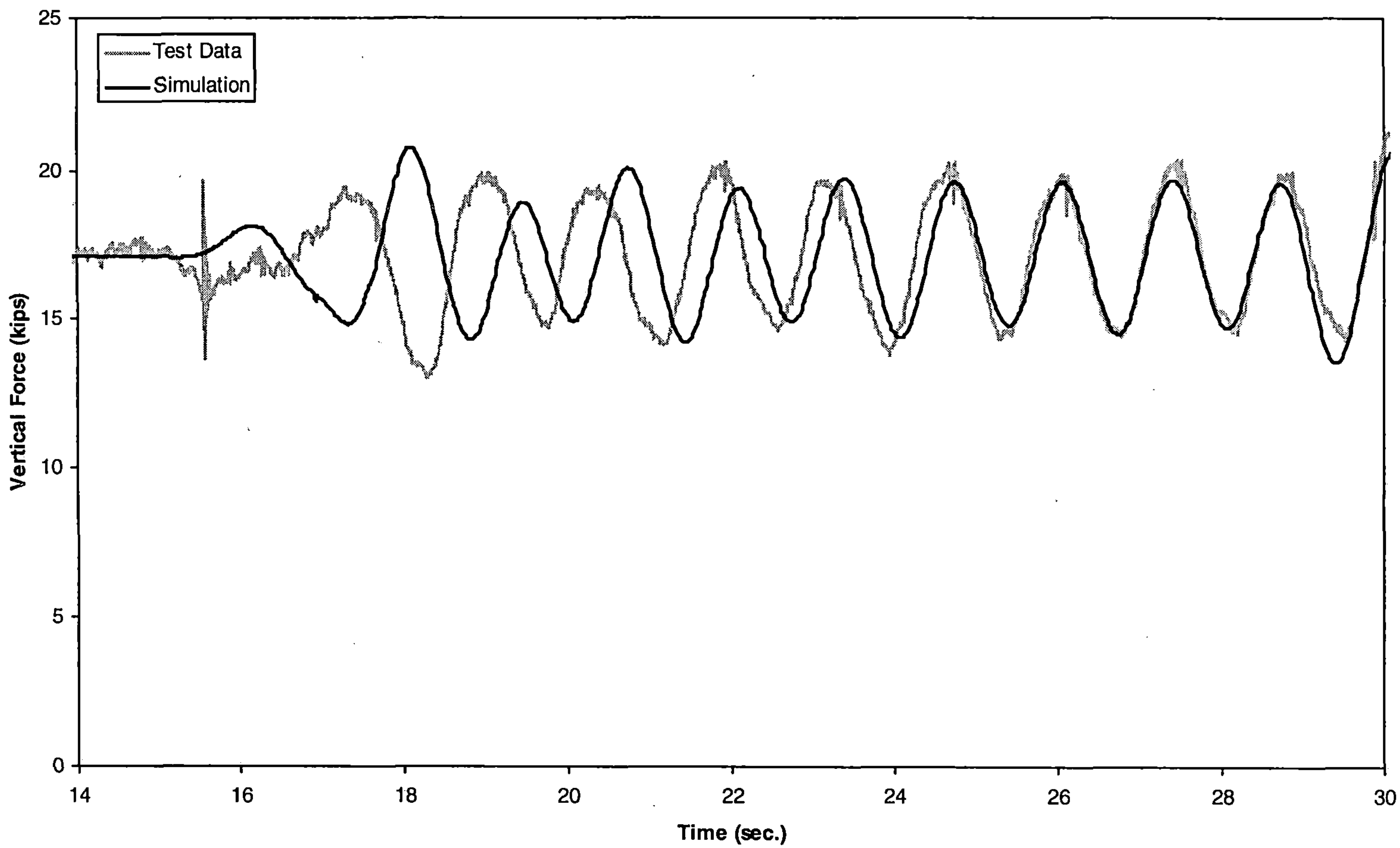

Figure 5-32(a). Twist and roll – vertical force time history, 20 mph (lead left wheel)

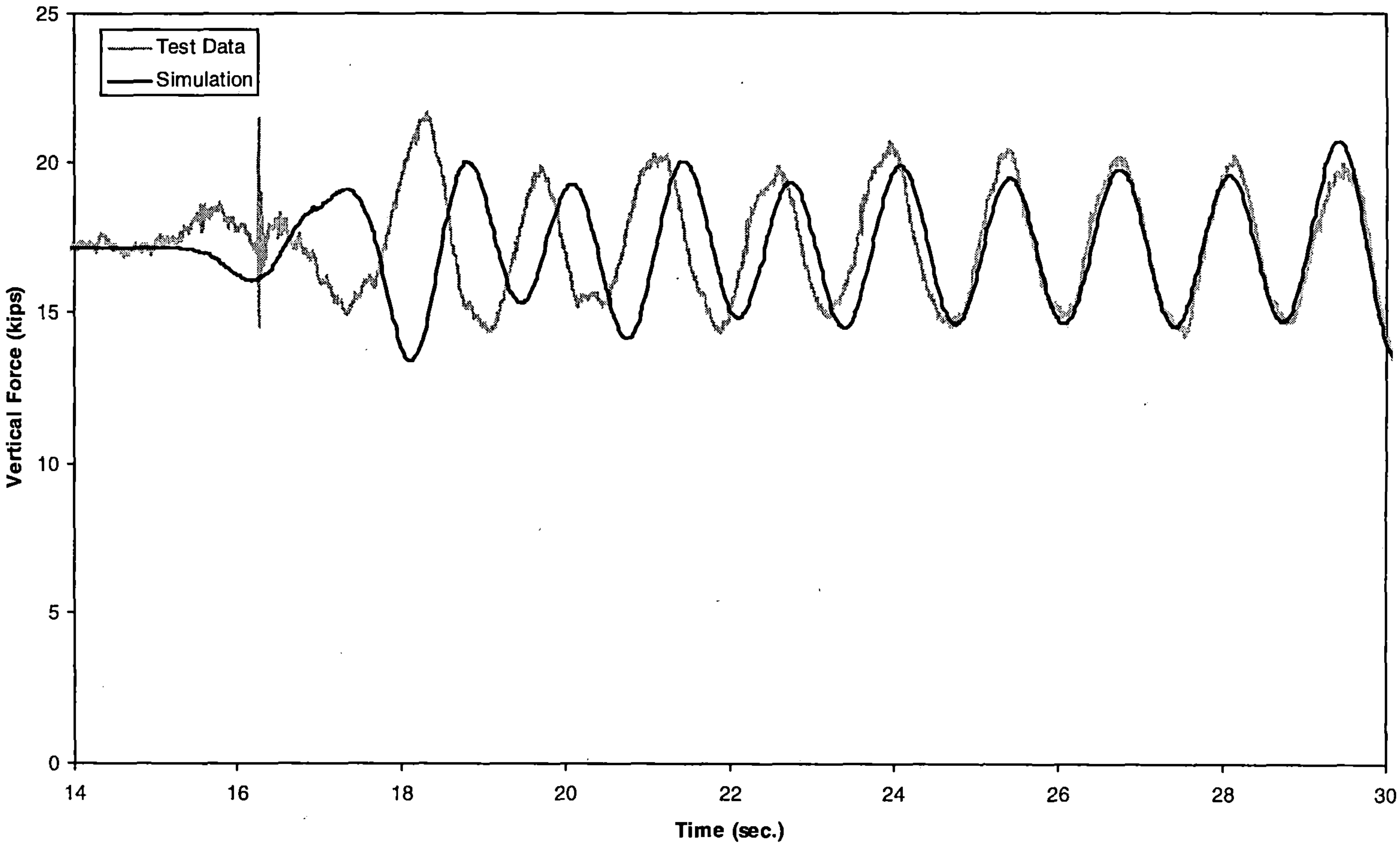

Figure 5-32(b). Twist and roll – vertical force time history, 20 mph (lead right wheel)

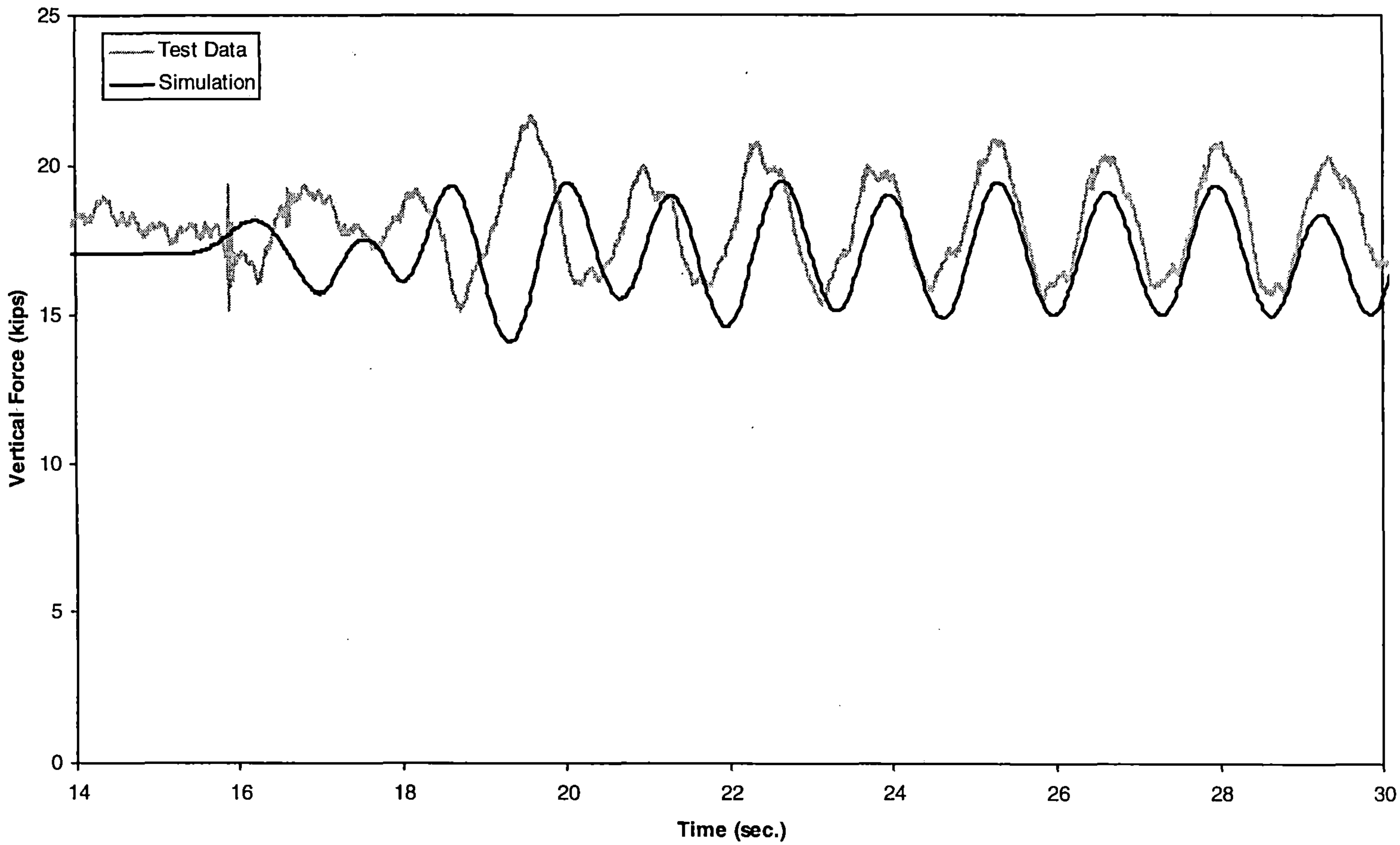

Figure 5-32(c). Twist and roll – vertical force time history, 20 mph (trailing left wheel)

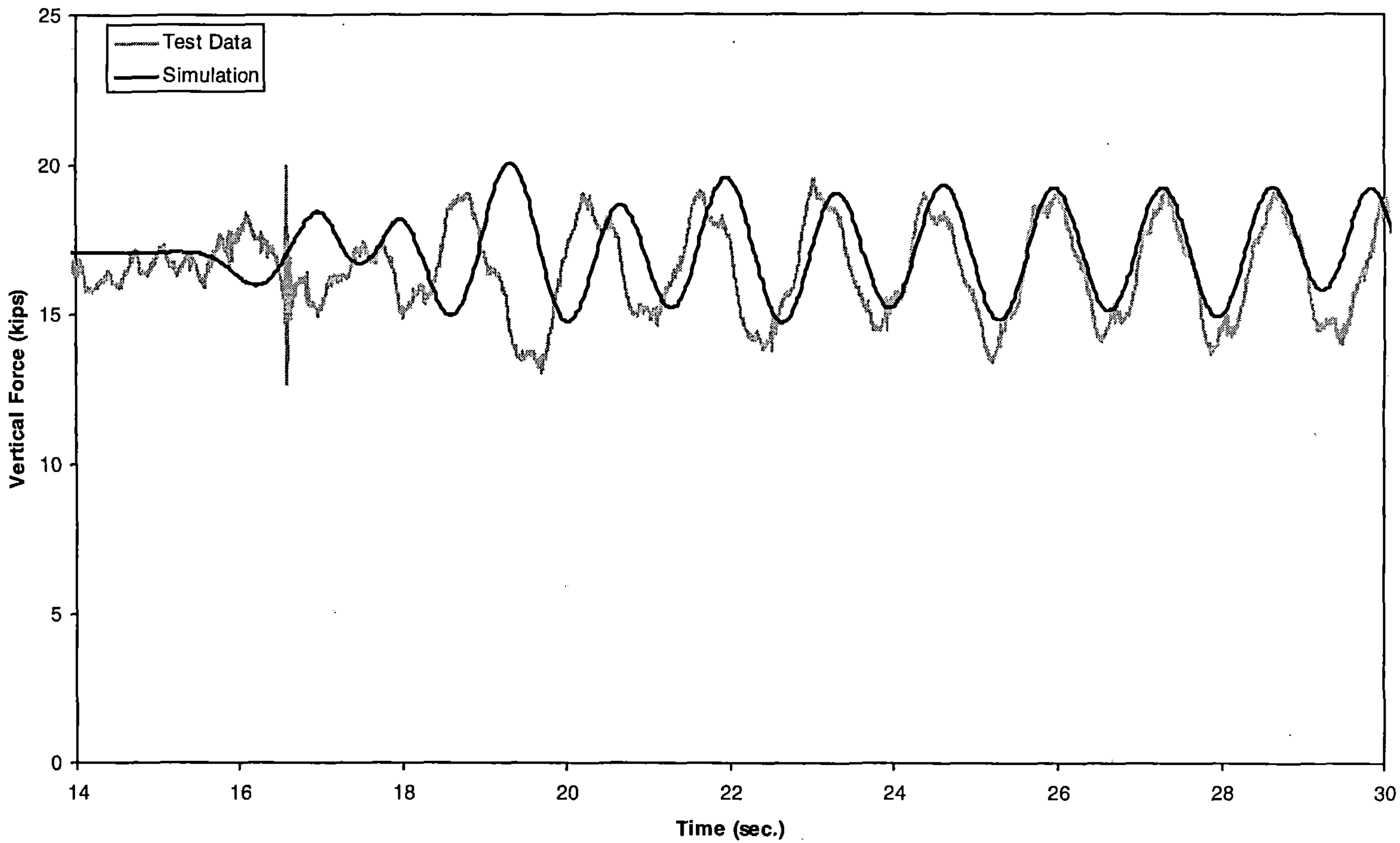

Figure 5-32(d). Twist and roll – vertical force time history, 20 mph (trailing right wheel)

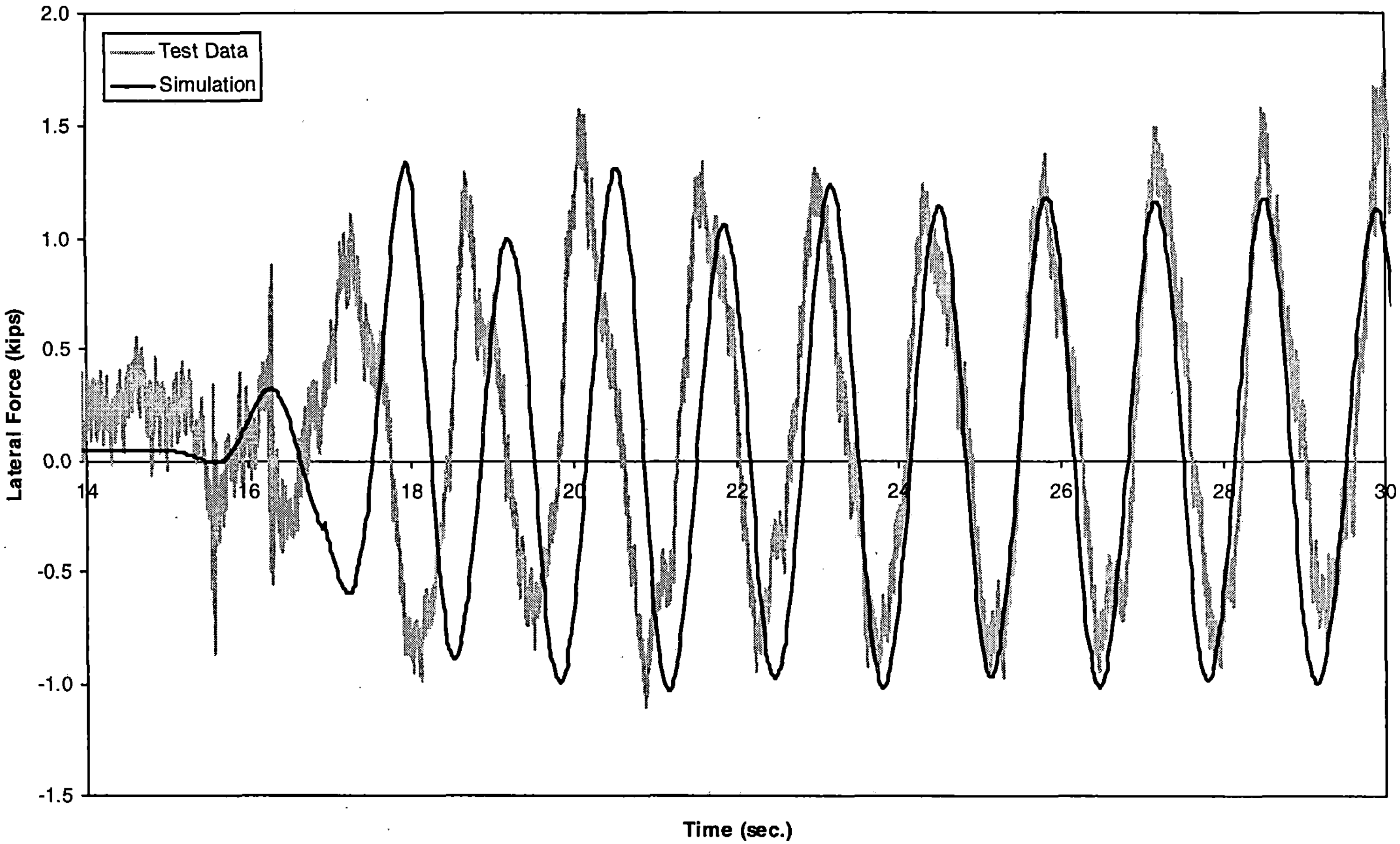

Figure 5-33(a). Twist and roll – lateral force time history, 20 mph (lead left wheel)

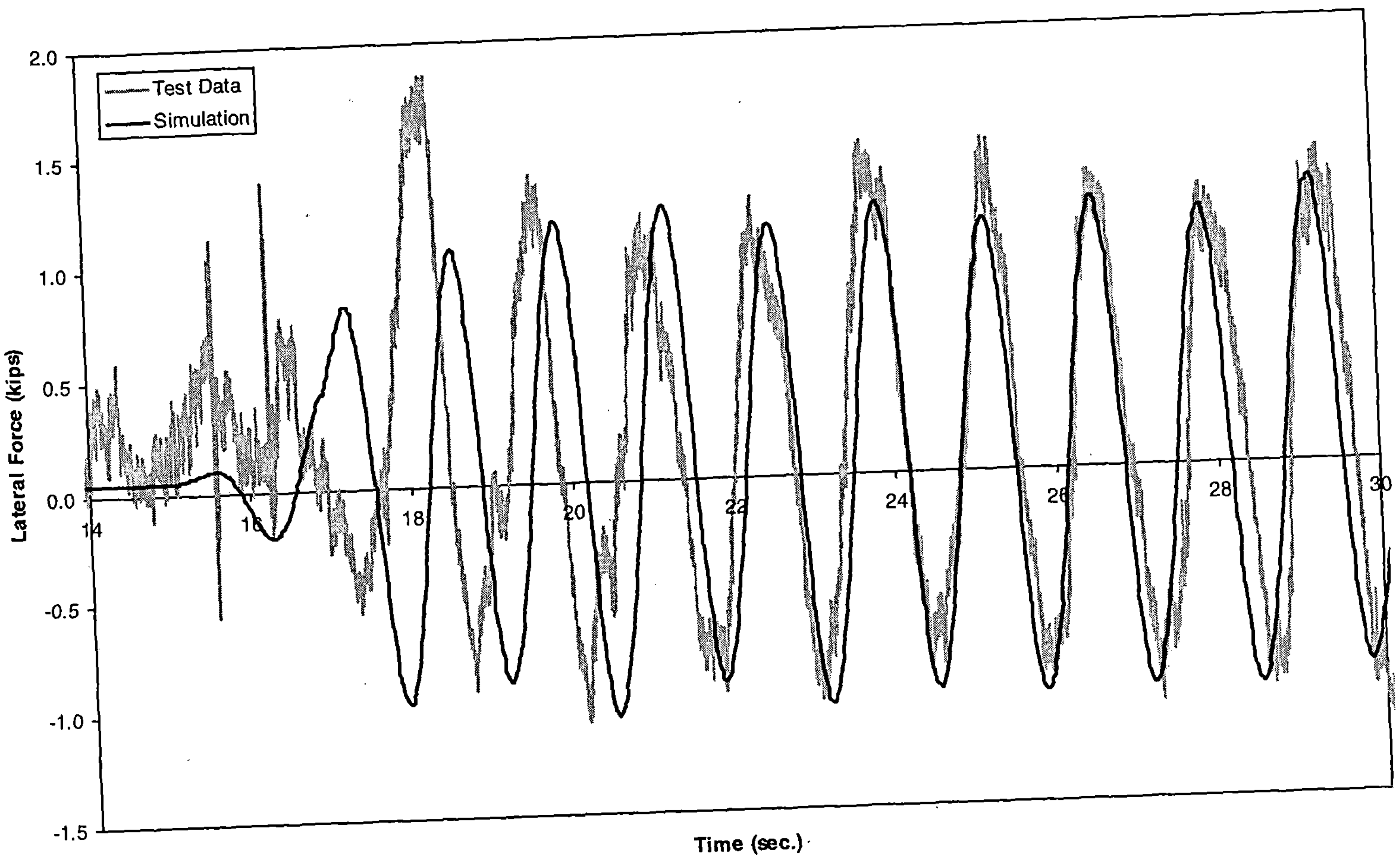

Figure 5-33(b). Twist and roll – lateral force time history, 20 mph (lead right wheel)

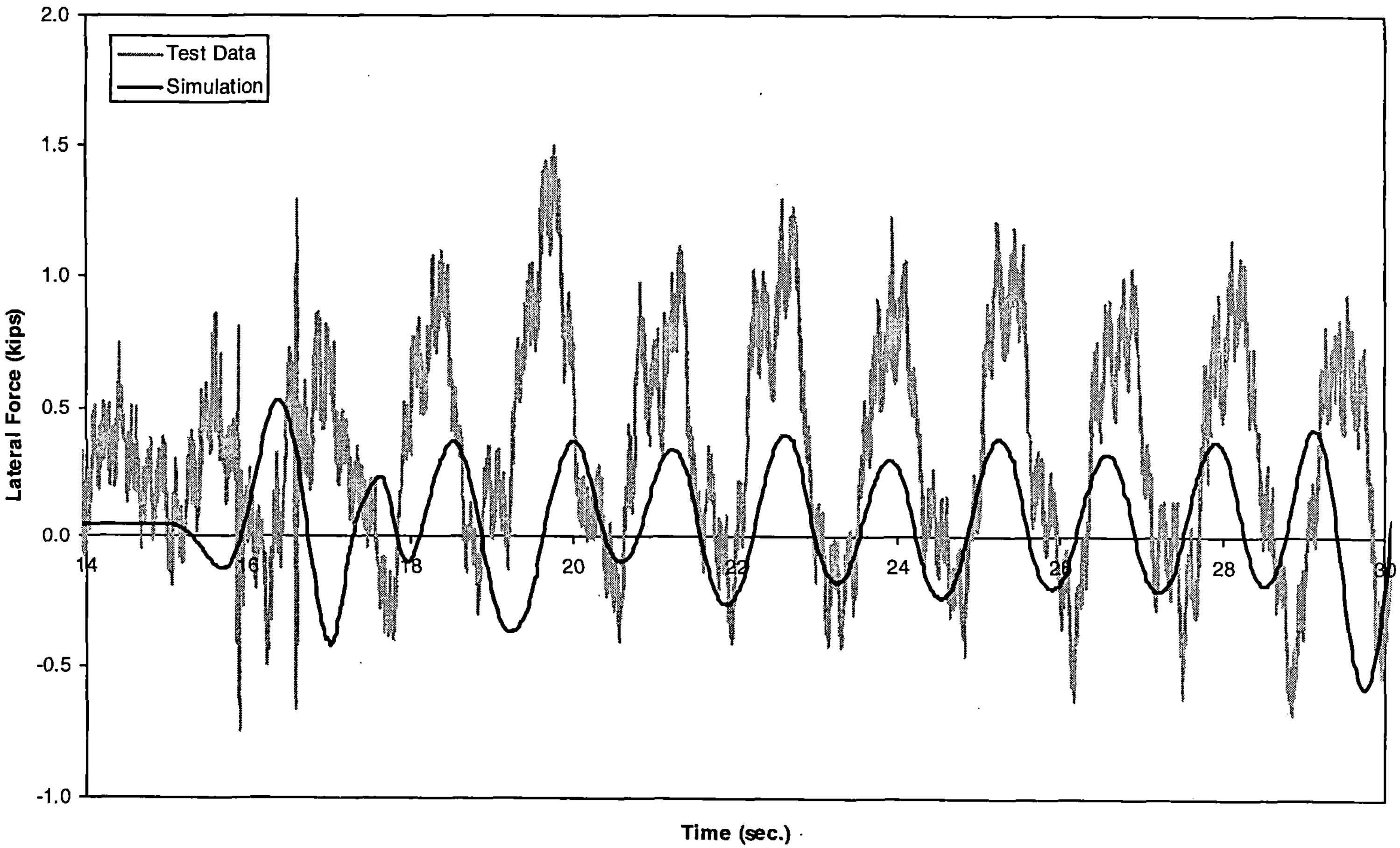

Figure 5-33(c). Twist and roll – lateral force time history, 20 mph (trailing left wheel)

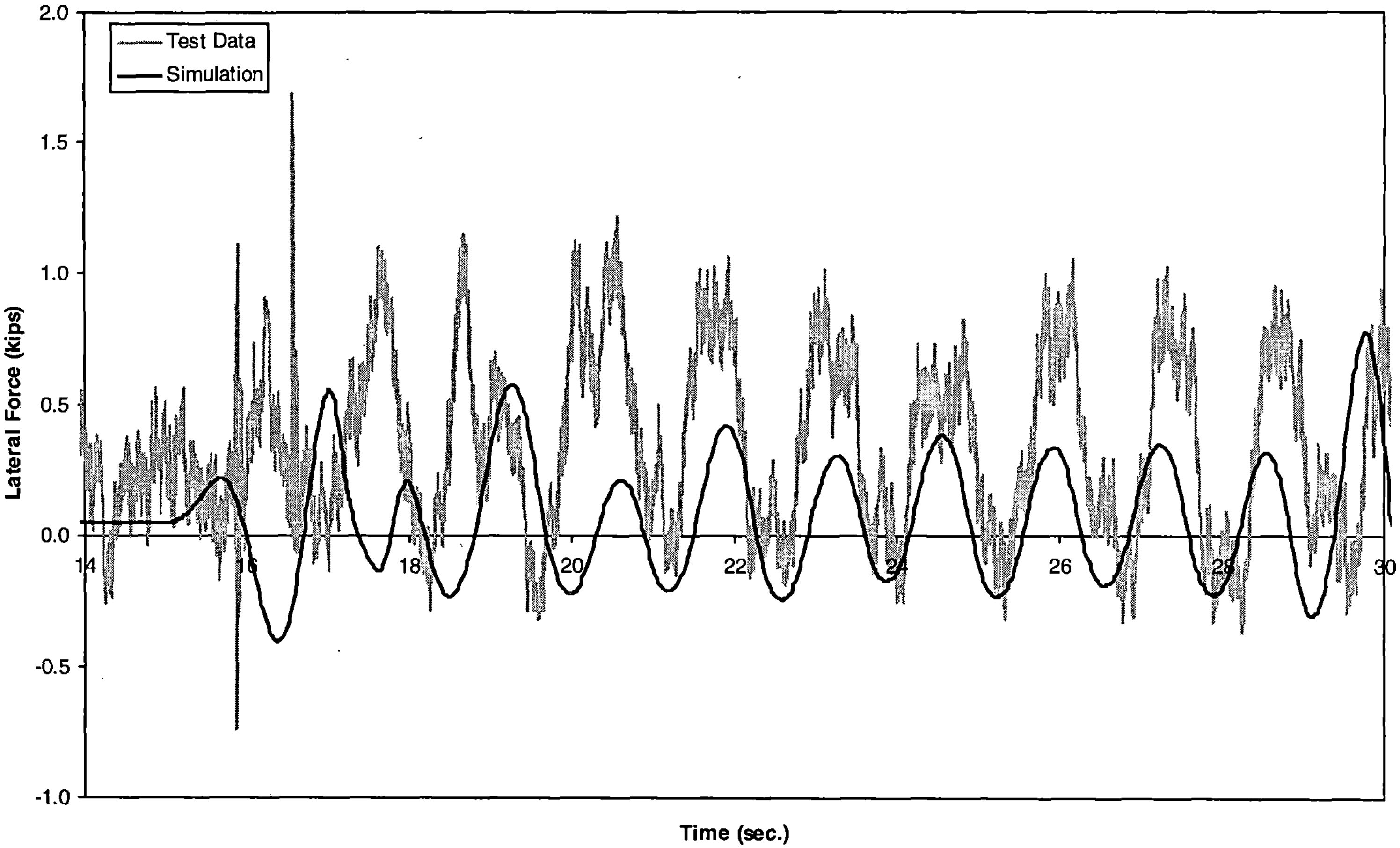

Figure 5-33(d). Twist and roll – lateral force time history, 20 mph (trailing right wheel)

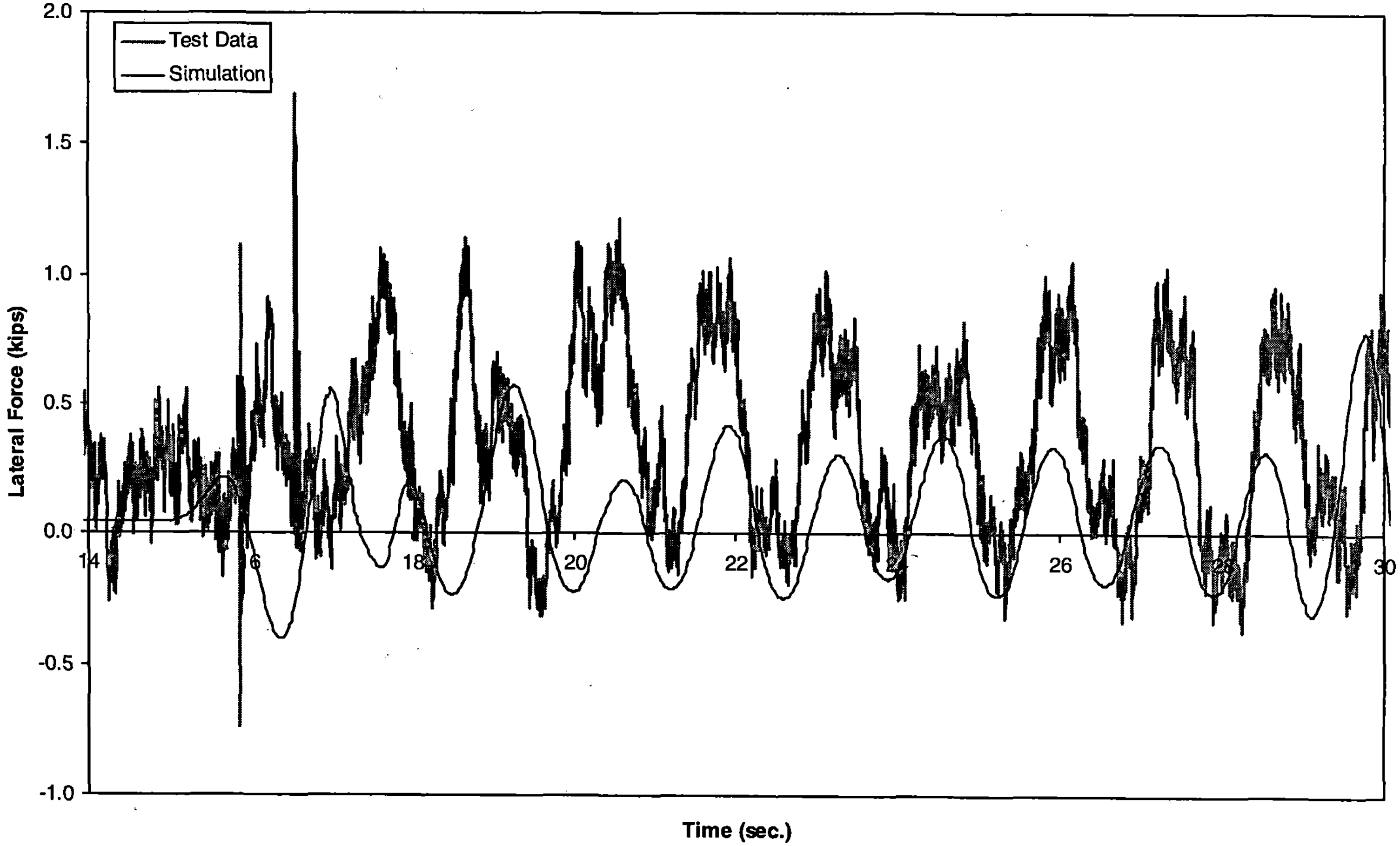

Figure 5-33(d). Twist and roll – lateral force time history, 20 mph (trailing right wheel)

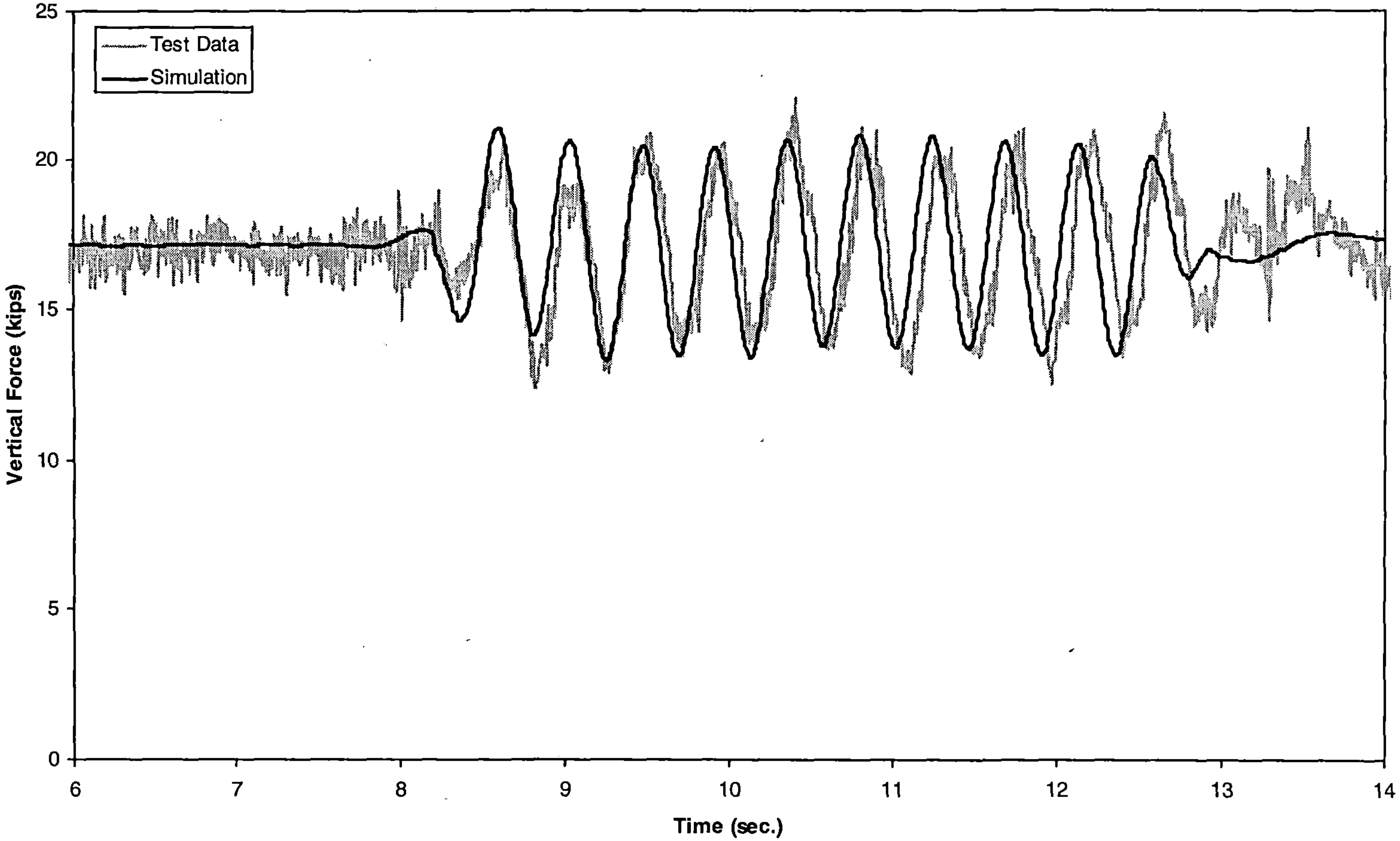

Figure 5-34(a). Twist and roll – vertical force time history, 60 mph (lead left wheel)

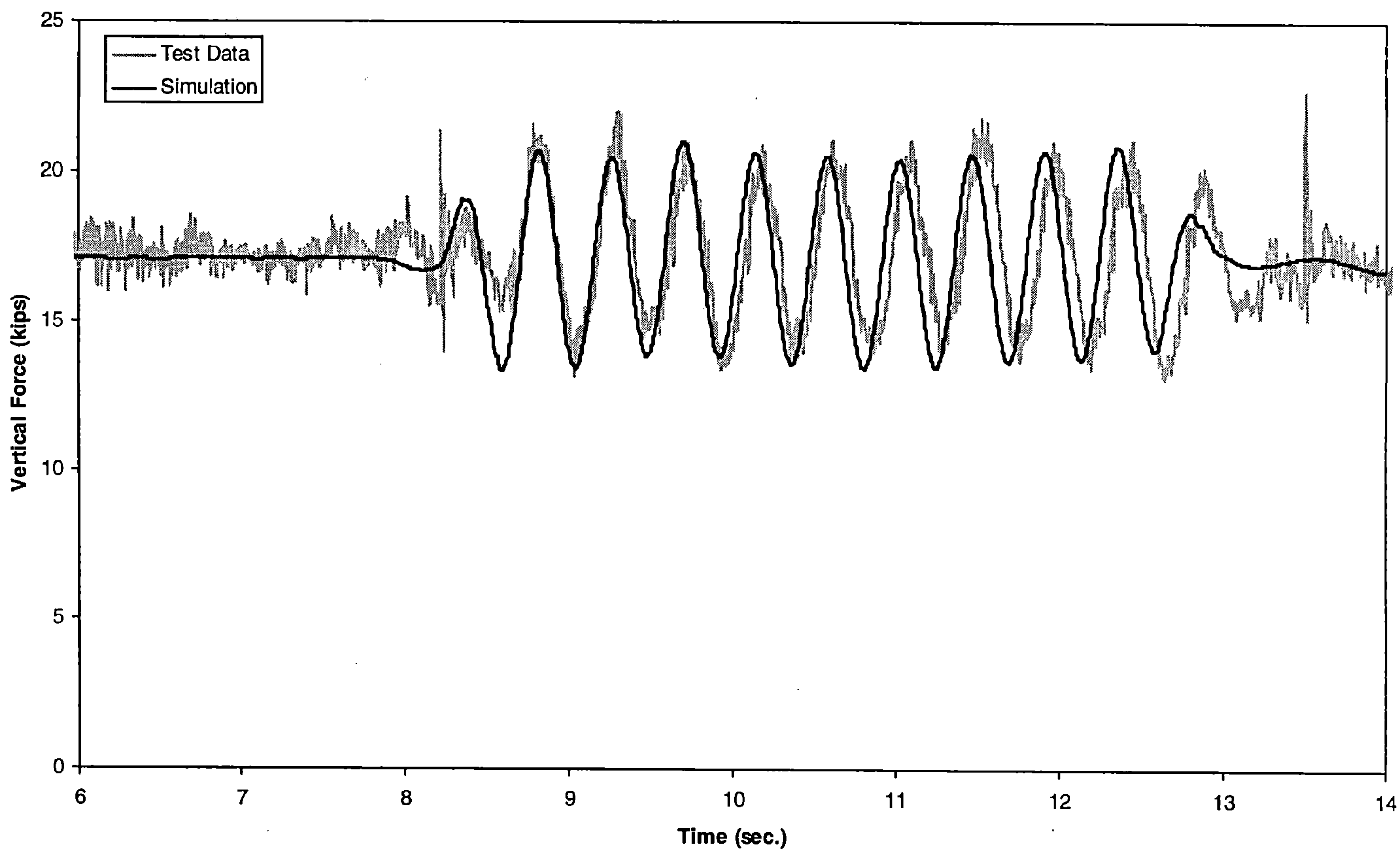

Figure 5-34(b). Twist and roll – vertical force time history, 60 mph (lead right wheel)

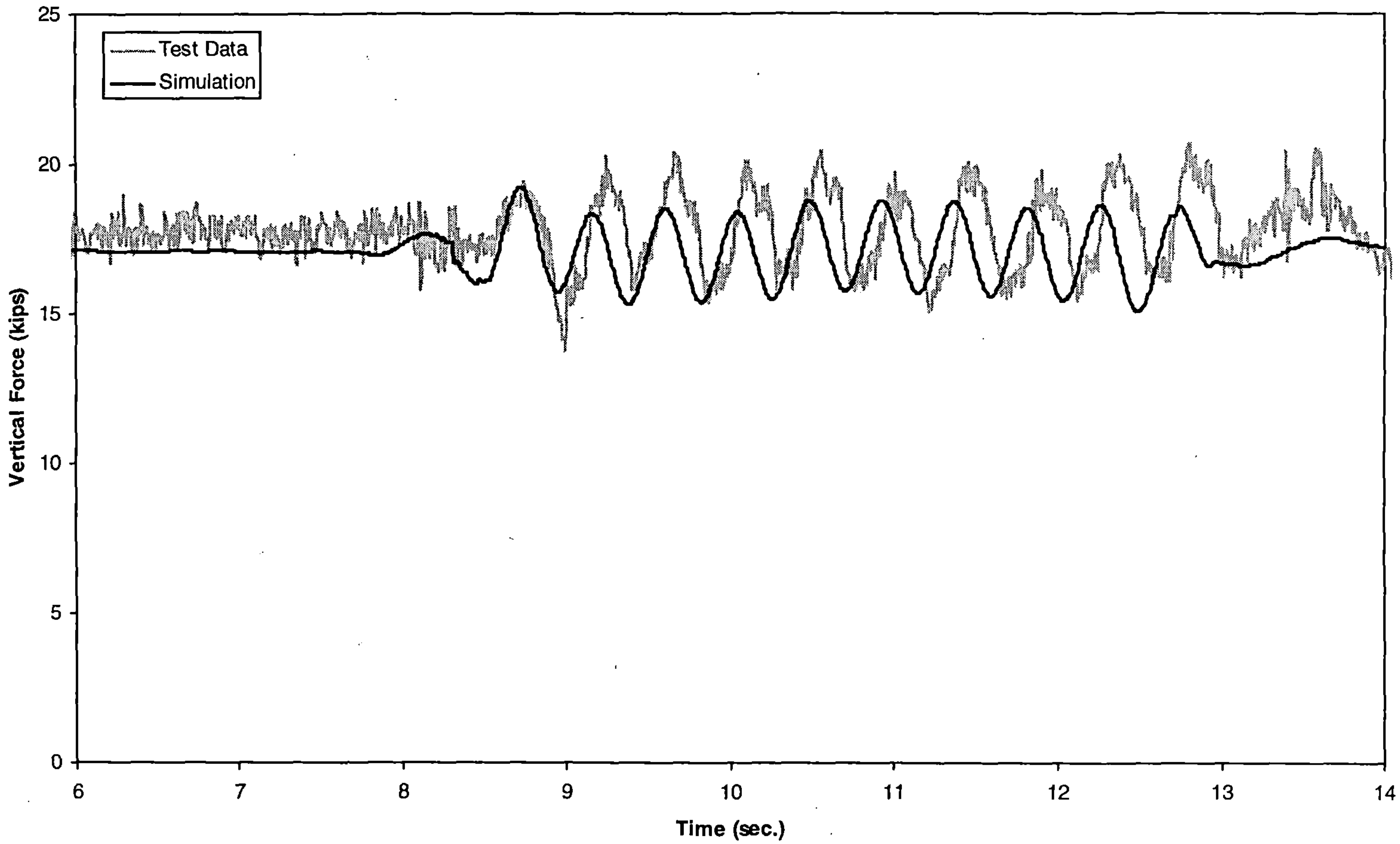

Figure 5-34(c). Twist and roll – vertical force time history, 60 mph (trailing left wheel)

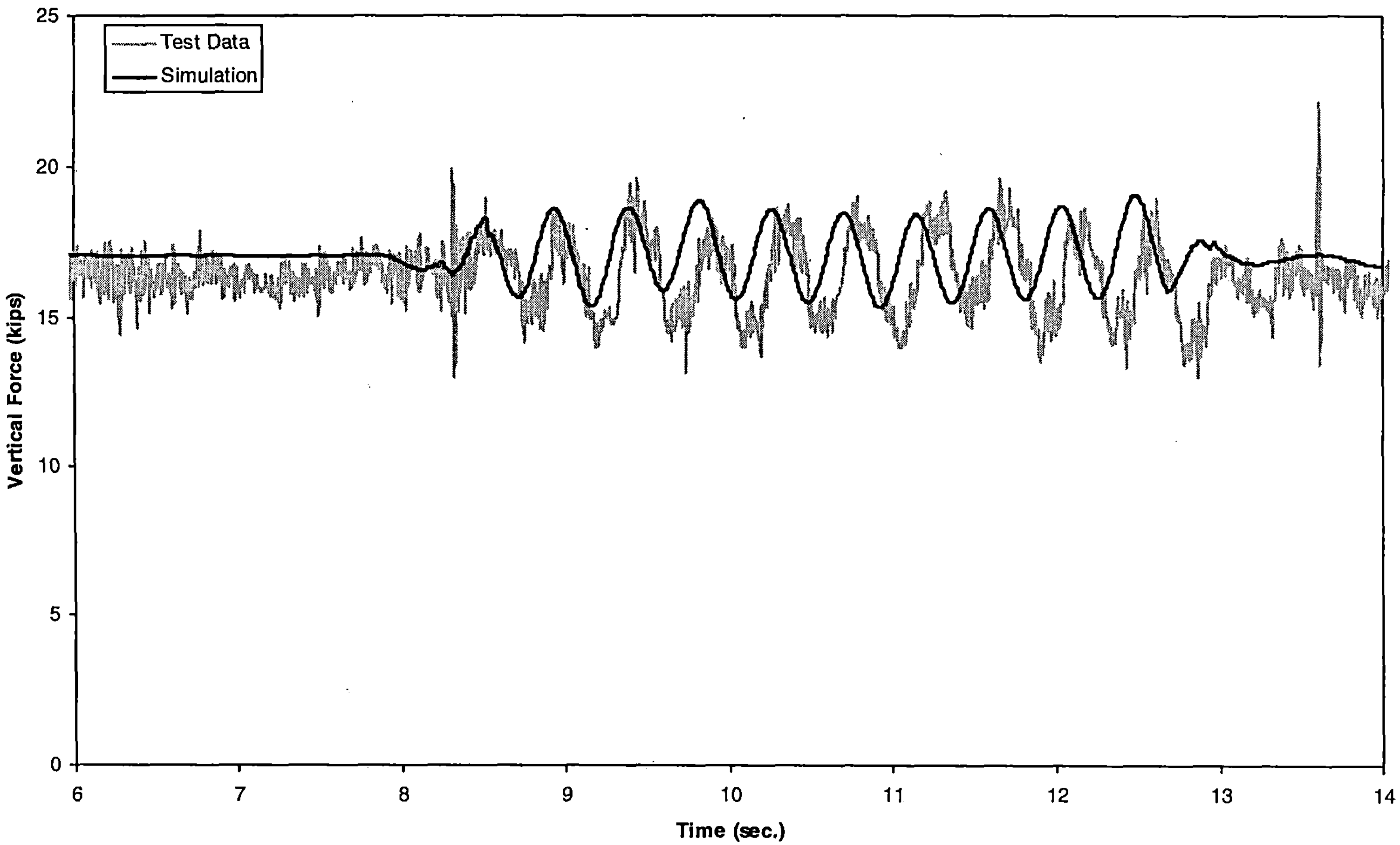

Figure 5-34(d). Twist and roll – vertical force time history, 60 mph (trailing right wheel)

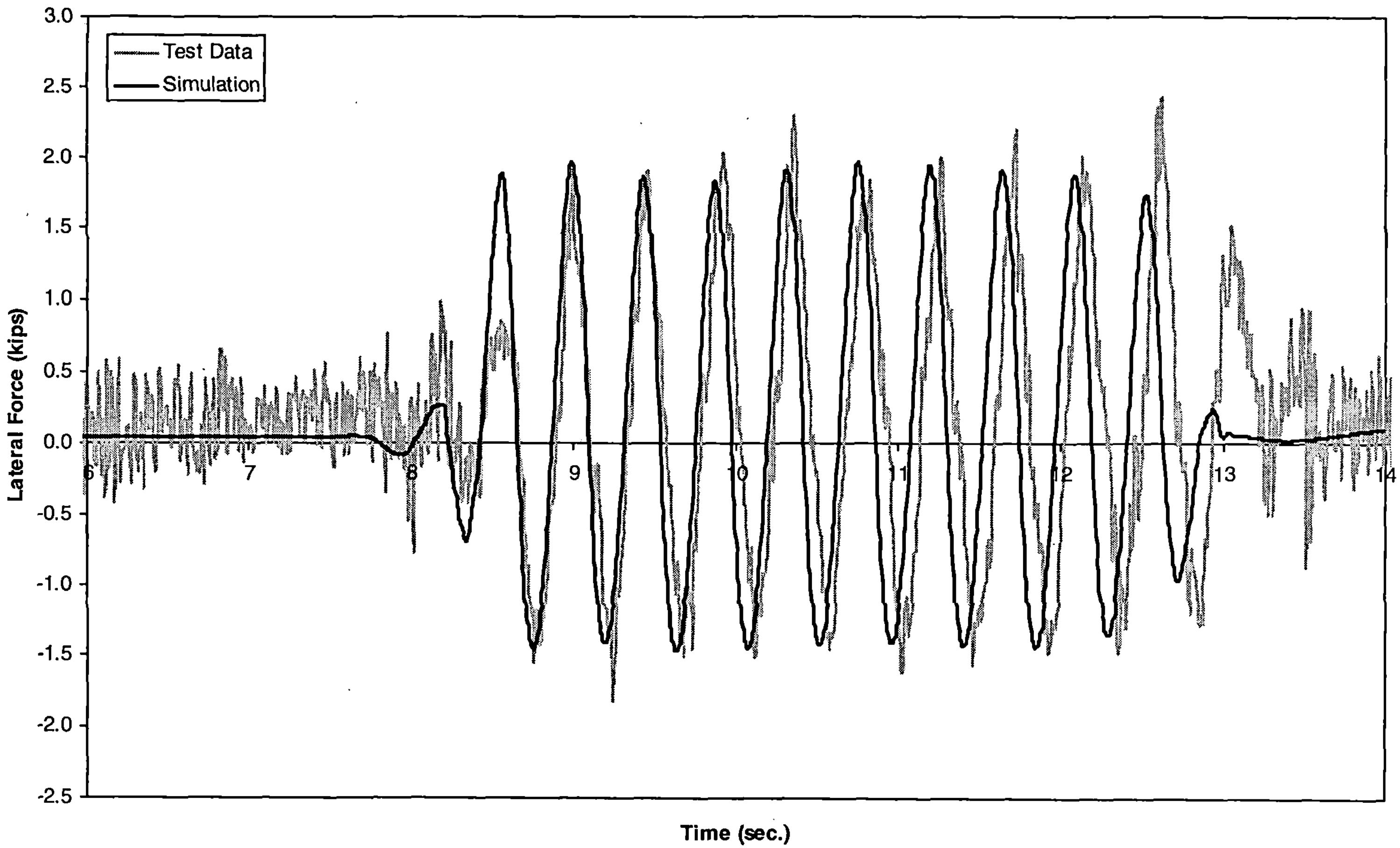

Figure 5-35(a). Twist and roll – lateral force time history, 60 mph (lead left wheel)

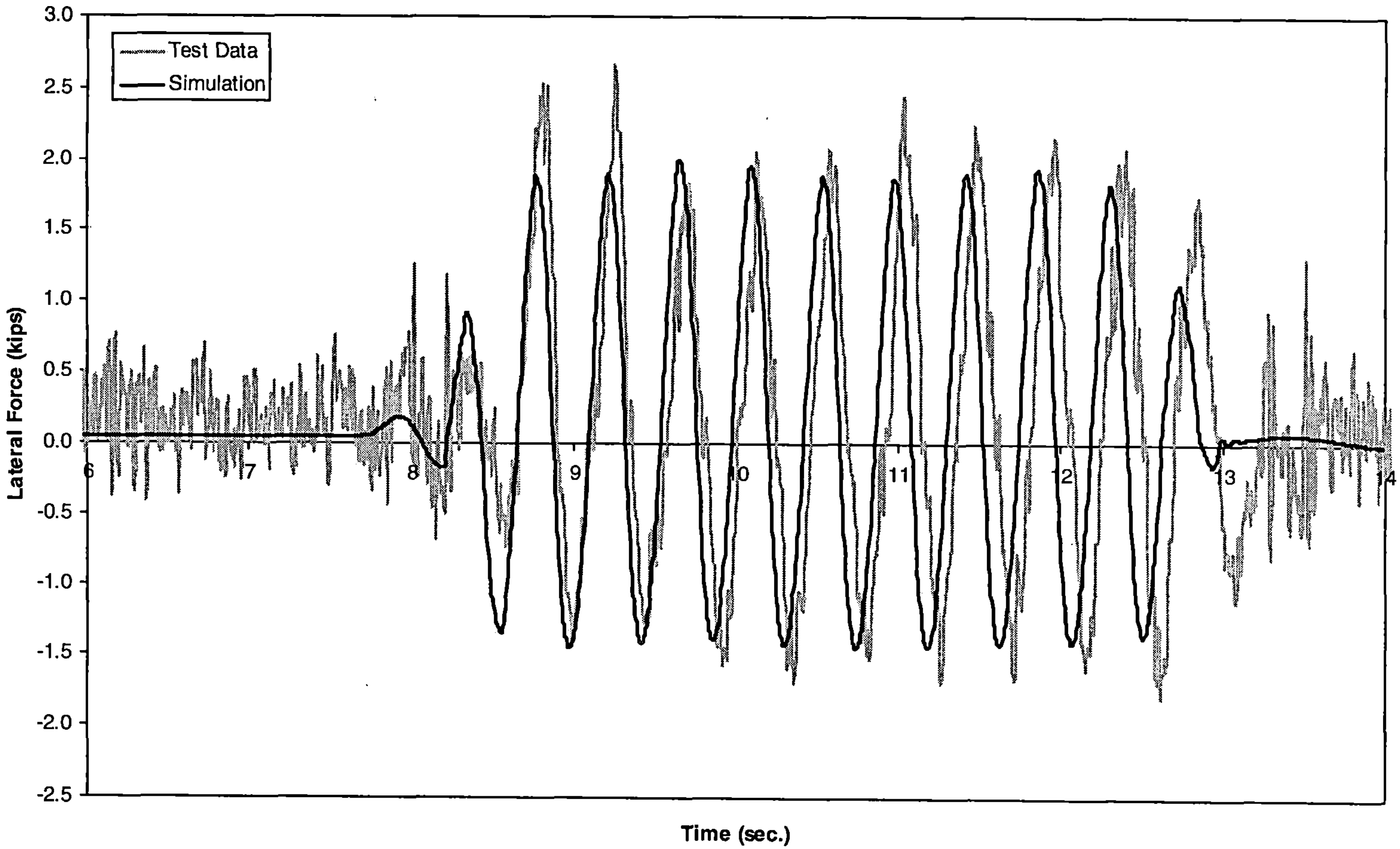

Figure 5-35(b). Twist and roll – lateral force time history, 60 mph (lead right wheel)

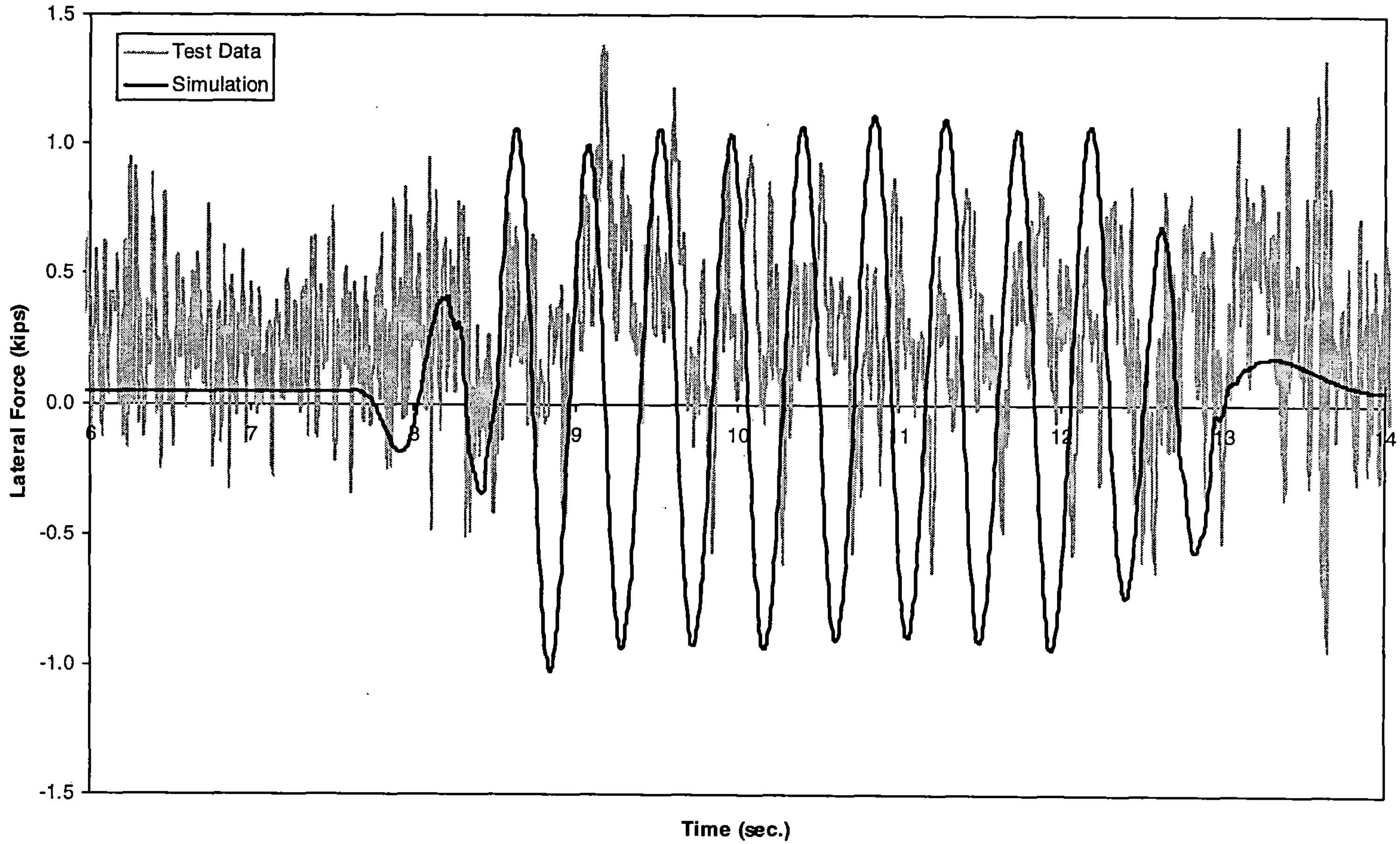

Figure 5-35(c). Twist and roll – lateral force time history, 60 mph (trailing left wheel)

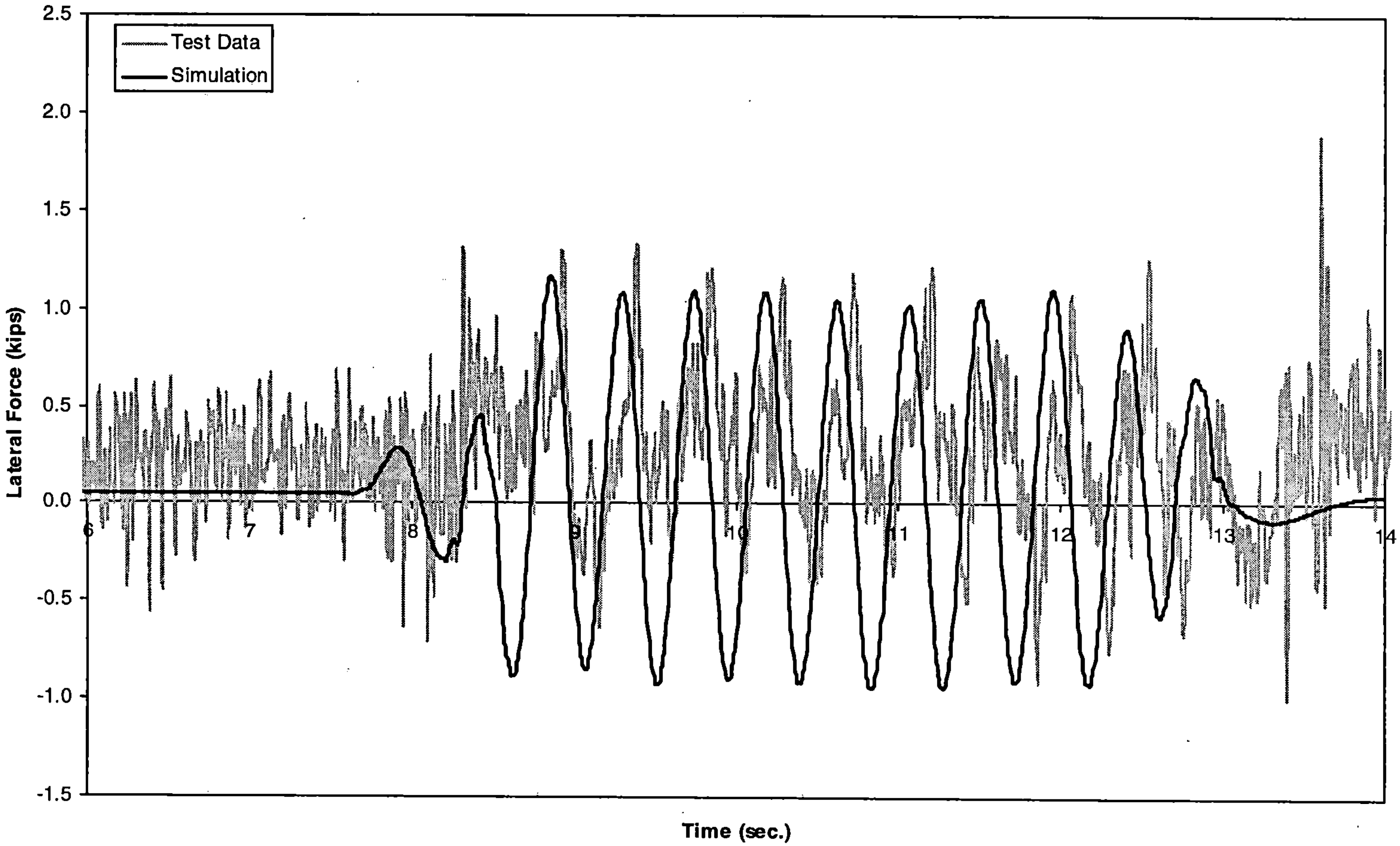

Figure 5-35(d). Twist and roll – lateral force time history, 60 mph (trailing right wheel)

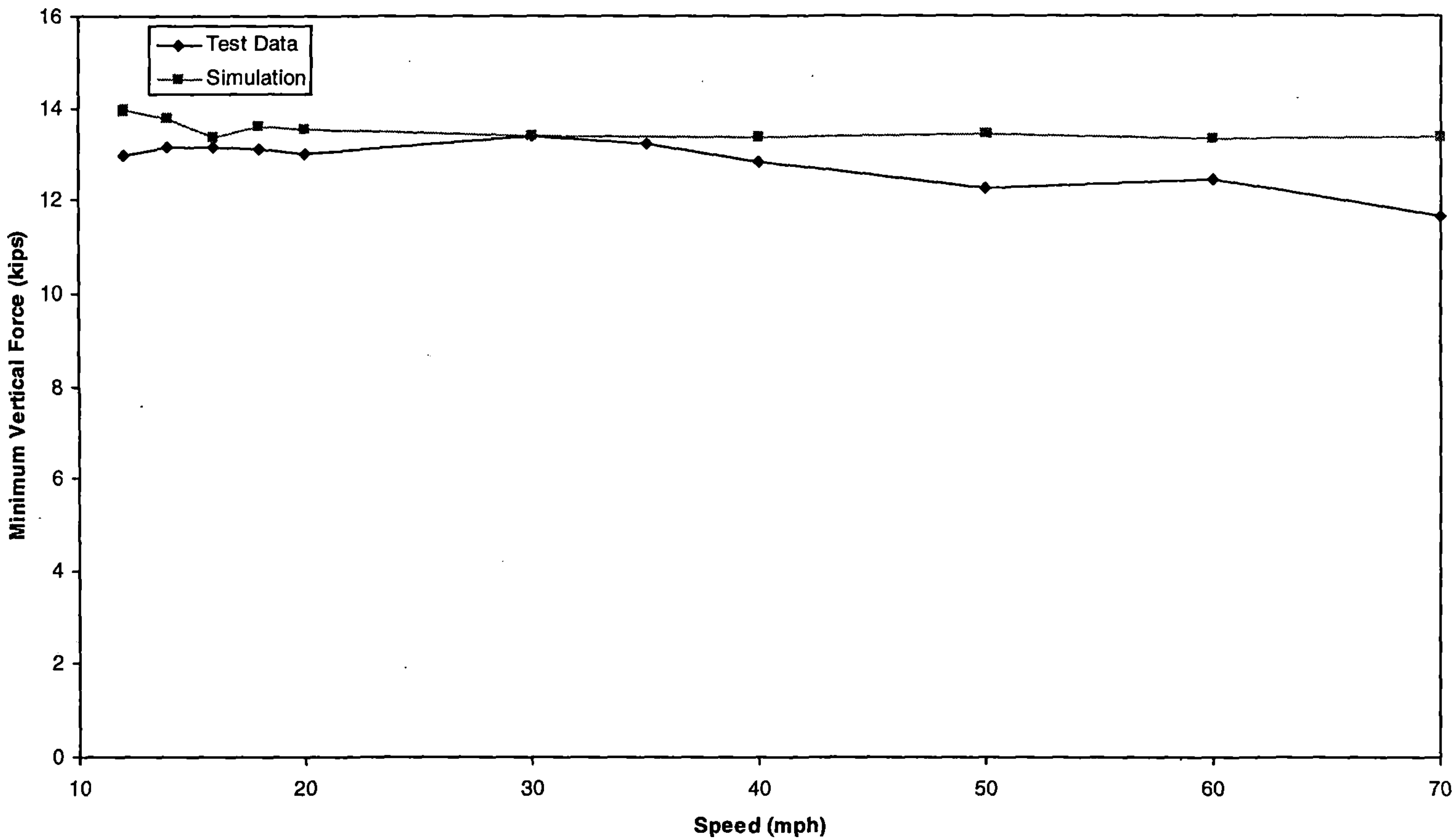

Figure 5-36. Twist and roll – minimum vertical force

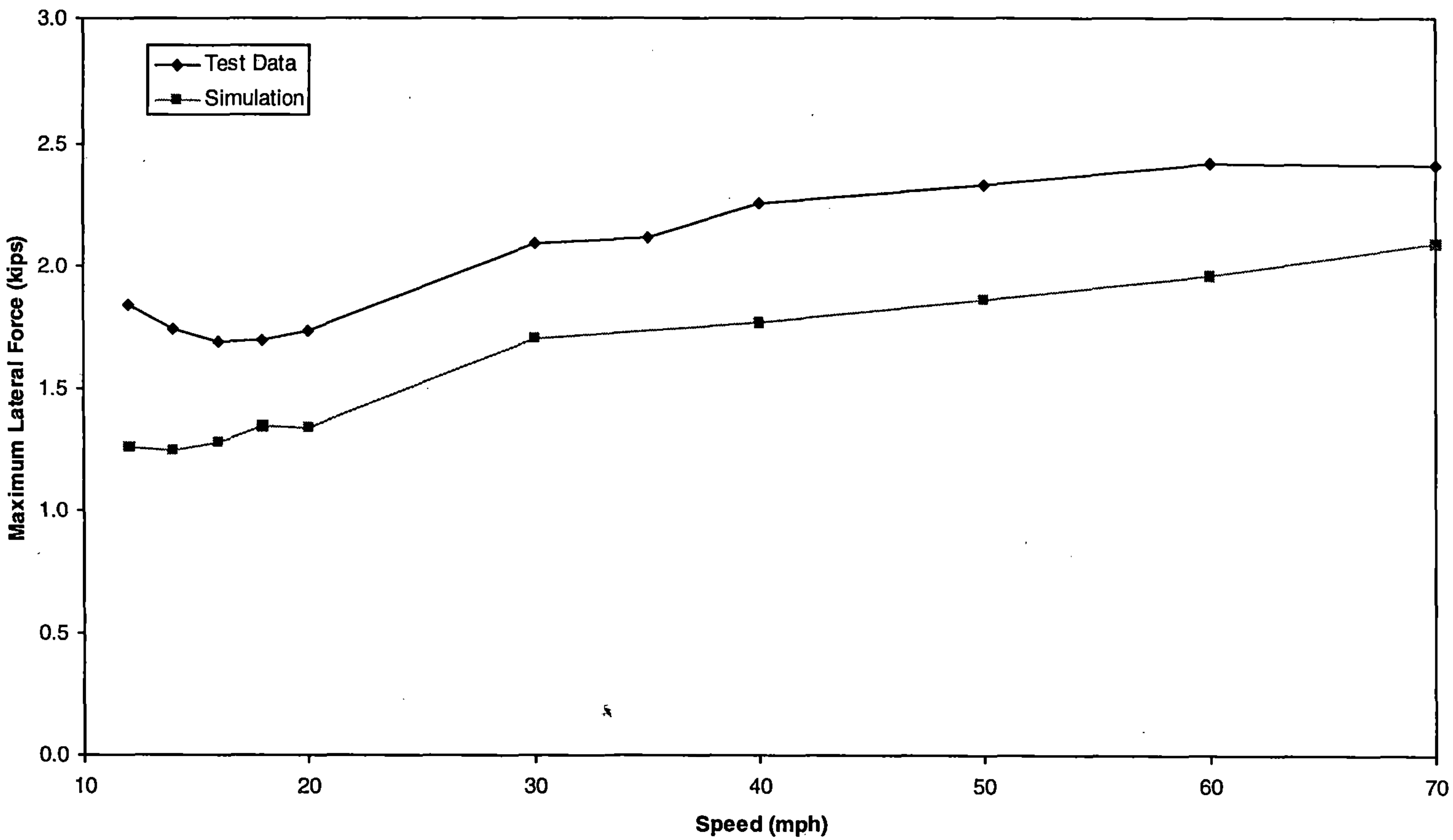

Figure 5-37. Twist and roll – maximum lateral force

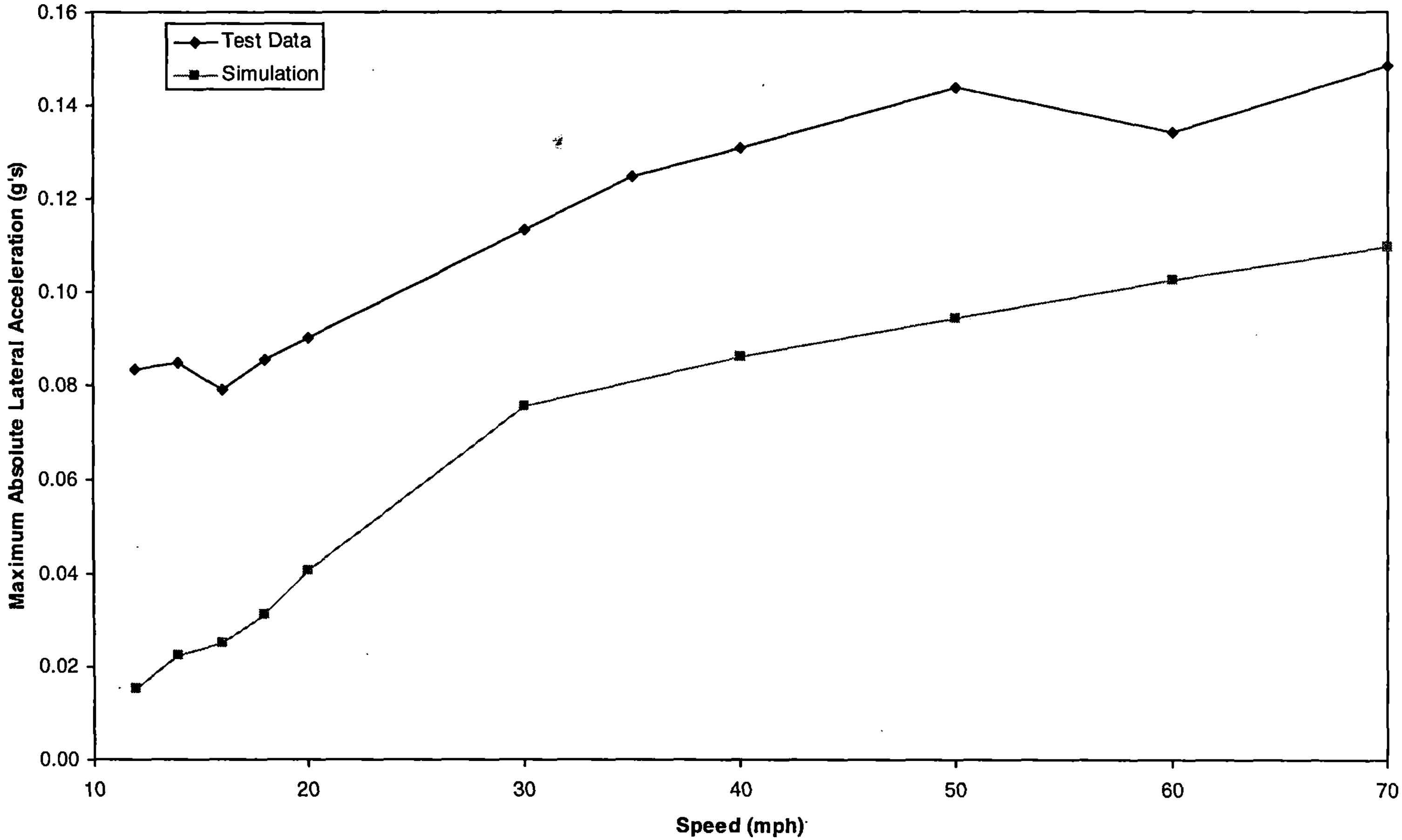

Figure 5-38. Twist and roll – maximum absolute lateral carbody acceleration

5.6 Pitch and Bounce

Test Description

This test was designed to evaluate the car safety as it negotiates track perturbations which generate pitch and bounce oscillations. An example is a track constructed with parallel joints and/or track structure with changes in the vertical track stiffness. The analyses and tests show the margin of safety in the wheel-rail forces against any tendency for the car to derail. The track included 10 parallel, vertical perturbations, 39 ft apart, with amplitude of 0.75 in. (see Figure 5-39). The tests were performed at speeds in the range of 10 to 70 mph, ensuring the capture of the resonant speed.

Correlation

Figure 5-40 illustrates the case of a pitch and bounce correlation of the vertical force for the four wheels of the trailing truck at a speed of 20 mph. Good correlation is seen between the test data and simulation results. The small fluctuations in the test data are attributed to the inherent variations in the rail vertical profile data, not modeled in the simulation. The lateral force levels are too small to be of any practical significance and are not shown. Similar results were obtained for other speeds.

Figure 5-41 shows the vertical forces for the four wheels for a pitch and bounce test conducted at 60 mph. The correlation for the vertical force levels is good for all wheels.

A plot of the correlation of test and simulation data of minimum vertical force is shown in Figure 5-42 for the left wheel on the lead axle of the trailing truck. Good correlation is shown

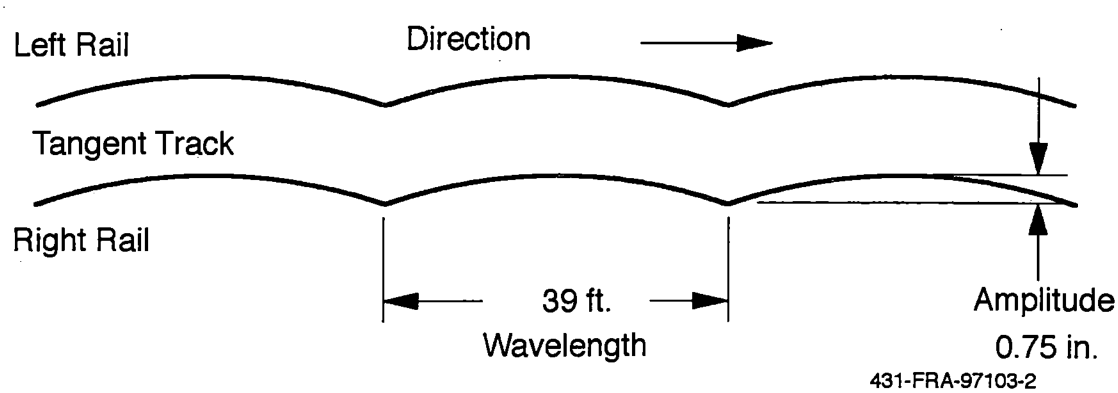

Figure 5-39. Track surface variation for pitch and bounce

through the speed range for the vertical force. The minimum vertical force is about 31 mph in both the test data and simulation. This occurs at the resonance speeds. The resonant condition is not noticeably strong.

Conclusion

The simulation tool shows very good correlation for the vertical force throughout the speed range. OMNISIM is able to predict the shape and amplitude of the vertical forces. The predicted lateral forces are small, consistent with the test data.

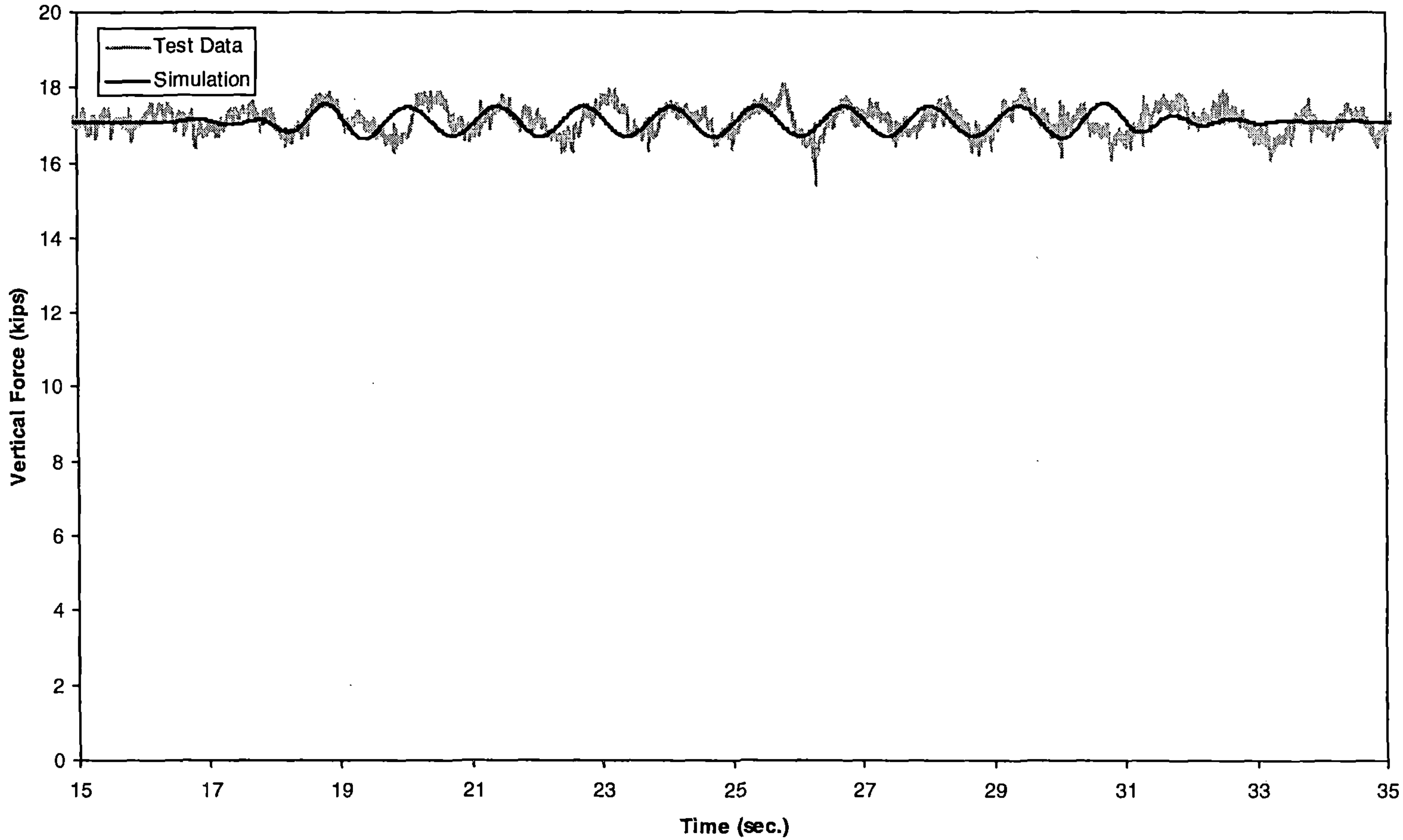

Figure 5-40(a). Pitch and bounce – vertical force time history, 20 mph (lead left wheel)

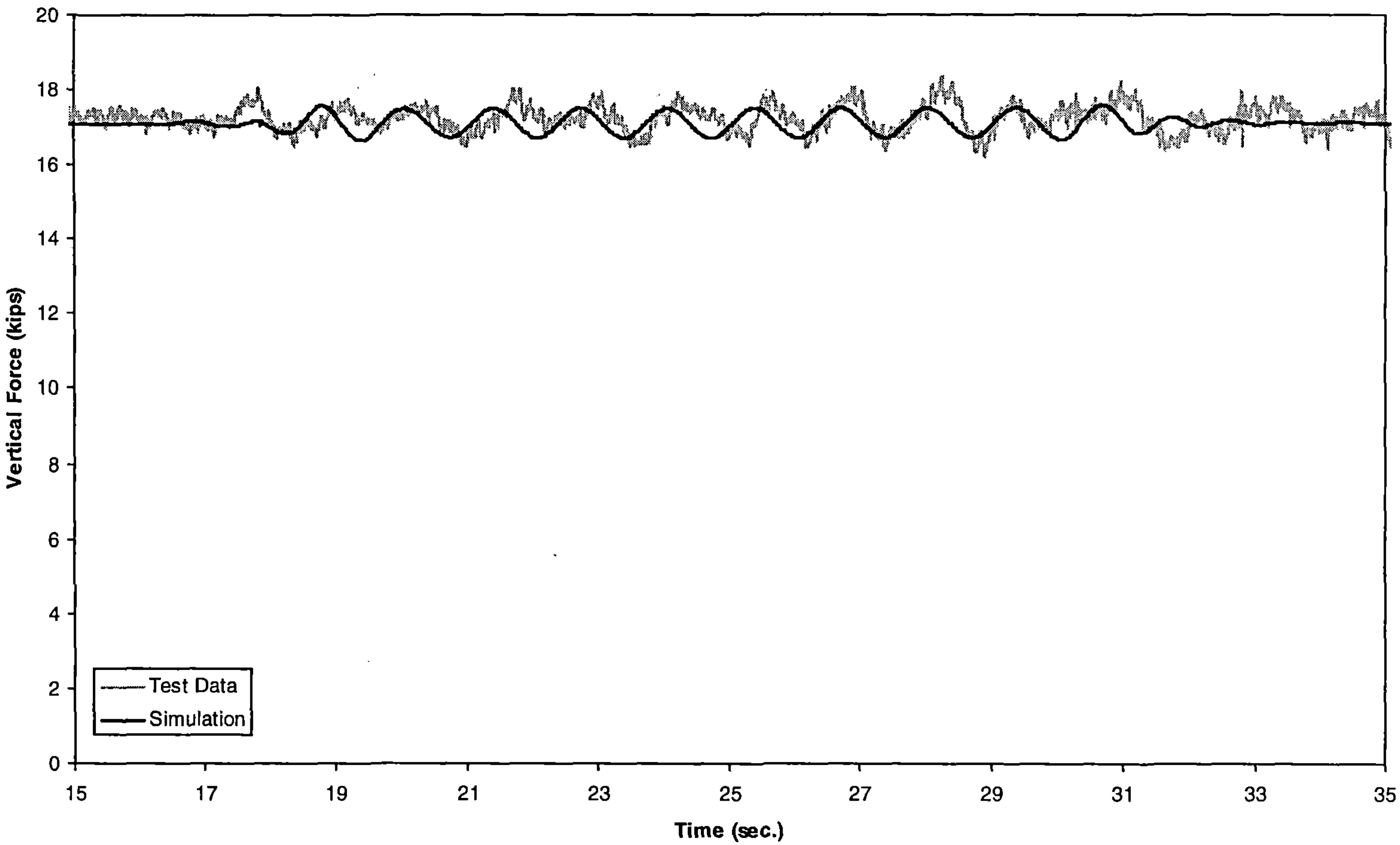

Figure 5-40(b). Pitch and bounce – vertical force time history, 20 mph (lead right wheel)

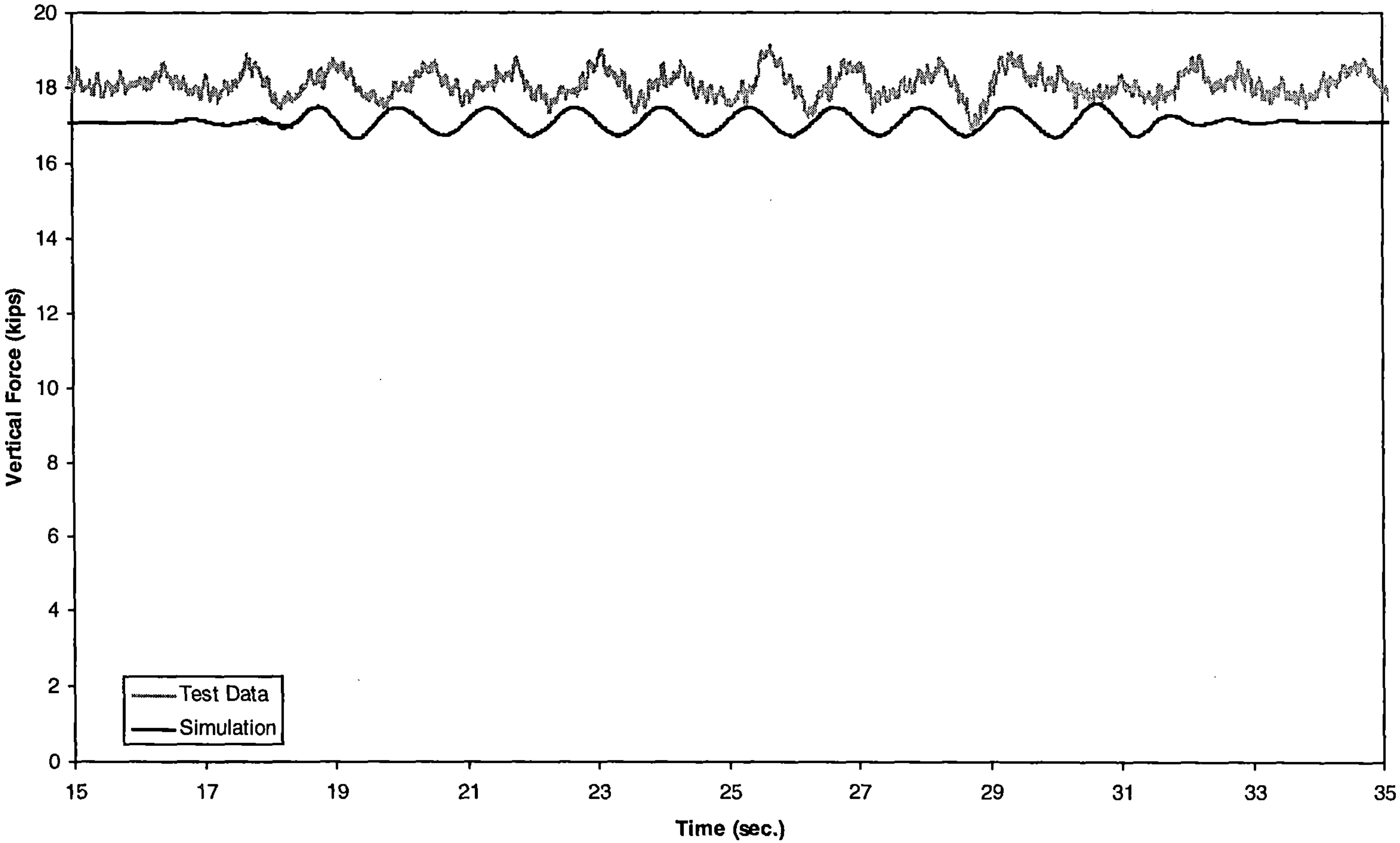

Figure 5-40(c). Pitch and bounce – vertical force time history, 20 mph (trailing left wheel)

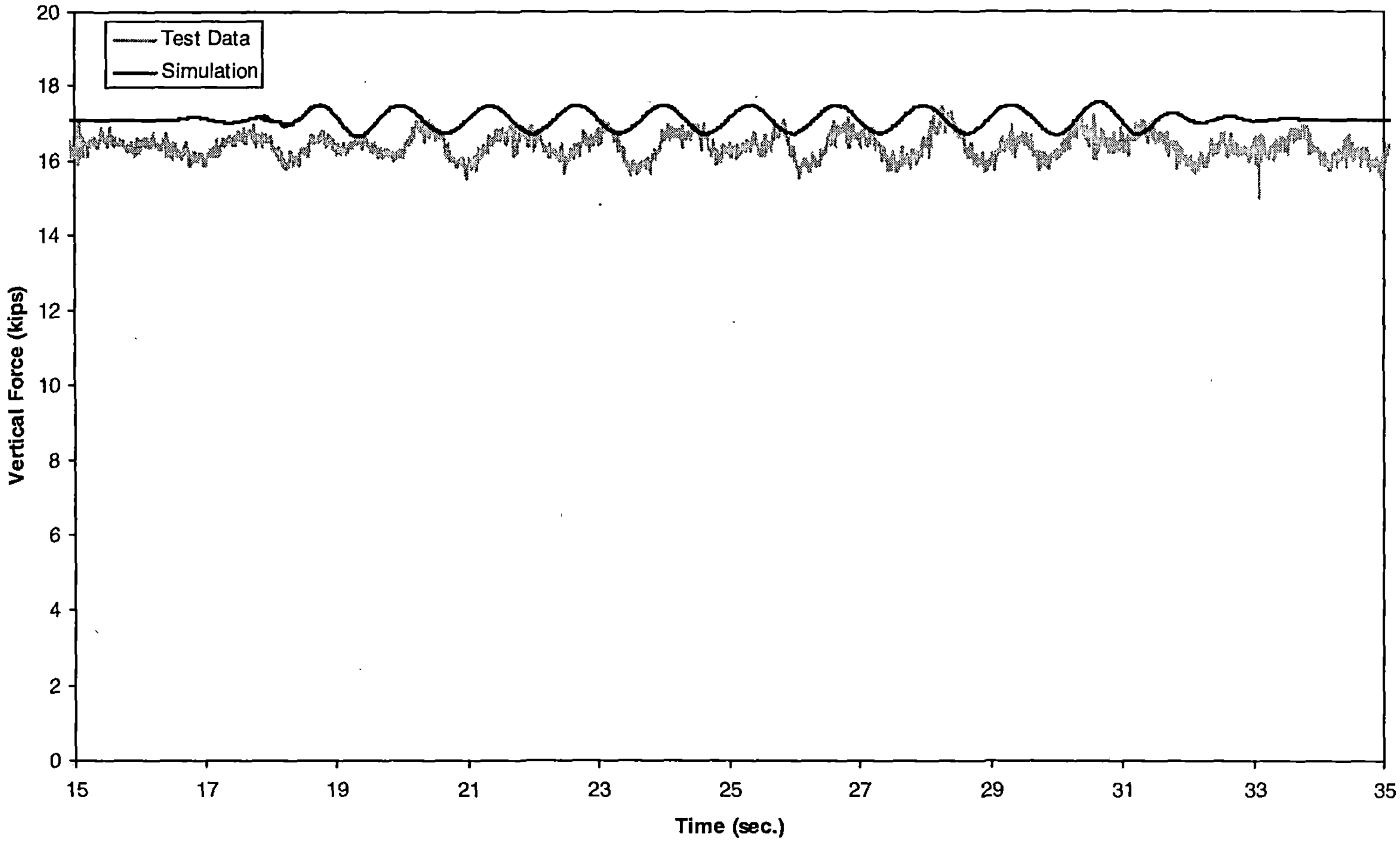

Figure 5-40(d). Pitch and bounce – vertical force time history, 20 mph (trailing right wheel)

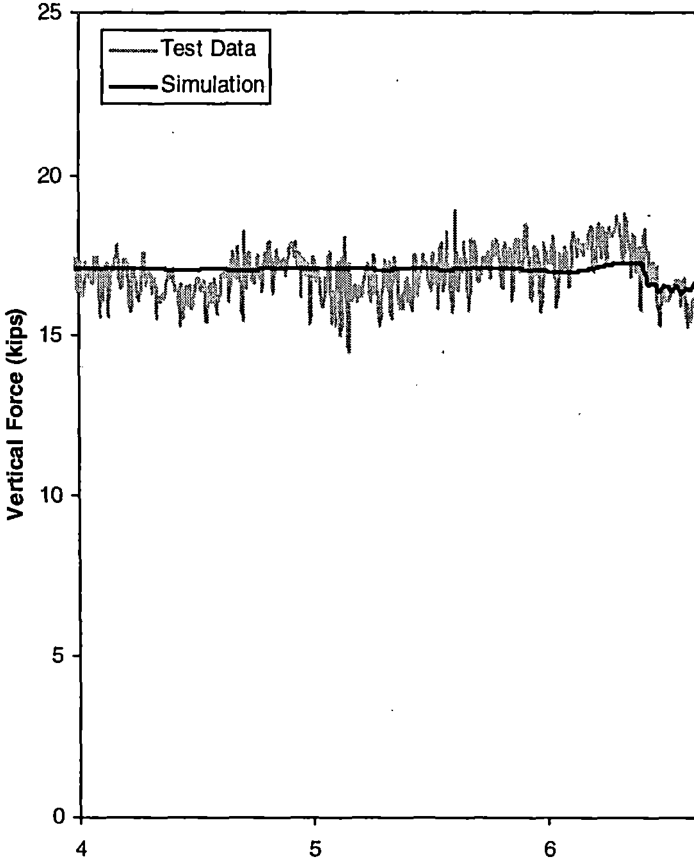

Figure 5-41(a). Pitch and bounce –

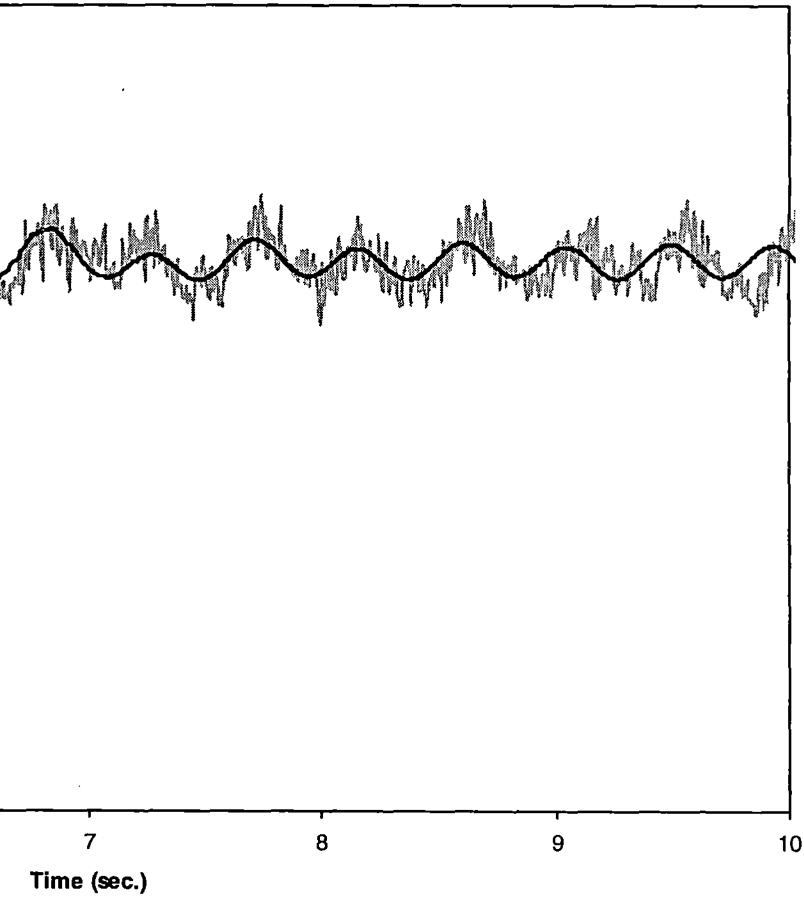

vertical force time history, 60 mph (lead left wheel)

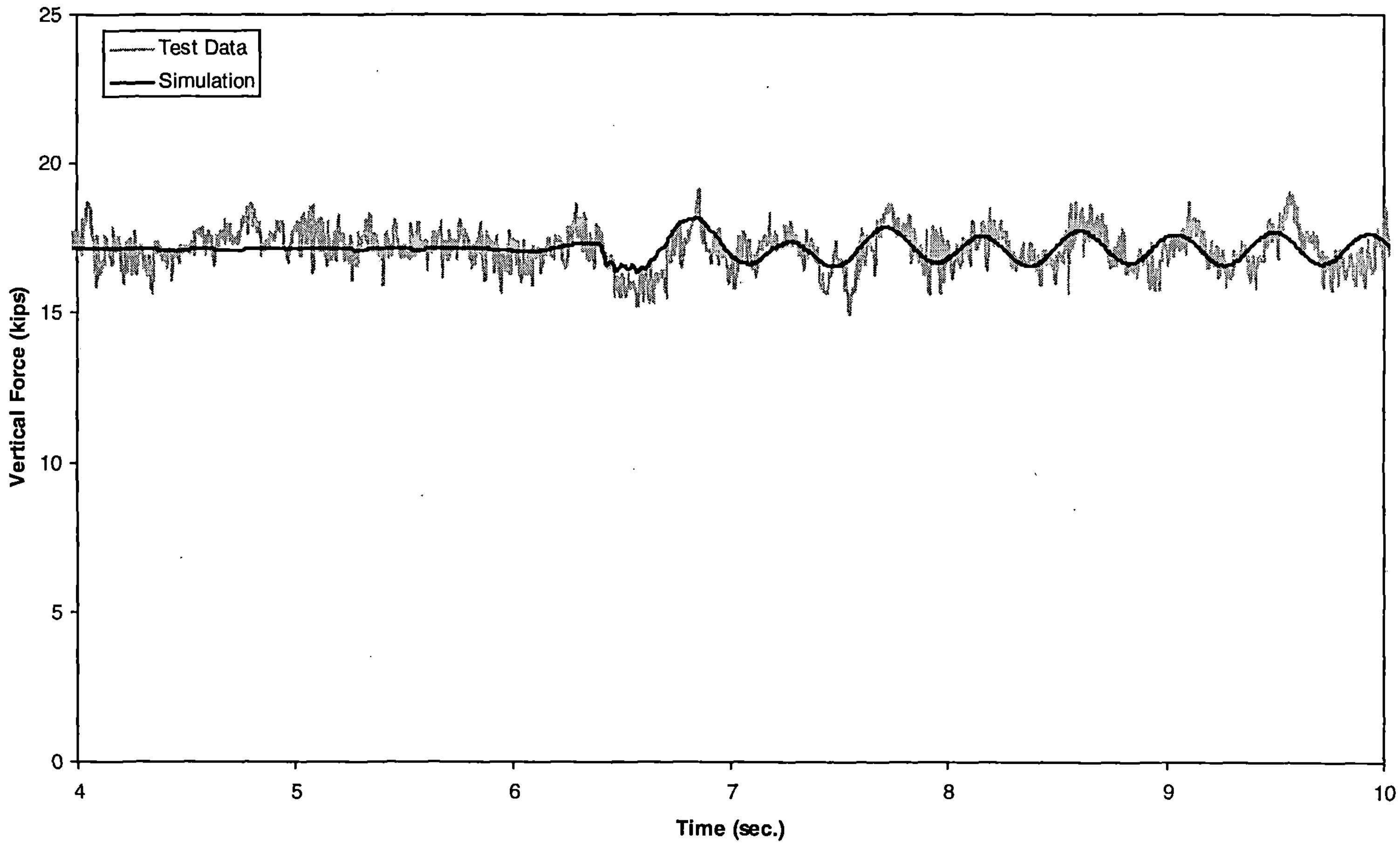

Figure 5-41(b). Pitch and bounce – vertical force time history, 60 mph (lead right wheel)

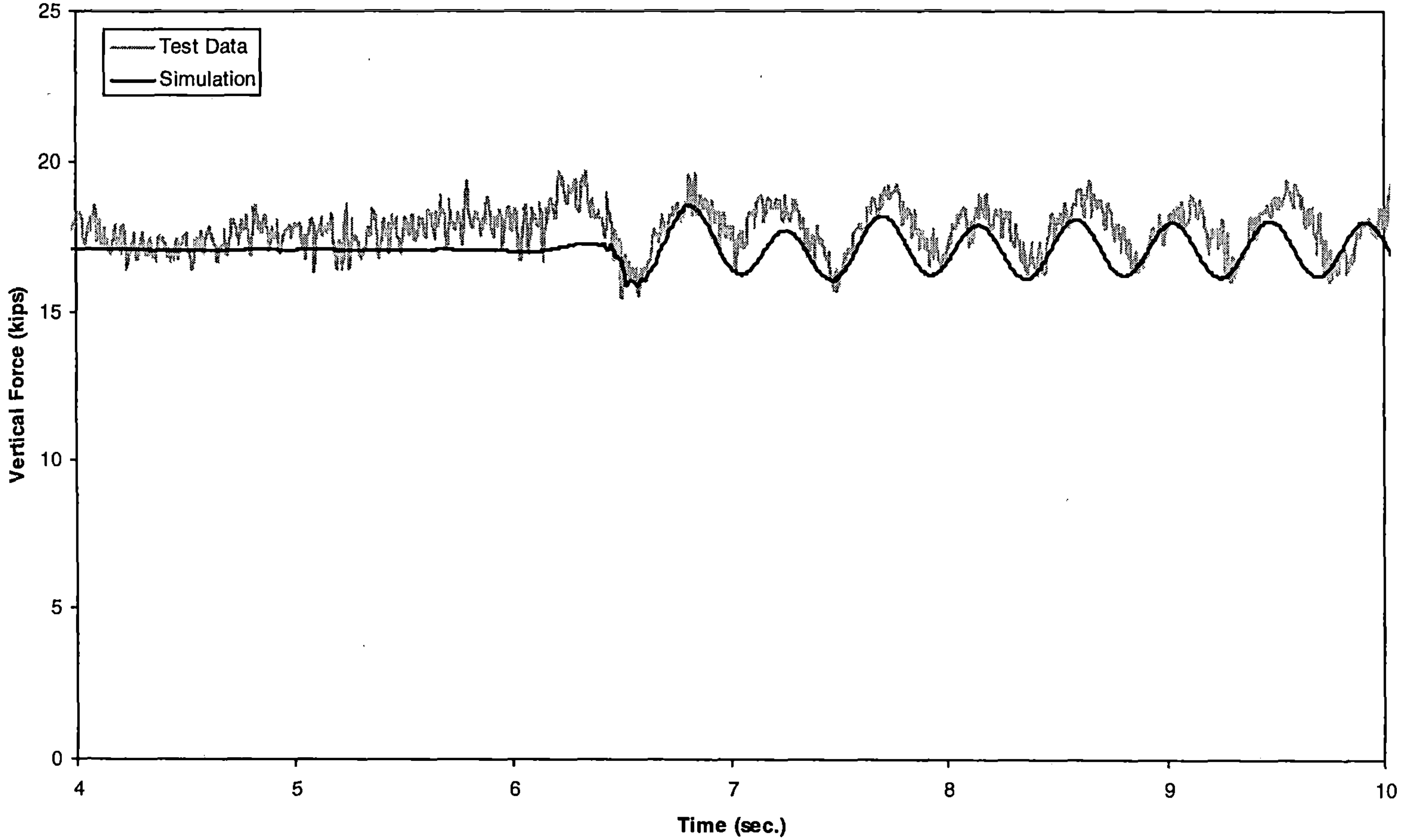

Figure 5-41(c). Pitch and bounce – vertical force time history, 60 mph (trailing left wheel)

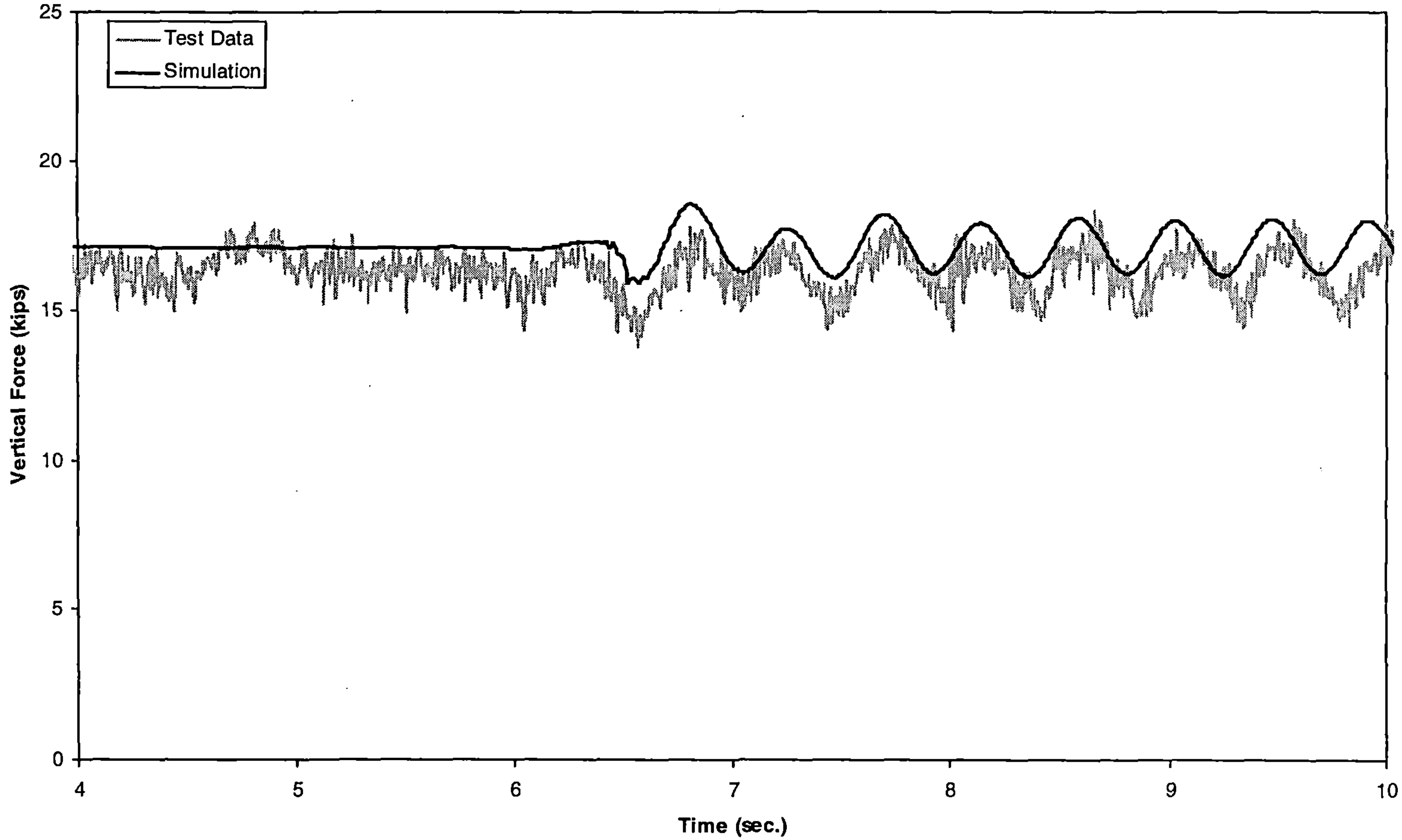

Figure 5-41(d). Pitch and bounce – vertical force time history, 60 mph (trailing right wheel)

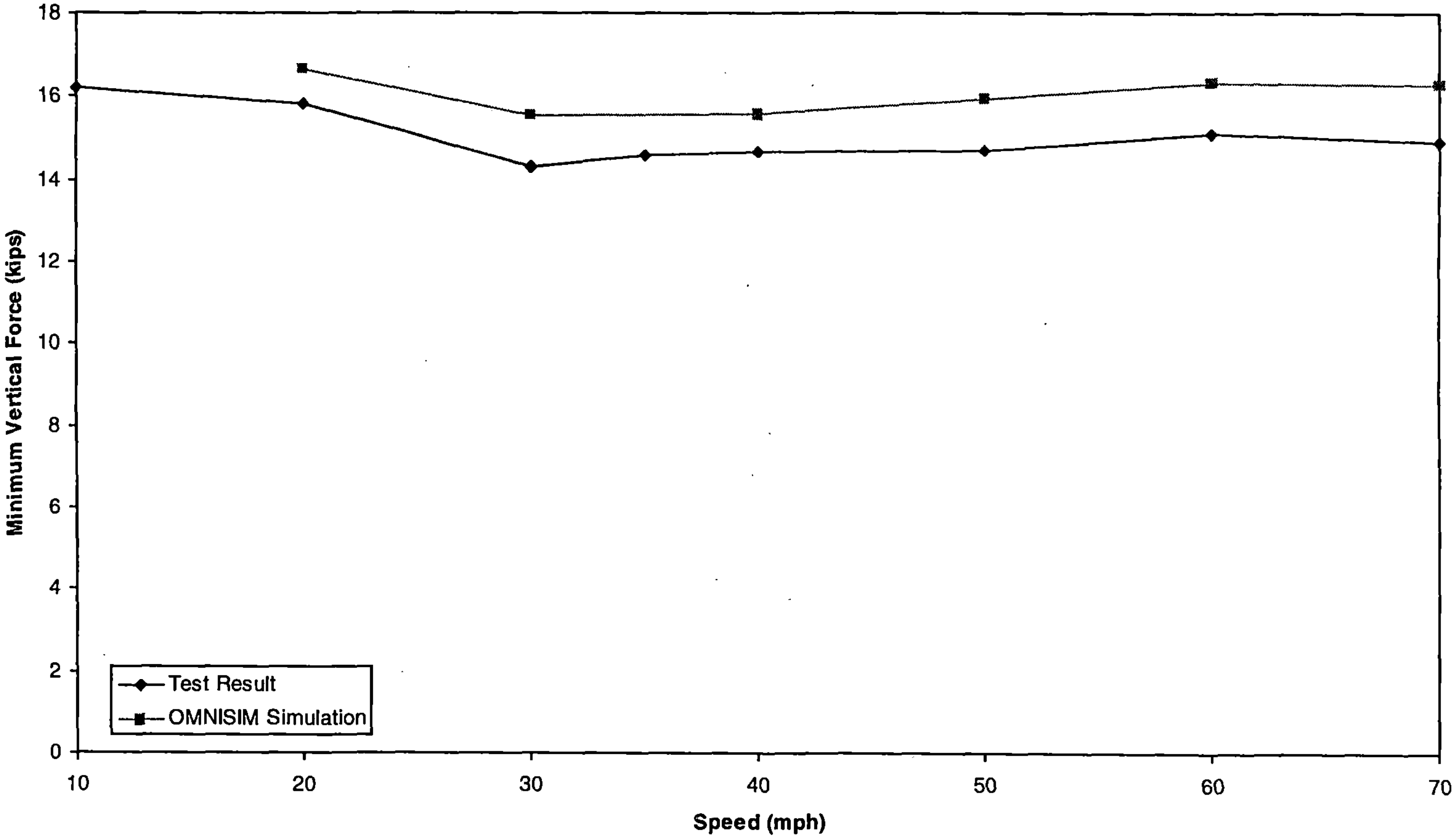

Figure 5-42. *Pitch and bounce – minimum vertical force*

5.7 Hunting Test with Initial Alignment Defects

Test Description

The hunting test was conducted to provide information on lateral vehicle stability at various operating speeds on tangent track. Tests were conducted on the Railroad Test Track (RTT) during dry conditions while recording carbody accelerations and wheel/rail forces. The tests were performed at speeds in the range of 80 to 130 mph. The test vehicle was operated over the test track through a single lateral perturbation of 9/16 in. with a 22 ft wavelength to initiate a lateral dynamic response. The installed lateral perturbation is equal on both rails and is shown in Figure 5-43.

Correlation

In both the test data and the simulations, no evidence of sustained vehicle hunting is observed in the 80 to 130 mph speed range. Additional computer simulations conducted at higher speeds indicated that the vehicle hunting speed is in excess of 200 mph. Comparisons of lateral measured and simulated forces resulting from track perturbation are plotted in Figure 5-44 for all four wheels of the trailing truck for the 130 mph case. Both the test and simulation data show no evidence of sustained hunting and in general have lateral force variations of less than ±2 kips.

Conclusion

OMNISIM predicts that the hunting speed for this vehicle is well above the test maximum speed (130 mph). Lower conicity wheels or other truck modifications would be required to generate a practical hunting speed that can be achieved in the tests for comparisons with the simulation.

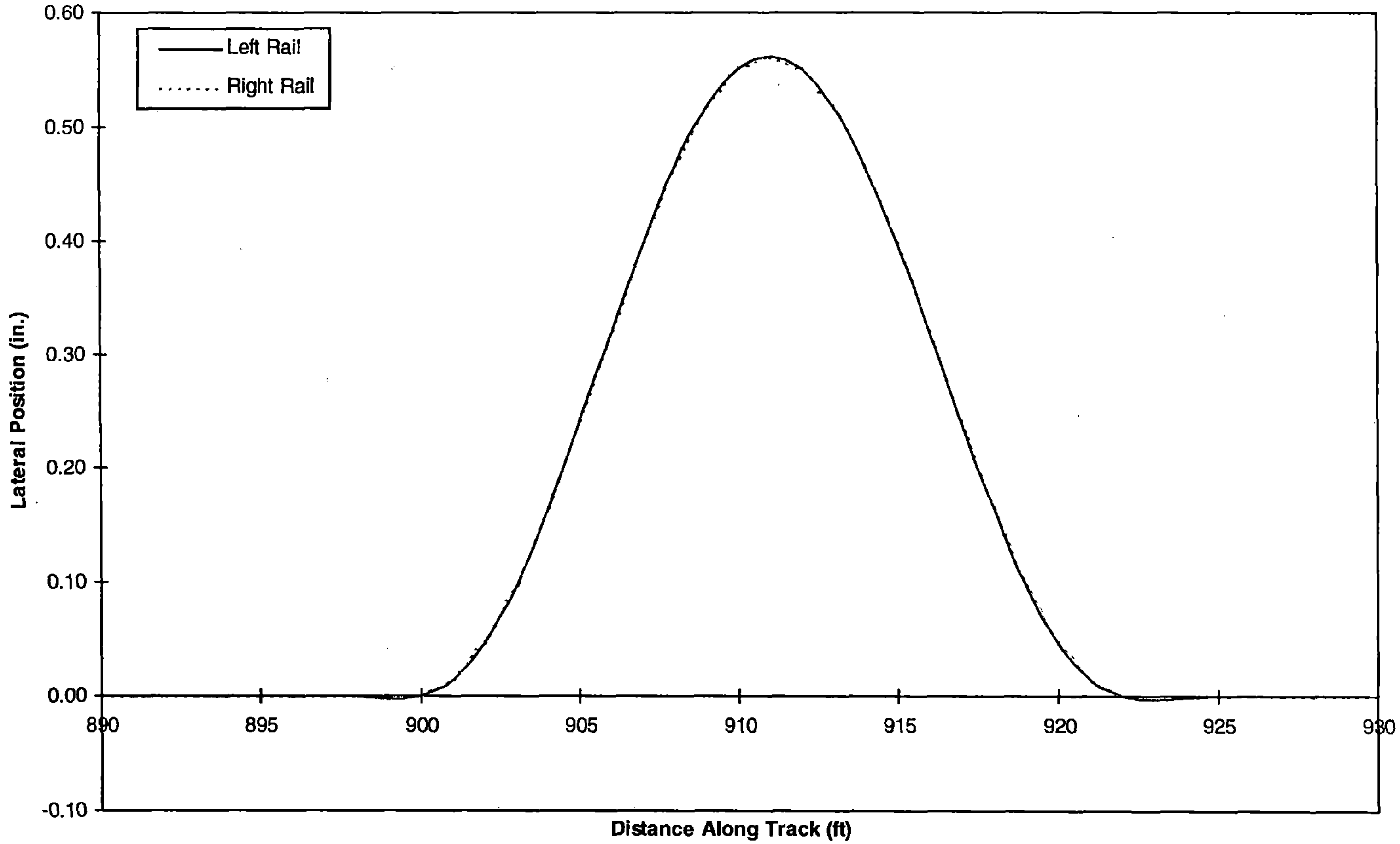

Figure 5-43. Lateral perturbation for hunting test

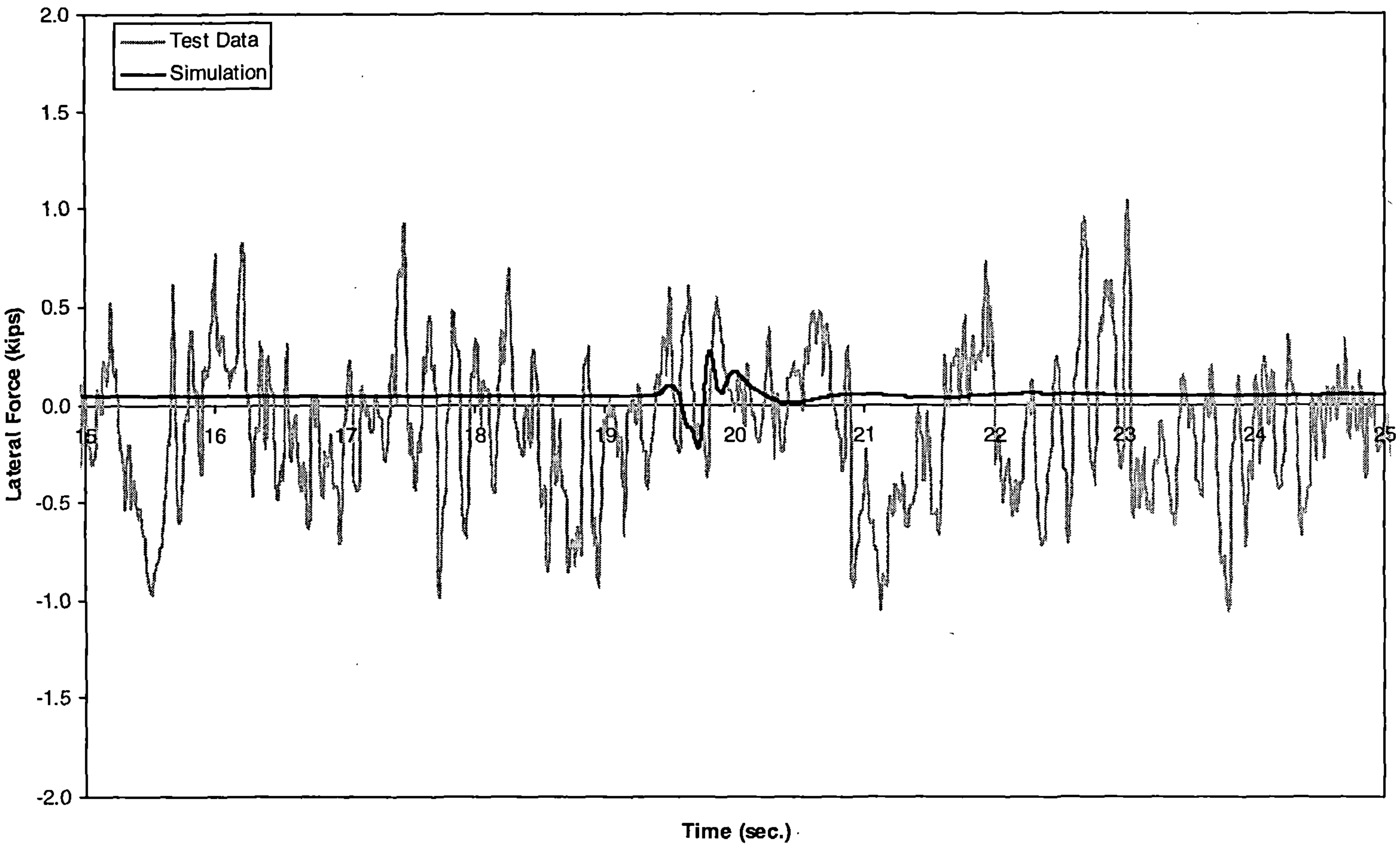

Figure 5-44(a). Hunting test – lateral force time history, 130 mph (lead left wheel)

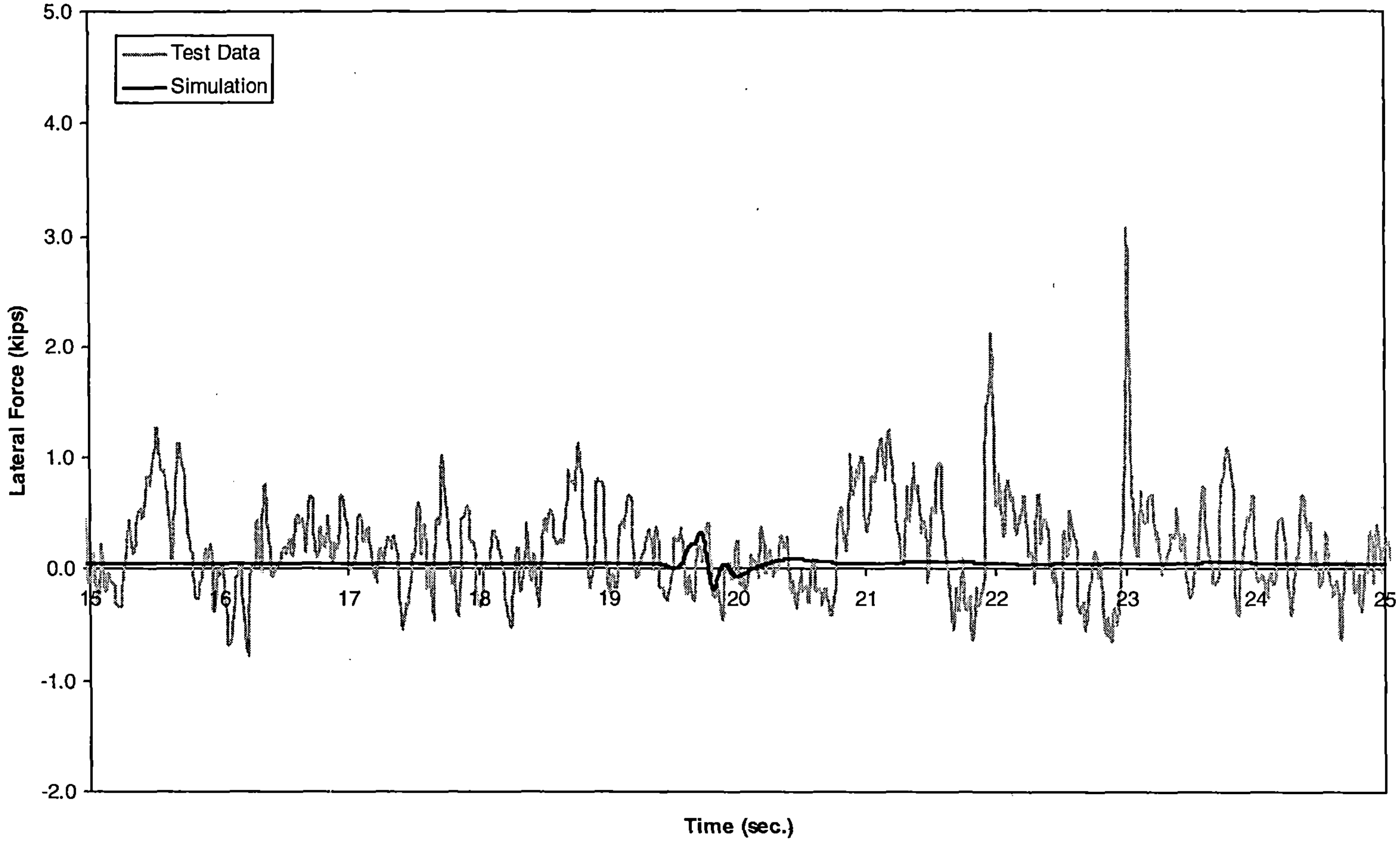

Figure 5-44(b). Hunting test – lateral force time history, 130 mph (lead right wheel)

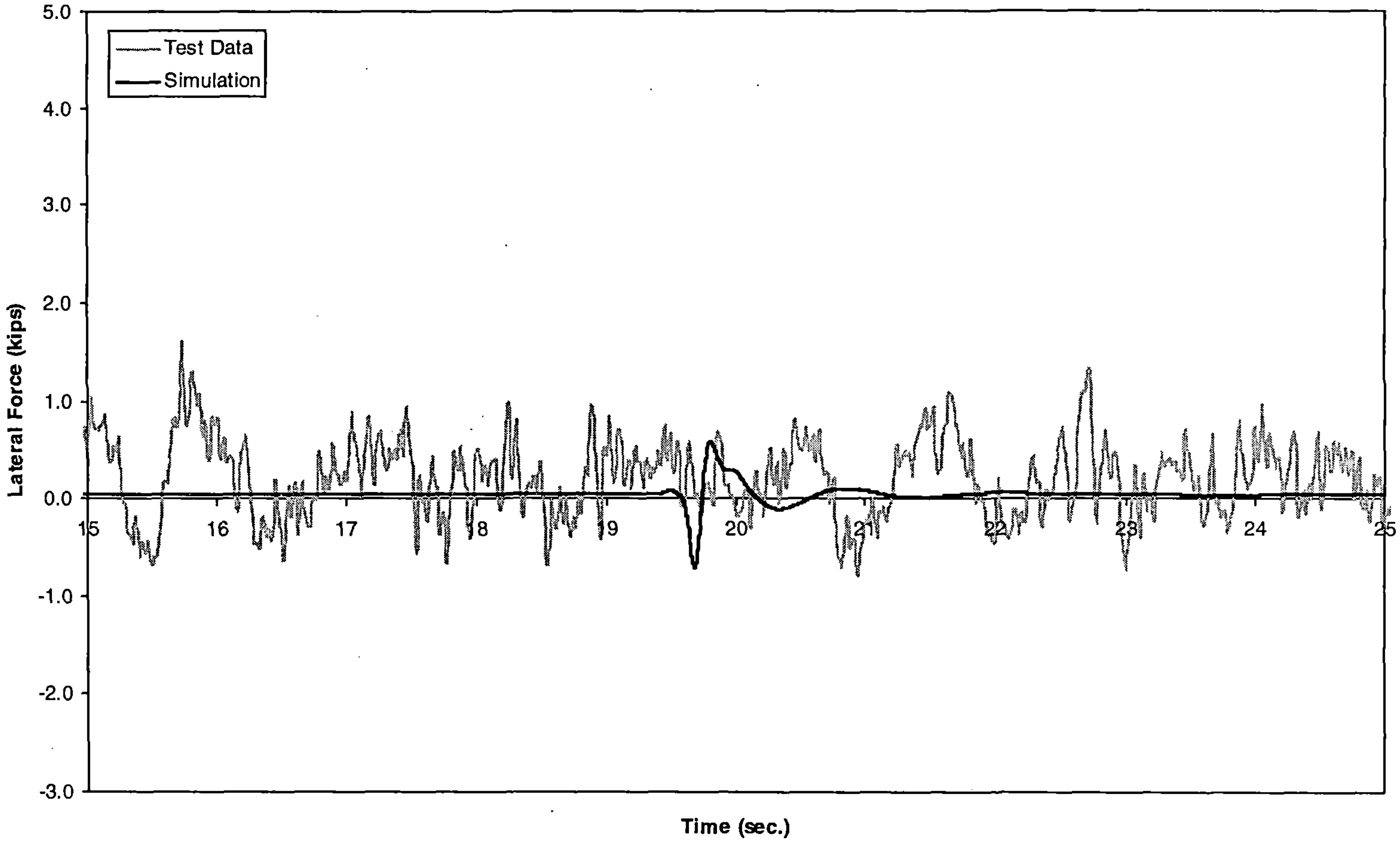

Figure 5-44(c). Hunting test – lateral force time history, 130 mph (trailing left wheel)

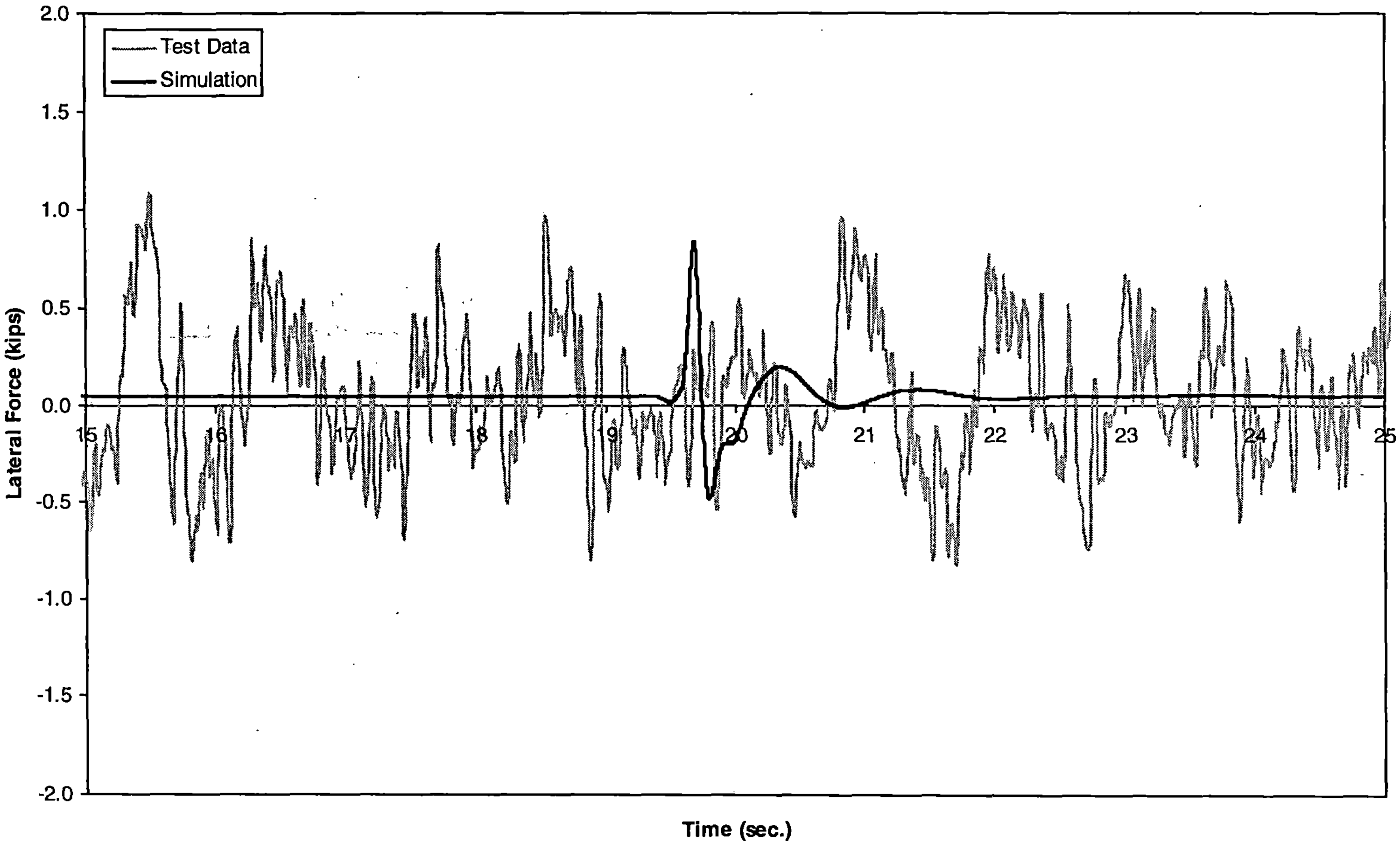

Figure 5-44(d). Hunting test – lateral force time history, 130 mph (trailing right wheel)

6. CONCLUSIONS

The simulation tool, OMNISIM has been exercised to predict the dynamic response of a vehicle negotiating various track scenarios including transient response to vertical and lateral perturbations in the track alignment, steady-state curving, dynamic curving, and truck hunting. For the study the following conclusions are reached with respect to correlations between test and computer simulation data:

1. The vehicle response to a variation in vertical alignment shows that simulation results for vertical forces agree closely with test data at all speeds. The simulation predicts wheel lift in close agreement with test data.

2. In the steady curving tests with spirals the simulation has good correlation with the measured vertical forces at all speeds. The correlation for the lateral force on individual wheels is not as good; however, the lateral net axle forces are in relatively good agreement between simulation and test results both at balance and over balance speeds.

3. In the dynamic curving tests the simulation is able to accurately predict the shape and amplitude of the vertical forces. The simulation has very good correlation for the vertical forces at all speeds. The correlation for the lateral force is not as good. The distribution of predicted lateral forces have the same shape as test lateral forces but are larger in amplitude, at all test speeds. Both the simulation and test data indicate that a wheel climb condition is not approached for the conditions studied.

4. In yaw and sway tests, the simulation has very good correlation with test data for the vertical force at all speeds. The correlation for the lateral force is not as good. The simulation is able to predict the shape and amplitude of the vertical forces. The predicted lateral force distributions have similar shape as in test lateral forces but the simulation under predicts the amplitude.

5. In twist and roll tests the simulation has very good correlation with test data for the amplitude of the vertical and lateral forces at all speeds.

6. In pitch and bounce tests the simulation has good correlation with test data for the vertical force throughout the speed range. The simulation predicts the shape and amplitude of the vertical forces. The predicted lateral forces are small, as are the test results.

7. The vehicle did not show any truck or body hunting oscillations up to the speed limits achieved in the test program (130 mph). This is consistent with the theory, which predicted a hunting speed of well over 200 mph.

8. In considering the cases where safety related limits were approached, the simulations and tests both identified in a similar manner the presence or absence of such conditions. In cases where wheel lift occurred, the simulation and test results were similar. Throughout the correlation study, good agreement was achieved between vertical force test data and simulation data.

9. Although agreement in the predicted and test data on the lateral force is not good in certain cases (dynamic curving and yaw and sway), the levels of forces are small and no unsafe condition is predicted by OMNISIM and witnessed in the tests.

7. REFERENCES

1. Samavedam, G., et al., "Conventional Passenger Rail Vehicle Safety, Volume I: Summary of Safe Performance Limits," Foster-Miller, Inc., Final Report, October 1997.
2. Samavedam, G., et al., "Conventional Passenger Rail Vehicle Safety, Technical Report Volume II: Detailed Analyses and Simulation Results," Foster-Miller, Inc., Draft Report, November 1997.
3. Samavedam, G., et al., "Analyses of Track Shift Under High-Speed Vehicle-Track Interaction – Safety of High-Speed Ground Transportation," DOT Report No. DOT/FRA/ ORD-97/02, June 1997.
4. Cooperrider, N.K., and Heller, R., "User's Manual for the Asymmetric Wheel/Rail Contact Characterization Program," Federal Railroad Administration Report FRA/ORD-78/05, December 1977.
5. Kalker, J.J., "The Computation of Three Dimensional Rolling Contact with Dry Friction," International Journal for Numerical Methods in Engineering, Vol.14, pp. 1293-1307, 1979.